

---

---

JSCSEN 87(1)1–168(2022)

---

---

ISSN 1820-7421(Online)

---

---

---

---

---

---

# Journal of the Serbian Chemical Society

---

---

e  
l  
e  
c  
t  
r  
o  
n  
i  
c



---

VOLUME 87

---

No 1

---

BELGRADE 2022

---

Available on line at



[www.shd.org.rs/JSCS/](http://www.shd.org.rs/JSCS/)

---

The full search of JSCS  
is available through

**DOAJ** DIRECTORY OF  
OPEN ACCESS  
JOURNALS  
[www.doaj.org](http://www.doaj.org)

The **Journal of the Serbian Chemical Society** (formerly Glasnik Hemijskog društva Beograd), one volume (12 issues) per year, publishes articles from the fields of chemistry. The **Journal** is financially supported by the **Ministry of Education, Science and Technological Development of the Republic of Serbia**.

Articles published in the **Journal** are indexed in Clarivate Analytics products: **Science Citation Index-Expanded<sup>TM</sup>** – accessed via **Web of Science®** and **Journal Citation Reports®**.

**Impact Factor** announced 2021: **1.240; 5-year Impact Factor: 1.144.**

Articles appearing in the **Journal** are also abstracted by: **Scopus**, **Chemical Abstracts Plus (Cplus<sup>SM</sup>)**, **Directory of Open Access Journals**, **Referativniy Zhurnal (VINITI)**, **RSC Analytical Abstracts**, **EuroPub**, **Pro Quest** and **Asian Digital Library**.

**Publisher:**

**Serbian Chemical Society**, Karnežijeva 4/III, P. O. Box 36, 1120 Belgrade 35, Serbia  
tel./fax: +381–11–3370–467, E-mails: **Society** – shd@shd.org.rs; **Journal** – jscs@shd.org.rs  
Home Pages: **Society** – <http://www.shd.org.rs/>; **Journal** – <http://www.shd.org.rs/JSCS/>  
Contents, Abstracts and full papers (from Vol 64, No. 1, 1999) are available in the electronic form at the Web Site of the **Journal** (<http://www.shd.org.rs/JSCS/>).

**Internet Service:**

**Nikola A. Pušin** (1930–1947), **Aleksandar M. Leko** (1948–1954),

**Panta S. Tutundžić** (1955–1961), **Miloš K. Mladenović** (1962–1964),

**Đorđe M. Dimitrijević** (1965–1969), **Aleksandar R. Despić** (1969–1975),

**Slobodan V. Ribnikar** (1975–1985), **Dragutin M. Dražić** (1986–2006).

**BRANISLAV Ž. NIKOLIĆ**, Serbian Chemical Society (E-mail: jscs-ed@shd.org.rs)  
**DUŠAN SLADIĆ**, Faculty of Chemistry, University of Belgrade

**Former Editors:**

**DEJAN OPSENICA**, Institute of Chemistry, Technology and Metallurgy, University of Belgrade

**Editor-in-Chief:**  
**Deputy Editor:**  
**Sub editors:**

*Organic Chemistry*

**JÁNOS CSANÁDI**, Faculty of Science, University of Novi Sad

**OLGICA NEDIĆ**, INEP – Institute for the Application of Nuclear Energy, University of Belgrade

**MILOŠ DURAN**, Serbian Chemical Society

**IVAN JURANIĆ**, Serbian Chemical Society

**LJILJANA DAMJANOVIĆ-VASILIĆ**, Faculty of Physical Chemistry, University of Belgrade

**SNEŽANA GOJKOVIĆ**, Faculty of Technology and Metallurgy, University of Belgrade

**SLAVICA RAŽIĆ**, Faculty of Pharmacy, University of Belgrade

**BRANKO DUNJIĆ**, Faculty of Technology and Metallurgy, University of Belgrade

**MIRJANA KIJEVČANIN**, Faculty of Technology and Metallurgy, University of Belgrade

**TATJANA KALUDEROVIĆ RADOIĆIĆ**, Faculty of Technology and Metallurgy, University of Belgrade

**RADA PETROVIĆ**, Faculty of Technology and Metallurgy, University of Belgrade

**ANA KOSTOV**, Mining and Metallurgy Institute Bor, University of Belgrade

**VESNA ANTIĆ**, Faculty of Agriculture, University of Belgrade

**DRAGICA TRIVIĆ**, Faculty of Chemistry, University of Belgrade

**LYNNE KATSIKAS**, Serbian Chemical Society

**VLATKA VAJS**, Serbian Chemical Society

**JASMINA NIKOLIĆ**, Faculty of Technology and Metallurgy, University of Belgrade

**VLADIMIR PANIĆ, ALEKSANDAR DEKANSKI, VUK FILIPOVIĆ**, Institute of Chemistry, Technology and Metallurgy, University of Belgrade

**ALEKSANDAR DEKANSKI**, Institute of Chemistry, Technology and Metallurgy, University of Belgrade

**VERA ĆUŠIĆ**, Serbian Chemical Society

**Editorial Board:**

**From abroad:** **R. Adžić**, Brookhaven National Laboratory (USA); **A. Casini**, University of Groningen (The Netherlands); **G. Cobb**, Baylor University (USA); **D. Douglas**, University of British Columbia (Canada); **G. Inzelt**, Etvos Lorand University (Hungary); **N. Katsaros**, NCSR “Demokritos”, Institute of Physical Chemistry (Greece); **J. Kenny**, University of Perugia (Italy); **Ya. I. Korenman**, Voronezh Academy of Technology (Russian Federation); **M. D. Lechner**, University of Osnabrueck (Germany); **S. Macura**, Mayo Clinic (USA); **M. Spiteller**, INFU, Technical University Dortmund (Germany); **M. Stratakis**, University of Crete (Greece); **M. Swart**, University de Girona (Cataluna, Spain); **G. Vunjak-Novaković**, Columbia University (USA); **P. Worsfold**, University of Plymouth (UK); **J. Zagal**, Universidad de Santiago de Chile (Chile).

**From Serbia:** **B. Abramović**, **V. Antić**, **V. Beškoski**, **J. Csanadi**, **Lj. Damjanović-Vasilić**, **A. Dekanski**, **V. Dondur**, **B. Dunjić**, **M. Duran**, **S. Gojković**, **I. Gutman**, **B. Jovančićević**, **I. Juranić**, **T. Kaluderović Radiović**, **L. Katsikas**, **M. Kijevčanin**, **A. Kostov**, **V. Levac**, **S. Milonjić**, **V.B. Mišković-Stanković**, **O. Nedić**, **B. Nikolić**, **J. Nikolić**, **D. Oprešenica**, **V. Panić**, **M. Petkovska**, **R. Petrović**, **I. Popović**, **B. Radak**, **S. Ražić**, **D. Sladić**, **S. Sovilj**, **S. Šerbanović**, **B. Solaja**, **Z. Tešić**, **D. Trivić**, **V. Vajs**.

**Subscription:** The annual subscription rate is **150.00 €** including postage (surface mail) and handling. For Society members from abroad rate is **50.00 €**. For the proforma invoice with the instruction for bank payment contact the Society Office (E-mail: shd@shd.org.rs) or see JSCS Web Site: <http://www.shd.org.rs/JSCS/>, option Subscription.

**Godišnja preplata:** Za članove SHD: **2.500,00 RSD**, za penzionere i studente: **1000,00 RSD**, a za ostale: **3.500,00 RSD**; za organizacije i ustanove: **16.000,00 RSD**. Uplate se vrše na tekući račun Društva: **205-13815-62**, poziv na broj **320**, sa naznakom “preplata za JSCS”.

**Nota:** Radovi čiji su svi autori članovi SHD prioritetno se publikuju.

Odlukom Odbora za hemiju Republičkog fonda za nauku Srbije, br. 66788/1 od 22.11.1990. godine, koja je kasnije potvrđena odlukom Saveta Fonda, časopis je uvršten u kategoriju međunarodnih časopisa (M-23). Takođe, aktom Ministarstva za nauku i tehnologiju Republike Srbije, 413-00-247/2000-01 od 15.06.2000. godine, ovaj časopis je proglašen za publikaciju od posebnog interesa za nauku. **Impact Factor** časopisa objavljen 2021. godine iznosi **1,240**, a petogodišnji **Impact Factor 1,144**.

## INSTRUCTIONS FOR AUTHORS (2021)

### GENERAL

The *Journal of the Serbian Chemical Society* (the *Journal* in further text) is an international journal publishing papers from all fields of chemistry and related disciplines. Twelve issues are published annually. The Editorial Board expects the editors, reviewers, and authors to respect the well-known standard of professional ethics.

### Types of Contributions

|                            |   |
|----------------------------|---|
| Original scientific papers | (up to 15 typewritten pages, including Figures, Tables and References)<br>report original research which must not have been previously published. |
| Short communications       | (up to 8 pages) report unpublished preliminary results of sufficient importance to merit rapid publication.                                       |
| Notes                      | (up to 5 pages) report unpublished results of short, but complete, original research  |
| Authors' reviews           | (up to 40 pages) present an overview of the author's current research with comparison to data of other scientists working in the field            |
| Reviews <sup>a</sup>       | (up to 40 pages) present a concise and critical survey of a specific research area. Generally, these are prepared at the invitation of the Editor |
| Surveys                    | (about 25 pages) communicate a short review of a specific research area.  |
| Book and Web site reviews  | (1 - 2 pages)   |
| Extended abstracts         | (about 4 pages) of Lectures given at meetings of the Serbian Chemical Society Divisions   |
| Letters to the Editor      | report miscellaneous topics directed directly to the Editor   |

<sup>a</sup>Generally, Authors' reviews, Reviews and Surveys are prepared at the invitation of the Editor.

### Submission of manuscripts

Manuscripts should be submitted using the **OnLine Submission Form**, available on the JSCS Web Site (<http://www.shd-pub.org.rs/index.php/JSCS>). The manuscript must be uploaded as a Word.doc or .rtf file, with tables and figures (including the corresponding captions – above Tables and below Figures), placed within the text to follow the paragraph in which they were mentioned for the first time.

Please note that **Full Names** (First Name, Last Name), **Full Affiliation** and **Country** (from drop down menu) of **ALL OF AUTHORS** (written in accordance with English spelling rules - the first letter capitalized) must be entered in the manuscript Submission Form (Step 3). Manuscript Title, authors' names and affiliations, as well as the Abstract, **WILL APPEAR** in the article listing, as well as in **BIBLIOGRAPHIC DATABASES (WoS, SCOPUS...)**, in the form and in the order entered in the author details

### Graphical abstract

Graphical abstract is a one-image file containing the main depiction of the authors work and/or conclusion and must be supplied along with the manuscript. It must enable readers to quickly gain the main message of the paper and to encourage browsing, help readers identify which papers are most relevant to their research interests. Authors must provide an image that clearly represents the research described in the paper. The most relevant figure from the work, which summarizes the content, can also be submitted. The image should be submitted as a separate file in **Online Submission Form - Step 2**.

Specifications: The graphical abstract should have a clear start and end, reading from top to bottom or left to right. Please omit unnecessary distractions as much as possible.

- **Image size:** minimum of 500×800 pixels (W×H) and a minimum resolution of 300 dpi. If a larger image is sent, then please use the same ratio: 16 wide × 9 high. Please note that your image will be scaled proportionally to fit in the available window in TOC; a 150x240 pixel rectangle. Please be sure that the quality of an image cannot be increased by changing the resolution from lower to higher, but only by resampling or exporting the image with a higher resolution, which can be set in usual "settings" option.
- **Font:** Please use Calibri and Symbol font with a large enough font size, so it is readable even from the image of a smaller size (150 × 240 px) in TOC.
- **File type:** JPG and PNG only.  
No additional text, outline or synopsis should be included. Please do not use white space or any heading within the image.

## **Cover Letter**

Manuscripts must be accompanied by a cover letter (strictly uploaded in **Online Submission Step 2**) in which the type of the submitted manuscript and a warranty as given below are given. The Author(s) has(have) to warranty that the manuscript submitted to the *Journal* for review is original, has been written by the stated author(s) and has not been published elsewhere; is currently not being considered for publication by any other journal and will not be submitted for such a review while under review by the *Journal*; the manuscript contains no libellous or other unlawful statements and does not contain any materials that violate any personal or proprietary rights of any other person or entity. All manuscripts will be acknowledged on receipt (by e-mail).

## **Illustrations**

Illustrations (Figs, schemes, photos...) in TIF or EPS format (JPG format is acceptable for colour and greyscale photos, only), must be additionally uploaded (Online Submission Step 2) as a separate file or one archived (.zip, .rar or .arj) file. Figures and/or Schemes should be prepared according to the **Artwork Instructions** - [http://www.shd.org.rs/JSCS/jscs-pdf/Artwork\\_Instructions.pdf](http://www.shd.org.rs/JSCS/jscs-pdf/Artwork_Instructions.pdf)!

For any difficulties and questions related to **OnLine Submission Form** - <https://www.shd-pub.org.rs/index.php/JSCS/submission/wizard>, please refer to **User Guide** - <https://openjournal-systems.com/ojs-3-user-guide/>, Chapter **Submitting an Article** - <https://openjournalsystems.com/ojs-3-user-guide/submitting-an-article/>. If difficulties still persist, please contact JSCS Editorial Office at [JSCS@shd.org.rs](mailto:JSCS@shd.org.rs)

**A manuscript not prepared according to these instructions will be returned for resubmission without being assigned a reference number.**

**Conflict-of-Interest Statement\***: Public trust in the peer review process and the credibility of published articles depend in part on how well a conflict of interest is handled during writing, peer review, and editorial decision making. A conflict of interest exists when an author (or the author's institution), reviewer, or editor has financial or personal relationships that inappropriately influence (bias) his or her actions (such relationships are also known as dual commitments, competing interests, or competing loyalties). These relationships vary from those with negligible potential to those with great potential to influence judgment, and not all relationships represent true conflict of interest. The potential for a conflict of interest can exist whether or not an individual believes that the relationship affects his or her scientific judgment. Financial relationships (such as employment, consultancies, stock ownership, honoraria, paid expert testimony) are the most easily identifiable conflicts of interest and the most likely to undermine the credibility of the journal, the authors, and of science itself. However, conflicts can occur for other reasons, such as personal relationships, academic competition, and intellectual passion.

**Informed Consent Statement\***: Patients have a right to privacy that should not be infringed without informed consent. Identifying information, including patients' names, initials, or hospital numbers, should not be published in written descriptions, photographs, and pedigrees unless the information is essential for scientific purposes and the patient (or parent or guardian) gives written informed consent for publication. Informed consent for this purpose requires that a patient who is identifiable be shown the manuscript to be published. Authors should identify individuals who provide writing assistance and disclose the funding source for this assistance. Identifying details should be omitted if they are not essential. Complete anonymity is difficult to achieve, however, and informed consent should be obtained if there is any doubt. For example, masking the eye region in photographs of patients is inadequate protection of anonymity. If identifying characteristics are altered to protect anonymity, such as in genetic pedigrees, authors should provide assurance that alterations do not distort scientific meaning and editors should so note. The requirement for informed consent should be included in the journal's instructions for authors. When informed consent has been obtained it should be indicated in the published article.

**Human and Animal Rights Statement\*** When reporting experiments on human subjects, authors should indicate whether the procedures followed were in accordance with the ethical standards of the responsible committee on human experimentation (institutional and national) and with the Helsinki Declaration of 1975, as revised in 2000 (5). If doubt exists whether the research was conducted in accordance with the Helsinki Declaration, the authors must explain the rationale for their approach, and demonstrate that the institutional review body explicitly approved the doubtful aspects of the study. When reporting experiments on animals, authors should be asked to indicate whether the institutional and national guide for the care and use of laboratory animals was followed.

---

\*International Committee of Medical Journal Editors ("Uniform Requirements for Manuscripts Submitted to Biomedical Journals"), February 2006

## **PROCEDURE**

All contributions will be peer reviewed and only those deemed worthy and suitable will be accepted for publication. The Editor has the final decision. To facilitate the reviewing process, authors are encouraged to suggest up to three persons competent to review their manuscript. Such suggestions will be taken into consideration but not always accepted. If authors would prefer a specific person not be a reviewer, this should be announced. The Cover Letter must be accompanied by these suggestions. Manuscripts requiring revision should be returned according to the requirement of the Editor, within 60 days upon reception of the reviewing comments by e-mail.

The *Journal* maintains its policy and takes the liberty of correcting the English as well as false content of manuscripts **provisionally accepted** for publication in the first stage of reviewing process. In this second stage of manuscript preparation by JSCS Editorial Office, the author(s) may be required to supply some **additional clarifications and corrections**. This procedure will be executed during copyediting actions, with a demand to author(s) to perform corrections of unclear parts before the manuscript would be published OnLine as **finally accepted manuscript (OLF Section of the JSCS website)**. Please note that the manuscript can receive the status of **final rejection** if the author's corrections would not be satisfactory.

When finally accepted manuscript is ready for printing, the corresponding author will receive a request for proof reading, which should be performed within 2 days. Failure to do so will be taken as the authors agree with any alteration which may have occurred during the preparation of the manuscript for printing.

Accepted manuscripts of active members of the Serbian Chemical Society (all authors) have publishing priority.

## **MANUSCRIPT PRESENTATION**

Manuscripts should be typed in English (either standard British or American English, but consistent throughout) with 1.5 spacing (12 points Times New Roman; Greek letters in the character font Symbol) in A4 format leaving 2.5 cm for margins. For Regional specific, non-standard characters that may appear in the text, save documents with Embed fonts Word option: *Save as -> (Tools) -> Save Options... -> Embed fonts in the text*.

The authors are requested to seek the assistance of competent English language expert, if necessary, to ensure their English is of a reasonable standard. The Serbian Chemical Society can provide this service in advance of submission of the manuscript. If this service is required, please contact the office of the Society by e-mail ([jscs-info@shd.org.rs](mailto:jscs-info@shd.org.rs)).

**Tables, figures and/or schemes** must be embedded in the main text of the manuscript and should follow the paragraph in which they are mentioned for the first time. **Tables** must be prepared with the aid of the **WORD table function**, without vertical lines. The minimum size of the font in the tables should be **10 pt**. Table columns must not be formatted using multiple spaces. Table rows must not be formatted using any returns (enter key; ↵ key) and are **limited to 12 cm width**. Tables should not be incorporated as graphical objects. **Footnotes to Tables** should follow them and are to be indicated consequently (in a single line) in superscript letters and separated by semi-column.

**Table caption** must be placed above corresponding Table, while **Captions of the Illustrations** (Figs. Schemes...) must follow the corresponding item. **The captions, either for Tables or Illustrations**, should make the items comprehensible without reading of the main text (but clearly referenced in), must follow numerical order (Roman for Tables, Arabic for Illustrations), and should not be provided on separate sheets or as separate files.

**High resolution Illustrations** (named as Fig. 1, Fig. 2... and/or Scheme 1, Scheme 2...) in **TIF or EPS format** (JPG format is acceptable for photos, only) **must be additionally uploaded as a separate files or one archived (.zip, .rar) file**.

Illustrations should be prepared according to the [ARTWORK INSTRUCTIONS](http://www.shd.org.rs/JSCS/jscs-pdf/Artwork_Instructions.pdf) - [http://www.shd.org.rs/JSCS/jscs-pdf/Artwork\\_Instructions.pdf](http://www.shd.org.rs/JSCS/jscs-pdf/Artwork_Instructions.pdf) !

All pages of the manuscript must be numbered continuously.

## **DESIGNATION OF PHYSICAL QUANTITIES AND UNITS**

**IUPAC recommendations** for the naming of compounds should be followed. SI units, or other permissible units, should be employed. The designation of physical quantities must be in italic throughout the text (including figures, tables and equations), whereas the units and indexes (except for indexes having the meaning of physical quantities) are in upright letters. They should be in Times New Roman font. In graphs and tables, a slash should be used to separate the designation of a physical quantity from the unit

(example:  $p$  / kPa,  $j$  / mA cm<sup>-2</sup>,  $t$  / °C,  $T_0$  / K,  $\tau$ /h,  $\ln(j / \text{mA cm}^{-2})$ ...). Designations such as:  $p$  (kPa),  $t$  [min]..., are not acceptable. However, if the full name of a physical quantity is unavoidable, it should be given in upright letters and separated from the unit by a comma (example: Pressure, kPa; Temperature, K; Current density, mA cm<sup>-2</sup>...). Please do not use the axes of graphs for additional explanations; these should be mentioned in the figure captions and/or the manuscript (example: “pressure at the inlet of the system, kPa” should be avoided). The axis name should follow the direction of the axis (the name of y-axis should be rotated by 90°). Top and right axes should be avoided in diagrams, unless they are absolutely necessary.

**Latin words**, as well as the names of species, should be in *italic*, as for example: *i.e.*, *e.g.*, *in vivo*, *ibid*, *Calendula officinalis L.*, etc. The branching of organic compound should also be indicated in *italic*, for example, *n*-butanol, *tert*-butanol, etc.

**Decimal numbers** must have decimal points and not commas in the text (except in the Serbian abstract), tables and axis labels in graphical presentations of results. Thousands are separated, if at all, by a comma and not a point.

**Mathematical and chemical equations** should be given in separate lines and must be numbered, Arabic numbers, consecutively in parenthesis at the end of the line. All equations should be embedded in the text. Complex equations (fractions, integrals, matrix...) should be prepared with the aid of the **Microsoft Equation 3.0** (or higher) or **MathType** (Do not use them to create simple equations and labels). Using the **Insert -> Equation option, integrated in MS Office 2010 and MS Office 2013, as well as insertion of equation objects within paragraph text IS NOT ALLOWED.**

## ARTICLE STRUCTURE

- TITLE PAGE;
- MAIN TEXT – including Tables and Illustrations with corresponding captions;
- SUPPLEMENTARY MATERIAL (optional)

### Title page

- Title in bold letters, should be clear and concise, preferably 12 words or less. The use of non-standard abbreviations, symbols and formulae is discouraged.
- AUTHORS' NAMES in capital letters with the full first name, initials of further names separated by a space and surname. Commas should separate the author's names except for the last two names when 'and' is to be used. In multi-affiliation manuscripts, the author's affiliation should be indicated by an Arabic number placed in superscript after the name and before the affiliation. Use \* to denote the corresponding author(s).
- *Affiliations* should be written in italic. The e-mail address of the corresponding author should be given after the affiliation(s).
- *Abstract:* A one-paragraph abstract written of 150 – 200 words in an impersonal form indicating the aims of the work, the main results and conclusions should be given and clearly set off from the text. Domestic authors should also submit, on a separate page, an Abstract - Izvod, the author's name(s) and affiliation(s) in Serbian (Cyrillic letters). (Домаћи аутори морају доставити Извод (укључујући имена аутора и афилијацију) на српском језику, исписане њирилицом, иза Захвалнице, а пре списка референци.) For authors outside Serbia, the Editorial Board will provide a Serbian translation of their English abstract.
- *Keywords:* Up to 6 keywords should be given. Do not use words appearing in the manuscript title
- RUNNING TITLE: A one line (maximum five words) short title in capital letters should be provided.

### Main text – should have the form:

- INTRODUCTION,
- EXPERIMENTAL (RESULTS AND DISCUSSION),
- RESULTS AND DISCUSSION (EXPERIMENTAL),
- CONCLUSIONS,
- NOMENCLATURE (optional) and
- Acknowledgements: If any.
- REFERENCES (Citation of recent papers published in chemistry journals that highlight the significance of work to the general readership is encouraged.)

The sections should be arranged in a sequence generally accepted for publication in the respective fields. They subtitles should be in capital letters, centred and NOT numbered.

- The INTRODUCTION should include the aim of the research and a concise description of background information and related studies directly connected to the paper.
- The EXPERIMENTAL section should give the purity and source of all employed materials, as well as details of the instruments used. The employed methods should be described in sufficient detail to enable experienced persons to repeat them. Standard procedures should be referenced and only modifications described in detail. On no account should results be included in the experimental section.

## Chemistry

Detailed information about instruments and general experimental techniques should be given in all necessary details. If special treatment for solvents or chemical purification were applied that must be emphasized.

*Example:* Melting points were determined on a Boetius PMHK or a Mel-Temp apparatus and were not corrected. Optical rotations were measured on a Rudolph Research Analytical automatic polarimeter, Autopol IV in dichloromethane (DCM) or methanol (MeOH) as solvent. IR spectra were recorded on a Perkin-Elmer spectrophotometer FT-IR 1725X.  $^1\text{H}$  and  $^{13}\text{C}$  NMR spectra were recorded on a Varian Gemini-200 spectrometer (at 200 and 50 MHz, respectively), and on a Bruker Ultrashield Advance III spectrometer (at 500 and 125 MHz, respectively) employing indicated solvents (*vide infra*) using TMS as the internal standard. Chemical shifts are expressed in ppm ( $\delta$  / ppm) values and coupling constants in Hz ( $J$  / Hz). ESI-MS spectra were recorded on Agilent Technologies 6210 Time-Of-Flight LC-MS instrument in positive ion mode with  $\text{CH}_3\text{CN}/\text{H}_2\text{O}$  1/1 with 0.2 % HCOOH as the carrying solvent solution. Samples were dissolved in  $\text{CH}_3\text{CN}$  or MeOH (HPLC grade purity). The selected values were as follows: capillary voltage = 4 kV, gas temperature = 350 °C, drying gas flow 12 L min $^{-1}$ , nebulizer pressure = 310 kPa, fragmentator voltage = 70 V. The elemental analysis was performed on the Vario EL III- C,H,N,S/O Elemental Analyzer (Elementar Analysensysteme GmbH, Hanau-Germany). Thin-layer chromatography (TLC) was performed on precoated Merck silica gel 60 F254 and RP-18 F254 plates. Column chromatography was performed on Lobar LichroPrep Si 60 (40-63  $\mu\text{m}$ ), RP-18 (40-63  $\mu\text{m}$ ) columns coupled to a Waters RI 401 detector, and on Biotope SP1 system with UV detector and FLASH 12+, FLASH 25+ or FLASH 40+ columns pre packed with KP-SIL [40-63  $\mu\text{m}$ , pore diameter 6 nm (60 Å)], KP-C18-HS (40-63  $\mu\text{m}$ , pore diameter 9 nm (90 Å) or KP-NH [40-63  $\mu\text{m}$ , pore diameter 10 nm (100 Å)] as adsorbent. Compounds were analyzed for purity (HPLC) using a Waters 1525 HPLC dual pump system equipped with an Alltech, Select degasser system, and dual  $\lambda$  2487 UV-VIS detector. For data processing, Empower software was used (methods A and B). Methods C and D: Agilent Technologies 1260 Liquid Chromatograph equipped with Quat Pump (G1311B), Injector (G1329B) 1260 ALS, TCC 1260 (G1316A) and Detector 1260 DAD VL+ (G1315C). For data processing, LC OpenLab CDS ChemStation software was used. For details, see Supporting Information.

### 1. Synthesis experiments

Each paragraph describing a synthesis experiment should begin with the name of the product and any structure number assigned to the compound in the Results and Discussions section. Thereafter, the compound should be identified by its structure number. Use of standard abbreviations or unambiguous molecular formulas for reagents and solvents, and of structure numbers rather than chemical names to identify starting materials and intermediates, is encouraged.

When a new or improved synthetic method is described, the yields reported in key experimental examples, and yields used for comparison with existing methods, should represent amounts of isolated and purified products, rather than chromatographically or spectroscopically determined yields. Reactant quantities should be reported in weight and molar units and for product yields should be reported in weight units; percentage yields should only be reported for materials of demonstrated purity. When chromatography is used for product purification, both the support and solvent should be identified.

### 2. Microwave experiments

Reports of syntheses conducted in microwave reactors must clearly indicate whether sealed or open reaction vessels were used and must document the manufacturer and model of the reactor, the method of monitoring the reaction mixture temperature, and the temperature-time profile. Reporting a wattage rating or power setting is not an acceptable alternative to providing temperature data. Manuscripts describing work done with domestic (kitchen) microwave ovens will not be accepted except for studies where the unit is used for heating reaction mixtures at atmospheric pressure.

### 3. Compound characterization

The Journal upholds a high standard for compound characterization to ensure that substances being added to the chemical literature have been correctly identified and can be synthesized in known yield and purity by the reported preparation and isolation methods. For **all new** compounds, evidence adequate to establish both **identity** and **degree of purity** (homogeneity) must be provided.

**Identity - Melting point.** All homogeneous solid products (*e.g.* not mixtures of isomers) should be characterized by melting or decomposition points. The colors and morphologies of the products should also be noted.

**Specific rotations.** Specific rotations based on the equation  $[\alpha]^l; D = (100 \alpha) / (l c)$  should be reported as unitless numbers as in the following example:  $[\alpha]^{20}; D = -25.4$  (*c* 1.93, CHCl<sub>3</sub>), where *c* / g mL<sup>-1</sup> is concentration and *l* / dm is path length. The units of the specific rotation, (deg mL) / (g dm), are implicit and are not included with the reported value.

**Spectra/Spectral Data.** Important IR absorptions should be given.

For all new diamagnetic substances, NMR data should be reported (<sup>1</sup>H, <sup>13</sup>C, and relevant heteronuclei). <sup>1</sup>H NMR chemical shifts should be given with two digits after the decimal point. Include the number of protons represented by the signal, signal multiplicity, and coupling constants as needed (*J* italicized, reported with up to one digit after the decimal). The number of bonds through which the coupling is operative, <sup>x</sup>*J*, may be specified by the author if known with a high degree of certainty. <sup>13</sup>C NMR signal shifts should be rounded to the nearest 0.01 ppm unless greater precision is needed to distinguish closely spaced signals. Field strength should be noted for each spectrum, not as a comment in the general experimental section. Hydrogen multiplicity (C, CH, CH<sub>2</sub>, CH<sub>3</sub>) information obtained from routine DEPT spectra should be included. If detailed signal assignments are made, the type of NOESY or COSY methods used to establish atom connectivity and spatial relationships should be identified in the Supporting Information. Copies of spectra should also be included where structure assignments of complex molecules depend heavily on NMR interpretation. Numbering system used for assignments of signals should be given in the Supporting Information with corresponding general structural formula of named derivative.

HPLC/LCMS can be substituted for biochemistry papers where the main focus is not on compound synthesis.

**HRMS/elemental analysis.** To support the molecular formula assignment, HRMS data accurate within 5 ppm, or combustion elemental analysis [carbon and hydrogen (and nitrogen, if present)] data accurate within 0.5 %, should be reported for new compounds. HRMS data should be given in format as is usually given for combustion analysis: calculated mass for given formula following with observed mass: (+)ESI-HRMS *m/z*: [molecular formula + H]<sup>+</sup> calculated mass, observed mass. Example: (+)ESI-HRMS *m/z*: calculated for [C<sub>13</sub>H<sub>8</sub>BrCl<sub>2</sub>N + H]<sup>+</sup> 327.92899, observed 327.92792.

NOTE: in certain cases, a crystal structure may be an acceptable substitute for HRMS/elemental analysis.

**Biomacromolecules.** The structures of biomacromolecules may be established by providing evidence about sequence and mass. Sequences may be inferred from the experimental order of amino acid, saccharide, or nucleotide coupling, from known sequences of templates in enzyme-mediated syntheses, or through standard sequencing techniques. Typically, a sequence will be accompanied by MS data that establish the molecular weight.

**Example:** Product was isolated upon column chromatography [dry flash (SiO<sub>2</sub>, eluent EA, EA/MeOH gradient 95/5 → 9/1, EA/MeOH/NH<sub>3</sub> gradient 18/0.5/0.5 → 9/1/1, and flash chromatography (Biotage SP1, RP column, eluent MeOH/H<sub>2</sub>O gradient 75/25 → 95/5, N-H column, eluent EA/Hex gradient 6/3 → EA)]. was obtained after flash column chromatography (Biotage SP NH column, eluent hexane/EA 4:6 → 2:6). Yield 968.4 mg (95 %). Colorless foam softens at 96–101 °C.  $[\alpha]^{20}; D = +0.163$  (*c* = 2.0 × 10<sup>-3</sup> g/mL, CH<sub>2</sub>Cl<sub>2</sub>). IR (ATR): 3376w, 2949m, 2868w, 2802w, 1731s, 1611w, 1581s, 1528m, 1452m, 1374s, 1331w, 1246s, 1171m, 1063w, 1023m, 965w, 940w, 881w, 850w, 807w, cm<sup>-1</sup>. <sup>1</sup>H NMR (500 MHz, CDCl<sub>3</sub>, δ): 8.46 (*d*, 1H, *J* = 5.4, H-2'), 7.89 (*s*, 1H, *J* = 2.0, H-8'), 7.71 (*d*, 1H, *J* = 8.9, H-5'), 7.30 (*dd*, 1H, *J*<sub>1</sub> = 8.8, *J*<sub>2</sub> = 2.1, H-6'), 6.33 (*d*, 1H, *J* = 5.4, H-3'), 6.07 (*s*, HN-Boc, exchangeable with D<sub>2</sub>O), 5.06 (*s*, 1H, H-12), 4.92–4.88 (*m*, 1H, H-7), 4.42 (*bs*, H-3), 3.45 (*s*, CH<sub>3</sub>-N), 3.33 (*bs*, H-9'), 3.05–2.95 (*m*, 2H, H-11'), 2.70–2.43 (*m*, 2H, H-24) and HN, exchangeable with D<sub>2</sub>O), 2.07 (*s*, CH<sub>3</sub>COO), 2.04 (*s*, CH<sub>3</sub>COO), 1.42 (*s*, 9H, (CH<sub>3</sub>)<sub>3</sub>C-N(Boc)), 0.88 (*s*, 3H, CH<sub>3</sub>-10), 0.79 (*d*, 3H, *J* = 6.6, CH<sub>3</sub>-20), 0.68 (*s*, 3H, CH<sub>3</sub>-13). <sup>13</sup>C NMR (125 MHz, CDCl<sub>3</sub>, δ): 170.34, 170.27, 151.80, 149.92, 148.87, 134.77, 128.36, 125.11, 121.43, 117.29, 99.98, 75.41, 70.82, 50.43, 49.66, 47.60, 47.33, 44.97, 43.30, 41.83, 41.48, 37.65, 36.35, 35.44, 34.89,

34.19, 33.23, 31.24, 28.79, 28.35, 27.25, 26.45, 25.45, 22.74, 22.63, 21.57, 21.31, 17.85, 12.15. (+)ESI-HRMS (*m/z*): calculated for [C<sub>45</sub>H<sub>67</sub>ClN<sub>4</sub>O<sub>6</sub> + H]<sup>+</sup> 795.48219, observed 795.48185. Combustion analysis for C<sub>45</sub>H<sub>67</sub>ClN<sub>4</sub>O<sub>6</sub>: Calculated. C 67.94, H 8.49, N 7.04; found C 67.72, H 8.63, N 6.75. HPLC purity: method A: RT 1.994, area 99.12 %; method C: RT 9.936, area 98.20 %.

**Purity** - Evidence for documenting compound purity should include one or more of the following:

- a) Well-resolved high field 1D <sup>1</sup>H NMR spectrum showing at most only trace peaks not attributable to the assigned structure and a standard 1D proton-decoupled <sup>13</sup>C NMR spectrum. Copies of the spectra should be included as figures in the Supporting Information.
- b) Quantitative gas chromatographic analytical data for distilled or vacuum-transferred samples, or quantitative HPLC analytical data for materials isolated by column chromatography or separation from a solid support. HPLC analyses should be performed in two diverse systems. The stationary phase, solvents (HPLC), detector type, and percentage of total chromatogram integration should be reported; a copy of the chromatograms may be included as a figure in the Supporting Information.
- c) Electrophoretic analytical data obtained under conditions that permit observing impurities present at the 5 % level.

HRMS data may be used to support a molecular formula assignment **but cannot be used as a criterion of purity**.

#### 4. Biological Data

Quantitative biological data are required for all tested compounds. Biological test methods must be referenced or described in sufficient detail to permit the experiments to be repeated by others. Detailed descriptions of biological methods should be placed in the experimental section. Standard compounds or established drugs should be tested in the same system for comparison. Data may be presented as numerical expressions or in graphical form; biological data for extensive series of compounds should be presented in tabular form. Tables consisting primarily of negative data will not usually be accepted; however, for purposes of documentation they may be submitted as supporting information. Active compounds obtained from combinatorial syntheses should be resynthesized and retested to verify that the biology conforms to the initial observation.

Statistical limits (statistical significance) for the biological data are usually required. If statistical limits cannot be provided, the number of determinations and some indication of the variability and reliability of the results should be given. References to statistical methods of calculation should be included. Doses and concentrations should be expressed as molar quantities (*e.g.*, mol/kg,  $\mu$ mol/kg, M, mM). The routes of administration of test compounds and vehicles used should be indicated, and any salt forms used (hydrochlorides, sulfates, *etc.*) should be noted. The physical state of the compound dosed (crystalline, amorphous; solution, suspension) and the formulation for dosing (micronized, jet-milled, nanoparticles) should be indicated. For those compounds found to be inactive, the highest concentration (*in vitro*) or dose level (*in vivo*) tested should be indicated.

- The RESULTS AND DISCUSSION should include concisely presented results and their significance discussed and compared to relevant literature data. The results and discussion may be combined or kept separate.
- The inclusion of a CONCLUSION section, which briefly summarizes the principal conclusions, is recommended.
- NOMENCLATURE is optional but, if the authors wish, a list of employed symbols may be included.
- REFERENCES should be numbered sequentially as they appear in the text. Please note that any reference numbers appearing in the Illustrations and/or Tables and corresponding captions must follow the numbering sequence of the paragraph in which they appear for the first time. When cited, the reference number should be superscripted in Font 12, following any punctuation mark. In the reference list, they should be in normal position followed by a full stop. Reference entry must not be formatted using Carriage returns (enter key; ↵ key) or multiple space key. The formatting of references to published work should follow the *Journal's* style as follows:

|                         |   |
|-------------------------|---|
| Journals <sup>a</sup> : | A. B. Surname1, C. D. Surname2, <i>J. Serb. Chem. Soc.</i> <b>Vol</b> (Year) first page Number<br>( <a href="https://doi.org/doi">https://doi.org/doi</a> ) <sup>b</sup>  |
| Books:                  | A. B. Surname1, C. D. Surname2, <i>Name of Book</i> , Publisher, City, Year, pp. 100-101<br>( <a href="https://doi.org/doi">https://doi.org/doi</a> ) <sup>b</sup>  |
| Compilations:           | A. B. Surname1, C. D. Surname2, in <i>Name of Compilation</i> , A. Editor1, C. Editor2, Ed(s)., Publisher, City, Year, p. 100 ( <a href="https://doi.org/doi">https://doi.org/doi</a> ) <sup>b</sup>                    |
| Proceedings:            | A. B. Surname1, C. D. Surname2, in <i>Proceedings of Name of the Conference or Symposium</i> , (Year), Place of the Conference, Country, <i>Title of the Proceeding</i> , Publisher, City, Year, p. or Abstract No. 100 |
| Patents:                | A. B. Inventor1, C. D. Inventor2, (Holder), Country Code and patent number (registration year)  |
| Chemical Abstracts:     | A. B. Surname1, C. D. Surname2, <i>Chem. Abstr.</i> CA 234 567a; For non-readily available literature, the Chemical Abstracts reference should be given in square brackets: [C.A. 139/2003 357348t] after the reference |
| Standards:              | EN ISO 250: <i>Name of the Standard</i> (Year)  |
| Websites:               | Title of the website, URL in full (date accessed)   |

<sup>a</sup> When citing Journals, the International Library Journal abbreviation is required. Please consult, e.g., [https://images.webofknowledge.com/WOK46/help/WOS/A\\_abrvjt.html](https://images.webofknowledge.com/WOK46/help/WOS/A_abrvjt.html)

<sup>b</sup> doi should be replaced by doi number of the Article, for example: <http://dx.doi.org/10.2298/JSC161212085B> (as active link). If doi do not exist, provide the link to the online version of the publication.

#### **Only the last entry in the reference list should end with a full stop.**

The names of all authors should be given in the list of references; the abbreviation *et al.* may only be used in the text. The original journal title is to be retained in the case of publications published in any language other than English (please denote the language in parenthesis after the reference). Titles of publications in non-Latin alphabets should be transliterated. Russian references are to be transliterated using the following transcriptions:

ж→zh, х→kh, ц→ts, ч→ch, ш→sh, щ→shch, ы→y, ю→yu, я→ya, ё→e, ѕ→i, ъ→’.

#### **Supplementary material**

Authors are encouraged to present the information and results non-essential to the understanding of their paper as SUPPLEMENTARY MATERIAL (can be uploaded in Step 4 of Online Submission). This material may include as a rule, but is not limited to, the presentation of analytical and spectral data demonstrating the identity and purity of synthesized compounds, tables containing raw data on which calculations were based, series of figures where one example would remain in the main text, etc. The Editorial Board retain the right to assign such information and results to the Supplementary material when deemed fit. Supplementary material does not appear in printed form but can be downloaded from the web site of the JSCS.

Mathematical and chemical equations should be given in separate lines and must be numbered, Arabic numbers, consecutively in parenthesis at the end of the line. All equations should be embedded in the text. Complex equations (fractions, integrals, matrix...) should be prepared with the aid of the Microsoft Equation 3.0 (or higher) or MathType (Do not use them to create simple equations and labels). Using the Insert -> Equation option, integrated in MS Office 2010 and MS Office 2013, as well as insertion of equation objects within paragraph text IS NOT ALLOWED.

#### **Deposition of crystallographic data**

Prior to submission, the crystallographic data included in a manuscript presenting such data should be deposited at the appropriate database. Crystallographic data associated with organic and metal-organic structures should be deposited at the Cambridge Crystallographic Data Centre (CCDC) by e-mail to [deposit@ccdc.cam.ac.uk](mailto:deposit@ccdc.cam.ac.uk)

Crystallographic data associated with inorganic structures should be deposited with the Fachinformationszentrum Karlsruhe (FIZ) by e-mail to [crysdata@fiz-karlsruhe.de](mailto:crysdata@fiz-karlsruhe.de). A deposition number will then be provided, which should be added to the reference section of the manuscript.

**For detailed instructions please visit the JSCS website:  
<https://www.shd-pub.org.rs/index.php/JSCS/Instructions>**

## **ARTWORK INSTRUCTIONS**

JSCS accepts only **TIFF** or **EPS** formats, as well as **JPEG** format (only for colour and greyscale photographs) for electronic artwork and graphic files. **MS files** (Word, PowerPoint, Excel, Visio) **NOT acceptable**. Generally, scanned instrument data sheets should be avoided. Authors are responsible for the quality of their submitted artwork. Every single Figure or Scheme, as well as any part of the Figure (A, B, C...) should be prepared according to following instructions (every part of the figure, A, B, C..., must be submitted as an independent single graphic file):

### **TIFF**

Virtually all common artwork and graphic creation software is capable of saving files in TIFF format. This 'option' can normally be found under 'the 'Save As...' or 'Export...' commands in the 'File' menu.

TIFF (Tagged Image File Format) is the recommended file format for bitmap, greyscale and colour images.

- Colour images should be in the RGB mode
- When supplying TIFF files, please ensure that the files are supplied at the correct resolution:
  1. Line artwork: minimum of 1000 dpi
  2. RGB image: minimum of 300 dpi
  3. Greyscale image: minimum of 300 dpi
  4. Combination artwork (line/greyscale/RGB): minimum of 500 dpi
- Images should be tightly cropped, without frame and any caption.
- If applicable please re-label artwork with a font supported by JSCS (Arial, Helvetica, Times, Symbol) and ensure it is of an appropriate font size.
- Save an image in TIFF format with LZW compression applied.
- It is recommended to remove Alpha channels before submitting TIFF files.
- It is recommended to flatten layers before submitting TIFF files.

Please be sure that quality of an image cannot be increased by changing the resolution from lower to higher, but only by rescanning or exporting the image with higher resolution, which can be set in usual "settings" facilities.

### **EPS**

Virtually all common artwork creation software, such as Canvas, ChemDraw, CorelDraw, SigmaPlot, Origin Lab..., are capable of saving files in EPS format. This 'option' can normally be found under the 'Save As...' or 'Export...' commands in the 'File' menu.

For vector graphics, EPS (Encapsulated PostScript) files are the preferred format as long as they are provided in accordance with the following conditions:

- when they contain bitmap images, the bitmaps should be of good resolution (see instructions for TIFF files)
- when colour is involved, it should be encoded as RGB
- an 8-bit preview/header at a resolution of 72 dpi should always be included
- embed fonts should always included and only the following fonts should be used in artwork: Arial, Helvetica, Times, Symbol
- the vertical space between the parts of an illustration should be limited to the bare necessity for visual clarity
- no data should be present outside the actual illustration area
- line weights should range from 0.35 pt to 1.5 pt
- when using layers, they should be reduced to one layer before saving the image (Flatten Artwork)

## JPEG

Virtually all common artwork and graphic creation software is capable of saving files in JPEG format. This 'option' can normally be found under the 'Save As...' or 'Export...' commands in the 'File' menu.

JPEG (Joint Photographic Experts Group) is the acceptable file format **only for colour and greyscale photographs**. JPEG can be created with respect to photo quality (low, medium, high; from 1 to 10), ensuring file sizes are kept to a minimum to aid easy file transfer. Images should have a minimum resolution of 300 dpi. Image width: minimum 3.0 cm; maximum 12.0 cm.

**Please be sure that quality of an image cannot be increased by changing the resolution from lower to higher, but only by rescanning or exporting the image with higher resolution, which can be set in usual "settings" facilities.**

## SIZING OF ARTWORK

- JSCS aspires to have a uniform look for all artwork contained in a single article. Hence, it is important to be aware of the style of the journal.
- Figures should be submitted in black and white or, if required, colour (charged). If coloured figures or photographs are required, this must be stated in the cover letter and arrangements made for payment through the office of the Serbian Chemical Society.
- As a general rule, the lettering on an artwork should have a finished, printed size of 11 pt for normal text and no smaller than 7 pt for subscript and superscript characters. Smaller lettering will yield a text that is barely legible. This is a rule-of-thumb rather than a strict rule. There are instances where other factors in the artwork, (for example, tints and shadings) dictate a finished size of perhaps 10 pt. Lines should be of at least 1 pt thickness.
- When deciding on the size of a line art graphic, in addition to the lettering, there are several other factors to address. These all have a bearing on the reproducibility/readability of the final artwork. Tints and shadings have to be printable at the finished size. All relevant detail in the illustration, the graph symbols (squares, triangles, circles, etc.) and a key to the diagram (to explain the explanation of the graph symbols used) must be discernible.
- The sizing of halftones (photographs, micrographs,...) normally causes more problems than line art. It is sometimes difficult to know what an author is trying to emphasize on a photograph, so you can help us by identifying the important parts of the image, perhaps by highlighting the relevant areas on a photocopy. The best advice that can be given to graphics suppliers is not to over-reduce halftones. Attention should also be paid to magnification factors or scale bars on the artwork and they should be compared with the details inside. If a set of artwork contains more than one halftone, again please ensure that there is consistency in size between similar diagrams.

General sizing of illustrations which can be used for the Journal of the Serbian Chemical Society:

- Minimum fig. size: 30 mm width
- Small fig. size - 60 mm width
- Large fig. size - 90 mm width
- Maximum fig. size - 120 mm width

Pixel requirements (width) per print size and resolution for bitmap images:

|                     | Image width | A           | B           | C           |
|---------------------|-------------|-------------|-------------|-------------|
| <b>Minimal size</b> | 30 mm       | <b>354</b>  | <b>591</b>  | <b>1181</b> |
| <b>Small size</b>   | 60 mm       | <b>709</b>  | <b>1181</b> | <b>2362</b> |
| <b>Large size</b>   | 90 mm       | <b>1063</b> | <b>1772</b> | <b>3543</b> |
| <b>Maximal size</b> | 120 mm      | <b>1417</b> | <b>2362</b> | <b>4724</b> |

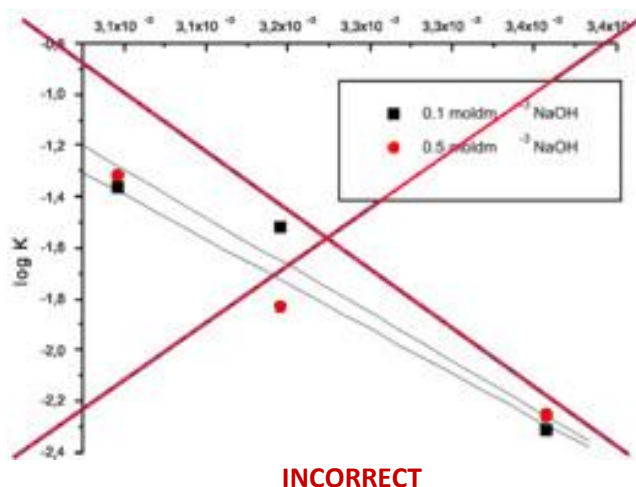
A: 300 dpi > RGB or Greyscale image

B: 500 dpi > Combination artwork (line/greyscale/RGB)

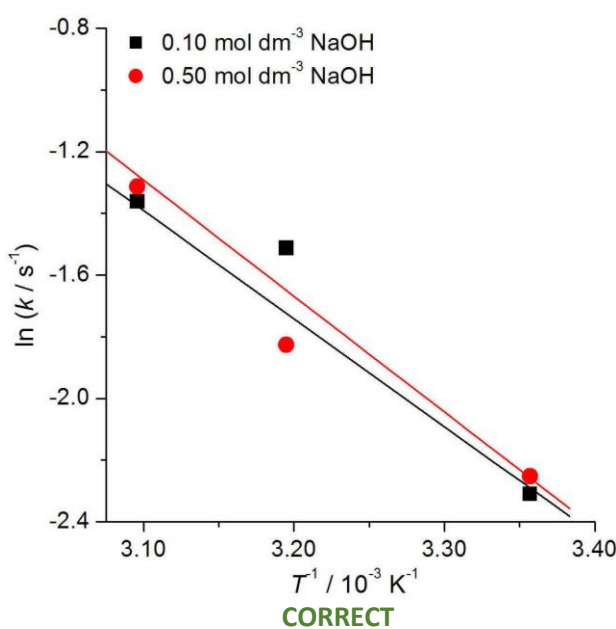
C: 1000 dpi > Line artwork

### The designation of physical quantities and graphs formatting

The designation of physical quantities on figures must be in italic, whereas the units are in upright letters. They should be in Times New Roman font. In graphs a slash should be used to separate the designation of a physical quantity from the unit (example:  $p / \text{kPa}$ ,  $t / \text{^{\circ}C}$ ,  $T_0 / \text{K}$ ,  $\tau / \text{h}$ ,  $\ln(j / \text{mA cm}^{-2})$ ...). Designations such as:  $p (\text{kPa})$ ,  $t [\text{min}]$ ..., are not acceptable. However, if the full name of a physical quantity is unavoidable, it should be given in upright letters and separated from the unit by a comma (example: Pressure, kPa, Temperature, K...). Please do not use the axes of graphs for additional explanations; these should be mentioned in the figure captions and/or the manuscript (example: “pressure at the inlet of the system, kPa” should be avoided). The axis name should follow the direction of the axis (the name of y-axis should be rotated by 90°). Top and right axes should be avoided in diagrams, unless they are absolutely necessary. Decimal numbers must have decimal points and not commas in the axis labels in graphical presentations of results. Thousands are separated, if at all, by a comma and not a point.



INCORRECT



CORRECT

**This is In Memoriam issue decicated to late Professor Petar Pfendt**

**Publication of this issue is financially co-supported by**

**University of Belgrade  
Faculty of Chemistry**



**Innovative Centre,  
Faculty of Chemistry Belgrade, Ltd.**



**University of Belgrade  
Faculty of Technology and Metallurgy**



**Innovative Center of the Faculty of  
Technology and Metallurgy in Belgrade Ltd.**



**Institute of General and Physical Chemistry**





CONTENTS\*

|   |     |
|---|-----|
| Editorial.....  | 1   |
| B. S. Jovančićević, G. D. Gajica, G. D. Veselinović, M. P. Kašanin-Grubin, T. M. Šolević Knudsen, S. R. Šrbac and A. M. Šajnović: The use of biological markers in organic geochemical investigations of the origin and geological history of crude oils (I) and in the assessment of oil pollution of rivers and river sediments of Serbia (II) (Review) ..... | 7   |
| A. Popović, B. Andelković, D. Đorđević, S. Sakan, Lj. Vujišić, S. Veličković and D. Relić: To Professor Petar Pfendt, <i>In calidum, et plurium retributivus memoriae</i> : FTIR-ATR analysis of post stamps of the Principality of Serbia issued in 1866 and 1868 and their forgeries .....  | 27  |
| J. Z. Stevanović, A. R. Rakitin, I. D. Kojić, N. S. Vuković and K. A. Stojanović: Significance of infrared spectroscopic branching factor for investigation of structural characteristics of alkanes, geochemical properties and viscosity of oils.....   | 41  |
| S. D. Savić, G. M. Roglić, V. V. Avdin, D. A. Zherebtsov, D. M. Stanković and D. D. Manojlović: In-house-prepared carbon-based Fe-doped catalysts for electro-Fenton degradation of azo dyes.....   | 57  |
| J. Orlić, M. Aničić Urošević, K. Vergel, I. Zinicovscaia, S. Stojadinović, I. Gržetić and K. Iljević: Comparison of non-destructive techniques and conventionally used spectrometric techniques for determination of elements in plant samples (coniferous leaves) .....  | 69  |
| Z. Nikolovski, J. Isailović, D. Jeremić, S. Kovač and I. Brčeski: Some examples of interactions between certain rare earth elements and soil .....  | 83  |
| A. Žeradjanin, K. Joksimović, J. Avdalović, G. Gojgić-Cvijović, T. Nakano, S. Miletić, M. Ilić and V. P. Beškoski: Bioremediation of river sediment polluted with polychlorinated biphenyls: A laboratory study .....   | 95  |
| D. Savić, M. Balaban, N. Pantelić, D. N. Savić, M. Antić, R. Dekić and V. Antić: Determination of bisphenol A traces in water samples from the Vrbas River and its tributaries, Bosnia and Herzegovina .....  | 109 |
| B. B. Obrovski, I. J. Mihajlović, M. B. Vojinović Miloradov, M. M. Sremački, I. Španik and M. Z. Petrović: Groundwater quality assessment of protected aquatic eco-systems in cross-border areas of Serbia and Croatia .....  | 121 |
| M. Dubovina, N. Grba, D. Krčmar, J. Agbaba, S. Rončević, D. Kerkez and B. Dalmacija: Characterization of landfill deposited sediment from dredging process during different maturation stages .....   | 133 |
| T. D. Andelković, D. S. Bogdanović, I. S. Kostić Kokić, G. M. Kocić and R. M. Pavlović: UV light impact on phthalates migration from children's toys into artificial saliva ...   | 145 |
| M. Vojinović Miloradov, M. Turk Sekulić, L. Ignatović, S. Krajinović, D. Adamović and J. Radonić: Modelling of gas-particle partitioning of PAHs according to ab/adsorption approach.....   | 157 |

Published by the Serbian Chemical Society  
Karnegijeva 4/III, P. O. Box 36, 11120 Belgrade, Serbia  
Printed by the Faculty of Technology and Metallurgy  
Karnegijeva 4, P. O. Box 35-03, 11120 Belgrade, Serbia

\* For colored figures in this issue please see electronic version at the Journal Home Page:  
<http://www.shd.org.rs/JSCS/>





## EDITORIAL

This issue is an In Memoriam issue dedicated to Professor Peter Pfendt, who passed away on January 14, 2021. Professor Pfendt is considered the founder of the scientific discipline of Environmental Chemistry in Serbia.

In the late 1980s, studying the humic substances of recent sediments, he entered the field of environment. In the years that followed, he devoted almost all his research to this field, which is today considered one of the most important in the natural sciences. For decades, he was one of the most active members of the Serbian Chemical Society and founder of the Section for Environmental Chemistry.

It was a great honor for us to organize the collection and evaluation of scientific papers from various fields of environmental chemistry. We would like to express our gratitude to the authors, and to the editors of the *Journal* for their understanding and help. They enabled us to prepare this special issue, which will bring back memories of the Professor in the future. We would also like to take this opportunity to thank Dr. Gorica Veselinović for her selfless help in the technical part of the preparation of this issue.

Belgrade, January 11, 2022

Guest Editors,  
Branimir Jovančićević, PhD, Full Professor  
Vladimir Beškoski, PhD, Associate Professor

## Petar Pfendt (1934–2021)

Petar Pfendt, a longtime professor at the Faculty of Chemistry, outstanding expert in the field of environmental chemistry and founder of the said scientific discipline in Serbia, passed away in January 2021.

Peter Pfendt was born in November 1934 in the village of Jaša Tomić, district of Zrenjanin, to his mother Marija, née Proklet, housewife, and father Anton, glass cutter and trader.

The Second World War saw him in Jaša Tomić where he was together with his parents. He finished elementary school in Hungarian and Romanian in Romania, followed by a year at the Teacher-training College in Timisoara and the Serbian Gymnasium in Vršac, where he graduated in 1955.

In 1955, he enrolled in the Chemistry Department, Faculty of Mathematics and Natural Sciences, Belgrade. During his studies in the period 1957–1960 he was engaged as a laboratory assistant and demonstrator at the Institute of Chemistry's analytical laboratory, while simultaneously being an active member of the Student Union: for three years he was a member of the Student Union Board within the Chemistry Division, member of the Founding Board of the "Sima Lozanić" Professional Club of Chemistry Students, Vice-President of its first Management Board and its longtime Chairman. He served in the army from September 1961 to February 1963 and graduated in March 1964 with an average grade of 9.00.

He was appointed Assistant at the Department of Applied Chemistry in October 1964. In 1971 he finished his graduate studies after completing his Master's thesis entitled "Determination of unsaturation of Aleksinac oil shale kerogen by modified methods for iodine number". He received his PhD degree in 1975 after defending his thesis entitled "A study of the Chemical Nature of Kerogens by Bromination".

In 1975, he was appointed Assistant Professor for the course Chemical Technology at the Department of Applied Chemistry. He was re-appointed twice,



in 1983 and 1991, for the courses Industrial Chemistry and Environmental Chemistry. In 1992 he was appointed Associate Professor, followed by tenureship as Full Professor in 1997.

While initially in the capacity of an assistant and then as a full professor as well, he improved teaching of the courses on which he was engaged in terms of both holding exercises and lectures. He drafted new curriculums for courses taught in undergraduate and graduate studies and introduced several courses in the field of biochemistry and applied chemistry.

During his first years as an assistant (1964–65) he expanded exercises held in Chemical Technology by introducing a number of latest, state-of-the-art and problem-solving exercises for students while devising tailor-made instructions for exercises.

On the occasion of Students' Day (April, 4), he was recognized as one of the best assistants at the University of Belgrade and awarded a diploma and a badge by the University Board of the Student Union (1972/73).

In addition to teaching undergraduate studies (Industrial Chemistry and Environmental Chemistry), as of 1979 he taught the elective courses Environmental Chemistry and Chemistry of Water Technology, as well as a part of the course Selected Processes of Chemical Industry. He devised pertinent curriculums and unauthorized course readers for these courses.

He taught the courses Basics of Chemical Technology and Chemical Technology in the period 1980–1987, followed by Industrial Chemistry with Environmental Chemistry as of 1989.

In addition to working at the Faculty of Chemistry in Belgrade, he taught in Priština, Kragujevac, Niš, Center for Multidisciplinary studies in Belgrade, Faculty of Physical Sciences and Faculty of Geography in Belgrade.

In the late 1970s and early 1980s, he instituted the courses Environmental Chemistry (1978) and Chemistry of Water and Wastewater (1982) at the Faculty, while initiating research in the said fields. At his initiative, the Environmental Chemistry division was established in post-graduate studies in 1987, whereas Environmental Chemistry was introduced as a course for all fourth year students at the Faculty (1990). In 1993, he initiated establishment of the Environmental Chemistry Section with the Department of Applied Chemistry in the fourth year of undergraduate studies, which included the following courses: Pollutant Hemodynamics, Chemistry of Water and Wastewater, Instrumental Analysis 2 and Environmental Chemistry 2.

He is the author of the textbook entitled "Environmental Chemistry" (2009) and co-author of "The Practicum and Workbook for Industrial Chemistry" (2021). He wrote course readers for Environmental Chemistry, Water Chemistry and Technology, and Selected Processes of Chemical Industry. He is the author of instructions for student exercises for multiple courses and co-author of three secondary school textbooks in Applied Chemistry.

He was engaged in scientific research in the field of Organic Geochemistry and Environmental Chemistry. With regards to Organic Geochemistry he undertook research on structures of organic substances of old sediments, primarily of bituminous shale kerogens. His Master's and Doctoral theses both pertain to this scientific field. In addition to chemistry of kerogens, he studied humic acids and local peats. Regarding organic and geochemistry studies, he was dedicated to researching reactivity of inorganic constituents of organic substances, primarily pyrites. Prof. Petar Pfendt published more than 40 scientific papers. He mentored more than 65 diploma theses, eight specialist theses, 14 Master's theses and four doctoral theses.

In the position of Deputy Chairman or Chairman of the Organizing Committee, he organized three large symposiums (amongst which one was international) dedicated to environmental chemistry.

He was a peer reviewer of papers published in *Organic Geochemistry* and *The Journal of the Serbian Chemical Society*. He was a contributor to the Encyclopedia and worked on entries until the end of his life.

As of 1973, he participated in organizing Federal and International competitions for chemistry students. On several occasions he led the summer school for young researchers in the Petnica Research Center.

He went on several study visits abroad. In 1966 he attended the "Borderline Fields of Chemistry" summer school at BASF (Ludwigshafen, FR Germany). He went on two short visits to the Department of Development of Wastewater Treatment Procedures in 1982 and 1983 at Linde Ag in Munich (1978 and 1979). Later on, in 1991, he proceeded with professional training at KF Jülich (Institute of Applied Physical Chemistry – Laboratory for Studying Pollutant Hemodynamics), Henkel AG (Institute of Ecotoxicology – Biochemodynamics of Surfactants) in Dusseldorf and at BASF's Laboratory for Studying Wastewater Treatment Procedures, Ludwigshafen.

He held several positions at the Faculty, amongst which some were highest-ranking managerial functions: Deputy Head of the Institute of Chemistry (1976–1978), Head of the Institute of Chemistry (1978–1980), Head of the Department of Applied Chemistry (1988–1997), Dean of the Faculty of Chemistry (1998–2001).

He headed the Faculty in extremely difficult and sensitive times (1998–2001). When the University was deprived of its autonomy, and freedom was taken away from professors, he acted wisely and bravely while protecting the professors and the entire staff from inadequate laws and the authorities disinclined towards the Faculty and its tradition. Despite the new rules of conduct and the hitherto unheard of authorizations bequest to Faculty Deans, Pfendt respected the tradition of academic conduct in all his acts while making decisions in agreement with Heads of Departments and while respecting the will of the Teaching-Scientific Council.

After meeting the requirements for retirement in 1999, his employment was extended until 2003. Even after he had retired, Petar Pfendt came to the Faculty every day to pursue his scientific research until late 2020.

He was fluent in German and English and had a working knowledge of French, Russian, Hungarian and Romanian.

He was married to Lidija Pfendt, née Sumilin, Full Professor at the Faculty of Chemistry, with whom he has two sons, Eduard and Robert.

Petar Pfendt, who dedicated his entire working life to teaching and science, or that is to say to the Faculty of Chemistry and his Department, will be remembered by the professors of the Faculty of Chemistry and many a generation of students as an outstanding scholar, teacher and expert, while at the same time being a quiet and modest, unobtrusive, correct and tolerant person, ready to help and listen. On the other hand, he was creative and active in his endeavors to contribute to modernization and expansion of his Department and the entire Faculty while instituting new courses and initiating establishment of new scientific disciplines.

Snežana Bojović, PhD, Full Professor





*J. Serb. Chem. Soc.* 87 (1) 7–25 (2022)  
JSCS-5501

# Journal of the Serbian Chemical Society

JSCS@tmf.bg.ac.rs • www.shd.org.rs/JSCS

Review  
Published 1 October 2021

## REVIEW

### The use of biological markers in organic geochemical investigations of the origin and geological history of crude oils (I) and in the assessment of oil pollution of rivers and river sediments of Serbia (II)

BRANIMIR S. JOVANIĆ<sup>1#</sup>, GORDANA Đ. GAJICA<sup>2\*</sup>, GORICA D. VESELINović<sup>2</sup>, MILICA P. KAŠANIN-GRUBIN<sup>2</sup>, TATJANA M. ŠOLEVIĆ KNUDSEN<sup>2</sup>, SNEŽANA R. ŠTRBAC<sup>2</sup> and ALEKSANDRA M. ŠAJNOVić<sup>2</sup>

<sup>1</sup>University of Belgrade, Faculty of Chemistry, Studentski trg 12–16 11001 Belgrade, Serbia  
and <sup>2</sup>University of Belgrade, Institute of Chemistry, Technology, and Metallurgy, Department of Chemistry, Njegoševa 12, 11000 Belgrade, Serbia

(Received 1 July, revised 30 August, accepted 31 August 2021)

**Abstract:** Biological markers (BMs) are organic compounds in oils in which a precursor is known, and during the transformation of organic matter these compounds undergo certain structural and stereochemical changes. Based on the established precursors of BMs, the origin of the examined oils can be estimated, and based on the intensity and the type of changes and also geological history. It includes defining the deposition medium, the degree of maturation, the length of the oil migration path, the degree of biodegradation. The most studied and applied BMs are normal alkanes, isoprenoid aliphatic alkanes pristane and phytane, and polycyclic alkanes of the sterane and terpane type. On the other hand, in the environmental chemistry, these compounds can significantly contribute to the identification of petroleum pollutants, as well as to the assessment of the migration mechanism and the intensity of biodegradation. This review paper first presents the results related to the application of BMs in the organic geochemical correlations of oil in the south-eastern part of the Pannonian Basin (I). The second part provides an overview of those researches in which the same BMs were used in the identification of oil pollutants and in monitoring their changes during the migration and the biodegradation in rivers and river sediments of Serbia (II).

**Keywords:** organic matter; biomarkers; geochemical correlation; petroleum pollutants; biodegradation.

\*Corresponding author. E-mail: gordana.gajica@ihtm.bg.ac.rs

# Serbian Chemical Society member.

<https://doi.org/10.2298/JSC210701072J>

## CONTENTS

1. INTRODUCTION
2. BIOLOGICAL MARKERS IN ORGANIC GEOCHEMICAL CORRELATIONS OF OIL IN THE SOUTHEASTERN PART OF THE PANNONIAN BASIN ON THE TERRITORY OF SERBIA
3. THE USE OF BIOLOGICAL MARKERS IN OIL-TYPE POLLUTANTS IDENTIFICATION AND MONITORING OF THEIR FATE IN RIVERS AND RIVER SEDIMENTS OF SERBIA
  - 3.1. Identification
  - 3.2. Migration
  - 3.3. Biodegradation
4. CONCLUSIONS

## INTRODUCTION

The crude oil is a product of geochemical transformations of biogenic organic matter in the sedimentary rocks of the lithosphere. Geochemical processes have been taking place over the past 600 million years, since the Cambrian period until the present days. During these processes, the organic matter passes through four consecutive alteration stages, that are in organic geochemistry called diagenesis, catagenesis, metagenesis and metamorphism.<sup>1–7</sup>

After they accumulate in sedimentary rocks, the organic compounds from the biosphere undergo both structural and configurational changes in order to create thermodynamically more stable forms. During the early diagenesis, these changes are primarily governed by microorganisms. During the late diagenesis, catagenesis, and in the final stages methogenesis and metamorphism, heat, the pressure and the aluminosilicate minerals acting as catalysts, have a dominant role in the transformations of organic compounds. The most important factors in these changes are temperature and geologic time, which is measured in millions of years.<sup>1–6</sup>

In addition to graphite and gas, the final product of these changes in the sedimentary organic matter is crude oil. As a result of the aforementioned processes, crude oil consists mainly of thermodynamically stable compounds that usually differ significantly from their biological precursors.<sup>1–7</sup>

The first compounds of biogenic origin identified in crude oil were porphyrins.<sup>8</sup> That was in 1931. This discovery still has a great and historical significance. The identification of porphyrins in crude oil marked the beginning of an era of biogenesis or biogenetic origin of petroleum. During the seventies and the eighties of the twentieth century, a large number of compounds were discovered in crude oils and their biological precursors were precisely determined.<sup>9–13</sup>

In organic geochemistry, these compounds are called molecular fossils, biological markers, or biomarkers.<sup>1–13</sup> So far, a large number of biomarkers in crude

oils have been identified. Even nowdays, identification of a new biomarker in oil, or its geochemically related form, represents a research challenge. The most studied biomarkers are *n*-alkanes, isoprenoid aliphatic alkanes (first of all C19, pristane and C20, phytane) and polycyclic alkanes of the terpane type (tricyclic and tetracyclic diterpanes and pentacyclic triterpanes) and the sterane type (including diasteranes and mono- and triaromatic steroids).<sup>1–7</sup> Today, it is possible to reliably determine the origin, *i.e.*, the precursor organic matter type of an individual oil. On the other hand, interpretation of the transformation pathways of these compounds from the unstable biolipid isomers to thermodynamically stable geolipid structural and configurational forms, allows us to examine the geologic history of a crude oil which includes the estimation of the characteristics of the depositional environment, degree of thermal maturity, length of the migration pathway from a source to the reservoir rock, are the extent of microbiological degradation, *etc.*<sup>1–17</sup>

The largest number of biological markers in oil is found in very low quantities. Practically only *n*-alkanes and the isoprenoids pristane and phytane can be successfully identified “only” by gas chromatographic (GC) analysis of the iphatic fraction of oil. For the identification of all other biomarker compounds, the application of more complex and sophisticated techniques is required. These analytical techniques include primarily mass spectrometry (MS). Because of that, it can be said that the development of organic-chemical investigations of biological markers was developing parallel with the development of instrumental techniques in organic chemistry, primarily gas chromatography - mass spectrometric (GC-MS) and gas chromatography-mass spectrometry-mass spectrometric (GC-MS-MS) systems.<sup>18</sup>

The use of oil started its rapid growth at the beginning of the twentieth century with the invention of the internal combustion engine. Organic geochemistry gave crucial importance to the prospective oil exploration, especially in the second half of the twentieth century.<sup>1–6</sup> With geological and geophysical surveys, organic geochemical methods have become irreplaceable in finding new oil deposits. Among them, the methods involving biological markers are considered the most important.

These same compounds have a completely different role in the environmental chemistry. When oil, or some of its derivatives, comes in the contact with the environment, its role completely changes its character, because from a very important fossil fuel, without which it is almost impossible to imagine life nowdays, it transforms into a very dangerous organic pollutant. This can be understood because oil is a complex mixture of iphatic, aromatic, and many other nitrogen, sulfur, and oxygen organic compounds. Many of them are toxic, carcinogenic, mutagenic, and even teratogenic. The biological markers in ecochem-

ical tests are invaluable for the identification of oil pollutants and for assessing their aim in the environment.<sup>19</sup>

The analysis of biological markers, *n*-alkanes, isoprenoid aliphatic alkanes, terpanes, and steranes, in oil as a form of the organic substance of the geosphere, *i.e.*, as a fossil fuel, and in oil as a pollutant in the environment is performed in an almost identical way.<sup>18</sup> However, the interpretation of the obtained results in organic geochemistry and in environmental chemistry goes in completely different directions. This review paper will first present the results, *i.e.*, the research related to the application of biological markers in the organic geochemical correlations of oil in the southeastern part of the Pannonian Basin in the territory of Serbia (I). The second part will provide an overview of those researches in which the same biological markers were used in the identification of oil pollutants and in monitoring their changes during migration and biodegradation in rivers and river sediments of Serbia (II).

## 2. BIOLOGICAL MARKERS IN ORGANIC GEOCHEMICAL CORRELATIONS OF OIL IN THE SOUTHEASTERN PART OF THE PANNONIAN BASIN ON THE TERRITORY OF SERBIA

The first geochemical explorations of oil in the southeastern part of the Pannonian Basin are dated from the early 1970s.<sup>20</sup> Based on the results of analyses of trace elements and physicochemical properties, they are classified into three genetic types. According to their origin, the oil fields of the Kikinda and Kikinda Varoš form the first group. The Mokrin and Palić oil fields are classified in the second, and the Velebit oil field in the third genetic group.

In most oils that have not been exposed to the effect of biodegradation, *n*-alkanes and isoprenoid aliphatic alkanes, pristane and phytane are the dominant hydrocarbons in alkane fractions. Therefore, they are relatively easily identified by GC analysis of the alkanes previously isolated from the oil maltene fraction by the column chromatography using petroleum ether as eluent. For this reason, these biological markers were first applied in organic geochemical studies in the southeastern part of the Pannonian Basin (Serbia). The results for the crude oils of the Banat, South Bačka, and Kostolac Depressions were announced at the II Yugoslav Symposium on Hydrocarbons, within the Conference of the Serbian Chemical Society in 1986.<sup>21</sup>

A detailed correlation study of these oils later included polycyclic alkanes of the steranes and terpanes type for the first time. They were identified from carbamide (urea) non-adducts of iphatic fractions by GC–MS technique, with application of single ion monitoring (SIM) method, and using ions *m/z* 217 (for steranes) and *m/z* 191 (for terpanes). The results were announced at the organic geochemical conference in Venice in 1987,<sup>22</sup> and published in the journal Organic Geochemistry, at that time the most important journal in this scientific field.<sup>23</sup>

Based on the distributions of *n*-alkanes, isoprenoids pristane, and phytane,  $14\alpha(\text{H})17\alpha(\text{H})20(\text{R}) \text{C}_{27}\text{--C}_{29}$  steranes, tricyclic  $\text{C}_{19}\text{--C}_{26}$  diterpanes, pentacyclic triterpanes of the hopane type, gammacerane and oleanane, 19 oil samples from the above mentioned Pannonian depressions basins (labeled A–D and E in the publication) were classified into only two genetic types. Based on the steranes and terpanes migration parameters, it was concluded that they originate from different source rocks. Based on the maturation parameters  $22(\text{S})/22(\text{R}) \text{C}_{32}$  hopanes and  $14\alpha(\text{H})17\alpha(\text{H})20(\text{S})/14\alpha(\text{H})17\alpha(\text{H})20(\text{R}) \text{C}_{29}$  steranes, it was concluded that all tested oils were of relatively uniform degree of maturity. The abundances of *n*-alkanes and isoprenoids pristane and phytane, in alkane fractions, showed that only three of the total 19 tested oils were moderately biodegraded.<sup>22,23</sup> As an example, Fig. 1 shows the gas chromatograms of alkane fractions, typical for the non-biodegraded and moderately biodegraded oils of the southeastern part of the Pannonian Basin, and the fingerprints of steranes (*m/z* 217) and terpanes (*m/z* 191) obtained by GC–MS analysis of branched and cyclic alkanes, and using the SIM method. Peak identifications are given in Tables I and II.

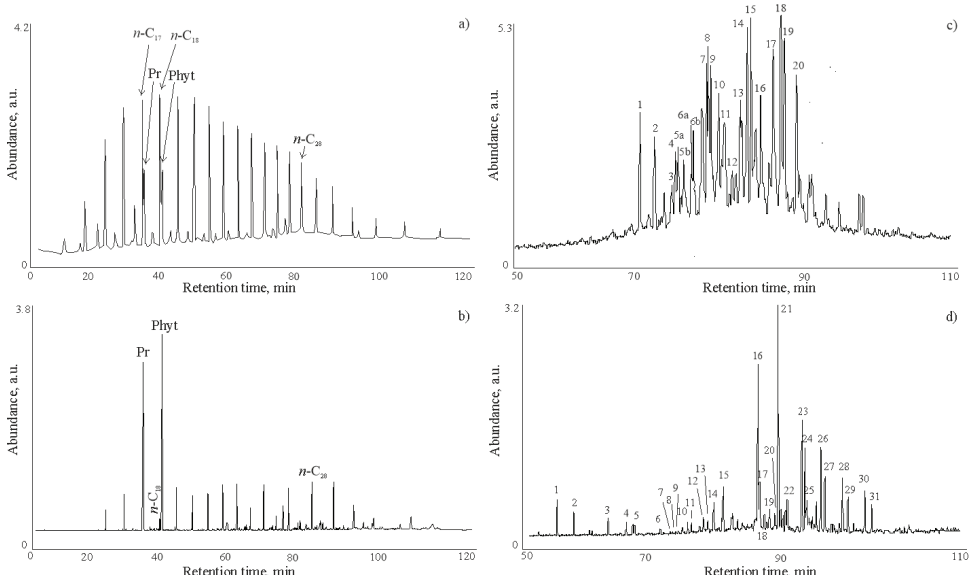


Fig. 1. Gas chromatograms of: a) iphatic fractions, typical for non-biodegraded and b) moderately biodegraded oils of the southeastern part of the Pannonian Basin and c) fingerprints of steranes (*m/z* 217) and d) terpanes (*m/z* 191) obtained from GC–MS analysis of branched and cyclic alkanes.<sup>23–27</sup>

The special attention in organic geochemical research was attracted by the naphthalene-type oils from the oil field of the North Bačka Depression. Thirteen samples of the Velebit field marked “W” were analyzed in detail. All group and

specific correlation parameters, that were applied in similar studies worldwide in the late eighties of the twentieth century, were applied in these studies.<sup>24,25</sup>

TABLE I. Identification of the compounds in the Fig. 1c

| Peak | Compound  |
|------|---|
| 1    | $C_{27} 13\beta(H)17\alpha(H)20(S)$ -diasterane   |
| 2    | $C_{27} 13\beta(H)17\alpha(H)20(R)$ -diasterane   |
| 3    | $C_{27} 13\alpha(H)17\beta(H)20(S)$ -diasterane   |
| 4    | $C_{27} 13\alpha(H)17\beta(H)20(R)$ -diasterane   |
| 5a   | $C_{28} 13\beta(H)17\alpha(H)20(S)24(S)$ -diasterane  |
| 5b   | $C_{28} 13\beta(H)17\alpha(H)20(S)24(R)$ -diasterane  |
| 6a   | $C_{28} 13\beta(H)17\alpha(H)20(R)24(S)$ -diasterane  |
| 6b   | $C_{28} 13\beta(H)17\alpha(H)20(R)24(R)$ -diasterane  |
| 7    | $C_{28} 13\alpha(H)17\beta(H)20(S)$ -diasterane + $C_{27} 14\alpha(H)17\alpha(H)20(S)$ -sterane |
| 8    | $C_{29} 13\beta(H)17\alpha(H)20(S)$ -diasterane + $C_{27} 14\beta(H)17\beta(H)20(R)$ -sterane   |
| 9    | $C_{28} 13\alpha(H)17\beta(H)20(R)$ -diasterane + $C_{27} 14\beta(H)17\beta(H)20(S)$ -sterane   |
| 10   | $C_{27} 14\alpha(H)17\alpha(H)20(R)$ -sterane   |
| 11   | $C_{29} 13\beta(H)17\alpha(H)20(R)$ -diasterane   |
| 12   | $C_{29} 13\alpha(H)17\beta(H)20(S)$ -diasterane   |
| 13   | $C_{28} 14\alpha(H)17\alpha(H)20(S)$ -sterane   |
| 14   | $C_{29} 13\alpha(H)17\beta(H)20(R)$ -diasterane + $C_{28} 14\beta(H)17\beta(H)20(R)$ -sterane   |
| 15   | $C_{28} 14\beta(H)17\beta(H)20(S)$ -sterane   |
| 16   | $C_{28} 14\alpha(H)17\alpha(H)20(R)$ -sterane   |
| 17   | $C_{29} 14\alpha(H)17\alpha(H)20(S)$ -sterane   |
| 18   | $C_{29} 14\beta(H)17\beta(H)20(R)$ -sterane   |
| 19   | $C_{29} 14\beta(H)17\beta(H)20(S)$ -sterane   |
| 20   | $C_{29} 14\alpha(H)17\alpha(H)20(R)$ -sterane   |

Based on the absence of *n*-alkanes in all tested oils, it was confirmed that the oils were exposed to microbiological degradation in reservoir rocks (reservoir temperatures: 62–70 °C). In the aliphatic fractions of the three samples, neither pristane nor phytane were identified, due to a slightly higher degree of biodegradation. Specific steranes and terpanes source parameters showed that the tested field W oils were of mixed terrestrial-marine origin. Based on the parameters  $C_{30}$  moretane/hopane and  $C_{29} 14\alpha(H)17\alpha(H)20(S)/14\alpha(H)17\alpha(H)20(S) + 20(R)$  steranes, and also based on the presence of oleanane it was estimated that the oils originated from the source rocks of Pre-Tertiary age (Upper Creataceous).

Many years later, the Velebit oil and gas field was examined in even more detail.<sup>26</sup> Twenty-five geologically very well-characterized samples were analyzed. Modern instrumental techniques have enabled very good identification of biological markers from the total aliphatic fractions. In other words, there was no need to separate the aliphatic fraction with urea into the *n*-alkane fraction (adduct) and the fraction of branched and cyclic alkanes (non-adduct). In this paper, due to the GC–MS–MS analysis of total aliphatic fractions, a number of very reliable specific correlation parameters were determined. The estimates of

previous research with a more precise definition of geological history have been confirmed. For example, it was determined that the maturity of the source rocks of the Velebit crude oil was at the level of vitrinite reflection  $Ro > 0.80\%$ .

TABLE II. Identification of the compounds in the Fig. 1d

| Peak | Compound   |
|------|--|
| 1    | C <sub>19</sub> -tricyclic terpane                         |
| 2    | C <sub>20</sub> -tricyclic terpane                         |
| 3    | C <sub>21</sub> -tricyclic terpane                         |
| 4    | C <sub>23</sub> -tricyclic terpane                         |
| 5    | C <sub>24</sub> -tricyclic terpane                         |
| 6    | C <sub>25</sub> -tricyclic terpane                         |
| 7    | C <sub>24</sub> -tetracyclic terpane                       |
| 8    | C <sub>26</sub> 22(S)- tricyclic terpane                   |
| 9    | C <sub>26</sub> 22(R)- tricyclic terpane                   |
| 10   | C <sub>28</sub> 22(S)- tricyclic terpane                   |
| 11   | C <sub>28</sub> 22(R)- tricyclic terpane                   |
| 12   | C <sub>29</sub> 22(S)- tricyclic terpane                   |
| 13   | C <sub>29</sub> 22(R)- tricyclic terpane                   |
| 14   | C <sub>27</sub> 18 $\alpha$ (H),22,29,30-trisnorhopane, Ts |
| 15   | C <sub>27</sub> 17 $\alpha$ (H),22,29,30-trisnorhopane, Tm |
| 16   | C <sub>29</sub> 17 $\alpha$ (H)21 $\beta$ (H)-hopane       |
| 17   | C <sub>29</sub> 18 $\alpha$ (H),30-norhopane               |
| 18   | C <sub>30</sub> 17 $\alpha$ (H)-diahopane                  |
| 19   | C <sub>29</sub> 17 $\beta$ (H)21 $\alpha$ (H)-moretane     |
| 20   | Oleanane   |
| 21   | C <sub>30</sub> 17 $\alpha$ (H)21 $\beta$ (H)-hopane       |
| 22   | C <sub>30</sub> 7 $\beta$ (H)21 $\alpha$ (H)-moretane      |
| 23   | C <sub>31</sub> 17 $\alpha$ (H)21 $\beta$ (H)22(S)-hopane  |
| 24   | C <sub>31</sub> 17 $\alpha$ (H)21 $\beta$ (H)22(R)-hopane  |
| 25   | Gammacerane  |
| 26   | C <sub>32</sub> 17 $\alpha$ (H)21 $\beta$ (H)22(S)-hopane  |
| 27   | C <sub>32</sub> 17 $\alpha$ (H)21 $\beta$ (H)22(R)-hopane  |
| 28   | C <sub>33</sub> 17 $\alpha$ (H)21 $\beta$ (H)22(S)-hopane  |
| 29   | C <sub>33</sub> 17 $\alpha$ (H)21 $\beta$ (H)22(R)-hopane  |
| 30   | C <sub>34</sub> 17 $\alpha$ (H)21 $\beta$ (H)22(S)-hopane  |
| 31   | C <sub>34</sub> 17 $\alpha$ (H)21 $\beta$ (H)22(R)-hopane  |

In the most GC-MS or GC-MS-MS correlation studies, the analyses of aliphatic fractions of crude oils are used to determine numerous values of individual source, maturation, or migration parameters. However, in some cases it is possible to make a very reliable correlation of crude oils only on the basis of “fingerprints” of steranes ( $m/z$  217) and terpanes ( $m/z$  191) obtained using the SIM method (Fig. 1a and b). This is shown in the example of six crude oils from the Kikinda, Mokrin and Požarevac fields.<sup>27</sup> The derived conclusions were in agree-

ment with those drawn earlier on the basis of numerous values of the calculated specific correlation parameters.<sup>22</sup>

The period of the end of the eighties and the first half of the nineties of the last century was marked by the numerous organic geochemical correlations of crude oils from the southeastern part of the Pannonian Basin. The research from the mentioned period was summarized in a review paper from 1998.<sup>28</sup> This correlation study included 80 samples of crude oils from the Banat Depression (18 crude oil fields) and 8 samples from the Drmno Depression (4 fields; Fig. S-1 of the Supplementary material to this paper). The crude oils were correlated based on the number of group and specific correlation parameters (Table III).

TABLE III. Organic geochemical correlation parameters applied in crude oils study of the southeastern part of the Pannonian Basin on the territory of Serbia<sup>28</sup>

| Bulk correlation parameter                 | Specific correlation parameters   |
|--|---|
| <i>API</i> -density                        | <i>CPI</i> ; most abundant <i>n</i> -alkane   |
| Sulphur                                    | Pr/Phyt   |
| Asphaltenes                                | Pr/ <i>n</i> -C <sub>17</sub> , Phyt/ <i>n</i> -C <sub>18</sub>   |
| Bulk composition (alkanes, aromatics, NSO) | Regular sterane distribution<br>Oleanane/gammacerane index<br>Geolipid/biolipid sterane isomers<br>Biolipid/geolipid hopane isomers |

Most of the crude oils in this basin have not been exposed to biodegradation in reservoir rocks. The samples from the fields Janošik, Jermenovci, Lokve and Velika Greda-jug have a minimal degree of biodegradation, Kikinda Gornje and ten samples from the Velebit field have a medium degree, and three samples from the Velebit field and one from both Kelebijja and Gaj fields are in the category of more intensive biodegradation. The source parameters confirmed the conclusions of previous studies on the existence of two genetic types of crude oil. In this review paper, the crude oil from the Subotica field is singled out as the third type, which has not been investigated in previous research. According to the maturation parameters, crude oils were classified in the category of low-maturity crude oils formed in the phase of early catagenesis.

During the eighties of the last century, the reservoir rocks of crude oils were also found in the localities of the Stiška valley near the town of Požarevac (Drmno depression; crude oil fields: Sirakovo, Bradarac, Maljurevac, Bubušinac). These samples were also included in the first correlation studies of the Pannonian Basin crude oils on the territory of Serbia (Drmno Depression, E1–E4).<sup>22</sup> The paper presenting these results was published at 2001.<sup>29</sup>

The crude oils of the Drmno Depression are characterized by the dominance of *n*-alkanes with an odd number of C-atoms (carbon preference index, *CPI*, is slightly above unity). The pristane is more abundant than phytane, and in the dis-

tribution of regular steranes C<sub>27</sub>–C<sub>29</sub>, 14 $\alpha$ (H)17 $\alpha$ (H)20(R), the C<sub>29</sub> isomer dominates. These three parameters unequivocally show that an organic matter of terrestrial origin also participated in the formation of these crude oils in a larger share than in the case of crude oils from reservoir rocks from Vojvodina. The maturation parameters of steranes and terpanes showed that crude oils are of a slightly lower degree of maturity, formed in the early stages of the catagenetic sequence of crude oil formation ( $Ro$  in range 0.70–0.80 %). The source rocks of Stig crude oil are of Tertiary age.<sup>29</sup> The special examination of sediments from boreholes from the Sirakovo, Bubušinac and Bradarac locations (organic carbon content, bitumen and hydrocarbon content, distribution of biological markers) also defined their source rocks.<sup>30</sup>

The crude oil samples from the fields in Serbia were often used for fundamental research. For example, in the early 1980's, there was a controversy in the organic-geochemical research community, when it came to the use of the ratios of relative concentrations of pristane and phytane in iphatic oil fractions (Pr/Phyt) as a maturation parameter. According to some authors, the value of this ratio decreases with increasing maturity.<sup>31</sup> To shed light on this question, Pr/Phyt ratios were determined in 63 crude oil samples of the Banat and Drmno depressions of the Pannonian Basin, and the obtained values were correlated with the values of more reliable terpane maturity parameters, as well as with *API* densities and ratios Pr/n-C<sub>17</sub> and Phyt/n-C<sub>18</sub>.<sup>32</sup> The correlation analysis has unequivocally shown that the value of the parameter Pr/Phyt increases with the maturity. Also, in order to assess the impact of microbiological degradation in the reservoir rocks on sterane and terpane changes, the best known maturity parameters of sterane and terpane of 36 crude oil samples from the southeastern part of the Pannonian Basin, together with 8 samples of oil fields from the eastern Russia were correlated. The results showed that steranes were more resistant to biodegradation than terpanes.<sup>33</sup>

Finally, the significance of maturation parameters determined from the distribution and abundance of saturated biomarkers and alkylaromatics in crude oil correlation studies was evaluated using a new approach in factor and cluster analysis. For this fundamental research, 23 crude oils from the part of the Pannonian Basin that belongs to Serbia were used.<sup>34</sup>

The experiences gained by studying biological markers in crude oils belonging to the southeastern part of the Pannonian Basin on the territory of Serbia have been applied in similar studies regarding the crude oils of the most important oil fields in the world. For example, a detailed correlation study of crude oils from 9 oil fields of Sakhalin Island (Russia) enabled the definition of phenanthrene content in the aromatic fraction as a very reliable maturation parameter.<sup>35</sup> On the other hand, the approaches used to define the origin and geological history of crude oils from the basins from the territory of Serbia, have also been success-

fully applied to the organic geochemical correlation of crude oils in Libya's most important oil fields.<sup>36–38</sup>

### 3. THE USE OF BIOLOGICAL MARKERS IN OIL-TYPE POLLUTANTS IDENTIFICATION AND MONITORING OF THEIR FATE IN RIVERS AND RIVER SEDIMENTS OF SERBIA

#### 3.1. Identification

In recent sediment deposits, surface and groundwaters, and soils, the presence of oil-type pollutants cannot be determined only based on the amount of organic extract (bitumen). Namely, from the theoretical, organic geochemical aspect, the amount of native bitumen in the surface parts of the lithosphere can be in the range from zero to one hundred percent.<sup>1–7</sup> There are numerous examples of the surface sediments without any of organic substances. On the other hand, there is the phenomenon of “seeping crude oil” (natural oil lakes), which can be defined as sedimentary formations with 100 % native organic matter. Therefore, to determine the presence of oil-type pollutants in these segments of the environment, it is necessary to geochemically characterize the organic substance (organic extract) isolated from a sample.

This approach is based on the fact that crude oil is a highly mature organic matter. On the other hand, the organic substance of recent sediments is of a rather low degree of thermal maturity. As a consequence, the distributions of biomarkers differ as well. Crude oil contains an incomparably higher concentration of thermodynamically most stable structural and stereochemical biomarker isomers. For the first time this was shown on the example of *n*-alkane distributions in a total of 17 samples of alluvial sediments taken from the localities of Zrenjanin (Begej River, 13 samples), Pančevo (Danube River, 3 samples), and Kraljevo (Ibar River, 1 sample).<sup>39</sup> Based on the *n*-alkane distribution, the oil-type pollutant was found only in a sample belonging to the Ibar River. In some samples there was a mixture of native and anthropogenic oil substances, and in some the oil-type pollutant was not even identified. Conclusions were made based on the organic geochemical knowledge that in crude oils, as a consequence of a high degree of maturation, there is a uniform distribution of odd and even homologues (*CPI* is around 1). Fig. 2 shows examples with the distribution of *n*-alkanes belonging to a native organic matter, then an organic matter that is a mixture of native and anthropogenic, and *n*-alkanes from an oil-type organic pollutant.

Due to the high degree of maturation, oil has the highest concentration of the heavier, <sup>13</sup>C isotope, compared to the other forms of organic matter in the geosphere. The isotopic analysis was performed from the samples of Begej, Danube, and Ibar River sediments. Gas chromatography–mass spectrometry–isotope ratio (GC–MS–IR) technique determined the values for  $\delta^{13}\text{CPDB}$  for individual *n*-alkanes C<sub>25</sub>, C<sub>27</sub>, C<sub>29</sub> and C<sub>31</sub>. The highest concentrations of the heavier, <sup>13</sup>C, iso-

tope (least negative values for  $\delta^{13}\text{CPDB}$ ) in the sample belonging to the Ibar River, provided the additional confirmation of the presence of oil pollutants in this sample.<sup>39</sup>

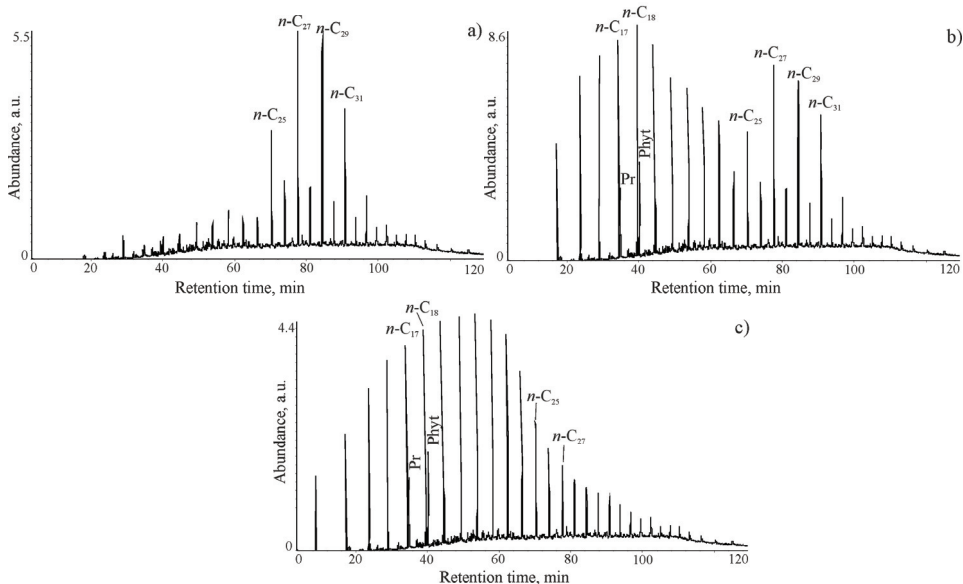


Fig. 2. Examples of the distribution of *n*-alkanes fitting to: a) the native organic matter, b) an organic matter that is a mixture of native and anthropogenic, and c) *n*-alkanes from the organic matter which represents the oil pollutant.<sup>39</sup>

*n*-Alkanes in the organic extracts of river sediments can also be a tool for determining the presence of the non-petroleum type organic pollutants. For example, 6 samples of sediments of the Lim River in Bjelo Polje (Montenegro) were investigated.<sup>40</sup> One sample was taken above the place of sewage waste discharge into the river, and five samples downstream from it. The dominance of odd homologues in the first sample was the proof that this sample contained a native organic substance. In all other samples, a pronounced dominance of even *n*-alkane homologues was identified (*CPI* in range 0.01–0.45). This was an unequivocal proof that these samples contained sewage, where microorganisms developed and produced even *n*-alkane homologues as their metabolites.

The polycyclic alkanes of sterane and triterpene type may serve as the most useful tools for the identifying of oil-type pollution in recent sediments (*m/z* 217 and *m/z* 191, Fig. 1c and d). In addition to regular, biolipid isomers C<sub>27</sub>–C<sub>29</sub> 14 $\alpha$ (H)17 $\alpha$ (H)20(R), *n*-alkane fractions of crude oils contain high concentrations of geolipid isomers, such as diasteranes and C<sub>27</sub>–C<sub>29</sub> steranes with hydrogen atoms at C<sub>14</sub> and C<sub>17</sub>  $\beta$  position and *S*-configuration at the C<sub>20</sub> chiral center.

When it comes to triterpanes, in addition to biolipid moretane isomers, olestanane and gammacerane, the significant presence of homologous series of  $17\alpha(H)21\beta(H)$  ( $22S$  and  $22R$ ) hopanes in the range of  $C_{29}$ – $C_{35}$  are also characteristic of crude oil. Such distributions of steranes and terpenes in organic extracts of river sediments, soil, or some other recent sediments (examples are displayed in Fig. 1c and d), are a strong indication of the presence of oil-type pollutants.<sup>41–45</sup> These polycyclic alkanes can be considered as a very sensitive “forensic tool”. If oil-type pollutants are present in some samples and in very low concentrations, GC–MS analysis of steranes and terpanes will allow their identification. This was confirmed, for example, in the research of surface sediments of the Great War Island (Belgrade)<sup>46</sup> and sludge from the Techirghiol Lake (Romania).<sup>47</sup>

### 3.2. Migration

When an oil-type pollutant reaches the environment, it does not stay at the accident site. It migrates, either as a consequence of its fluidity or with the help of water. Based on the changes in the biomarker composition, during the migration of crude oil into the environment, the mechanism of this process can be assessed.

The migration of oil-type pollutants into the environment by water can be related to the migration of bitumen in natural geological conditions from the source to the reservoir rock. This migration is called secondary migration in the organic geochemical literature, and it takes place mainly by water. The assumed mechanisms are: 1) solutions, 2) colloidal solutions, 3) globules and droplets and 4) continuous phases mechanism.<sup>3,6</sup>

During the accident at the Ušće station near Kraljevo, a certain amount of oil was spilled. The accident happened in 1996<sup>48</sup> during rainy days, which is, from the research point of view, very important. The oil migrated through the crushed stone. In such a process of natural geochromatography, the stone had the role of the adsorbent and water the role of the eluent. It has been observed that with the migration the amount of nitrogen, sulfur, oxygen (NSO) compounds is increasing, that the amount of pristane and phytane also increases in the relation to *n*-alkanes  $C_{17}$  and  $C_{18}$ , and that the amount of higher homologues of *n*-alkanes increases in the relation to lower ones. Namely, there was a shift of the *n*-alkane maximum in the five tested samples from  $C_{19}$  to  $C_{26}$ . It was concluded that NSO compounds and water formed colloidal solutions, with the colloidal micelle channel having a diameter of 0.7 nm. The isoprenoid alkanes with a volume slightly smaller than 0.7 nm in diameter and *n*-alkanes with a volume diameter of 0.5 nm were incorporated into such a channel. Higher homologues made stronger inclusions and thus migrated to a greater extent than those with fewer C-atoms.

In the early organic geochemical studies, an interesting phenomenon related to the migration of bitumen through sedimentary rocks in natural geological con-

ditions was proven. Namely, those compounds that elute the fastest during chromatographic separation (analytical procedure in the laboratory), migrate the fastest in natural catagenetic conditions.<sup>49,50</sup> On the other hand, by examining the mechanism of oil pollutant migration in river sediments of the Vrbas River (Banja Luka) it was proven that the amount of lower *n*-alkanes during the migration increases relative to higher homologues.<sup>51</sup> In the case of polycyclic alkanes, the amount of C<sub>27</sub> 13β(H)17α(H)20(S) and C<sub>27</sub> 13β(H)17α(H)20(R) diasteranes increases relative to C<sub>27</sub> 14α(H)17α(H)20(R) sterane, and C<sub>28</sub> 14α(H)17α(H)20(S) relative to C<sub>28</sub> 14α(H)17α(H)20(R). These results, for the first time, proved that the migration phenomenon that occurs with the diasteranes oil pollutants in the environment is the same as with bitumen in catagenetic geological conditions.<sup>51</sup>

### 3.3. Biodegradation

Once it reaches the environment, the oil pollutant is exposed to a number of changes. Its composition is influenced by reactions of adsorption, photodegradation, evaporation, oxidation. However, the greatest changes in an oil pollutant occur as a result of microbiological degradation.

During the period from November 1997 to February 2000, five groundwater samples were taken from the same piezometer of the Pančevo Oil Refinery. The biological markers were analyzed in the isolated extracts by GC–MS technique (Fig. 3).<sup>52–56</sup> In these extracts a phenomenon, related to the fate of biological markers during oil biodegradation in groundwater of an alluvial sedimentary formation, was defined.

In the first sample, the relative concentrations of *n*-alkanes C<sub>17</sub> and C<sub>18</sub> were lower than the concentrations of pristane and phytane isoprenoids. Such a distribution of the *n*-alkane fraction peaks is typical for the oil in which the biodegradation process has already started.<sup>52</sup>

The process continued until the complete degradation of *n*-alkanes in the fourth sample taken in September 1999.<sup>53</sup> In the sampled groundwater a few months later, in February 2000, *n*-alkanes with an even number of C-atoms appeared.<sup>54,55</sup> The identification of even homologues of fatty acids (their methyl-esters) and even homologues of alcohols as well as of cholesterol, in this sample, is the evidence that even *n*-alkanes were synthesized by the single-celled, non-photosynthetic algae Pyrophyta, known as “fire algae”, which are easily grown on an oil substrate.

The comprehensive understanding of the behaviour of biological markers in the process of oil biodegradation in natural geological conditions, as well as in the environment, has enabled their very efficient use in monitoring of the bio-remediation process, as a procedure for purification of water, soil and sediment from oil type organic pollutants in *ex situ*<sup>56</sup> and *in situ* conditions (Fig. 4).<sup>57</sup>

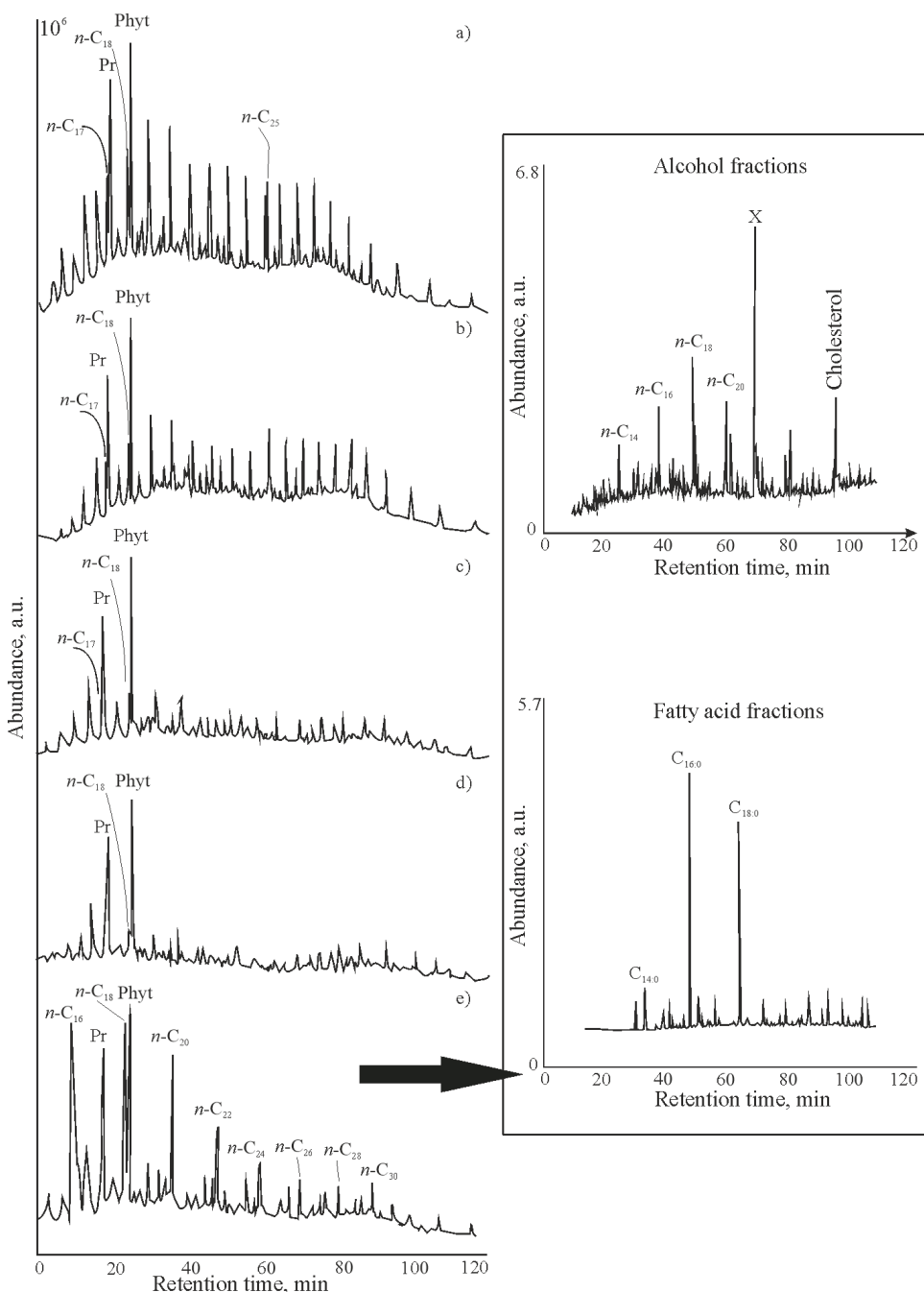


Fig. 3. Biological markers in the groundwater oil pollutant of the Pančevo Oil Refinery, samples of contaminated groundwater were taken from the same piezometer: a) November 1997, b) May 1998, c) September 1998, d) September 1999 and e) February 2000.<sup>52-56</sup>

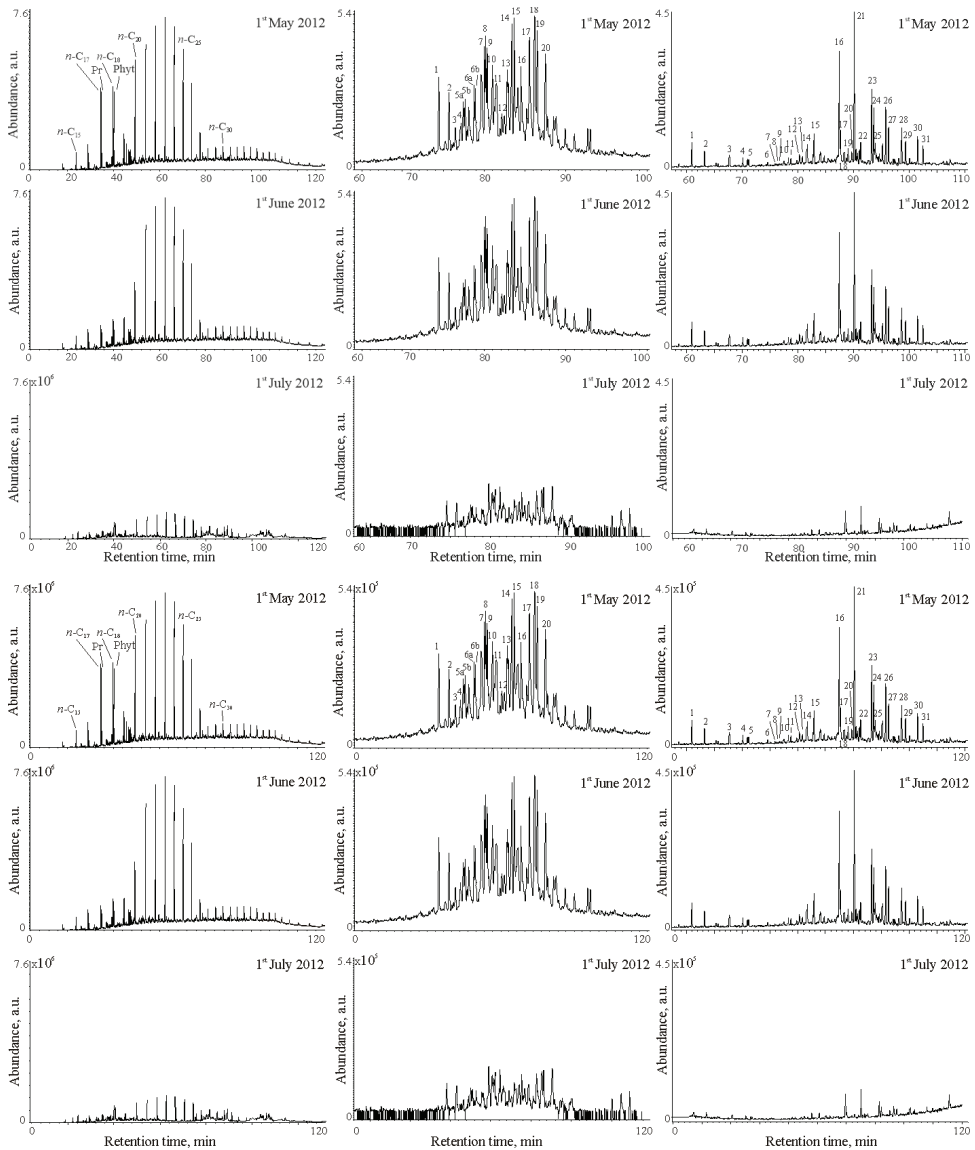


Fig. 4. An example of the degradation of biological markers of the *n*-alkane, sterane and triterpane type in groundwater petroleum pollutant during the in situ bioremediation process;<sup>57</sup> the identification of individual sterane and terpane isomers is given in Tables I and II.

#### 4. CONCLUSIONS

The organic geochemical research of oil in the Southeastern part of the Panonian Basin in Serbia, as well as the process of identifying oil pollutants and monitoring its fate in rivers and river sediments in Serbia, in the last three dec-

ades, have shown which biological markers can be used as the geochemical, *i.e.*, chemical tool.

In the first case, *n*-alkanes, isoprenoid aliphatic alkanes, diasteranes, steranes, tricyclic and tetracyclic diterpanes and pentacyclic triterpanes enabled a very successful assessment of the type of oil biomass precursor and classified the tested oils from one or more oil fields. Furthermore, they allowed the assessment of the sedimentation environment, the degree of maturation, the length of the migration path from the source to the reservoir rock and the degree of biodegradation in the reservoir rocks.

In the environmental chemistry, these organic compounds are indispensable in the identification of oil pollutants and their sources, in different parts of the environment, in monitoring changes during its migration, as well as in defining the manner and the intensity of microbiological degradation. Additionally, they also enable the successful monitoring of the bioremediation process efficiency in the *ex situ* and *in situ* conditions.

#### SUPPLEMENTARY MATERIAL

Additional data and information are available electronically at the pages of journal website: <https://www.shd-pub.org.rs/index.php/JSCS/article/view/10916>, or from the corresponding author on request.

*Acknowledgement.* This study was supported by the Ministry of Education, Science and Technological Development of the Republic of Serbia (Grant No: 451-03-9/2021-14/200026 and Contract number: 451-03-9/2021-14/200168).

#### ИЗВОД

#### УПОТРЕБА БИОЛОШКИХ МАРКЕРА У ОРГАНСКО-ГЕОХЕМИЈСКИМ ИСПИТИВАЊИМА ПОРЕКЛА И ГЕОЛОШКЕ ИСТОРИЈЕ СИРОВИХ НАФТИ (I) И У ПРОЦЕНИ НАФТНОГ ЗАГАЂЕЊА РЕКА И РЕЧНИХ СЕДИМЕНТА СРБИЈЕ (II)

БРАНИМИР С. ЈОВАНЧИЋЕВИЋ<sup>1</sup>, ГОРДАНА Ђ. ГАЈИЦА<sup>2</sup>, ГОРИЦА Д. ВЕСЕЛИНОВИЋ<sup>2</sup>, МИЛИЦА П. КАШАНИН-ГРУБИН<sup>2</sup>, ТАТЈАНА М. ШОЛЕВИЋ КНУДСЕН<sup>2</sup>, СНЕЖАНА Р. ШТРБАЦ<sup>2</sup>  
и АЛЕКСАНДРА М. ШАЈНОВИЋ<sup>2</sup>

<sup>1</sup>Универзитет у Београду, Хемијски факултет, Студентски трг 16, 11158 Београд и <sup>1</sup>Универзитет у Београду, Центар за хемију, Институт за хемију, технолоџију и металургију, Његошева 12, 11001 Београд

Биолошки маркери у нафтама су једињења за које се зна прекурсор, у току трансформација органске супстанце ова једињења трпе извесне структурне и стереохемијске промене. На основу установљеног прекурсора појединачних биомаркера, процењује се порекло испитиваних нафти, а на основу интензитета и типа промена, геолошка историја. Она укључује дефинисање средине таложења, степена матурисаности, дужине миграционог пута нафте, степена биодеградације. Највише изучавани и примењивани биолошки маркери су нормални алканси, изопреноидни алифатични алакани пристан и фитан, и полициклични алканси типа стерана и терпана. С друге стране, у хемији животне средине ова једињења у значајној мери могу да допринесу идентификацији нафтног полутанта, као и процени механизма миграције и интензитета биодеградације. У овом прегледном раду прво су приказани резултати који се односе на примену биолошких

маркера у органско геохемијским корелацијама нафти југоисточног дела Панонског басена (I). У другом делу дат је преглед оних радова у којима су исти биолошки маркери коришћени у идентификацији нафтних полутаната и у праћењу његових промена у току миграције и биодеградације у рекама и речним седиментима Србије (II).

(Примљено 1. јула, ревидирано 30. августа, прихваћено 31. августа 2021)

#### REFERENCES

1. G. Eglinton, M. T. J. Murphy, *Organic Geochemistry*, Springer-Verlag, Heidelberg, 1969, p. 20 (ISBN: 70-107318)
2. B.P. Tissot, D.H. Welte, *Petroleum Formation and Occurrence*, 2<sup>nd</sup> ed., Springer-verlag, Heidelbarg, 1984, p. 3 (ISBN: 0-387-08698-6)
3. D. Waples, *Geochemistry in Petroleum Exploration*, Interantaional Human Resources Development Corporation, Boston, MA, 1985, p. 1 (ISBN: 90-277-208-8)
4. R. P. Philp, *Fossil Fuel Biomarkers, Applications and Spectra*, Elsevier, Amsterdam, 1985, p. 1 (ISBN: 0444424717)
5. K. E. Peters, C. C. Walters, J. M. Moldowan, *The biomarker Guide, Vol. 2: Biomarkers and Isotopes in Petroleum Exploration and Earth History*, Cambridge University Press, Cambridge, 2005, p. 475 (ISBN: 0-521-83763-4)
6. J. Schwarzbauer, B. Jovančićević, *Fundamentals in Organic Geochemistry – Fossil Matter in the Geosphere*, Springer, Heidelberg, 2015, p. 1 (ISBN: 978-3-319-11552-8)
7. J. Schwarzbauer, B. Jovančićević, *Fundamentals in Organic Geochemistry – From Biomolecules to Chemosfossils*, Springer, Heidelberg, 2016, p. 1 (ISBN: 978-3-319-27241-2)
8. A. Trieb, *Ann. Chemie* **509** (1934) 103 (<https://doi.org/10.1002/ange.19360493803>)
9. D. H. Welte, D. Waples, *Sci. Nat.* **60** (1973) 516 (<https://doi.org/10.1007/BF00603253>)
10. J. M. Moldowan, W. K. Seifert, *Science* **204** (1979) 169 (<https://doi.org/10.1126/science.204.4389.169>)
11. W. K. Seifert, J.M. Moldowan, *Geochim. Cosmochim. Acta* **45** (1981) 783 ([https://doi.org/10.1016/0016-7037\(81\)90108-3](https://doi.org/10.1016/0016-7037(81)90108-3))
12. P. A. Albrecht, *Evaluation geochimique des polyterpanes et des sterols*, Prix Rousel, Paris, 1986, p. 1
13. H. L. Ten Haven, M. Rohmer, J. Rullkötter, P. Bisseret, *Geochim. Cosmochim. Acta* **53** (1989) 3073 ([https://doi.org/10.1016/0016-7037\(89\)90186-5](https://doi.org/10.1016/0016-7037(89)90186-5))
14. W. K. Seifert, R. M. K. Carlson, J. M. Moldowan, in *Advances in Organic Geochemistry 1981*, M. Bjorøy, P. Albrecht, C. Cornford, K. de Groot, G. Eglinton, E. Galimov, D. Leythaeuser, R. Pelet, J. Rullkötter, G. Speers., Eds., Wiley, Chichester, 1983, p. 710 (ISBN: 0-471-26229-3)
15. W. K. Seifert, J. M. Moldowan, G. J. Demaioson, *Org. Geochem.* **10** (1984) 633 ([https://doi.org/10.1016/0146-6380\(84\)90085-8](https://doi.org/10.1016/0146-6380(84)90085-8))
16. Z. Sofer, J. E. Zumberge, V. Lay, *Org. Geochem.* **10** (1986) 377 ([https://doi.org/10.1016/0146-6380\(86\)90037-9](https://doi.org/10.1016/0146-6380(86)90037-9))
17. J. Rullkötter, T. M. Peakman, H. L. ten Haven, *Org. Geochem.* **21** (1994) 215 ([https://doi.org/10.1016/0146-6380\(94\)90186-4](https://doi.org/10.1016/0146-6380(94)90186-4))
18. J. Schwarzbauer, B. Jovančićević, *Fundamentals in Organic Geochemistry – Introduction to Analytical Methods in Organic Geochemistry*, Springer, Heidelberg, 2020, p. 1 (ISBN: 978-3-030-38591-0)
19. J. Schwarzbauer, B. Jovančićević, *Fundamentals in Organic Geochemistry – Organic Pollutants in the Geosphere*, Springer, Heidelberg, 2018, p. 1 (ISBN: 978-3-319-68937-1)

20. M. Šarković, *Geochemical characteristics of layered fluids of oil and gas deposits in the southeastern part of the Pannonian Basin and their use in research*, Matica srpska, Novi Sad, 1973, p. 1 (in Serbian)
21. M. Šaban, B. Jovančićević, D. Vitorović, in *Proceedings of the II Yugoslav Symposium on Hydrocarbons*, 1986, Belgrade, Yugoslavia, II Yugoslav Symposium on Hydrocarbons, Serbian Chemical Society, Belgrade, 1986, p. 142 (in Serbian)
22. M. Šaban, B. S. Jovančićević, A. Hollerbach, D. Vitorović, in *Proceedings of 13<sup>th</sup> International Meeting on Organic Geochemistry*, 1987, Venezia, Italia, Organic Geochemistry in Petroleum Exploration, Pergamon Press, Frankfurt, 1987, p. 224
23. M. Šaban, B. S. Jovančićević, S. Saračević, A. Hollerbach, D. Vitorović, *Org. Geochem.* **13** (1988) 325 ([https://doi.org/10.1016/0146-6380\(88\)90052-6](https://doi.org/10.1016/0146-6380(88)90052-6))
24. M. M. Šaban, B. Jovančićević, T. Glumičić, S. Saračević, in *Abstracts of 14<sup>th</sup> International Meeting on Organic Geochemistry*, 1989, Paris, France, Organic Geochemistry in Petroleum Exploration, Pergamon Press, Paris, 1989, p. 197
25. M. M. Šaban, B. S. Jovančićević, T. Glumičić, S. Saračević, *Org. Geochem.* **16** (1990) 477 ([https://doi.org/10.1016/0146-6380\(90\)90063-6](https://doi.org/10.1016/0146-6380(90)90063-6))
26. T. Šolević, K. Stojanović, J. Bojesen-Koefod, H. P. Nytoft, B. Jovančićević, D. Vitorović, *Org. Geochem.* **39** (2008) 118 (<https://doi.org/10.1016/j.orggeochem.2007.09.003>)
27. M. Šaban, B. S. Jovančićević, T. Glumičić, N. Dogović, *Rapid Commun. Mass Spectrom.* **4** (1990) 505 (<https://doi.org/10.1002/rcm.1290041207>)
28. B. Jovančićević, P. Polić, D. Vitorović, *J. Serb. Chem. Soc.* **63** (1998) 397 (<https://doi.org/10.2298/JSC161129022M>)
29. B. Jovančićević, H. Wehner, G. Scheeder, D. Plečaš, M. Ercegovac, D. Vitorović, *J. Serb. Chem. Soc.* **66** (2001) 297 (<https://doi.org/10.2298/JSC0105297J>)
30. B. Jovančićević, H. Wehner, G. Scheeder, K. Stojanović, A. Šainović, O. Cvetković, M. Ercegovac, D. Vitorović, *J. Serb. Chem. Soc.* **67** (2002) 553 (<https://doi.org/10.2298/JSC0209553J>)
31. B. Durand, in *Advances in Organic Geochemistry 1981*, M. Bjørøy, P. Albrecht, C. Cornford, K. de Groot, G. Eglinton, E. Galimov, D. Leythaeuser, R. Pelet, J. Rullkötter, G. Speers, Eds., Wiley, Chichester, 1983, p. 117 (ISBN: 0-471-26229-3)
32. B. Jovančićević, P. Polić, M. Šaban, D. Vitorović, *J. Serb. Chem. Soc.* **59** (1994) 983
33. B. Jovančićević, Lj. Tasić, P. Polić, J. Nedeljković, A. Golovko, D. Vitorović, *J. Serb. Chem. Soc.* **61** (1996) 817
34. K. Stojanović, B. Jovančićević, D. Vitorović, Y. Golovko, G. Pevneva, A. Golovko, *J. Serb. Chem. Soc.* **72** (2007) 1237 (<https://doi.org/10.2298/JSC0712237S>)
35. K. Stojanović, B. Jovančićević, G. S. Pevneva, J. A. Golovko, A. K. Golovko, P. Pfendt, *Org. Geochem.* **32** (2001) 721 ([https://doi.org/10.1016/S0146-6380\(01\)00004-3](https://doi.org/10.1016/S0146-6380(01)00004-3))
36. M. A. M. Faraj, T. Šolević-Knudsen, H. P. Nytoft, B. Jovančićević, *J. Pet. Sci. Eng.* **147** (2016) 605 (<https://doi.org/10.1016/j.petrol.2016.09.030>)
37. M. A. M. Faraj, T. Šolević-Knudsen, K. Stojanović, S. Ivković-Pavlović, H. P. Nytoft, B. Jovančićević, *J. Serb. Chem. Soc.* **82** (2017) 1315 (<https://doi.org/10.2298/JSC170419075A>)
38. R. M. S. Saheed, T. Šolević-Knudsen, M. A. M. Faraj, Z. Nikolovski, H. P. Nytoft, B. Jovančićević, *J. Serb. Chem. Soc.* **85** (2020) 1489 (<https://doi.org/10.2298/JSC200501055S>)
39. B. Jovančićević, Lj. Tasić, H. Wehner, E. Faber, N. Šušić, P. Polić, *Fresenius Environ. Bull.* **6** (1997) 667 (<https://doi.org/10.2298/JSC200501055S>)

40. B. Jovančićević, Lj. Tasić, H. Wehner, D. Marković, P. Polić, *Fresenius Environ. Bull.* **7** (1998) 320
41. B. Jovančićević, P. Polić, B. Mikašinović, G. Scheeder, M. Teschner, H. Wehner, *Fresenius Environ. Bull.* **10** (2001) 527 ([https://www.prt-parlar.de/download\\_afs\\_2001/](https://www.prt-parlar.de/download_afs_2001/))
42. S. Grujić, B. Jovančićević, P. Polić, H. Wehner, *Fresenius Environ. Bull.* **12** (2003) 359 ([https://www.prt-parlar.de/download\\_feb\\_2003/](https://www.prt-parlar.de/download_feb_2003/))
43. I. Samelak, M. Balaban, N. Vidović, N. Koljančić, M. Antić, T. Šolević Knudsen, B. Jovančićević, *J. Serb. Chem. Soc.* **83** (2018) 1167 (<https://doi.org/10.2298/JSC180501061S>)
44. Z. Milićević, D. Marinović, G. Gajica, M. Kašanin-Grubin, V. Jovanović, B. Jovančićević, *J. Serb. Chem. Soc.* **82** (2014) 593 (<https://doi.org/10.2298/JSC161129022M>)
45. S. Šrbac, G. Gajica, A. Šajnović, N. Vasić, K. Stojanović, B. Jovančićević, *J. Serb. Chem. Soc.* **79** (2014) 597 (<https://doi.org/10.2298/JSC130614087S>)
46. M. Kašanin-Grubin, S. Šrbac, S. Antonijević, S. Djogo-Mračević, D. Randjelović, J. Orlić, A. Šajnović, *J. Environ. Manage.* **251** (2019) 109574 (<https://doi.org/10.1016/j.jenvman.2019.109574>)
47. S. Stojadinović, B. Jovančićević, A. Šajnović, M. Golumbeanu, R. Almasan, Dj. Jovanović, I. Brčeski, *Fresenius Environ. Bull.* **30** (2021) 1595 ([https://www.prt-parlar.de/download\\_feb\\_2021/](https://www.prt-parlar.de/download_feb_2021/))
48. B. Jovančićević, Lj. Tasić, S. Vujsinović, I. Matić, D. Malović, P. Pfendt, *J. Serb. Chem. Soc.* **61** (1996) 1025
49. A. Golovko, V. Ivanov, in *Proceedings of 19<sup>th</sup> International Meeting on Organic Geochemistry*, 1991, Istanbul, Turkey, Organic Geochemistry, TÜBITAK, Istanbul, 1999, p. 585
50. W. K. Seifert, J. M. Moldowan, *Geochim. Cosmochim. Acta* **42** (1978) 77 ([https://doi.org/10.1016/0016-7037\(79\)90051-6](https://doi.org/10.1016/0016-7037(79)90051-6))
51. I. Samelak, M. Balaban, M. Antić, T. Šolević-Knudsen, B. Jovančićević, *Environ. Chem. Lett.* **18** (2020) 459 (<https://doi.org/10.1007/s10311-019-00937-2>)
52. B. Jovančićević, P. Polić, *Fresenius Environ. Bull.* **9** (2000) 232
53. B. Jovančićević, P. Polić, D. Vitorović, G. Scheeder, M. Teschner, H. Wehner, *Fresenius Environ. Bull.* **10** (2001) 178 ([https://www.prt-parlar.de/download\\_afs\\_2001/](https://www.prt-parlar.de/download_afs_2001/))
54. B. Jovančićević, P. Polić, M. Vrvić, G. Scheeder, M. Teschner, H. Wehner, *Environ. Chem. Lett.* **1** (2003) 73 (<https://doi.org/10.1007/s10311-002-0002-7>)
55. B. Jovančićević, M. Vrvić, J. Schwarzbauer, H. Wehner, G. Scheeder, D. Vitorović, *Water Air Soil Pollut.* **183** (2007) 225 (<https://doi.org/10.1007/s11270-007-9371-7>)
56. V. Beškoski, M. Takić, J. Milić, M. Ilić, G. Gojgić-Cvijović, B. Jovančićević, M. M. Vrvić, *J. Serb. Chem. Soc.* **75** (2010) 1605 (<https://doi.org/10.2298/JSC100505091B>)
57. V. Beškoski, S. Miletić, M. Ilić, G. Gojgić-Cvijović, P. Papić, M. Marić, T. Šolević-Knudsen, B. Jovančićević, T. Nakano, M. Vrvić, *CLEAN – Soil, Air, Water* **45** (2017) 1600023 (<https://doi.org/10.1002/clen.201600023>).

SUPPLEMENTARY MATERIAL TO  
**The use of biological markers in organic geochemical investigations of the origin and geological history of crude oils (I) and in the assessment of oil pollution of rivers and river sediments of Serbia (II)**

BRANIMIR S. JOVANČIĆ<sup>1#</sup>, GORDANA D. GAJICA<sup>2\*</sup>, GORICA D. VESELINEVIĆ<sup>2</sup>, MILICA P. KAŠANIN-GRUBIN<sup>2</sup>, TATJANA M. ŠOLEVIĆ KNUDSEN<sup>2</sup>, SNEŽANA R. ŠTRBAC<sup>2</sup> and ALEKSANDRA M. ŠAJNOVIĆ<sup>2</sup>

*J. Serb. Chem. Soc.* 87 (1) (2022) 7–25

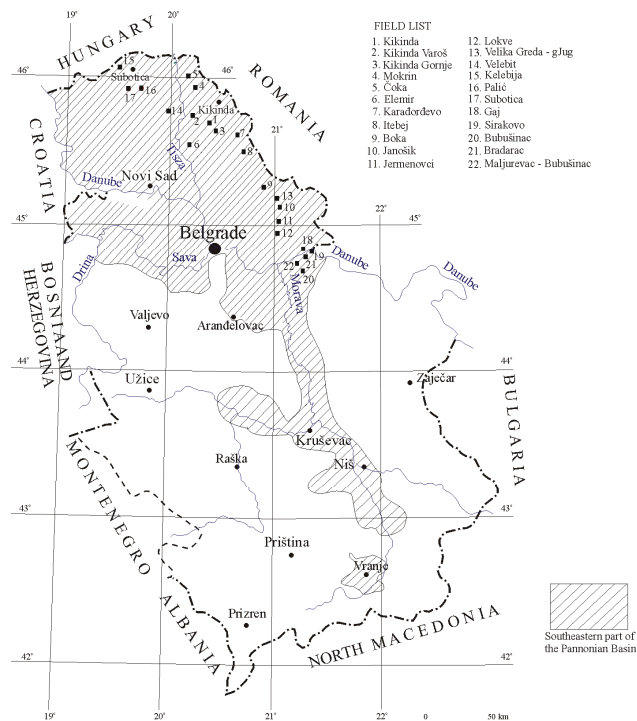


Fig. S-1. Locations of the most important oil and oil-gas fields in the southeastern part of the Pannonian Basin on the territory of Serbia.<sup>28</sup>

\*Corresponding author. E-mail: gordana.gajica@ihtm.bg.ac.rs





J. Serb. Chem. Soc. 87 (1) 27–40 (2022)  
JSCS-5502

# Journal of the Serbian Chemical Society

JSCS-info@shd.org.rs • www.shd.org.rs/JSCS

Original scientific paper

Published 14 January 2022

## To Professor Petar Pfendt, *In calidum, et plurium retributivus memoriae: FTIR-ATR analysis of post stamps of the Principality of Serbia issued in 1866 and 1868 and their forgeries*

ALEKSANDAR POPOVIĆ<sup>1\*</sup>, BOBAN ANĐELOKOVIC<sup>2</sup>, DRAGANA ĐORĐEVIĆ<sup>3</sup>,  
SANJA SAKAN<sup>3</sup>, LJUBODRAG VUJISIĆ<sup>1\*\*</sup>, SAVA VELIČKOVIĆ<sup>4</sup>  
and DUBRAVKA RELIĆ<sup>1</sup>

<sup>1</sup>Faculty of Chemistry, University of Belgrade, Studentski Trg 12–16, Belgrade, Serbia,  
<sup>2</sup>University of Belgrade, ICTM-Center of Chemistry, Njegoševa 12, Belgrade, Serbia, <sup>3</sup>Centre  
of Excellence in Environmental Chemistry and Engineering – ICTM, University of Belgrade,  
Njegoševa 12, 11000 Belgrade, Serbia and <sup>4</sup>Faculty of Technology and Metallurgy,  
University of Belgrade, Karnegijeva 4, Belgrade, Serbia

(Received 1 September, revised 29 October, accepted 1 November 2021)

**Abstract:** In order to further define the potential use of FTIR-ATR spectroscopy, as a non-destructive and reliable technique, for the analysis of the characteristics of post stamps, certified originals of the Principality of Serbia stamps (“Prince Michael issues”) issued in 1866 and 1868 as well as their forgeries were analyzed. Spectra enabling the comparison of the paper, dye and glue of stamps of so-called “Vienna issues”, having denominations of 10 (orange-yellow), 20 (pink) and 40 para (blue) and “Belgrade issues” (1 para-green and 2 para-reddish brown), as well as 24 expert-certified forgeries, were taken. It was shown that the applied technology was, in most of the cases, a fast and suitable technique for establishing clear differences between the spectral characteristics of the paper and dye used for the original stamps, and forgeries that were most probably made decades after the printing of the genuine stamps. The differences between printings of the same issues of the genuine stamps were also elaborated. It is proposed, for the first time in philatelic history, the possibility that “Vienna issues” stamps may have been printed on two different papers, and, having in mind the technology of printing in the 19<sup>th</sup> century, potentially, not even at the same time or in the same printing house.

**Keywords:** philately; stamps of Serbia; Prince Michael; “Vienna Issues”; “Belgrade Issues”.

\*\*\* Corresponding authors. E-mail: (\*)apopovic@chem.bg.ac.rs, (\*\*)ljubaw@chem.bg.ac.rs  
<https://doi.org/10.2298/JSC210901090P>

## INTRODUCTION

Professor Petar Pfendt (Jaša Tomić 1934–Belgrade 2021) was the first author's teacher, with whom he shared not only the passion for chemistry, but also numerous other fields, history being among them. Their conversations, during active service of Professor Pfendt at the University, were often devoted to this subject, emphasizing especially regional contemporary history. Probably due to sad past of the population of German origin in the Danube Basin during and after World War Two,<sup>1</sup> these conversations were brief, with occasional reminiscences of the professor from his childhood. In most occasions, historical facts were only inspiration for more applicative ideas, elaborating and connecting history (and other topics) with chemistry, over viewing the potential application of chemical methods, including analytical ones, in other areas of contemporary life, such as art, archaeology or sport. His passion was not only history, it is the fact that the late Professor Pfendt was a person of different and wide areas of interest, and deep and profound knowledge of chemistry, with publication in chemistry of oil shales,<sup>2</sup> aquifers and alluvial sediments,<sup>3</sup> coal,<sup>4</sup> water quality,<sup>5</sup> environmental consequences of war activities,<sup>6</sup> laboratory equipment,<sup>7</sup> processes occurring in soil,<sup>8</sup> air<sup>9</sup> and chemical education.<sup>10</sup> For these reasons, the authors of this paper decided unanimously to devote the study below, which includes history and applied chemistry, to the memory of Professor Petar Pfendt, a scholar and teacher.

Almost from the very moment of their invention and beginning of use, post stamps became the subject of collection<sup>11</sup> and forging.<sup>12</sup> Their basic issues and numerous variations were attractive forging targets due to their nature, rareness and very often the unpredictability of variations caused, among other reasons, by imperfections of the printing process.<sup>13</sup> Political changes, including those provoked by wars,<sup>14</sup> increased number of post stamp issues printed in limited quantities and for very short periods of time, sometime counted in days.<sup>15</sup> Like in the case of other collectables, the number of stamps printed as well as their quantity and availability on the market determine their values.

For decades, practically more than a century, the comparison between original and forged stamps was realised without any analytical methods, and was subject to the judgement and expertise of verified experts. The quality of forgeries were, in some cases, very close to the originals,<sup>16</sup> thus leading to mistakes in certification and the building of collections or their substantial parts that were not based on originals. Certainly, the introduction of instrumental analytical techniques that are non-destructive and that can differentiate paper,<sup>17–20</sup> dye<sup>21,22</sup> or the glue used in the printing of post stamps (and other documents) could improve their analysis, eliminate, at least to the large extent, potential errors that were involuntarily made due to subjectivity of experts. FTIR-ATR spectroscopy is one of such methods that could be used for the analysis of post stamps. It has

been used for the analysis of the stamps from Germany,<sup>23</sup> the United Kingdom,<sup>24</sup> Italy<sup>25</sup> and other countries, thus joining other non-destructive methods, such as Raman spectroscopy,<sup>26</sup> PIXE...<sup>27</sup>

The Principality of Serbia issued its first post stamps in 1866 (so called “Grbuše”), used for post tariffs of newspapers. In July of the same year, three post stamps used for mailing common letters were also issued, portraying Prince Mihajlo Obrenović. They were printed in Vienna’s “Die Kaiserliche Wiener Hof-Und Staatsdruckerei” and thus are known as “Vienna Issues”, designed by Anastas Jovanović, with denominations of 10 (orange yellow), 20 (pink) and 40 (blue) para.

Stamps with same design were issued five more times by Belgrade’s “Praviljstvena knjigopečatnja” (“State Printing House”) in November 1866–February 1867 (the 10 para stamp being orange-yellow, 20 para stamp pale pink and 40 para stamp – ultramarine), March 1867 (1 para stamp – light green, 2 para stamp – yellowish-olive brown), July 1868 (20 para – pink, 40 para – blue), November 1868 (1 para – dark green, 2 para – reddish-brown) and in still unknown month in 1868 (1 para – pale to dark olive, 2 para yellow-olive). All of them are known in literature as “Belgrade issues”. Forgeries of all the Prince Mihajlo Obrenović portrait definitive stamps are plentiful.<sup>28</sup> Their market values are different, the most expensive being the 1 para pale to dark olive stamp (1868) having not more than twenty known genuine samples at the present time, with a catalogue value of 6000 EUR.<sup>29</sup>

In this study, the authors present the potential use of FTIR-ATR spectroscopy for the analysis of similarities and differences of post stamps of the so-called “Vienna issue” of 10, 20 and 40 para and stamps of 1 para and 2 para issued in 1868, as well as of 24 proven forgeries of these stamps, being obtained from the collection of the late Professor Jovan Veličković (1927–2012), official expert of the Union of Philatelists of Serbia.

#### EXPERIMENTAL

Photographs of the examined original stamps are shown in Fig. 1, while their characteristics are given in Table I.<sup>27</sup>



Fig. 1. 10, 20 and 40 para Prince Mihajlo “Vienna Issue” (1866) and 1 and 2 para “Belgrade Issue” (1868) post stamps.

Infrared spectra were recorded for all stamps from collections using Fourier transform infrared spectroscopy (FTIR) with attenuated total reflectance (ATR) at 4 cm<sup>-1</sup> resolution

(Nicolet 6700 FT IR, software Omnic, Version 7.0, Thermo Scientific, USA). The spectra were recorded on a diamond crystal with signal beam in the range of 400 to 4000 cm<sup>-1</sup>. Crystal was cleaned with alcohol between samples. The background was recorded with 50 and sepal with 100 scans. The differences in the collected spectrum were shown by automatic subtraction of the spectra in Omnic software.

TABLE I. Characteristics of the 10, 20 and 40 para Prince Mihajlo "Vienna Issue" (1866) and 1 and 2 para "Belgrade Issue" (1868) post stamps

| Stamp   | Printing       | Colour        | Paper               | Glue           |
|---------|----------------|---------------|---------------------|----------------|
| 10 para | 1866, Vienna   | Orange yellow | Regular, soft       | White, cracked |
| 20 para | 1866, Vienna   | Pink          | Regular, soft       | White, cracked |
| 40 para | 1866, Vienna   | Blue          | Regular, soft       | White, cracked |
| 1 para  | 1868, Belgrade | Dark green    | Different thickness | Yellow-grey    |
| 2 para  | 1868, Belgrade | Reddish-brown | Different thickness | Yellow-grey    |

#### RESULTS AND DISCUSSION

The results obtained by FTIR-ATR spectroscopy of the described samples or original and forged post stamps are shown at Figs. 2–11.

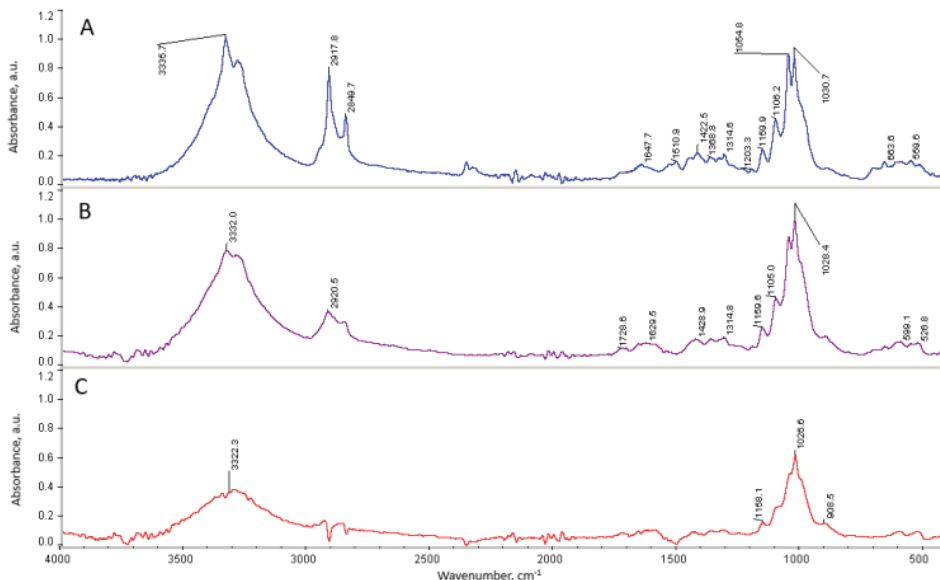


Fig. 2. FTIR spectra of: A) 10 para original stamps paper printed in Vienna 1866, B) 10 para confirmed forgery stamps paper and C) subtraction result of the original and the forgery stamp papers.

Comparison of certified original and forgery paper spectra revealed the differences between the paper used for printing of original and false stamps. This should not be a surprise, since certainly years if not decades elapsed between the

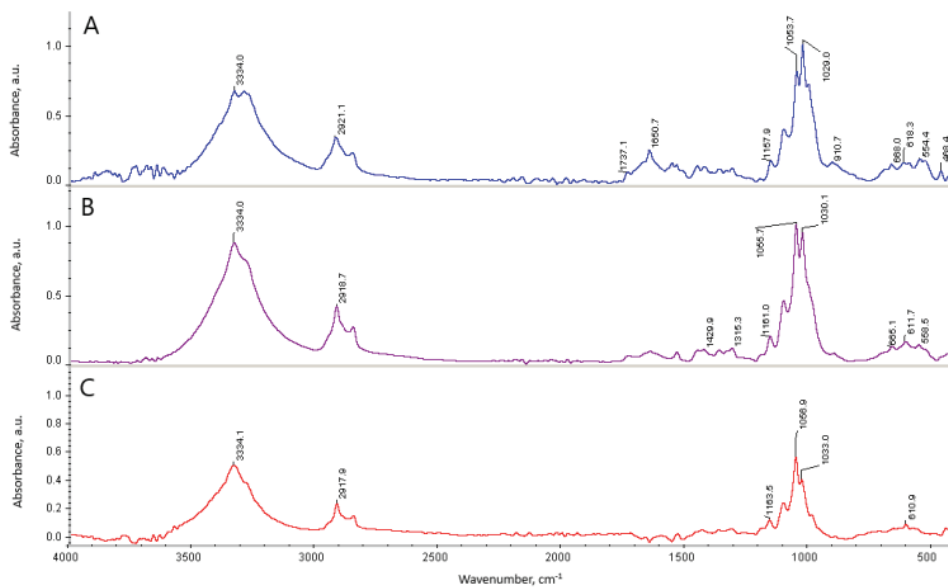


Fig. 3. FTIR spectra of: A) 20 para original stamps paper printed in Vienna 1866, B) 20 para confirmed forgery stamps paper and C) subtraction result of the original and the forgery stamp papers.

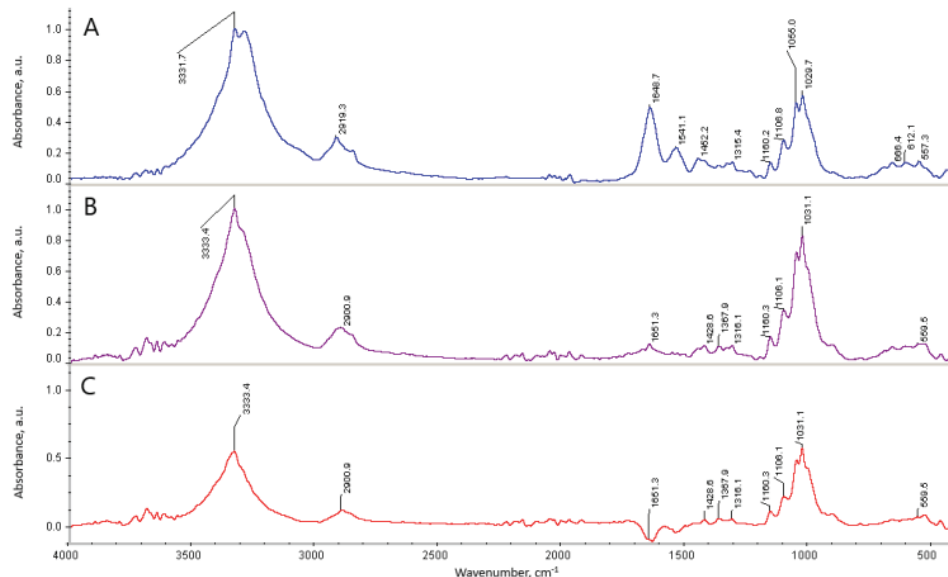


Fig. 4. FTIR spectra of: A) 40 para original stamps paper printed in Vienna 1866, B) 40 para confirmed forgery stamps paper and C) subtraction result of the original and the forgery stamp papers.

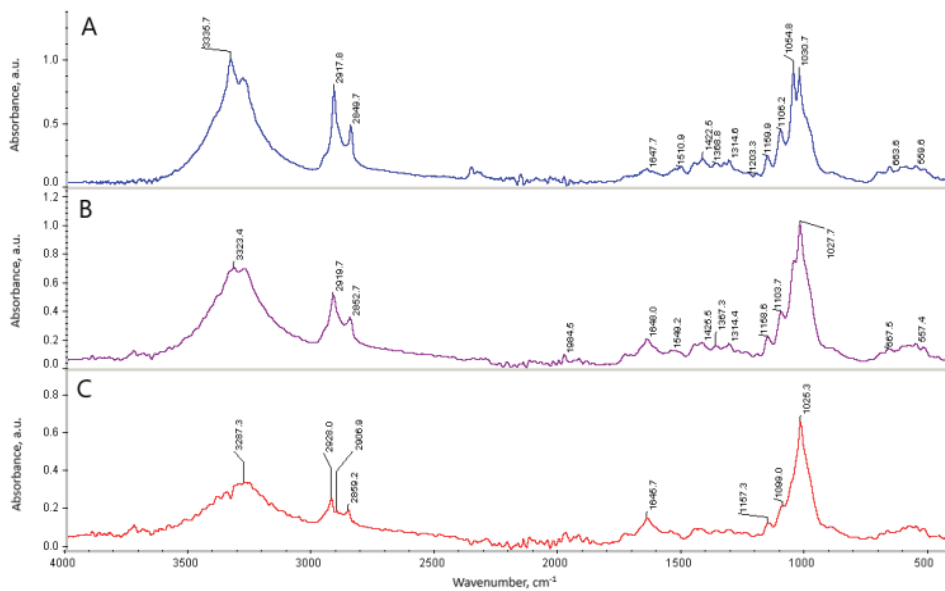


Fig. 5. FTIR spectra of: A) 10 para original stamps dye printed in Vienna 1866, B) 10 para confirmed forgery stamps dye and C) subtraction result of the original and the forgery stamp dyes.

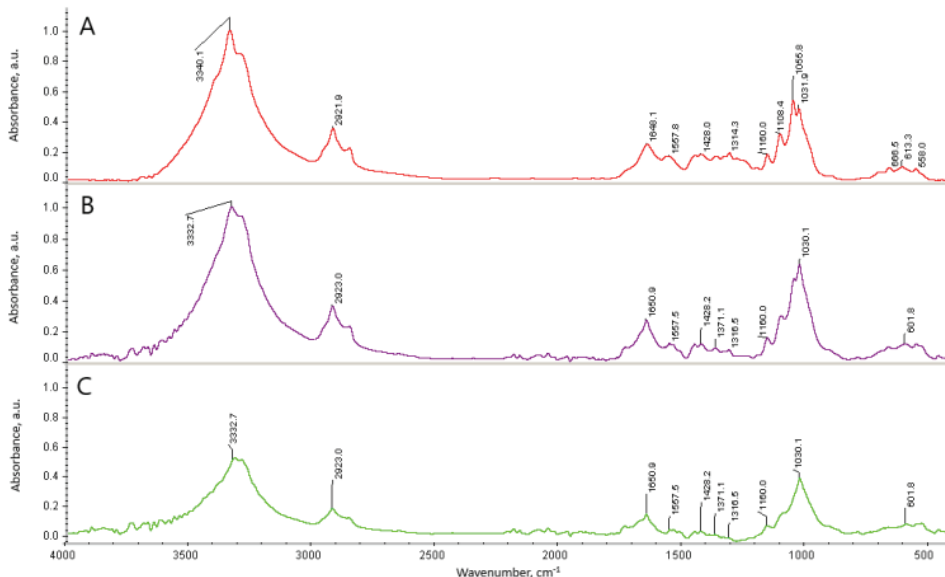


Fig. 6. FTIR spectra of: A) 20 para original stamps dye printed in Vienna 1866, B) 20 para confirmed forgery stamps dye and C) subtraction result of the original and the forgery stamp dyes.

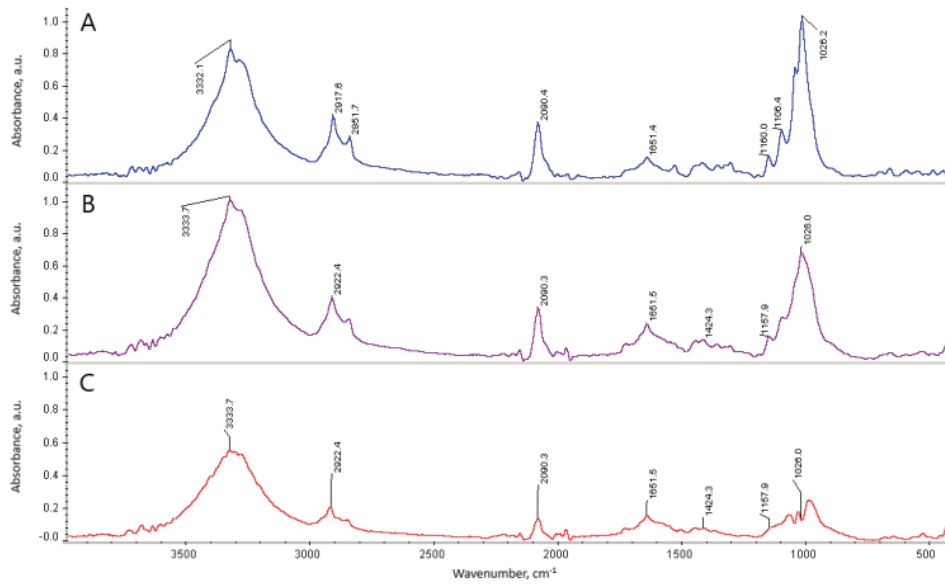


Fig. 7. FTIR spectra of: A) 40 para original stamps dye printed in Vienna 1866, B) 40 para confirmed forgery stamps dye and C) subtraction result of the original and the forgery stamp dyes.

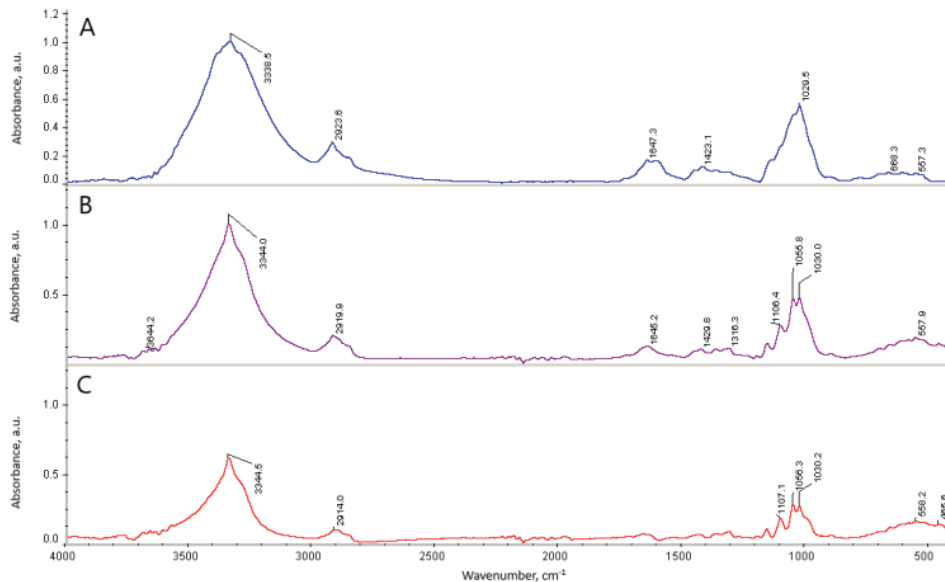


Fig. 8. FTIR spectra of: A) 1 para original dark green stamps paper printed in Belgrade 1868, B) 1 para confirmed forgery stamps paper and C) subtraction result of the original and the forgery stamp papers.

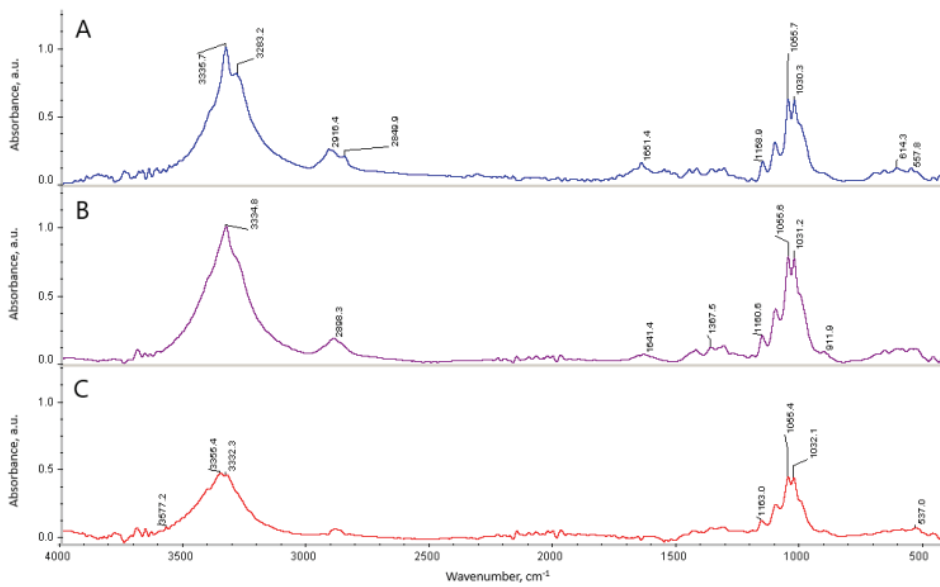


Fig. 9. FTIR spectra of: A) 2 para original stamps paper printed in Belgrade 1868, B) 2 para confirmed forgery stamps paper and C) subtraction result of the original and the forgery stamp papers.

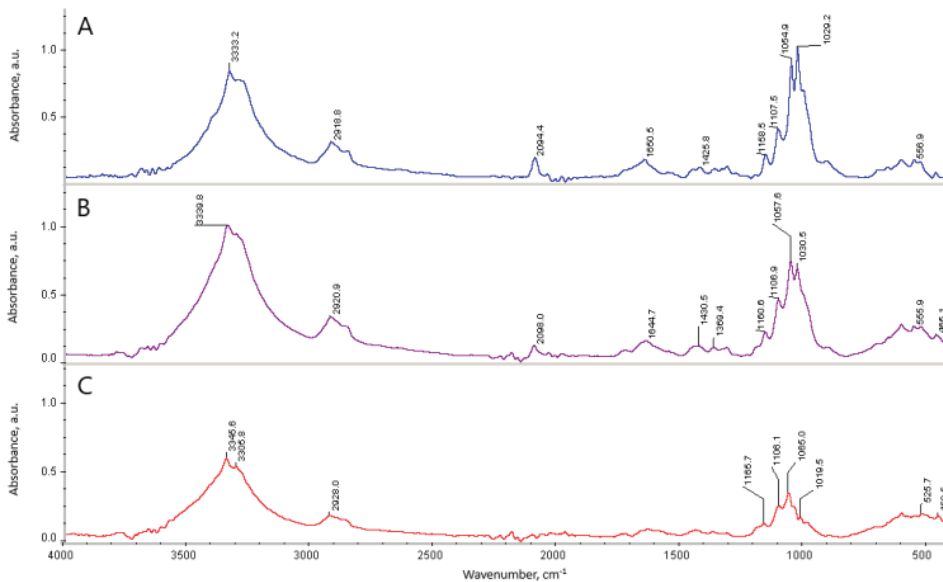


Fig. 10. FTIR spectra of: A) dye of 1 para original dark green stamp printed in Belgrade 1868, B) dye of 1 para confirmed forgery stamp and C) subtraction result of the original and the forgery stamp dyes.

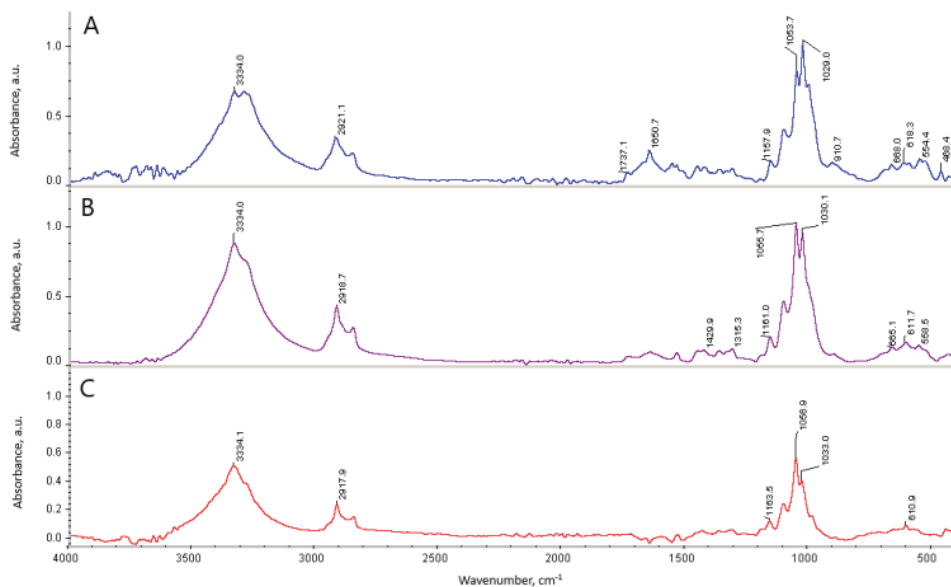


Fig. 11. FTIR spectra of: A) dye of 2 para original stamp printed in Belgrade 1868, B) dye of 2 para confirmed forgery stamps and C) subtraction result of the original and the forgery stamp dyes.

two processes, and it is not expectable that conspirators that produced false stamps could have the same paper available. In case of the 10 para stamp (Fig. 2), the intensity of peaks of the originals and fakes were different. In addition, the spectra of the genuine stamp exhibit a shoulder at  $984\text{ cm}^{-1}$  that the forgeries do not have, while peaks at  $533$  or  $910\text{ cm}^{-1}$  are absent in the spectra of the originals but are visible in the spectra of fake stamps. Differences also exist in the spectra of paper of the 20 para original and the certified forgeries (Fig. 3).

In the original stamp, the IR spectrum revealed the existence of a shoulder-like band at  $3100\text{ cm}^{-1}$ , which is not seen in the spectrum of the fake stamp of the same denomination. On the contrary, the counterfeit exhibited a band at  $1428\text{ cm}^{-1}$  not existing in the spectrum of the original stamp. Finally, the spectrum of the paper of the 40 para stamp (Fig. 4) was also different from those of known and proven forgeries. Its spectrum has a peak at  $1542\text{ cm}^{-1}$ , not existing in the fakes, as well a peak at  $1648\text{ cm}^{-1}$ , present in the spectra of some, but not all of the forgeries. However when present, they are never as intensive as in the spectrum of the original. Finally, forgeries exhibit different peaks not existing in the spectra of the originals, most commonly at  $470$  and  $911\text{ cm}^{-1}$ .

Since the original stamps having denomination of 10, 20 and 40 para were, according to the available literature,<sup>28,29</sup> printed at the same time in the same printing house, it should be reasonable to expect that the spectra of their papers should match. However, although this is the case for 20 and 40 para stamps, the

one with denomination of 10 para does not have a band at  $1551\text{ cm}^{-1}$  other two do. This raises the question of whether the 10 para orange-yellow stamp is original, as claimed by experts, and, if so, were two different sorts of papers used for printing the same set of stamps in Vienna?

If the spectra of the dyes of original and fake stamps are compared, in most, but not all cases, there are differences between the legal issues and those made for criminal purposes. When 10 para orange-yellow colour was compared (Fig. 5), ribbons existing in spectra of original stamp at  $1510$  and  $1536\text{ cm}^{-1}$  do not exist in the spectra of the forgeries. The pink dye used for printing the 20 para stamp (Fig. 6) in Vienna exhibits peaks at  $1284$ ,  $1253$  and  $1557\text{ cm}^{-1}$ , not seen in the forgeries, while some, but not all fakes, do have a specific peak at  $1733\text{ cm}^{-1}$  not observed in the original. Minimal differences exist in the spectra of the blue dye used for the 40 para stamp, some of the peaks in original ( $1543$  and  $558\text{ cm}^{-1}$ ) are more intense than in the forgeries (Fig. 7).

Comparison between spectra of original stamps of 1 para and 2 para, as well as between the certified originals and proven forgeries did not show such spectacular results as in case of the "Vienna issues". When the spectra of the paper of two originals were compared (Figs. 8 and 9), they did not show any differences, which is to be expected since they were printed in same printing house in Belgrade, and at the same time. However, more interesting and a bit unexpected is the fact that there is no differences between the original of 1 para and the compared fake, and between of original of 2 para and the analyzed fakes (Figs. 8 and 9). Bearing in mind that the stamps were issued in 1868 and that, most probably, the forgeries were made decades later, when philately and values of rare post stamps came into the focus of collectors worldwide, the credit is due to counterfeiters who used the same paper as the original one, at a time when analytical methods were not widely accessible.

Based on the information extracted from the IR spectra after their processing with PeakFit software, the values of the wavenumbers for dyes of 1 and 2 para originals stamps and proven forgeries were obtained and are shown in Tables II and III.

TABLE II. Wavenumber values ( $\text{cm}^{-1}$ ) of dyes of original and forged 1 para green post stamps

| Original | Forgery 1 | Forgery 2 | Forgery 3 | Forgery 4 | Forgery 5 | Forgery 6 | Forgery 7 | Forgery 8 |
|----------|-----------|-----------|-----------|-----------|-----------|-----------|-----------|-----------|
| 580      | 551       | 571       | 571       | 532       | 549       | 572       | 539       | 570       |
| 566      | 499       | 483       | 490       | 473       | 486       | 554       | 482       | 471       |
| 520      | 464       | 456       | 462       |           | 452       | 486       |           |           |
| 501      |           |           |           |           |           | 473       |           |           |
| 468      |           |           |           |           |           |           |           |           |
| 428      |           |           |           |           |           |           |           |           |

This information is compared to the spectral data of the most frequently used green (Table IV), red (Table V) and yellow (Table VI) pigments, and it was concluded that green malachite pigment ( $\text{CuCO}_3 \cdot \text{Cu(OH)}_2$ ) was used for the 1 para stamps, while a mixture of lead contained red ( $\text{Pb}_3\text{O}_4$ ), and yellow ( $\text{PbO}$ ) pigments was used for the 2 para stamps.

TABLE III. Wavenumber values ( $\text{cm}^{-1}$ ) of dyes of original and forged 2 para reddish-brown stamps

| Original red | Original yellow | Forgery 1 | Forgery 2 | Forgery 3 | Forgery 4 |
|--------------|-----------------|-----------|-----------|-----------|-----------|
| 526          | 581             | 596       | 568       | 548       | 578       |
| 511          | 504             | 574       | 485       | 491       | 481       |
| 450          | 494             | 466       |           | 463       |           |
| 440          | 482             |           |           |           |           |
|              | 466             |           |           |           |           |
|              | 413             |           |           |           |           |

TABLE IV. Wavenumbers ( $\text{cm}^{-1}$ ) of the most frequently used green pigments

| Bohemian Green | $\text{Cr}_2\text{O}_3$ | Cobalt Green ( $\text{CoO} \cdot \text{ZnO}$ ) | Malachite ( $\text{CuCO}_3 \cdot \text{Cu(OH)}_2$ ) | Vagone Green Earth | Verdigris Green ( $(\text{Cu}(\text{CH}_3\text{COO})_2 \cdot 2\text{Cu(OH)}_2$ ) | Green ( $\text{Cr}_2\text{O}_3 \cdot 2\text{H}_2\text{O}$ ) |
|----------------|-------------------------|--|---|--------------------|--|---|
| 497            | 571                     | 409  | 581   | 519                | 561  | 570   |
| 462            | 445                     | 327  | 571   | 498                | 521  | 559   |
| 437            | 416                     | 250  | 523   | 465                | 460  | 496   |
| 397            | 307                     | 230  | 501   | 415                | 374  | 477   |
|                | 227                     |  | 464   | 382                | 327  | 422   |
|                |                         |  | 427   | 315                | 271  | 386   |
|                |                         |  | 386   |                    | 253  |   |
|                |                         |  | 355   |                    |  |   |
|                |                         |  | 322   |                    |  |   |

TABLE V. Wavenumbers ( $\text{cm}^{-1}$ ) of the most frequently used red pigments

| Cadmium Red ( $\text{CdS} + \text{CdSe}$ ) | Caput Mortuum Reddish (Fe <sub>2</sub> O <sub>3</sub> +silicate) | Cinabarite (HgS) | Red Earth (Fe <sub>2</sub> O <sub>3</sub> +kaoline) | Pompeian Red (Fe <sub>2</sub> O <sub>3</sub> +kaoline) | Minium (Pb <sub>3</sub> O <sub>4</sub> ) | Venetian Red (Fe <sub>2</sub> O <sub>3</sub> +gypsum) |
|--|--|------------------|---|--|--|---|
| 272  | 528  | 342              | 537   | 534  | 528                                      | 460   |
| 268  | 458  | 301              | 467   | 466  | 513                                      | 446   |
| 258  | 379  | 284              | 431   | 428  | 454                                      | 422   |
| 230  | 294  | 280              | 396   | 334  | 442                                      | 377   |
|  |  | 268              | 366   | 318  | 381                                      | 354   |
|  |  |                  | 344   | 300  | 334                                      | 301   |
|  |  |                  | 336   | 272  | 326                                      | 255   |
|  |  |                  | 321   | 234  |  | 237   |
|  |  |                  | 297   |  |  |   |

The spectra of coloured sectors of the original stamps were different from the same spectra of the fake stamps, forged stamp of 1 para has a peak at  $2099\text{ cm}^{-1}$ , not seen in the original (Fig. 10), while in case of the 2 para stamp, there are peaks at  $910$  and  $2854\text{ cm}^{-1}$  which are not seen in the spectra of the fake stamps, while there is a band at  $1005\text{ cm}^{-1}$  in the spectrum of original, while the forged stamp exhibited a shoulder (Fig. 11).

TABLE VI. Wavenumbers ( $\text{cm}^{-1}$ ) of the most frequently used yellow pigments

| Barium yellow<br>( $\text{BaCrO}_4$ ) | Cadmium yellow<br>( $\text{CdS}$ ) | Chromium yellow<br>( $\text{PbCrO}_4$ ) | Lead yellow<br>( $\text{PbO}$ ) |
|---------------------------------------|------------------------------------|---|---------------------------------|
| 418                                   | 261                                | 464                                     | 582                             |
| 391                                   | 247                                | 384                                     | 503                             |
| 374                                   |                                    | 377                                     | 495                             |
| 336                                   |                                    | 279                                     | 484                             |
| 238                                   |                                    | 262                                     | 464                             |
|                                       |                                    |   | 415                             |
|                                       |                                    |   | 375                             |

#### CONCLUSIONS

FTIR-ATR spectroscopy, as a non-destructive and reliable technique, was used for the analysis of certified originals of Principality of Serbia stamps issued in 1866 and 1868 and their forgeries. Differences between the paper used for original and fake stamps was, in most but not all examined samples, clearly established. Moreover, the applied spectroscopy was a powerful tool not only for differentiation of the dyes used for originals and fakes, but also, in cases of 1 and 2 para issues of 1868, a tool for identification of pigments used (green malachite ( $\text{CuCO}_3\cdot\text{Cu}(\text{OH})_2$ ) for 1 para stamps, mixture of lead contained red ( $\text{Pb}_3\text{O}_4$ ) and yellow ( $\text{PbO}$ ) for the 2 para stamp). The difference between the papers used for the printing of 1866 issue has been established, and the possibility that the so-called "Vienna issues" may not have been printed at the same time or in the same printing house has been proposed. FTIR-ATR spectroscopy was proven to be valuable method for comprehensive analysis of potential philatelic forgeries.

*Acknowledgement.* This study was supported by the Ministry of Education, Science and Technological Development of Republic of Serbia (Contract Nos.: 451-03-9/2021-14/200168 and 451-03-9/2021-14/200026).

## И З В О Д

ПРОФЕСОРУ ПЕТРУ ПФЕНТУ, *IN CALIDUM, ET PLURIUM RETRIBUTIVUS MEMORIAE:*  
 FTIR-ATR АНАЛИЗА ОРИГИНАЛНИХ ПОШТАНСКИХ МАРАКА КНЕЖЕВИНЕ СРБИЈЕ  
 ИЗДАТИХ ИЗМЕЂУ 1866. И 1868. ГОДИНЕ И ЊИХОВИХ ФАЛСИФИКАТА

АЛЕКСАНДАР ПОПОВИЋ<sup>1</sup>, БОБАН АНЂЕЛКОВИЋ<sup>2</sup>, ДРАГАНА ЂОРЂЕВИЋ<sup>3</sup>, САЊА САКАН<sup>3</sup>, ЉУБОДРАГ  
 ВУЈИСИЋ<sup>1</sup>, САВА ВЕЛИЧКОВИЋ<sup>4</sup> и ДУБРАВКА РЕЛИЋ<sup>1</sup>

<sup>1</sup>Хемијски факултет, Универзитет у Београду, Студентски трг 12–16, Београд, <sup>2</sup>ИХТМ – Центар за хемију, Универзитет у Београду, Нђетошева 12, Београд, <sup>3</sup>Центар изузетних вредносци за хемију и  
 нановерине живојне средине – ИХТМ, Универзитет у Београду, Нђетошева 12, Београд и  
<sup>4</sup>Технолошко-мешавински факултет, Универзитет у Београду, Карнејевића 4, Београд

Како би се утврдиле могућности коришћења FTIR-ATR као недеструктивне и поуздане технике за анализу поштанских марака, анализирани су оригинални и фалсификати марака Кнезевине Србије издате 1866. и 1868. године. Снимљени су спектри који су омогућили поређење папира, боја и гуме оригинална такозваних „Бечког издања“ вредности 10 (наранџасто-жута), 20 (ружичаста) и 40 (плава) пара, „Београдског издања“ (1 паре-светло и тамно зелена и 2 паре – црвенкасто-смеђа) као и 12 фалсификата, које су као и оригиналне, сертификовали овлашћени испитивачи. Показано је да је примењена аналитичка метода у већини случајева погодна и да је њеним коришћењем могуће разликовати папир и боју оригинална од фалсификата који су, готово извесно, штампани неколико деценија касније. Утврђене су и разлике у папиру између оригинална истог издања, па је предложена могућност, по први пут у филателистичкој историји, да су марке „Бечког издања“ штампане на два различита папира, а имајући у виду тадашњу технологију штампања, могуће чак и у различито време или различитој штампарији.

(Примљено 1. септембра, ревидирано 29. октобра, прихваћено 1. новембра 2021)

## REFERENCES

1. Z. Sevic, in: *German Minorities in Europe: Ethnic Identity and Cultural Belonging*, S. Wolff, Ed., Berghahn Books, New York, 2001, pp. 143–164 (ISBN 978-1-57181-504-0)
2. D. Vitorović, P. Pfendt, *An. Acad. Bras. Ciencia* **45** (1974) 49
3. P. Polić, P. Pfendt, *J. Serb. Chem. Soc.* **56** (1991) 241
4. G. J. Dević, M. M. Šaban, P. A. Pfendt, *J. Serb. Chem. Soc.* **61** (1996) 985
5. D. Manojlović, M. Todorović, J. Jovićić, V. D. Krsmanović, P. A. Pfendt, R. Golubović, *Desalination* **213** (2007) 104 (<https://doi.org/10.1016/j.desal.2006.05.058>)
6. M. Radenković, D. Đorđević, J. Joksić, S. Đogo, P. Pfendt, J. Raičević, *Cent. Eur. J. Occup. Environ. Med.* **9** (2003) 327 ([https://www.nnk.gov.hu/cejoem/Volume9/Vol9\\_No4/CE03\\_4-15.html](https://www.nnk.gov.hu/cejoem/Volume9/Vol9_No4/CE03_4-15.html))
7. P. A. Pfendt, B. Janković, J. Čučković, *Kem. Ind.* **29** (1980) 479
8. A. Topalovic, L. B. Pfendt, N. Perovic, D. Djordjevic, S. Trifunovic, P. A. Pfendt, *J. Serb. Chem. Soc.* **71** (2006) 1219 (<https://doi.org/10.2298/JSC0611219T>)
9. V. Z. Jovanović, P.A. Pfendt, A. J. Filipović, *Russ. J. Phys. Chem., A* **81** (2007) 1482 (<https://doi.org/10.1134/S0036024407090269>)
10. P. Pfendt, *Hemisiski pregled* **20** (1979) 22 (in Serbian)
11. B. G. Harrison, *J. Royl. Soc. Arts* **88** (1940) 650
12. T. Lewes, E. L. Pemberton, *Forged stamps: how to detect them*. Colston and Son, Edinburgh, 1863, p. 36 ([https://openlibrary.org/works/OL16522625W/Forged\\_stamps](https://openlibrary.org/works/OL16522625W/Forged_stamps))

13. V. Fleck, *Handbook of stamps of Croatian countries*, Hrvatski filatelički savez, Zagreb, 1942 (in Croatian)
14. L. Suranyi, *Barely Emissions of Baranya*, Magyar Beleyeggyujtok Orszagos Szovetsege, Budapest, 1979 (in Hungarian)
15. P. Strpić, *Postage stamps Croatia 2009/2010*, Lokas dizajn, Zagreb, 2009 (ISBN 978-953-95978-3-0) (in Croatian)
16. C. E. Brainard, *Catalogue of Hungarian Occupation Issues*, C. E. Brainard, Ed., Cherry Hill, NJ, 2006
17. I. J. Maybury, D. Howell, M. Terras, H. Viles, *Herit. Sci.* **6** (2018) 42 (<https://doi.org/10.1186/s40494-018-0206-1>)
18. J. S. Gomez-Jeria, E. Clavijo, *Chem. Res. J.* **2** (2017) 191 (<https://chemrj.org/download/vol-2-iss-4-2017/chemrj-2017-02-04-191-197.pdf>)
19. A. Munajad, C. Subroto, Suwarno, *Energies* **11** (2018) 364 (<https://doi.org/10.3390/en11020364>)
20. V. Librando, Z. Minniti, S. Lorusso, *Conserv. Sci. Cult. Heritage* **11** (2011) 249 (<https://doi.org/10.6092/issn.1973-9494/2700>)
21. W. Dirwono, J. Sook Park, M.vR. Agustin-Camacho, J. Kim, H.-M. Park, Y. Lee, K.-B. Lee, *Forensic Sci. Int.* **199** (2010) 6 (<https://doi.org/10.1016/j.forsciint.2010.02.009>)
22. J. Žiljak Gršić, *Polytechnic Design* **7** (2019) 199 (<https://doi.org/10.19279/TVZ.PD.2019-7-3-17>)
23. J. S. Gomez-Jeria, E. Clavijo, J. J. Carcamo-Vega, S. Gutierrez, *Res. J. Pharm. Biol. Chem. Sci.* **10** (2019) 1565 ([https://www.rjpbcos.com/pdf/2019\\_10\(2\)/\[213\].pdf](https://www.rjpbcos.com/pdf/2019_10(2)/[213].pdf))
24. N. Ferrer, A. Vila, *Anal. Chim. Acta* **555** (2006) 161 (<https://doi.org/10.1016/j.aca.2005.08.080>)
25. E. Imperio, G. Giancane, L. Valli, *Anal. Chem.* **85** (2013) 7085 (<https://pubs.acs.org/doi/10.1021/ac401067r>)
26. T. D. Chaplin, A. Jurado-Lopez, R. J. H. Clark, D. R. Beech, *J. Raman Spectrosc.* **35** (2004) 600 (<https://doi.org/10.1002/jrs.1208>)
27. T. E. Gill, in: *Proceedings of the XI International Conference on PIXE and its Analytical Applications*, 2007, Puebla, Mexico [https://www fisica.unam.mx/pixe2007/Downloads/Proceedings/PDF\\_Files/PIXE2007-PI-42.pdf](https://www fisica.unam.mx/pixe2007/Downloads/Proceedings/PDF_Files/PIXE2007-PI-42.pdf)
28. *Stamp-Collecting-World*, [https://www.stamp-collecting-world.com/serbiastamps\\_1866d.html](https://www.stamp-collecting-world.com/serbiastamps_1866d.html) (accessed on July 25<sup>th</sup>, 2021)
29. Z. Šafar, *Catalogue of postage stamps in use on the territory of Serbia 1840–2011*, Srpski filatelički klub, Belgrade, 2011 (in Serbian).



## Significance of infrared spectroscopic branching factor for investigation of structural characteristics of alkanes, geochemical properties and viscosity of oils

JELENA Z. STEVANOVIĆ<sup>1</sup>, ANTON R. RAKITIN<sup>1</sup>, IVAN D. KOJIĆ<sup>2</sup>,  
NIKOLA S. VUKOVIĆ<sup>3</sup> and KSENIJA A. STOJANOVIC<sup>4\*</sup>

<sup>1</sup>STC-NIS Naftagas, Upstream Laboratory, Put šajkaškog odreda 9, 21000 Novi Sad, Serbia,

<sup>2</sup>University of Belgrade, Innovation Center of the Faculty of Chemistry, Studentski trg 12–16,  
11000 Belgrade, Serbia, <sup>3</sup>Municipality of Kladovo, Kralja Aleksandra 35, 19320 Kladovo,  
Serbia and <sup>4</sup>University of Belgrade, Faculty of Chemistry, Studentski trg 12–16,  
11000 Belgrade, Serbia

(Received 30 August, accepted 1 November 2021)

**Abstract:** A detailed investigation of significance of the infrared (IR) spectroscopic branching factor ( $\text{CH}_2/\text{CH}_3$ ; the ratio of methylene and methyl group peak heights at 2917–2921 and 2951–2954  $\text{cm}^{-1}$ , respectively in the IR spectra) for characterization of alkane structure, geochemical properties and viscosity of 76 oil samples was performed. These oils, originating from 13 Serbian oil fields in SE Pannonian Basin, differ according to source and depositional environment of organic matter (OM), as well as by thermal maturity and biodegradation stage. Methylene and methyl asymmetric stretching peak absorbances were used for the branching factor calculation.  $\text{CH}_2$  peak positions exhibited 3–4  $\text{cm}^{-1}$  red shift with increasing the  $\text{CH}_2/\text{CH}_3$  ratio, due to a greater contribution of *trans* vs. *gauche* rotamers in aliphatic chains. Comparing IR spectra of the oils and model *n*-alkanes, it was established that the average  $(\text{CH}_2)_n$  methylene chain length per  $\text{CH}_3$  group varied from  $n = 3.5$  to 6.5. The  $\text{CH}_2/\text{CH}_3$  ratio showed significant concordance with geochemical parameters, enabling clear distinction of the oils according to source and depositional environment of OM. At the same time, dependence of the  $\text{CH}_2/\text{CH}_3$  ratio on oil maturity in the range from immature to mature was not observed, allowing for an accurate determination of oil genetic types irrespective of maturity. The  $\text{CH}_2/\text{CH}_3$  ratio showed good accordance with oil biodegradation scale and oil viscosity.

**Keywords:** infrared spectroscopy; alkane branching; oil genetic types; viscosity; Serbian oil fields; Pannonian Basin.

\* Corresponding author. E-mail: ksenija@chem.bg.ac.rs  
<https://doi.org/10.2298/JSC210830091S>

## INTRODUCTION

Normal and branched alkanes, as the most thoroughly studied components of crude oil, play a crucial role in organic geochemistry, helping to genetically relate oils and source rocks.<sup>1,2</sup> Normal to branched alkane ratio is also an important characteristic of crude oil feedstock, determining detonability and performance characteristics of gasoline, kerosene pour point and diesel fuel flammability.<sup>3</sup>

Infrared spectroscopy is a rapid and robust analytical technique, which avoids the use of hazardous organic solvents. The method has a long and fruitful application history with group structure analysis of oil, allowing to collect information on all of its components regardless of class and molecular weight.<sup>4–6</sup> Methyl and methylene absorption bands are unhindered by aromatics and other functionalities peaks, thus offering several approaches to quantify a degree of alkane branching.<sup>7</sup>

For oil hydrocarbons, the stretching vibrations of CH bonds in the 2800 to 3000 cm<sup>-1</sup> region are the strongest. Zenker's early work on long-chain aliphatics<sup>8</sup> demonstrated linear dependence of the CH<sub>2</sub>/CH<sub>3</sub> asymmetric stretching peak ratio on (CH<sub>2</sub>)<sub>n</sub> methylene chain length for *n* = 5–18. This ratio was subsequently widely applied to characterize aliphatics branching in saturated fraction, polar fraction and asphaltenes in crude oils,<sup>9–11</sup> bitumens,<sup>12</sup> coals<sup>13,14</sup> and shales,<sup>15,16</sup> due to its convenient greater-than-unity scale and clear physical meaning as a measure of the average length of unsubstituted (CH<sub>2</sub>)<sub>n</sub> methylene chain per methyl group.

Considering the importance of alkane branching for organic geochemistry and oil refining, the authors believe that potential of the spectroscopic CH<sub>2</sub>/CH<sub>3</sub> branching factor (representing the ratio of methylene and methyl group peak heights at 2917–2921 cm<sup>-1</sup> and 2951–2954 cm<sup>-1</sup>, respectively in the IR spectra) has so far been largely underutilized. For the most part, the CH<sub>2</sub>/CH<sub>3</sub> ratio from IR experiments has been used solely as an indicator of the relative abundance of methylated saturated hydrocarbons.<sup>17–19</sup> Therefore, the paper is aimed at a more detailed investigation of the significance of this parameter for the characterization of alkane structure, geochemical properties and viscosity of oils.

## EXPERIMENTAL

### *Samples*

A set of 76 oil samples originating from 13 Serbian oil fields in SE Pannonian Basin was studied. The oils in this set differ according to source and depositional environment of precursor OM, as well as thermal maturity and biodegradation degree.

Experiments were performed on water-free crude oils, obtained by refluxing of well fluid at 60 °C for 48 h, and on individual model *n*-alkanes: *n*-octane (Alfa Aesar, Germany, > 98 % pure); *n*-nonane and *n*-dodecane (Fluka, Germany, > 99 % pure); *n*-tetradecane, *n*-pentadecane, *n*-hexadecane and *n*-heptadecane (Chem-Lab NV, Belgium, > 99 % pure).

### Methods

*Infrared spectroscopy (IR).* Absorbance IR spectra were recorded on a Thermo Nicolet 380 FTIR spectrometer, equipped with a DTGS detector and a Smart Orbit Diamond ATR accessory, by averaging over 1024 scans in the 500–4000 cm<sup>-1</sup> interval at 4 cm<sup>-1</sup> resolutions using OMNIC software, without additional corrections or processing. Background single-beam spectrum of air was collected prior to each single-beam sample spectrum. High viscosity and strong absorption of the oils precluded spectra collection using cells for liquid samples and KBr tablets. These difficulties were alleviated by the attenuated total reflectance (ATR) technique, providing measurement convenience and respectable signal-to-noise ratio. Repeatability and accuracy were confirmed by comparing spectra obtained from triplicate measurements on the same sample, the root-mean-square coordinate difference (*RSMD*) of peak positions being less than 0.5 cm<sup>-1</sup>.

*Gas chromatography (GC).* GC analysis of whole oils was performed using a Chromatec Chrystal 9000 gas chromatograph (non-polar capillary CP-Sil 5 CB column, 30 m×0.53 mm, 1.5 µm film thickness, He carrier gas at 17.2 cm<sup>3</sup> min<sup>-1</sup> flow rate) with a flame ionization detector (FID). On-column injection was performed using an autosampler. Prior to injection, the samples were diluted with carbon disulfide in 1:10 ratio. The inlet was heated from 40 °C to 310 °C at a rate of 50 °C min<sup>-1</sup>. The following oven temperature program was used: heating from 0 °C (with 2 min initial hold) to 305 °C, at a rate of 15 °C min<sup>-1</sup>, and then isothermal at 305 °C for 57 min. FID temperature was 350 °C. Individual peaks were identified by comparison of their retention times with those of a standard mixture of hydrocarbons. Quantification of the compounds used for calculation of geochemical molecular parameters was performed by integrating peak areas using Chromatec Analytic software.

*Viscosity measurements.* Dynamic viscosity of oils was measured using an Anton Paar MCR 302 rheometer in a rotational mode, at a shear rate of 10 s<sup>-1</sup> and following a temperature program from 50–60 °C to 10–15 °C with a rate of cooling of 1 °C min<sup>-1</sup>.

## RESULTS AND DISCUSSION

### *Significance of the branching factor for structural characterization of oils*

Typical IR spectra of the samples are shown in Fig. 1. Assignment of the principal absorption bands is straightforward: 2951–2954/2917–2921 cm<sup>-1</sup> and 2868–2871/2849–2852 cm<sup>-1</sup> are CH<sub>3</sub>/CH<sub>2</sub> asymmetric and symmetric stretching; 1462–1465 cm<sup>-1</sup> is CH<sub>2</sub> symmetric bending; 1456–1457 cm<sup>-1</sup> and 1376–1377 cm<sup>-1</sup> are CH<sub>3</sub> asymmetric and symmetric bending; 740–744 cm<sup>-1</sup> and 719–729 cm<sup>-1</sup> are (CH<sub>2</sub>)<sub>3</sub> and (CH<sub>2</sub>)<sub>4+</sub> rocking vibrations, respectively.<sup>7</sup> As opposed to other well-resolved CH<sub>2</sub> and CH<sub>3</sub> features, methyl symmetric stretching mode is evident in most spectra only in the form of a plateau. Tertiary CH vibrations absorb around 2890–2900 cm<sup>-1</sup> and are present as a weak shoulder on the low wavenumber slope of CH<sub>2</sub> asymmetric stretching peak.<sup>7</sup>

Classification of the oils into the groups is given in Tables I–III.

Near-baseline absorbance values in the 3000–3100 cm<sup>-1</sup> region, together with weak peaks around 1600 and 810 cm<sup>-1</sup> due to C=C and out-of-plane aromatic CH bending, respectively, point out to a low concentration of highly substituted aromatics in the oils studied, which is in agreement with a general trend of

alkylated aromatic rings prevalence over non-substituted ones in crude oils worldwide. Very weak absorbance around  $1700\text{ cm}^{-1}$  is registered in some samples, attesting to the presence of C=O stretching, that is in accordance with low acid numbers, not exceeding  $0.4\text{ mg KOH/g}$  for non-biodegraded oils.

$\text{CH}_2/\text{CH}_3$  branching factor was calculated as the ratio of methylene and methyl group peak heights at  $2917\text{--}2921\text{ cm}^{-1}$  and  $2951\text{--}2954\text{ cm}^{-1}$ , respectively. Peak heights were measured from a flat baseline drawn at  $3100\text{ cm}^{-1}$  absorbance value. From Fig. 1B it is evident that with increasing  $\text{CH}_2/\text{CH}_3$  branching factor, both methylene peak positions shift to lower wavenumbers. According to Fig. S-1A and B of the Supplementary material to this paper, when the  $\text{CH}_2/\text{CH}_3$  ratio increases from 2.0–2.4 to 3.0–3.4, the corresponding shift comprises 3–4  $\text{cm}^{-1}$ , while methyl peak position essentially fluctuates between 2952 and 2954  $\text{cm}^{-1}$  without a pronounced trend (Fig. S-1C).

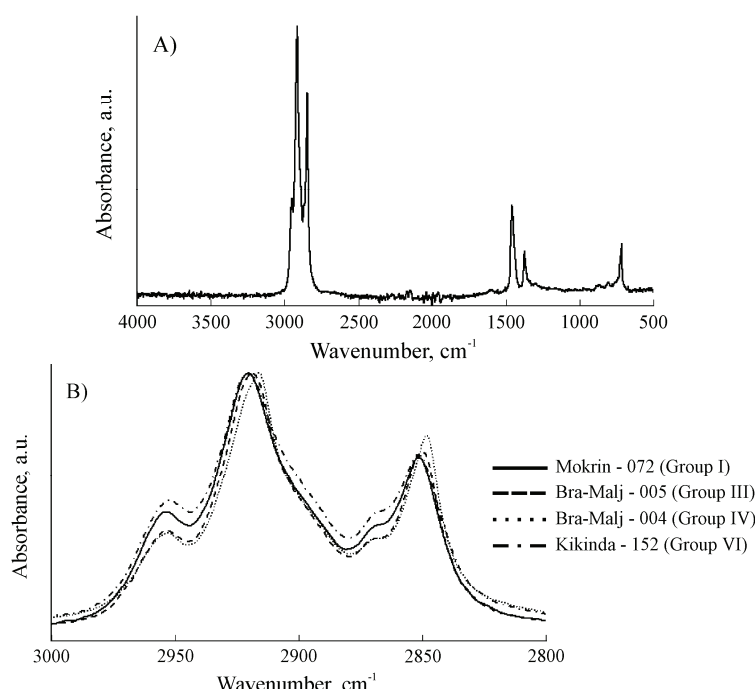


Fig. 1. A) Full IR spectrum of Maljurevac-Bubušinac-004 oil sample; B) stretching region of IR spectra of Mokrin-072 (group I), Bradarac-Maljurevac-005 (group III), Bradarac-Maljurevac-004 (group IV) and Kikinda-152 (group VI) samples.

From infrared studies of phospholipid cell membranes,<sup>20</sup> it is well known that  $\text{CH}_2$  stretching vibrations are sensitive to the *trans/gauche* ratio in lipids' hydrophobic tails. Gel to liquid crystal phase transition upon temperature increase is accompanied by a 3–4  $\text{cm}^{-1}$  methylene peak shift to higher wavenumbers simi-

TABLE I. Geochemical data, the IR branching factor ( $\text{CH}_2/\text{CH}_3$ ), geochemical parameters and the methylene to methyl group number ratio ( $N(\text{CH}_2)/N(\text{CH}_3)$ ) for group I (aquatic origin, reducing environment, non-biodegraded) and group II (oxic environment, non-biodegraded) oils; parameter average value and standard deviation (in parentheses)

| Group | Oil field                   | No. of samples maturity | $\text{CH}_2/\text{CH}_3$ | $I/HCP^a$ | $TAR^b$ | $P_{\text{r}}/P_{\text{h}}^c$ | $\text{Pr}/n\text{-C}_{17}^d$ | $\text{Ph}/n\text{-C}_{18}^e$ | $ACL$<br>$(n\text{-C}_{17}^f - n\text{-C}_{40})^f$ | $n\text{-Alkane}$<br>maximum(s)                     | $\Sigma(n\text{-C}_{10}-n\text{-C}_{40})^g$<br>$/\Sigma(i\text{-C}_{13}-i\text{-C}_{20})^g$ | $N(\text{CH}_2)/N(\text{CH}_3)^h$ |
|-------|-----------------------------|-------------------------|---------------------------|-----------|---------|-------------------------------|-------------------------------|-------------------------------|--|---|---|-----------------------------------|
| I     | Elemir                      | 1                       | M <sup>i</sup>            | 2.18      | 2.23    | 0.42                          | 0.96                          | 0.78                          | 0.86   | 16.80   | C <sub>9</sub>  | 5.09                              |
| I     | Kikinda-Varoš               | 1                       | M                         | 2.20      | 2.01    | 0.42                          | 0.67                          | 0.67                          | 0.85   | 17.43   | C <sub>14</sub>   | 5.94                              |
| I     | Mokrin (western part)       | 2                       | MM <sup>j</sup>           | 2.22      | 1.91    | 0.49                          | 0.76                          | 0.77                          | 1.04   | 17.63   | C <sub>14</sub> -C <sub>15</sub>  | 4.89 (0.01)                       |
| I     | Palić                       | 13                      | MM                        | 2.18      | 2.36    | 0.38                          | 0.74                          | 0.70                          | 1.00   | 18.05   | C <sub>13</sub> -C <sub>16</sub>  | 5.01 (0.42)                       |
| I     | Turija-sever (western part) | 7                       | IM <sup>k</sup>           | 2.22      | 1.41    | 0.38                          | 0.86                          | 0.98                          | 1.14   | 19.66   | C <sub>15</sub> , C <sub>19</sub>   | 5.26 (0.42)                       |
| I     | All group I oils            | 24                      | IM-M                      | 2.19      | 2.03    | 0.51                          | 0.79                          | 0.79                          | 1.04   | 18.45   | C <sub>9</sub> , C <sub>13</sub> -C <sub>16</sub> ,   | 5.08 (0.37)                       |
| II    | Kikinda-Kikinda-Polje       | 8                       | M                         | 2.26      | 2.49    | 0.32                          | 1.14                          | 0.48                          | 0.48   | 15.55   | C <sub>8</sub> , C <sub>9</sub> ,   | 6.01 (1.26)                       |
| II    | Mokrin (central part)       | 2                       | M                         | 2.43      | 2.78    | 0.29                          | 1.14                          | 0.37                          | 0.38   | 16.61   | C <sub>13</sub>   | 8.98 (0.03)                       |
| II    | Idoš (central part)         | 3                       | MM                        | 2.34      | 1.54    | 0.56                          | 1.38                          | 0.70                          | 0.59   | 18.14   | C <sub>14</sub> -C <sub>15</sub>  | 7.06 (0.40)                       |
| II    | All group II oils           | 13                      | MM-M                      | 2.31      | 0.37    | 1.19                          | 0.51                          | 0.49                          | 16.31  | C <sub>8</sub> , C <sub>9</sub> , C <sub>11</sub> , | 6.71 (1.47)   |                                   |
|       |                             |                         |                           | (0.08)    | (0.46)  | (0.11)                        | (0.13)                        | (0.12)                        | (0.08)   | (1.19)  | C <sub>13</sub> -C <sub>15</sub>  | (0.14)                            |

<sup>a</sup>Low vs. high carbon preference index of *n*-alkanes, calculated according to the following formula:  $I/HCP_I = (n\text{-C}_{17} + n\text{-C}_{18} + n\text{-C}_{19})/(n\text{-C}_{27} + n\text{-C}_{29} + n\text{-C}_{31})$ ; <sup>b</sup>terigenous/aquatic ratio of *n*-alkanes, calculated according to the following formula:  $TAR = (n\text{-C}_{15} + n\text{-C}_{17} + n\text{-C}_{19})/(n\text{-C}_{27} + n\text{-C}_{29} + n\text{-C}_{31})$ ; <sup>c</sup>pristane (2,6,10,14-tetramethylpentadecane)/phytane (2,6,10,14-tetramethylhexadecane) ratio calculated from peak areas of these compounds in gas chromatograms; <sup>d</sup>phytane (2,6,10,14-tetramethylpentadecane)/*n*-heptadecane ratio, calculated from peak areas of these compounds in gas chromatograms; <sup>e</sup>average chain length of *n*-alkanes; <sup>f</sup>average chain length of *n*-alkanes; <sup>g</sup> $\Sigma(i\text{-C}_{10}-i\text{-C}_{40})/\Sigma(i\text{-C}_{13}-i\text{-C}_{20})$  = sum of C<sub>10</sub> to C<sub>40</sub> *n*-alkanes/sum of C<sub>13</sub> to C<sub>20</sub> regular isoprenoids; <sup>h</sup>methylene to methyl group number ratio; <sup>i</sup>mature; <sup>j</sup>moderately mature; <sup>k</sup>immature

TABLE II. Geochemical data, the IR branching factor ( $\text{CH}_2/\text{CH}_3$ ), geochemical parameters and the methylene to methyl group number ratio ( $(\text{N}(\text{CH}_2)/\text{N}(\text{CH}_3))$ ) for group III (terrestrial origin,oxic environment, non-biodegraded), group IV (terrestrial origin, reducing environment, non-biodegraded) and group V (prevailing terrestrial origin, oxic environment, non-biodegraded) oils; parameter average value and standard deviation (in parentheses); for the abbreviations, see Table I

| Group             | Oil field                   | No. of samples | Oil maturity | $\text{CH}_2/\text{CH}_3$ | LHCPI          | TAR            | $\text{Pr}/\text{Ph}$ | $\text{Pr}/n\text{-C}_{17}$ | $\text{Ph}/n\text{-C}_{18}$ | $n\text{-C}_{17}/n\text{-C}_{40}$ | $n\text{-Alkane maximum(s)}$                                 | $\Sigma(n\text{-C}_{10}-n\text{-C}_{40})/\Sigma(i\text{-C}_{13}-i\text{-C}_{20})$ | $n\text{-C}_{10}/n(\text{CH}_2)$ |
|-------------------|-----------------------------|----------------|--------------|---------------------------|----------------|----------------|-----------------------|-----------------------------|-----------------------------|-----------------------------------|--|---|----------------------------------|
| III               | Iđoš (western part)         | 2              | IM           | 3.03<br>(0.11)            | 0.80<br>(0.04) | 1.07<br>(0.36) | 1.77<br>(0.08)        | 0.65<br>(0.12)              | 0.41<br>(0.03)              | 21.33<br>(0.03)                   | $\text{C}_{27}$  | 11.91 (1.43)  | 5.64 (0.22)                      |
| III               | Sirakovo                    | 3              | MM           | 3.14<br>(0.09)            | 1.33<br>(0.07) | 0.61<br>(0.04) | 1.05<br>(0.06)        | 0.29<br>(0.01)              | 0.30<br>(0.03)              | 20.60<br>(0.39)                   | $\text{C}_{15}$  | 12.59 (0.63)  | 5.85 (0.18)                      |
| III               | Bradarac-Maliurevac         | 2              | IM-MM        | 3.35<br>(0.13)            | 1.07<br>(0.01) | 0.75<br>(0.40) | 1.30<br>(0.03)        | 0.35<br>(0.08)              | 0.31<br>(0.08)              | 21.32<br>(0.86)                   | $\text{C}_{15}$  | 12.80 (0.24)  | 6.25 (0.25)                      |
| III               | All group III oils          | 7              | IM-MM        | 3.17<br>(0.16)            | 1.10<br>(0.24) | 0.78<br>(0.21) | 1.33<br>(0.39)        | 0.41<br>(0.17)              | 0.33<br>(0.08)              | 21.01<br>(0.57)                   | $\text{C}_{15}, \text{C}_{27}$                               | 12.46 (0.80)  | 5.90 (0.31)                      |
| IV                | Maliurevac-Bubušinac        | 5              | IM           | 2.78<br>(0.12)            | 0.92<br>(0.09) | 0.95<br>(0.11) | 0.60<br>(0.20)        | 0.46<br>(0.07)              | 0.65<br>(0.09)              | 21.11<br>(0.87)                   | $\text{C}_{23}, \text{C}_{25}, \text{C}_{27}$                | 10.62 (1.65)  | 5.15 (0.24)                      |
| All group IV oils |                             |                |              |                           |                |                |                       |                             |                             |                                   |  |   |                                  |
| V                 | Turija-sever (eastern part) | 7              | IM           | 2.60<br>(0.03)            | 0.93<br>(0.06) | 1.00<br>(0.09) | 1.08<br>(0.10)        | 0.63<br>(0.05)              | 0.63<br>(0.09)              | 20.50<br>(0.50)                   | $\text{C}_{14}, \text{C}_{15}, \text{C}_{29}, \text{C}_{31}$ | 9.36 (0.56)   | 4.82 (0.06)                      |
| All group V oils  |                             |                |              |                           |                |                |                       |                             |                             |                                   |  |   |                                  |

lar in magnitude to the one observed in the current study. The shift reflects higher tale mobility and disorder, as well as appearance of *gauche* conformations in the initially all-*trans* polymethylene fragments. In turn, quantum mechanical calculations predict significant lowering of *trans* to *gauche* transition energy barrier of linear alkanes upon methylation,<sup>21</sup> which is in line with methylene peak behavior from our IR spectra. dos Santos *et al.*<sup>22</sup> similarly concluded that the 2–3 cm<sup>-1</sup> shift of methylene peaks to lower wavenumbers upon rising bitumen crystallinity is due to an increase of the *trans/gauche* ratio in long-chain alkanes comprising the bulk of this material.

Spectra of individual C<sub>8</sub>–C<sub>17</sub> model *n*-alkanes were used to establish linear fit parameters for the dependence of methylene to methyl group number ratio,  $N(\text{CH}_2)/N(\text{CH}_3)$  on the branching factor from IR measurements (Fig. S-1D). Correlation factor  $r = 0.999$  is on par with fit quality for other model alkane series.<sup>10,12</sup> According to Fig. S-1D, CH<sub>2</sub>/CH<sub>3</sub> branching factor values between 2 and 3.5, established for the studied set of oils, correspond to  $N(\text{CH}_2)/N(\text{CH}_3)$  variation from 3.5 to 6.5.

#### *Significance of the CH<sub>2</sub>/CH<sub>3</sub> branching factor for characterization of geochemical properties and viscosity of oils*

Typical gas chromatograms of studied oils are shown in Fig. S-2 of the Supplementary material. In the majority of the samples (Fig. S-2A and B), *n*-alkanes are predominant compounds, indicating that these oils are not biodegraded. Microbially altered oils of 2<sup>nd</sup>–4<sup>th</sup> stage of biodegradation<sup>23</sup> were also analyzed (Fig. S-2C and D), in order to determine the influence of biodegradation on the CH<sub>2</sub>/CH<sub>3</sub> factor. Geochemical parameters<sup>24–27</sup> calculated from distributions of *n*-alkanes and regular isoprenoids, obtained by GC analysis of whole oil, are listed in Tables I–III.

Their values, in combination with our previous detailed investigations of other wells in the corresponding oil fields,<sup>28–32</sup> allowed a classification of the studied oils into 8 groups. All investigated oils are of mixed aquatic-terrestrial origin, but considerably differ according to the contribution of aquatic- vs. land-plants biomass, depositional environment of precursor OM, thermal maturity and biodegradation degree (Tables I–III).

Since the oils of the 2<sup>nd</sup> stage of biodegradation (group VI; Fig. S-2C) still contain *n*-alkanes and isoprenoids, geochemical parameters were calculated (Table III) as for non-biodegraded counterparts (Tables I and II). However, these values should be considered with great caution due to the destruction of original alkanes' distributions by microbial activity. Groups VII and VIII comprise the oils of the 3<sup>rd</sup>–4<sup>th</sup> and 4<sup>th</sup> degree of biodegradation, in which *n*-alkanes are almost absent and isoprenoids are either absent or their distributions are remarkably altered (Fig. S-2D), thus disabling any calculation of the parameters (Table III).

TABLE III. Geochemical data, the IR branching factor ( $\text{CH}_2/\text{CH}_3$ ), geochemical parameters and the methyl/ene to methyl group number ratio ( $\text{N}(\text{CH}_2)/\text{N}(\text{CH}_3)$ ) for group VI (aquatic origin, reducing environment, 2<sup>nd</sup> stage of biodegradation), group VII (aquatic origin, reducing and oxic environments, 3-4<sup>th</sup> and 4<sup>th</sup> stage of biodegradation) and group VIII (terrestrial origin, reducing environment, 4<sup>th</sup> stage of biodegradation) oils; parameter average value and standard deviation (in parentheses); N.C. – not calculated due to the absence of components, HM – highly mature; for other abbreviations, see Table I

| Group | Oil field              | No. of samples | Oil maturity | $\text{CH}_2/\text{CH}_3$ | LHCPI          | TAR            | Pr/Ph          | Pr/n-C <sub>17</sub> Ph/n-C <sub>18</sub> | $\Delta CL (n\text{-C}_1-n\text{-C}_{40})$ | n-Alkane maximum(s) | $\Sigma (n\text{-C}_{10}-n\text{-C}_{40})/C_5\text{-C}_6$ | $\Sigma (i\text{-C}_{13}-i\text{-C}_{20})/\text{N}(\text{CH}_2)/\text{N}(\text{CH}_3)$ |
|-------|------------------------|----------------|--------------|---------------------------|----------------|----------------|----------------|---|--|---------------------|---|--|
| VI    | Kikinda                | 3              | M            | 2.05<br>(0.05)            | 1.90<br>(0.53) | 0.59<br>(0.07) | 0.94<br>(0.04) | 2.29<br>(0.85)                            | 2.63<br>(0.91)                             | 18.44 (0.07)        | 2.00 (0.53)   | 3.77 (0.03)  |
|       | All group VI oils      |                |              |                           |                |                |                |   |  |                     |   |  |
| VII   | Kikinda, Kikinda-Polje | 2              | M            | 1.97<br>(0.05)            | N.C.           | N.C.           | N.C.           | N.C.                                      | N.C.                                       | N.C.                | N.C.  | 3.62 (0.09)  |
| VII   | Velebit                | 13             | HM           | 1.94<br>(0.01)            | N.C.           | N.C.           | N.C.           | N.C.                                      | N.C.                                       | N.C.                | N.C.  | 3.57 (0.02)  |
| VII   | All group VII oils     | 15             | M-HM         | 1.95<br>(0.02)            | N.C.           | N.C.           | N.C.           | N.C.                                      | N.C.                                       | N.C.                | N.C.  | 3.57 (0.04)  |
| VIII  | Jermenovci             | 2              | IM           | 2.55<br>(0.08)            | N.C.           | N.C.           | N.C.           | N.C.                                      | N.C.                                       | N.C.                | N.C.  | 4.71 (0.15)  |
|       | All group VIII oils    |                |              |                           |                |                |                |   |  |                     |   |  |

The data from Tables I and II show that the oil groups clearly differ according to the IR  $\text{CH}_2/\text{CH}_3$  branching factor, which continuously increases upon addition of terrigenous precursor material, enriched in long-chain *n*-alkanes and derived from epicuticular waxes of land plants. Lower values of the  $\text{CH}_2/\text{CH}_3$  ratio for group I and II oils are consistent with prevalence of short- and mid-chain *n*-alkanes, as well as greater content of methyl groups originating from methyl- and dimethylalkanes, typical for aquatic OM sources (*e.g.* cyanobacteria and *Botryococcus braunii* race A).<sup>2</sup>

In order to compare the results derived from IR and GC, a correlation diagram of the *n*-alkanes to regular isoprenoids ratio vs. the  $\text{CH}_2/\text{CH}_3$  branching factor was designed for 56 non-biodegraded oils belonging to groups I–V (Fig. 2A). To avoid the influence of evaporation and water washing on light hydrocarbons, *n*-alkanes containing less than 10 carbon atoms were excluded.

Consequently, the *n*-alkanes to isoprenoids ratio (as a “branching factor” derived from GC) represents the ratio between the sum of  $\text{C}_{10}$  to  $\text{C}_{40}$  *n*-alkanes and the sum of  $\text{C}_{13}$  to  $\text{C}_{20}$  acyclic regular isoprenoids:  $\Sigma(\text{n-C}_{10} \text{--n-C}_{40}) / \Sigma(\text{i-C}_{13} \text{--i-C}_{20})$ , assigned as “*n*-C/*i*-C” in the further text. Significant correlation between the two methods (IR and GC) is evident from Fig. 2A. The oils of predominantly aquatic origin (groups I and II) have values of  $\text{CH}_2/\text{CH}_3 < 2.5$  and *n*-C/*i*-C < 8, with the exception of two marginal samples of group II (Mokrin oil field;  $\text{CH}_2/\text{CH}_3 = 2.43$  and 2.44; *n*-C/*i*-C = 8.96 and 9.00, respectively). On the other hand, the oils which prevalently originate from terrestrial biomass show values of the above-mentioned parameters higher than 2.50 and 8.00, respectively (Tables I and II).

Besides that, the data from Fig. 2A indicate poorer correlation between IR and GC branching factors for the oils of predominantly aquatic origin (groups I and II, with a correlation coefficient  $r = 0.76$ , at a significance level  $p = 99.9\%$ ), comparing to the oils of prevalent terrestrial source (groups III–V:  $r = 0.86$ ,  $p = 99.9\%$ ). It is in accordance with the fact that terrestrial OM is enriched in long-chain *n*-alkanes and contains very low amounts of methyl- and dimethyl-alkanes. Consequently, in the oils from groups III–V, methyl-substituents mainly originate from isoprenoids.<sup>2</sup> Therefore, the obtained result indicates that the correlation of *n*-C/*i*-C and  $\text{CH}_2/\text{CH}_3$  factors can be used for an assessment of contribution of aquatic and terrestrial biomass in the precursor OM, in parallel with the numerical values of these parameters.

Furthermore, the data from Fig. 2A show that significant correlation between *n*-C/*i*-C and  $\text{CH}_2/\text{CH}_3$  factors exists up to  $\text{CH}_2/\text{CH}_3 \approx 3$  for dominantly terrestrially sourced oils, *i.e.*, for the oils in groups IV and V (Table II). With a further increase of content of methylene *vs.* methyl groups, the branching factor derived from GC (*n*-C/*i*-C) attains a plateau for the oils with the highest contribution of terrigenous OM deposited in the oxic environment (group III oils). This can be

attributed to the fact that routine GC analysis allows the identification of hydrocarbons up to C<sub>40</sub>, whereas IR considers higher molecular weight *n*-alkanes as well, which were observed in group III oils during a determination of paraffin content using a distillation method (BS EN 12606-1).<sup>33</sup>

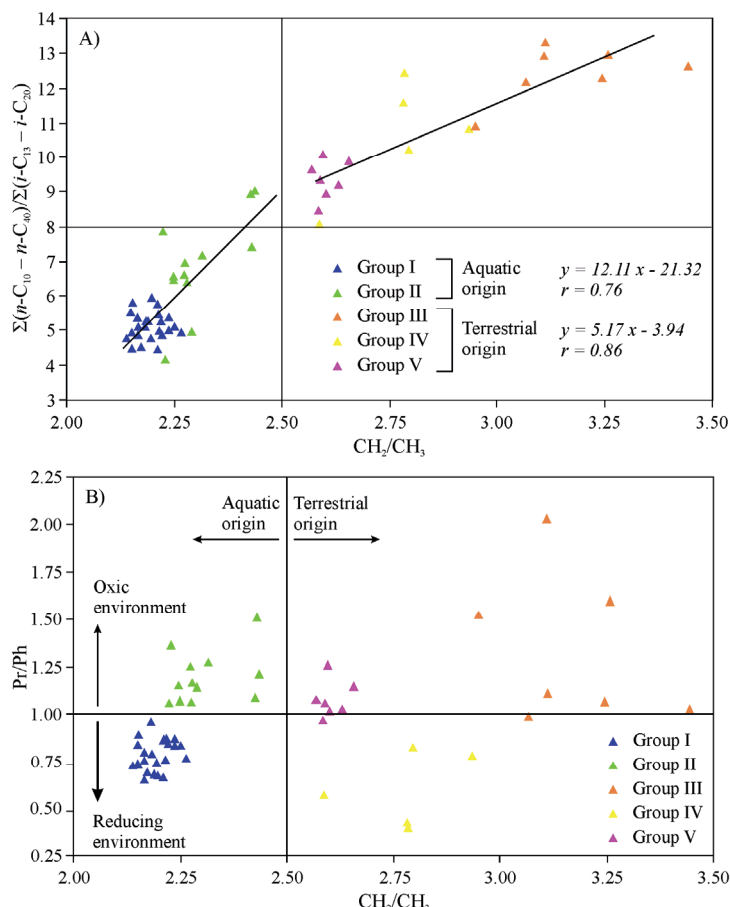


Fig. 2. A) Dependence of the *n*-C/*i*-C on the  $\text{CH}_2/\text{CH}_3$  branching factor and B) the Pr/Ph vs.  $\text{CH}_2/\text{CH}_3$  diagram, which indicates redox conditions of OM depositional environment.  $\text{CH}_2/\text{CH}_3$  – the branching factor (the ratio of methylene and methyl group peak heights at  $2917\text{--}2921\text{ cm}^{-1}$  and  $2951\text{--}2954\text{ cm}^{-1}$ , respectively in the IR spectra); Pr/Ph – pristane/phytane ratio, calculated from peak areas of these compounds in gas chromatograms.

The IR branching factor also demonstrated sensitivity to a depositional environment of oil precursor OM. Namely, a clear increase of the  $\text{CH}_2/\text{CH}_3$  factor is associated with the rising oxidizing properties of depositional environment for all the investigated oils, independently on their prevalent origin (aquatic or terrestrial; Fig. 2B).

The CH<sub>2</sub>/CH<sub>3</sub> branching factor is not substantially affected by thermal maturity in the range from immature to mature oils. This is reflected through almost identical average values of the CH<sub>2</sub>/CH<sub>3</sub> branching factor for immature (Turija-sever), moderately mature (Palić, Mokrin) and mature (Elemir) oils belonging to group I; very similar average values for moderately mature (Idoš) and mature (Kikinda) group II oils; and very similar average values for immature (Idoš) and moderately mature (Sirakovo) group III oils (Tables I and II). This can be explained by the fact that epimerization at chiral C-atoms, isomerization and rearrangement of methyl groups in the rings all together have an impact on molecules of biomarkers (resulting in formation of thermodynamically more stable isomers) during transformations from immature to mature oils,<sup>2</sup> but these processes do not affect the CH<sub>2</sub>/CH<sub>3</sub> ratio. A cracking of the long-chain alkanes producing shorter homologues can result in insignificant lowering of the CH<sub>2</sub>/CH<sub>3</sub> ratio; however, simultaneous reactions of degradation of side chains of cyclic and polycyclic hydrocarbons and/or their successive aromatization followed by demethylation<sup>2</sup> contribute to certain increasing of the ratio, resulting in the observed constancy of the CH<sub>2</sub>/CH<sub>3</sub> branching factor. Therefore, in a maturity range from immature to mature oils (corresponding to vitrinite reflectance of source rocks, *R<sub>r</sub>* in range 0.60–0.80 %), the CH<sub>2</sub>/CH<sub>3</sub> branching factor can be considered as an effective indicator of the origin and depositional environment of oils' precursor OM.

Biodegradation also affects the CH<sub>2</sub>/CH<sub>3</sub> factor independently on origin and maturity of oils. Predominantly aquatically sourced, mature oils of the 2<sup>nd</sup> stage of biodegradation from the Kikinda oil field (group VI) have lower values by *ca.* 0.20 of the CH<sub>2</sub>/CH<sub>3</sub> branching factor comparing to non-biodegraded oils from the same oil field (group II; Tables I and III). Prevalently aquatically sourced group VII oils, *i.e.*, mature Kikinda oil of the 3<sup>rd</sup>–4<sup>th</sup> stage of biodegradation and highly mature Velebit oil attaining the 4<sup>th</sup> stage of biodegradation, as well as immature terrigenous oils of the 4<sup>th</sup> stage of biodegradation (Jermenovci oil field, group VIII), have values of the CH<sub>2</sub>/CH<sub>3</sub> branching factor 0.25–0.30 lower than non-biodegraded oils of the same genetic type (groups I and IV, respectively; Tables I–III). The obtained results are in concordance with the biodegradation scale,<sup>23</sup> according to which normal alkanes are most prone to microbial alteration among all aliphatic hydrocarbons present in oils, being followed by branched methylated alkanes, including isoprenoids. Having the similar origin, oils of the VI and VII groups exhibit negligible decrease of the CH<sub>2</sub>/CH<sub>3</sub> branching factor from the 2<sup>nd</sup> to the 4<sup>th</sup> biodegradation stage (Table III), which can be explained by the fact that microbes primarily attack alkylnaphthalenes and alkylphenanthrenes in this range of biodegradation,<sup>23</sup> which does not influence infrared aliphatic stretching region.

Oils from groups III and IV, having the highest CH<sub>2</sub>/CH<sub>3</sub> branching factor, showed a notable increase of viscosity at temperatures below 40 °C. Group V oils

exhibited analogous viscosity growth at temperatures below 35 °C, whereas for group II and particularly for group I oils no intensive viscosity increase was observed even at lower temperatures (Fig. 3).

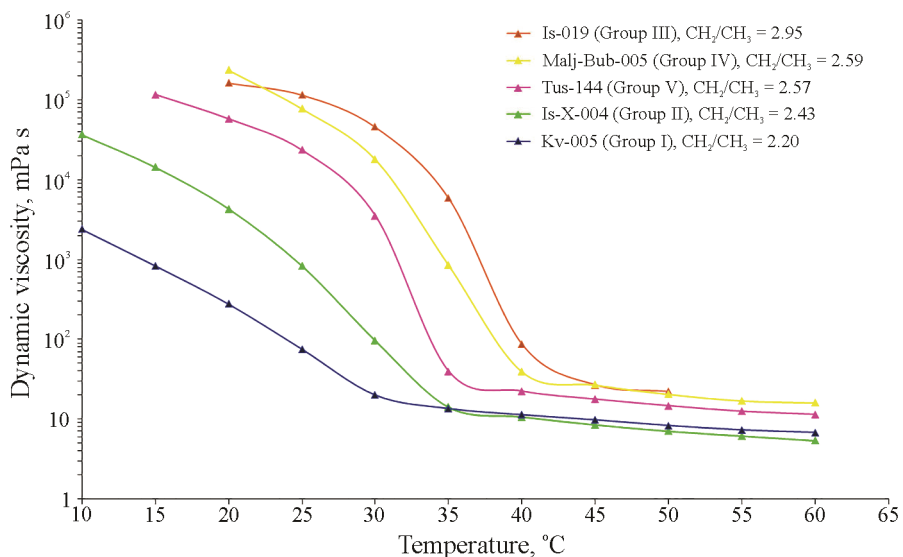


Fig. 3. Temperature dependence of dynamic viscosity for representative oil samples from groups I–V, reflecting variations of rheological behavior with the  $\text{CH}_2/\text{CH}_3$  branching factor; Is-019 – Idoš-019; Malj-Bub-005 – Maljurevac-Bubušinac-005; Tus-144 – Turija-sever-144; Is-X-004 – Idoš X-004; Kv-005 – Kikinda-Varoš-005. The lowest temperature of measurements differs, because the measurement is possible down to temperature 15 °C lower than the oil pour point.

This indicates that high viscosity is primarily related to a substantial content of high molecular weight *n*-alkanes in oils. It is typical for immature terrigenous oils having  $\text{CH}_2/\text{CH}_3 > 2.75$ , enriched in solid paraffins, which have been insignificantly affected by cracking due to their high thermal stability and low oil maturity.

#### CONCLUSION

Increase of the  $\text{CH}_2/\text{CH}_3$  branching factor determined from IR measurements on studied oil samples set resulted in a 3–4  $\text{cm}^{-1}$  shift of methylene stretching peaks to lower wavenumbers for alkanes containing on average from 3.5 to 6.5 methylenes per methyl group as established by comparison with IR spectra of C<sub>8</sub>–C<sub>17</sub> model *n*-alkanes. This effect may be explained by a corresponding increase of the *trans/gauche* conformer ratio of aliphatic chains.

The  $\text{CH}_2/\text{CH}_3$  branching factor showed significant concordance with geochemical parameters, enabling clear distinction of oils according to the source

and depositional environment of precursor OM. On the other hand, dependence of the CH<sub>2</sub>/CH<sub>3</sub> branching factor on oil maturity in the range from immature to mature (corresponding to vitrinite reflectance of source rocks, *R<sub>r</sub>* in range 0.60–0.80 %) was not observed, thus allowing the accurate determination of the oil genetic type irrespective of maturity. Values of the IR CH<sub>2</sub>/CH<sub>3</sub> branching factor and the ratio between sum of *n*-alkanes and sum of acyclic regular isoprenoids,  $\Sigma(n\text{-C}_{10}\text{--}n\text{-C}_{40})/\Sigma(i\text{-C}_{13}\text{--}i\text{-C}_{20})$ , derived from GC, as well as their mutual correlation are useful for the assessment of contribution of aquatic *vs.* terrestrial land plant biomass in the oil precursor OM.

Good accordance between the CH<sub>2</sub>/CH<sub>3</sub> branching factor and the oil biodegradation level up to the 4<sup>th</sup> stage of biodegradation was confirmed. Also, it was established that a notable increase of viscosity at temperatures below 40 °C is typical for immature oils of predominantly terrestrial origin, having values of the CH<sub>2</sub>/CH<sub>3</sub> branching factor above 2.75.

Therefore, using a relatively large oil sample set in the current study, quantitative data relating the IR CH<sub>2</sub>/CH<sub>3</sub> branching factor with structural characteristics of alkanes, geochemical properties and viscosity of oils were constituted.

#### SUPPLEMENTARY MATERIAL

Additional data and information are available electronically at the pages of journal website: <https://www.shd-pub.org.rs/index.php/JSCS/article/view/11114>, or from the corresponding author on request.

*Acknowledgment.* This study was financed by the Ministry of Education, Science and Technological Development of the Republic of Serbia (Contract numbers: 451-03-9/2021-14/200168 and 451-03-9/2021-14/200288).

#### ИЗВОД

#### ЗНАЧАЈ ИНФРАЦРВЕНО-СПЕКТРОСКОПСКОГ ФАКТОРА РАЧВАЊА ЗА ИСТРАЖИВАЊЕ СТРУКТУРНИХ КАРАКТЕРИСТИКА АЛКАНА, ГЕОХЕМИЈСКИХ СВОЈСТАВА И ВИСКОЗИТЕТА НАФТИ

ЈЕЛЕНА З. СТЕВАНОВИЋ<sup>1</sup>, АНТОН Р. РАКИТИН<sup>1</sup>, ИВАН Д. КОЈИЋ<sup>2</sup>, НИКОЛА С. ВУКОВИЋ<sup>3</sup>  
и КСЕНИЈА А. СТОЈАНОВИЋ<sup>4</sup>

<sup>1</sup>НТЦ-НИС Нафтиас, Лабораторија Upstream, Пут шајкашкој одреда 9, 21000 Нови Сад,

<sup>2</sup>Универзитет у Београду, Иновациони центар Хемијског факултета, Студенчески парк 12–16,

11000 Београд, <sup>3</sup>Општина Кладово, Краља Александра 35, 19320 Кладово и <sup>3</sup>Универзитет  
у Београду, Хемијски факултет, Студенчески парк 12–16, 11000 Београд

Урађено је детаљно испитивање значаја инфрацрвено (IC)-спектроскопског фактора рачвања, CH<sub>2</sub>/CH<sub>3</sub> (однос висина пикова метиленских и метил група на 2917–2921 cm<sup>-1</sup> и 2951–2954 cm<sup>-1</sup>, редом, у IC спектрима) за карактеризацију структуре алкане, геохемијских својстава и вискозитета нафти. Испитивано је 76 узорака нафти из 13 нафтних поља у Србији у југоисточном делу Панонског басена. Нафте се разликују према пореклу и средини таложења прекурсорске органске супстанце (OS), као и према степену термичке матурисаности и степену биодеградације. За израчунавање фактора рачвања коришћене су апсорбације пикова који одговарају антисиметричном истезању метиленских и метил група. Код положаја CH<sub>2</sub> пикова запажено је померање за 3–4 cm<sup>-1</sup>

ка већим таласним дужинама са порастом односа  $\text{CH}_2/\text{CH}_3$ , које потиче од већег доприноса *trans* у односу на *gaushe* изомере у алифатичним ланцима. Поређењем IC спектара нафти и стандардних *n*-алкана, утврђено је да средња дужина метиленског низа,  $(\text{CH}_2)_n$  по једној  $\text{CH}_3$  групи варира за *n* од 3,5 до 6,5. Однос  $\text{CH}_2/\text{CH}_3$  је показао значајну сагласност са геохемијским параметрима и омогућио прецизно разликовање нафти према пореклу и средини таложења прекурсорске OS. Истовремено, зависност односа  $\text{CH}_2/\text{CH}_3$  од матурисаности нафти у опсегу од незрелих до зрелих није запажена, што омогућава тачно одређивање генетског типа нафте, невезано од степена зрелости. Однос  $\text{CH}_2/\text{CH}_3$  је показао добру сагласност са скалом биодеградације и вискозитетом нафте.

(Примљено 30. августа, прихваћено 1. новембра 2021)

#### REFERENCES

1. K. E. Peters, C. C. Walters, J. M. Moldowan, *The Biomarker Guide, Volume 1: Biomarkers and Isotopes in Petroleum Systems and Earth History*, Cambridge University Press, Cambridge, 2005
2. K. E. Peters, C. C. Walters, J. M. Moldowan, *The Biomarker Guide, Volume 2: Biomarkers and Isotopes in the Petroleum Exploration and Earth History*, Cambridge University Press, Cambridge, 2005
3. A. K. Manoyyan, *Tekhnologiya pervichnoi pererabotki nefti i prirodnogo gaza*, Khimiya, Moscow, 2001
4. E. A. Glebovskaya, *Primenenie infrakrasnoi spektroskopii v neftyanoi geokhimii*, Nedra, Leningrad, 1971
5. B. K. Wilt, W. T. Welch, J. G. Rankin, *Energy Fuels* **12** (1998) 1008 (<https://doi.org/10.1021/ef980078p>)
6. M. Khanmohammadi, A. B. Garmarudi, A. B. Garmarudi, M. Dela Guardia, *Trends Anal. Chem.* **35** (2012) 135 (<https://doi.org/10.1016/j.trac.2011.12.006>)
7. L. Bellami, *Infrakrasnye spektry slozhnyh molekul*, Izdatel'stvo inostrannoi literatury, Moscow, 1963
8. W. Zenker, *Anal. Chem.* **44** (1972) 1235 (<https://doi.org/10.1021/ac60315a027>)
9. G. Genov, E. Nodland, B. B. Skaare, T. Barth, *Org. Geochem.* **39** (2008) 1229 (<https://doi.org/10.1016/j.orggeochem.2008.04.006>)
10. M. A. Khadim, M. A. Sarbar, *J. Pet. Sci. Eng.* **23** (1999) 213 ([https://doi.org/10.1016/S0920-4105\(99\)00024-8](https://doi.org/10.1016/S0920-4105(99)00024-8))
11. J. Douda, Ma. E. Llanos, R. Alvarez, J. Navarrete Bolaños, *Energy Fuels* **18** (2004) 736 (<https://doi.org/10.1021/ef034057t>)
12. R. R. Coelho, I. Hovell, M. B. D. Monte, A. Middea, A. L. de Souza, *Fuel Process. Technol.* **87** (2006) 325 (<https://doi.org/10.1016/j.fuproc.2005.10.010>)
13. P. C. Painter, R. W. Snyder, M. Starsinic, M. M. Coleman, D. W. Kuehn, A. Davis, *Appl. Spectrosc.* **35** (1981) 475 (<https://doi.org/10.1366/0003702814732256>)
14. S. Yao, K. Zhang, K. Jiao, W. Hu, *Energy Explor. Exploit.* **29** (2011) 1 (<https://doi.org/10.1260/0144-5987.29.1.1>)
15. R. W. Snyder, P. C. Painter, D. C. Cronauer, *Fuel* **62** (1983) 1205 ([https://doi.org/10.1016/0016-2361\(83\)90065-0](https://doi.org/10.1016/0016-2361(83)90065-0))
16. R. Lin, G. P. Ritz, *Appl. Spectrosc.* **47** (1993) 265 (<https://doi.org/10.1366/0003702934066794>)
17. G. S. Fedorova, L. S. Kosyakova, V. Yu. Artem'ev, *Vesti gazovoi nauki*, **2 (5)** (2010) 22 (<http://vesti-gas.ru/sites/default/files/attachments/033-045-1006-sbornik-plasty-v21-d.pdf>) (in Russian)

18. V. Yu. Artem'ev, E. B. Grigor'ev, O. A. Shigidin, *Vesti Gazovoi Nauki* **1** (2013) 21 ([http://vesti-gas.ru/sites/default/files/attachments/21-26\\_vgn-plasty-2013-v66.pdf](http://vesti-gas.ru/sites/default/files/attachments/21-26_vgn-plasty-2013-v66.pdf))
19. I. M. Abdrafikova, G. P. Kayukova, S. M. Petrov, A. I. Ramazanova, R. Z. Musin, V. I. Morozov, *Neftekhimiya* **55** (2015) 110 (<https://doi.org/10.7868/S0028242115020021>)
20. H. H. Mantsch, R. N. McElhaney, *Chem. Phys. Lipids* **57** (1991) 213 ([https://doi.org/10.1016/0009-3084\(91\)90077-O](https://doi.org/10.1016/0009-3084(91)90077-O))
21. K. B. Wiberg, M. A. Murcko, *J. Am. Chem. Soc.* **110** (1998) 8029 (<https://doi.org/10.1021/ja00232a012>)
22. S. dos Santos, L. D. Poulikakos, M. N. Partl, *Int. J. Pavement Res. Technol.* **10** (2017) 2 (<https://doi.org/10.1016/j.ijprt.2017.01.002>)
23. M. Head, D. Martin Jones, S. R. Larter, *Nature* **426** (2003) 344 (<https://doi.org/10.1038/nature02134>)
24. N. Vuković, Đ. Životić, J. G. Mendonça Filho, T. Kravić-Stevović, M. Hámor-Vidó, J. O. Mendonça, K. Stojanović, *Int. J. Coal Geol.* **154–155** (2016) 213 (<http://doi.org/10.1016/j.coal.2016.01.007>)
25. R. A. Bourbonnire, P. A. Meyers, *Limnol. Oceanogr.* **41** (1996) 352 (<https://doi.org/10.4319/lo.1996.41.2.0352>)
26. E. Eckmeier, G. L. B. Wiesenberg, *J. Archaeol. Sci.* **36** (2009) 1590 (<https://doi.org/10.1016/j.jas.2009.03.021>)
27. B. M. Didyk, B. R. T. Simoneit, S. C. Brassell, G. Eglinton, *Nature* **272** (1978) 216 (<https://doi.org/10.1038/272216a0>)
28. B. Jovančićević, P. Polić, D. Vitorović, *J. Serb. Chem. Soc.* **63** (1998) 397
29. K. Stojanović, B. Jovančićević, D. Vitorović, G. Pevneva, J. Golovko, A. Golovko, *Geochem. Int.* **45** (2007) 781 (<https://doi.org/10.1134/S0016702907080058>)
30. K. Stojanović, B. Jovančićević, D. Vitorović, J. Golovko, G. Pevneva, A. Golovko, *J. Pet. Sci. Eng.* **55** (2007) 237 (<https://doi.org/10.1016/j.petrol.2006.07.009>)
31. T. Šolević, K. Stojanović, J. Bojesen-Koefoed, H. P. Nytoft, B. Jovančićević, D. Vitorović, *Org. Geochem.* **39** (2008) 118 (<https://doi.org/10.1016/j.orggeochem.2007.09.003>)
32. B. Jovančićević, H. Wehner, G. Scheeder, K. Stojanović, A. Šainović, O. Cvetković, M. Ercegovac, D. Vitorović, *J. Serb. Chem. Soc.* **67** (2002) 553 (<https://doi.org/10.2298/JSC0209553J>)
33. X. Lu, P. Redelius, *Energy Fuels* **20** (2006) 653 (<https://doi.org/10.1021/ef0503414>).



SUPPLEMENTARY MATERIAL TO  
**Significance of infrared spectroscopic branching factor for investigation of structural characteristics of alkanes, geochemical properties and viscosity of oils**

JELENA Z. STEVANOVIĆ<sup>1</sup>, ANTON R. RAKITIN<sup>1</sup>, IVAN D. KOJIĆ<sup>2</sup>,  
NIKOLA S. VUKOVIĆ<sup>3</sup> and KSENIJA A. STOJANOVIC<sup>4\*</sup>

<sup>1</sup>STC-NIS Naftagas, Upstream Laboratory, Put šajkaškog odreda 9, 21000 Novi Sad, Serbia,

<sup>2</sup>University of Belgrade, Innovation Center of the Faculty of Chemistry, Studentski trg 12–16,

11000 Belgrade, Serbia, <sup>3</sup>Municipality of Kladovo, Kralja Aleksandra 35, 19320 Kladovo, Serbia and <sup>4</sup>University of Belgrade, Faculty of Chemistry, Studentski trg 12–16, 11000 Belgrade, Serbia

J. Serb. Chem. Soc. 87 (1) (2022) 41–55

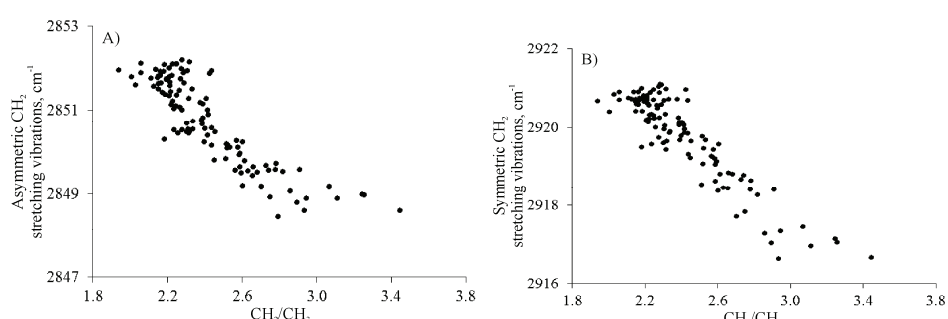


Fig. S-1. Peak positions depending on the CH<sub>2</sub>/CH<sub>3</sub> branching factor for the studied oils: (A) asymmetric CH<sub>2</sub> and (B) symmetric CH<sub>2</sub>. CH<sub>2</sub>/CH<sub>3</sub> – the branching factor (the ratio of methylene and methyl group peak heights at 2917–2921 cm<sup>-1</sup> and 2951–2954 cm<sup>-1</sup>, respectively in the IR spectra).

\* Corresponding author. E-mail: ksenija@chem.bg.ac.rs

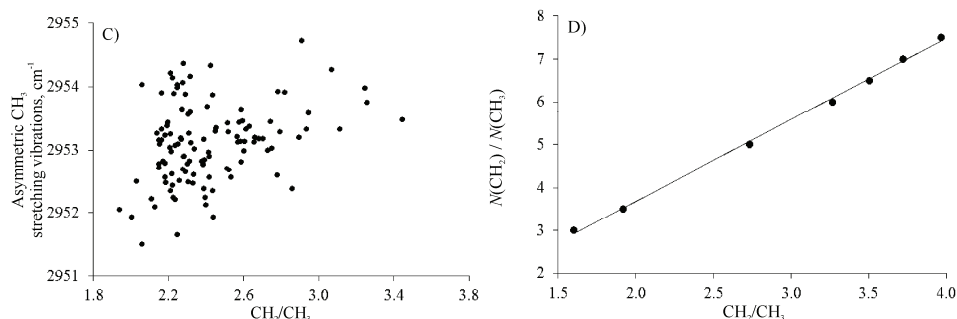


Fig. S-1. (Continued) Peak positions depending on the  $\text{CH}_2/\text{CH}_3$  branching factor for the studied oils: (C) asymmetric  $\text{CH}_3$  stretching vibrations and (D) correlation diagram of the methylene to methyl group number ratio,  $N(\text{CH}_2)/N(\text{CH}_3)$  vs.  $\text{CH}_2/\text{CH}_3$ .  $\text{CH}_2/\text{CH}_3$  – the branching factor (the ratio of methylene and methyl group peak heights at  $2917\text{--}2921\text{ cm}^{-1}$  and  $2951\text{--}2954\text{ cm}^{-1}$ , respectively in the IR spectra).

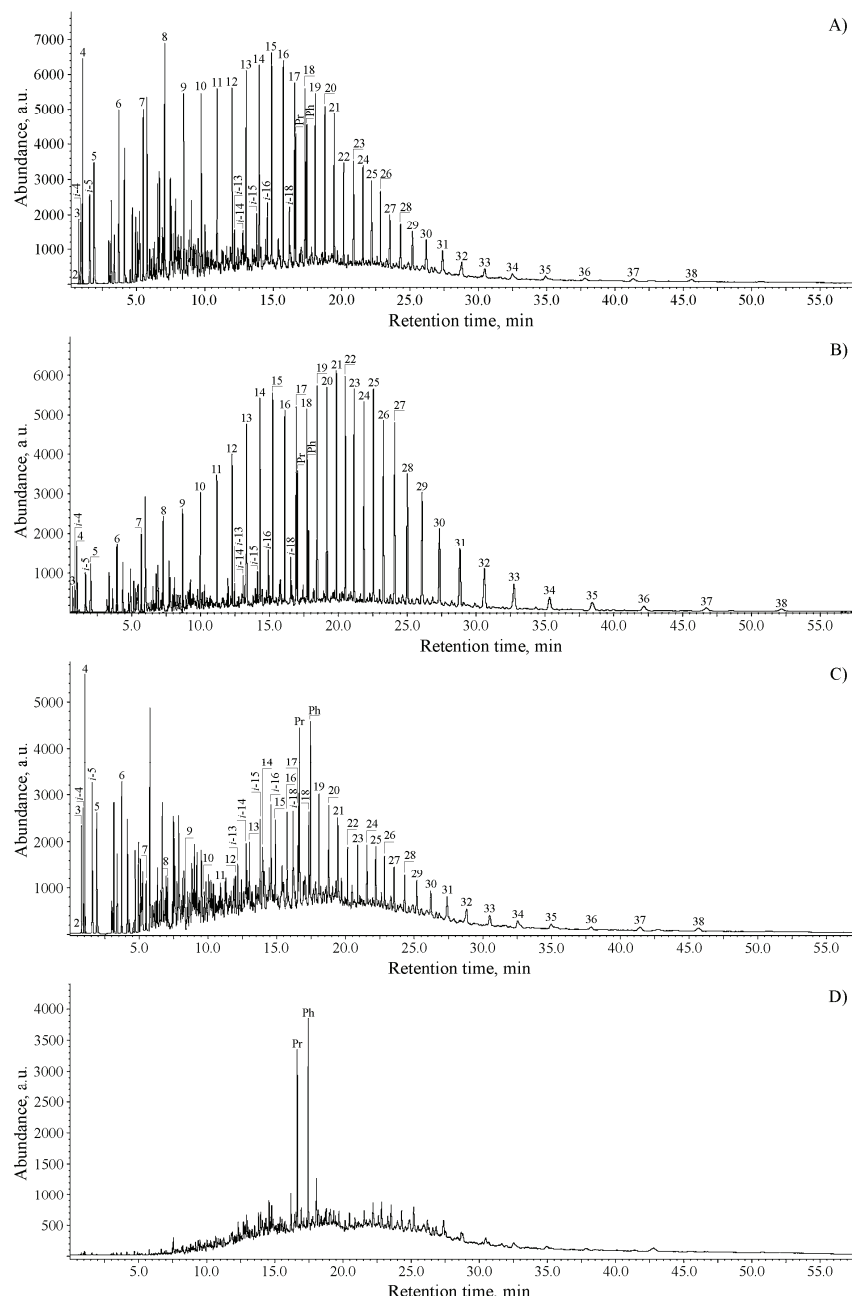


Fig. S-2. Typical gas chromatograms for the studied set of oils: (A) Elemir - 042 (group I), (B) Iđoš - 019 (group III), (C) Kikinda - 152 (group VI) and (D) Jermenovci - 045 (group VIII). *n*-Alkanes are labeled according to their carbon number; Pr – Pristane; Ph – Phytane; *i*-*x* – regular isoprenoid, where *x* represents its total number of carbon atoms.





J. Serb. Chem. Soc. 87 (1) 57–67 (2022)  
JSCS-5504

# Journal of the Serbian Chemical Society

JSCS@tmf.bg.ac.rs • www.shd.org.rs/JSCS

Original scientific paper  
Published 14 January 2022

## In-house-prepared carbon-based Fe-doped catalysts for electro-Fenton degradation of azo dyes

SLADANA D. SAVIĆ<sup>1\*</sup>, GORAN M. ROGLIĆ<sup>1#</sup>, VYACHESLAV V. AVDIN<sup>2</sup>, DMITRY A. ZHEREBTSOV<sup>2</sup>, DALIBOR M. STANKOVIĆ<sup>3,4#</sup> and DRAGAN D. MANOLOVIĆ<sup>2,3#</sup>

<sup>1</sup>University of Belgrade – Faculty of Chemistry, Department of Applied Chemistry, Studentski trg 12–16, Belgrade, Serbia, <sup>2</sup>South Ural State University, 76, Lenin prospect, Chelyabinsk, Russia, 454080, <sup>3</sup>University of Belgrade – Faculty of Chemistry, Department of Analytical Chemistry, Studentski trg 12–16, Belgrade, Serbia, <sup>4</sup>University of Belgrade, “Vinča” Institute of Nuclear Sciences, National Institute of the Republic of Serbia, Department of Radioisotopes, Mike Petrovića Alasa 12–14, Belgrade, Serbia

(Received 1 September, revised 27 November, accepted 29 November 2021)

**Abstract:** Compounds used in the fashion industry effect the water bodies in the vicinity of textile factories, resulting in the visible coloration of surface water. Fe-doped graphite-based in house prepared electrodes were used in the Fenton-like degradation of Reactive Blue 52 (RB52). The electrodes consisting of high-density graphite in three granulation sizes and three levels of Fe content were characterized using scanning electron microscopy (SEM). The amount of Fe in the electrodes and H<sub>2</sub>O<sub>2</sub> concentration in synthetic textile wastewater were optimized. Additionally, the size of graphite grains was varied to investigate whether it effects the degradation rate. Under only 10 min of electro-Fenton degradation, a system with 10 mmol dm<sup>-3</sup> of H<sub>2</sub>O<sub>2</sub> and an electrode made of 7 % of Fe and 70 µm of granulation size of graphite, degraded over 75 % of RB52, and over 99 % after 40 min of treatment. The obtained results indicate that the proposed approach could be beneficial in the field of novel materials for environmental application and that in house prepared carbon could be an excellent replacement for commercially available supports.

**Keywords:** Reactive Blue 52; granulation; decolorization; hydrogen peroxide; graphite; advanced oxidation processes.

### INTRODUCTION

There have been many improvements of the classic Fenton reaction, a homogenous system with Fe<sup>2+</sup> and H<sub>2</sub>O<sub>2</sub> in the acid environment, but the electro-Fenton reactions contribute to *in situ* generation of reactive species in water due to

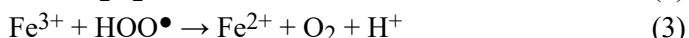
\* Corresponding author. E-mail: sladjana@chem.bg.ac.rs

# Serbian Chemical Society member.

<https://doi.org/10.2298/JSC210901103S>



the effect of the electric current.<sup>1,2</sup> Electro-Fenton oxidation processes occur at ambient pressure and ambient temperature and therefore belong to the electrochemical advanced oxidation processes (electro AOP).<sup>3,4</sup> In an acidic environment,  $\text{Fe}^{2+}$  oxidizes to  $\text{Fe}^{3+}$ , as shown in Eq. (1), but in pH neutral and aerobic conditions, Fenton-like reactions are possible that could lead to a respectable amount of generated oxidative species, as shown in Eqs. (2) and (3):<sup>5,6</sup>



To prevent Fe deposition and to increase the efficacy of Fenton reactions in pH neutral environment, a stable iron support is often needed.<sup>7,8</sup> Carbonaceous materials are commonly considered as readily available, cost-effective, and durable support materials for numerous electrochemical applications,<sup>9–12</sup> and especially graphite can be attractive in terms of different electrode preparation possibilities, due to its stability.<sup>13–15</sup> The effects of the ratio of iron and hydrogen peroxide on Fenton and Fenton-like reactions are well studied,<sup>16</sup> but novel electrode formulations open questions never asked before, such as granulation of the starting carbonaceous material. Techniques for electrodes production can strongly affect the efficiency, stability and reusability of electrodes.

Rapid fashion changes and mass production of clothes lead to enormous amounts of textile waste, compounds used in the fashion industry mostly effect the water bodies around textile factories, resulting in visible coloration of surface water. Therefore, effective, stable, and low-cost approaches are needed to combat this growing problem.<sup>17,18</sup>

This study was based on electro-Fenton oxidation of Reactive Blue 52 (RB52), a textile azo dye, where up to 10 ppm of  $\text{H}_2\text{O}_2$  was externally added to the electrochemical system. Fixed amounts of high-density graphite and phenol-formaldehyde resin were used to prepare nine electrodes with three ranges of graphite granulations and Fe contents. The electrodes were applied in the form of pellets to find the optimal combination of graphite granulation, iron content, and  $\text{H}_2\text{O}_2$  concentration to achieve the fastest removal of RB52 without pH adjustment.

## EXPERIMENTAL

### *Chemicals*

$\text{Fe}(\text{NO}_3)_3 \cdot 9\text{H}_2\text{O}$  (ACS reagent, ≥98 %, Sigma Aldrich, CAS 7782-61-8) was used as a doping material for the in house prepared carbon-based catalysts. A high-density graphite (trademark VPG-4) prepared in three granulation sizes was used as a precursor for the electrodes, while novolac phenol-formaldehyde resin SFPR-054 (Wego Chemical Group, CAS 9003-35-4, hereinafter SFPR binder), light-yellow powder with 26 % of hexamethylenetetramine (with 60 % of carbon content in SFPR binder heated at 950 °C) by weight served as a binder. Ethanol (95 vol. %, Sigma Aldrich) was needed for the preparation of precursors. Reactive Blue 52, a textile azo dye, a model compound (Clariant, CAS 12225-63-7, herein-

after RB52), Na<sub>2</sub>SO<sub>4</sub> ( $\geq 99\%$ , Sigma Aldrich, CAS 7757-82-6) a supporting electrolyte, and H<sub>2</sub>O<sub>2</sub> (30 vol. %, Sigma Aldrich, CAS 7722-84-1) were involved in the electrochemical degradation tests.

#### *Electrodes preparation*

The Fe-doped porous graphite electrodes were produced following a procedure published elsewhere.<sup>19,20</sup> Compared to work of Manojlović and colleagues,<sup>19</sup> this study was expanded by using three median granulation sizes of high-density graphite fractions cut on lathes. The grain size was controlled by adequate sieve openings, e.g. sieves with dimensions between 50 and 90 µm resulted in a median grain size of 70 µm, between 90 and 160 µm gave 125 µm, and those between 160 and 250 µm gave a median grain size of 205 µm (see more in Table I). A fixed amount of SFPR binder (0.9 g) and different amounts of Fe(NO<sub>3</sub>)<sub>3</sub>·9H<sub>2</sub>O were powdered and mixed. The content of Fe was proportional to the carbon content in the SFPR binder, hence 0, 0.078 and 0.273 g of Fe(NO<sub>3</sub>)<sub>3</sub>·9H<sub>2</sub>O was weighed to produce electrodes labelled as 0, 2 and 7 % of Fe. Three grams of graphite grains of appropriate size (*i.e.*, 70, 125 or 205 µm of medium size) was combined with the previous ingredients and again combined to make precursors for nine electrodes. These mixtures were then wetted, pelleted, and heated according to the procedure published by Petković *et al.*,<sup>20</sup> resulting in nine Fe-doped porous graphite electrodes, as listed in Table I. The electrodes were labeled according to the median size of graphite grains and Fe content, for example, electrode 70-0 container graphite with roughly 70 µm of grain size and 0 % of Fe. The morphology of the SFPR binder and the prepared electrodes were examined on a scanning electron microscope, Jeol JSM-7001F (SEM).

TABLE I. Properties of the studied Fe-doped porous graphite electrodes

| Electrode label | Content of Fe in relation to SFPR binder, % | Graphite grain size µm | Median grain size µm |
|-----------------|---|------------------------|----------------------|
| 70-0            | 0   | 50–90                  | 70                   |
| 70-2            | 2   | 50–90                  | 70                   |
| 70-7            | 7   | 50–90                  | 70                   |
| 125-0           | 0   | 90–160                 | 125                  |
| 125-2           | 2   | 90–160                 | 125                  |
| 125-7           | 7   | 90–160                 | 125                  |
| 205-0           | 0   | 160–250                | 205                  |
| 205-2           | 2   | 160–250                | 205                  |
| 205-7           | 7   | 160–250                | 205                  |

#### *Electro-Fenton decolorization experiments*

RB52 (30 mg dm<sup>-3</sup>) was used as a model compound for the comparison of electrode effectiveness, while 0.1 mol dm<sup>-3</sup> Na<sub>2</sub>SO<sub>4</sub> was chosen for the supporting electrolyte. The original divided electrochemical cell (Fig. 1) contained 50 cm<sup>3</sup> of azo dye with Na<sub>2</sub>SO<sub>4</sub> in the anodic part, with an applied anodic potential of 4.2 V and a current of 30 mA. Additionally, the cathodic part, separated by Nafion 117 perfluorinated membrane (178 µm thick) from the anodic part, was loaded only with supporting electrolyte solution. Fenton-like electrochemical degradation experiments involved all nine electrodes (see Table I) and four H<sub>2</sub>O<sub>2</sub> concentrations (namely, 0, 1, 5 and 10 mmol dm<sup>-3</sup>), including experiments at native pH value, without hydrogen peroxide. The effect of the optimal combination of graphite granulation, Fe content, and H<sub>2</sub>O<sub>2</sub> concentration on RB52 decolorization was monitored on UV-Vis spectro-

photometer (Evolution 200 Series, Thermo Fisher Scientific) at the  $\lambda_{\max} = 615$  nm. Each electro-Fenton degradation experiment lasted 50 min and samples were withdrawn after every 10 min. Graphs were generated using OriginPro® 8. The preparation of the electrodes was performed at the South Ural State University and the electro-Fenton degradation of RB52 at the University of Belgrade during 2018–2019.

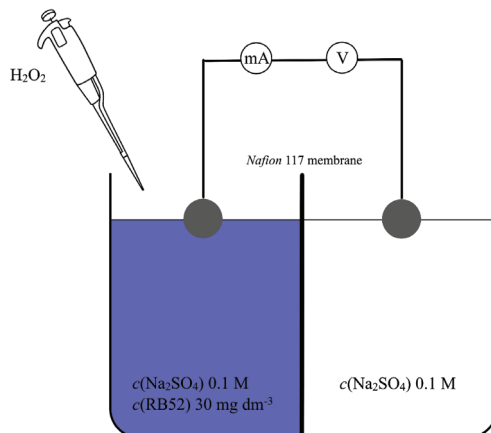


Fig. 1. Experimental setup.

## RESULTS AND DISCUSSION

In this study, three levels of Fe content in Fe-doped graphite electrodes were combined with three ranges of grain size of graphite used to obtain electrodes for optimal Reactive Blue 52 (RB52) degradation. Additionally,  $\text{H}_2\text{O}_2$  was added in four concentration levels to optimize electro-Fenton decolorization without pH value adjustment. The morphology of the SFPR binder at 5000 $\times$  and 100 $\times$  of magnification on SEM is shown Fig. 2.

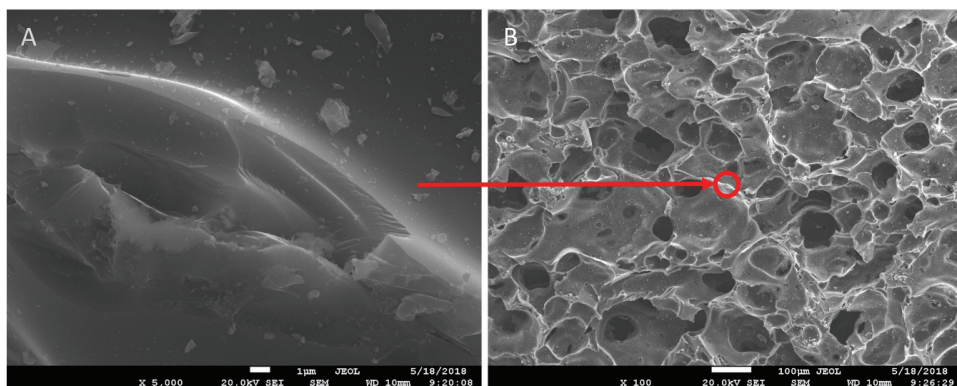


Fig. 2. SEM images of SFPR binder at: A – 5000 and B – 100 $\times$  of magnification using the secondary electron imaging (SEI) technique.

It could be concluded from Fig. 3 that each material was covered with large pores, formed in a heavily branched structure, and filled with spherical vacancies. By comparing the same magnification of the SEM images, it could be concluded that pore sizes were proportional to the grain size, indicating that the proposed procedure could serve as a controllable method for the preparation of the electrodes listed in Table I. Electrodes without iron are represented in Fig. 3A, D and G. The other electrodes shown in Fig. 3 represent the morphology of electrodes with 2 and 7 % of iron, where each material was covered with a thin layer of  $\text{Fe}_3\text{O}_4$  of high crystallinity and octahedral in shape, forming a high surface area, which is preferable for environmental use.

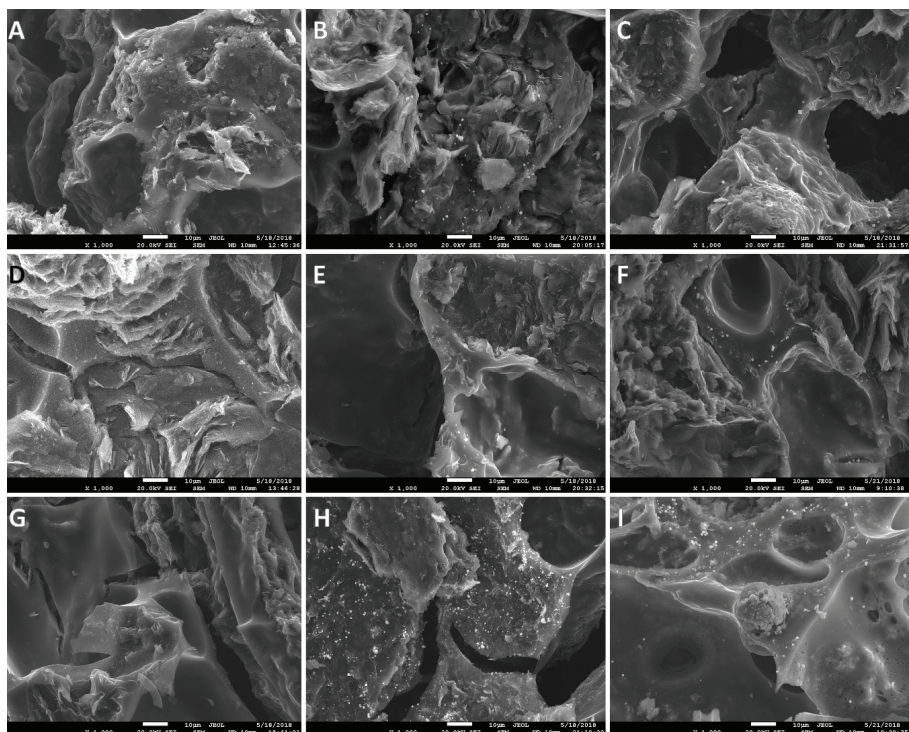


Fig. 3. SEM images of: A – 70-0, B – 70-2, C – 70-7, D – 125-0, E – 125-2, F – 125-7, G – 205-0, H – 205-2, I – 205-7 electrodes under 1000 $\times$  of magnification using SEI technique.

The first number stands for the granulation value and the second number for the amount of Fe (see Table I).

The changes in the decolorization rate of RB52 are shown in Fig. 4A–C as a function of Fe content and graphite grains size, with no added hydrogen peroxide. The highest degradation rate after 50 min of treatment was achieved (over 75 %) when the electrode with 2 % of Fe and 125  $\mu\text{m}$  of graphite granulation (label 125-2, see Table I) was applied, as shown in Fig. 4B. The raw data for

Figs. 4–8 are organized in Tables S-I–S-IX of the Supplementary material to this paper. On the other hand, RB52 was the least degraded (below 45 %) with electrodes of 70 µm grain size of graphite and without iron (Fig. 4A). In all cases (Fig. 4A–C), the middle level (125 µm) of graphite granulation accomplished higher decolorization rates, compared to the other two granulation sizes. Moreover, in the case of electrodes with 205 µm grains size (Fig. 4C), there were no significant differences in RB52 degradation efficiency between the electrodes with the lowest and the highest Fe content (almost 60 % and over 51 % of degraded RB52, respectively). The results showed in Fig. 4 were achieved without the addition of H<sub>2</sub>O<sub>2</sub> and could be attributed to the *in situ* electrochemical production of hydroxyl radical and other reactive species, as presented in Eqs. (1)–(3).<sup>5,6</sup>

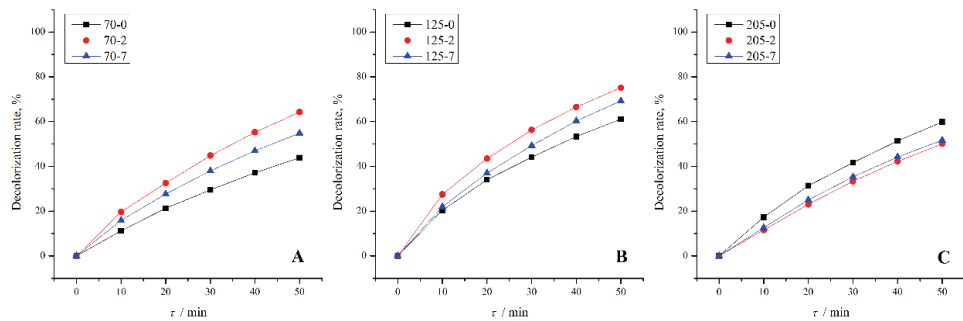


Fig. 4. Change in RB52 decolorization rate for electrodes made of different graphite granulation size; A – electrodes with no Fe, B – electrodes with 2 % of Fe and C – electrodes with 7 % of Fe (starting conditions: 30 mg dm<sup>-3</sup> RB52 solution in the absence of H<sub>2</sub>O<sub>2</sub>).

Completely different results were observed when 1 mmol dm<sup>-3</sup> of H<sub>2</sub>O<sub>2</sub> was added to all the prepared electrodes because in the presence of added hydrogen peroxide electro-Fenton reactions occurred to a greater extent (Fig. 5A–C). According to the results, 2 % of iron leads to the fastest RB52 degradation rates, achieving roughly 60 % degradation after only 10 min of treatment for all graphite granulation sizes, which could imply the mutual dependence of the iron content in the electrode and the quantity of H<sub>2</sub>O<sub>2</sub> for optimal Fenton reactions. Similar to the previous results, electrodes 70-2 and 125-2 with (Fig. 5) or without H<sub>2</sub>O<sub>2</sub> (Fig. 4) culminated in higher degradation rates compared to larger grain sizes (Fig.s 4C and 5C, respectively). Moreover, with 1 mmol dm<sup>-3</sup> of H<sub>2</sub>O<sub>2</sub> in the system, electrodes with no iron and lower grain sizes (70-0 and 125-0) also resulted in slightly higher endpoints (92 and 87 % after 50 min of treatment, respectively), compared to 205-0 with 83 % of RB52 degraded at the same point. The only exception to the observed rule in granulation size effect were electrodes with 7 % of Fe. Namely, 1 mmol dm<sup>-3</sup> of H<sub>2</sub>O<sub>2</sub> led to less than 80 % of degradation rate for the 70-7 electrode, but around 94 % for the other two electrodes (125-7 and 205-7) after 50 min of treatment.

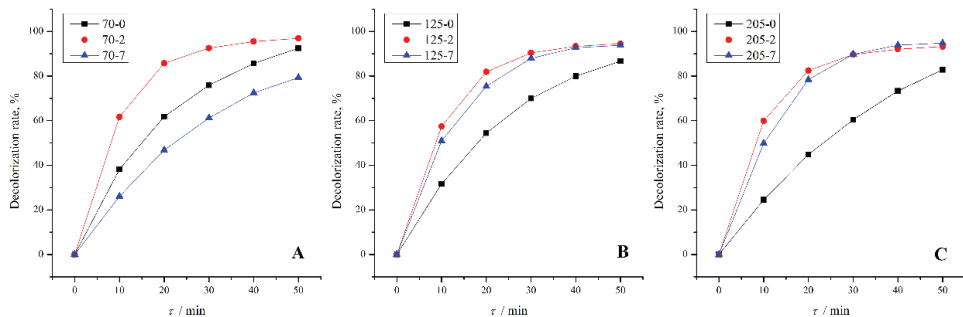


Fig. 5. Change in RB52 decolorization rate when using electrodes with different Fe contents; graphite granulation size: A – 70, B – 125 and C – 205  $\mu\text{m}$  (starting conditions: 30 mg dm<sup>-3</sup> RB52 solution and 1 mmol dm<sup>-3</sup> H<sub>2</sub>O<sub>2</sub>).

High degradation rates were also achieved with five times higher H<sub>2</sub>O<sub>2</sub> concentration (Fig. 6A–C). Furthermore, there was no significant difference in the decolorization rate (roughly 95 % at 50 min) between electrodes with 2 and 7 % of iron, for all three granulation levels, while the RB52 degradation was somewhat slower without iron present in the electrodes.

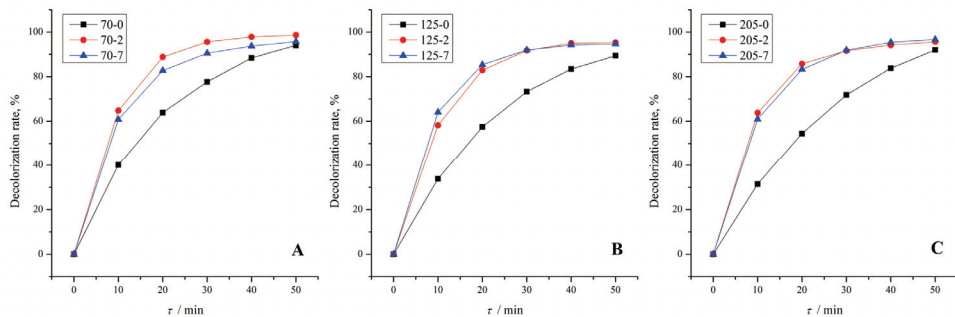


Fig. 6. Change in RB52 decolorization rate when using electrodes with different Fe content; graphite granulation size: A – 70, B – 125 and C – 205  $\mu\text{m}$  (starting conditions: 30 mg dm<sup>-3</sup> RB52 solution and 5 mmol dm<sup>-3</sup> H<sub>2</sub>O<sub>2</sub>).

The highest concentration of H<sub>2</sub>O<sub>2</sub> investigated in this study was 10 mmol dm<sup>-3</sup>, as depicted in Fig. 7. Under these conditions, almost 80 % of dye was degraded in only 10 min by electrodes 70-7 and 125-7 (Fig. 7A and B), the latter being the only system in which 7 % of iron led to the fastest decolorization. Although endpoints in all systems were remarkable and comparable with lower C (H<sub>2</sub>O<sub>2</sub>), this extent of hydrogen peroxide slightly suppressed the decolorization by electrodes with 2 % of Fe (Fig. 7A–C).

The best results shown in the previous figures, selected for each amount of H<sub>2</sub>O<sub>2</sub> combined with various electrodes, are summarized in Fig. 8. Obviously, the highest hydrogen peroxide concentration led to the quickest, but also the most

effective RB52 degradation, as already shown in Fig. 7C. All of the systems with added H<sub>2</sub>O<sub>2</sub> enable more efficient electro-Fenton reactions, which lead to similar outcomes, in terms of RB52 decolorization in 50 min of treatment. What also stands out, electrodes with the lowest graphite grains size (70 µm) came out to give higher degradation rates, compared to the other two tested sizes. In most cases, iron improved degradation percentage, and the optimal iron content was 2 % (1 and 5 mmol dm<sup>-3</sup> of H<sub>2</sub>O<sub>2</sub>), except for the 10 mmol dm<sup>-3</sup> of H<sub>2</sub>O<sub>2</sub>, where a higher amount of Fe was needed.

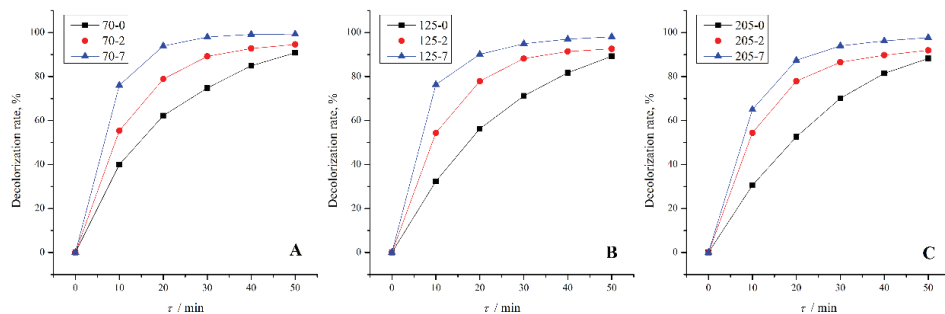


Fig. 7. Change in RB52 decolorization rate when using electrodes with different Fe contents; graphite granulation size: A – 70, B – 125 and C – 205 µm (starting conditions: 30 mg dm<sup>-3</sup> RB52 solution and 10 mmol dm<sup>-3</sup> H<sub>2</sub>O<sub>2</sub>).

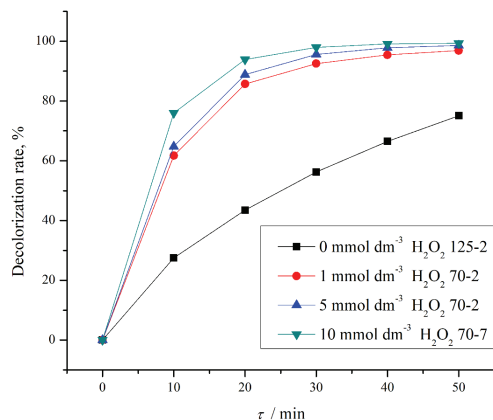


Figure 8. Comparison of the best RB52 decolorization rates for selected electrodes – with different Fe content, H<sub>2</sub>O<sub>2</sub> concentration, and graphite granulation size.

This result also indicates that Fe and H<sub>2</sub>O<sub>2</sub> ratio follows a certain positive correlation trend, and the outcome of electro-Fenton oxidation could be predicted and adjusted to the desired results, mostly based on the Fe/H<sub>2</sub>O<sub>2</sub>. On the other hand, decolorization of RB52 was still possible, even without H<sub>2</sub>O<sub>2</sub> – the 125-2 electrode and no H<sub>2</sub>O<sub>2</sub>, which resulted in almost 30 % degradation efficiency after 10 min of treatment, had the endpoint for the same electrode comparable to the result achieved with 70-7 and 10 mmol dm<sup>-3</sup> H<sub>2</sub>O<sub>2</sub> in the first 10 min when

roughly 80 % of azo dye was removed. This result could imply that the degradation system without added hydrogen-peroxide could be compensated with longer treatment time, and *vice versa* – the degradation time could be shortened with higher content of oxidation agent.

In the electro-Fenton oxidation of an azo dye Reactive Blue 52 presented here the maximal concentration of H<sub>2</sub>O<sub>2</sub> was 50 times less than reported elsewhere.<sup>21</sup> Although higher concentration of H<sub>2</sub>O<sub>2</sub> often leads to better degradation rates, the excess of hydrogen peroxide added can have a scavenging effect on hydroxyl radicals.<sup>1</sup> Even though the degradation efficiencies are often tested by the degradation rate of colored substances, their applicability is not limited to the textile industry, but could be expanded to many other organic chemicals with similar functional groups.

#### CONCLUSIONS

The proposed study contributes to a better understanding of electro-Fenton degradation of Reactive Blue 52, in terms of the role of the graphite granulation size, iron, and H<sub>2</sub>O<sub>2</sub> content. Under only 10 min of electro-Fenton degradation, a system with 10 mmol dm<sup>-3</sup> of H<sub>2</sub>O<sub>2</sub> and an electrode made of 7 % of Fe and 70 µm granulation size of graphite, degraded over 75 % of the treated azo dye. Additionally, less than 1 % of dye remained after 40 min of treatment. It should be emphasized that even lower H<sub>2</sub>O<sub>2</sub> concentrations lead to a satisfactory degradation rate, when 70-2 electrodes were used. Even though the removal efficiency of the presented system was tested by the degradation rate of colored substance, this study could serve as a basis for similar electrochemical degradations and its applicability could be expanded to many other organic chemicals with analogous functional groups, with further optimization of the experimental parameters.

#### SUPPLEMENTARY MATERIAL

Additional data and information are available electronically at the pages of journal website: <https://www.shd-pub.org.rs/index.php/JSCS/article/view/11130>, or from the corresponding author on request.

*Acknowledgements.* We want to express thankfulness to passed Prof. Dr. Petar Pfendt for his scientific and educational contribution to Environmental Chemistry in Serbia, and for inspiring many chemists to pursue a career in this discipline, including the authors of this study. This study was funded by Ministry of Education, Science and Technological Development of Republic of Serbia, Contract number: 451-03-9/2021-14/200168.

## ИЗВОД

ИЗРАДА И СВОЈСТВА КАТАЛИЗATORА НА БАЗИ УГЉЕНИКА ДОПОВАНИХ ГВОЖЂЕМ  
ЗА ЕЛЕКТРО-ФЕНТОНСКУ РАЗГРАДЊУ АЗО-БОЈА

СЛАЂАНА Д. САВИЋ<sup>1</sup>, ГОРАН М. РОГЛИЋ<sup>1</sup>, ВЈАЧЕСЛАВ В. АВДИН<sup>2</sup>, ДМИТРИЈ ЖЕРЕБЕЦОВ<sup>2</sup>,  
ДАЛИВОР М. СТАНКОВИЋ<sup>3,4</sup> и ДРАГАН Д. МАНОЈЛОВИЋ<sup>2,3</sup>

<sup>1</sup>Универзитет у Београду – Хемијски факултет, Кафедра за примењену хемију, Студеначки трг 12–16, Београд, <sup>2</sup>South Ural State University, 76, Lenin prospect, Chelyabinsk, Russia, 454080,

<sup>3</sup>Универзитет у Београду – Хемијски факултет, Кафедра за аналитичку хемију, Студеначки трг 12–16, Београд и <sup>4</sup>Универзитет у Београду, Институт за нуклеарне науке „Винча“, Национални институт Републике Србије, Лабораторија за радиоизотоце, Мике Пејшровић Аласа 12–14, Београд

Једињења која се користе у модној индустрији утичу на водна тела у околини текстилних фабрика, што резултира видљивим обојењем површинских вода. Домаће електроде на бази графита допирани гвожђем биле су укључене у деградацију Reactive Blue 52 (RB52) механизма попут Фентонове реакције. Електроде су се састојале од графита велике густине у три величине гранулације и три количине Fe и окарактерисане су помоћу скенирајуће електронске микроскопије (SEM). Оптимизоване су количина Fe у електродама и концентрација H<sub>2</sub>O<sub>2</sub> у синтетичној текстилној отпадној води. Додатно, величина графитних зрна је варирана како би се испитало да ли утиче на брзину разградње. За само 10 min електро-Фентонове деградације систем са 10 mmol dm<sup>-3</sup> H<sub>2</sub>O<sub>2</sub> и електродом од 7 % Fe и 70 μm величине гранулације графита разградило се преко 75 % RB52 и преко 99 % након 40 min третмана. Добијени резултати указују на то да предложени приступ може бити користан у области нових материјала за примену у животној средини и да домаће припремљени угљеник може бити одлична замена за комерцијално доступне носаче.

(Примљено 1. септембра, ревидирано 27. новембра, прихваћено 29. новембра 2021)

## REFERENCES

1. *Electro-Fenton Process: New Trends and Scale-Up*, M. Zhou, M. A. Oturan, I. Sirés, Eds., Springer, Singapore, 2018 (<https://doi.org/10.1007/978-981-10-6406-7>)
2. O. Ganzenko, C. Trellu, N. Oturan, D. Huguenot, Y. Péchaud, E. D. van Hullebusch, M. A. Oturan, *Chemosphere* **253** (2020) 126659 (<https://doi.org/10.1016/j.chemosphere.2020.126659>)
3. E. Brillas, I. Sirés, M. A. Oturan, *Chem. Rev.* **109** (2009) 6570 (<https://doi.org/10.1021/cr900136g>)
4. K. V. Plakas, A. J. Karabelas, in: *Electro-Fenton Process New Trends Scale-Up*, M. Zhou, M. A. Oturan, I. Sirés, Eds., Springer, Singapore, 2018, pp. 343–378 ([https://doi.org/10.1007/698\\_2017\\_52](https://doi.org/10.1007/698_2017_52))
5. C. K. Duesterberg, S. E. Mylon, T. D. Waite, *Environ. Sci. Technol.* **42** (2008) 8522 (<https://doi.org/10.1021/es081720d>)
6. F. C. Moreira, R. A. R. Boaventura, E. Brillas, V. J. P. Vilar, *Appl. Catal., B* **202** (2017) 217 (<https://doi.org/10.1016/j.apcatb.2016.08.037>)
7. K. M. Nair, V. Kumaravel, S. C. Pillai, *Chemosphere* **269** (2021) 129325 (<https://doi.org/10.1016/j.chemosphere.2020.129325>)
8. S. O. Ganiyu, M. Zhou, C. A. Martínez-Huitile, *Appl. Catal., B* **235** (2018) 103 (<https://doi.org/10.1016/j.apcatb.2018.04.044>)

9. R. N. Goyal, S. Bishnoi, *Bioelectrochemistry* **79** (2010) 234 (<https://doi.org/10.1016/j.bioelechem.2010.06.004>)
10. B. Vahid, A. Khataee, *Electrochim. Acta* **88** (2013) 614 (<https://doi.org/10.1016/j.electacta.2012.10.069>)
11. D. M. Stanković, A. Kukuruzar, S. Savić, M. Ognjanović, I. M. Janković-Častvan, G. Roglić, B. Antić, D. Manojlović, B. Dojčinović, *Mater. Chem. Phys.* **273** (2021) 125154 (<https://doi.org/10.1016/j.matchemphys.2021.125154>)
12. D. M. Stanković, M. Ognjanović, M. Fabián, V. V. Avdin, D. D. Manojlović, S. Vranješ, Đurić, B. B. Petković, *Surf. Interfaces* **25** (2021) 101211 (<https://doi.org/10.1016/j.surfin.2021.101211>)
13. P. Kariyajjanavar, N. Jogtappa, Y. A. Nayaka, *J. Hazard. Mater.* **190** (2011) 952 (<https://doi.org/10.1016/j.jhazmat.2011.04.032>)
14. W. Xu, S. Lai, S. C. Pillai, W. Chu, Y. Hu, X. Jiang, M. Fu, X. Wu, F. Li, H. Wang, *J. Colloid Interface Sci.* **574** (2020) 110 (<https://doi.org/10.1016/j.jcis.2020.04.038>)
15. G. Ren, M. Zhou, M. Liu, L. Ma, H. Yang, *Chem. Eng. J.* **298** (2016) 55 (<https://doi.org/10.1016/j.cej.2016.04.011>)
16. S. Bouafia-Chergui, N. Oturan, H. Khalaf, M. A. Oturan, *J. Environ. Sci. Health, A* **45** (2010) 622 (<https://doi.org/10.1080/10934521003595746>)
17. D. Marković, S. Milovanović, M. Radoičić, Ž. Radovanović, I. Zizović, Z. Šaponjić, M. Radetić, *J. Serb. Chem. Soc.* **83** (2018) 1379 (<https://doi.org/10.2298/JSC180913089M>)
18. M. Singh, D. Vaya, R. Kumar, B. Das, *J. Serbian Chem. Soc.* **86** (2021) 327 (<https://doi.org/10.2298/JSC200711074S>)
19. D. Manojlović, K. Lelek, G. Roglić, D. Zhrebtssov, V. Avdin, K. Buskina, C. Sakthidharan, S. Sapozhnikov, M. Samodurova, R. Zakirov, D. M. Stanković, *Int. J. Environ. Sci. Technol.* **17** (2020) 2455 (<https://doi.org/10.1007/s13762-020-02654-8>)
20. B. B. Petković, M. Ognjanović, B. Antić, V. V. Avdin, D. D. Manojlović, S. V. Đurić, D. M. Stanković, *Electroanalysis* **33** (2021) 446 (<https://doi.org/10.1002/elan.202060290>)
21. D. Gümüş, F. Akbal, *Process Saf. Environ. Prot.* **103** (2016) 252 (<https://doi.org/10.1016/j.psep.2016.07.008>).



SUPPLEMENTARY MATERIAL TO  
**In-house-prepared carbon-based Fe-doped catalysts for  
electro-Fenton degradation of azo dyes**

SLAĐANA D. SAVIĆ<sup>1\*</sup>, GORAN M. ROGLIĆ<sup>1</sup>, VYACHESLAV V. AVDIN<sup>2</sup>, DMITRY A. ZHEREBTSOV<sup>2</sup>, DALIBOR M. STANKOVIĆ<sup>3,4</sup> and DRAGAN D. MANOJLOVIĆ<sup>2,3</sup>

<sup>1</sup>University of Belgrade – Faculty of Chemistry, Department of Applied Chemistry, Studentski trg 12- 16, Belgrade, Serbia, <sup>2</sup>South Ural State University, 76, Lenin prospect, Chelyabinsk, Russia, 454080, <sup>3</sup>University of Belgrade – Faculty of Chemistry, Department of Analytical Chemistry, Studentski trg 12- 16, Belgrade, Serbia, <sup>4</sup>University of Belgrade, “Vinča” Institute of Nuclear Sciences, National Institute of the Republic of Serbia, Department of Radioisotopes, Mike Petrovića Alasa 12-14, Belgrade, Serbia

J. Serb. Chem. Soc. 87 (1) (2022) 57–67

TABLE S-I. RB52 degradation rate for 70-0 electrodes (70 µm granulation and 0 % of Fe) with different amounts H<sub>2</sub>O<sub>2</sub>

| τ, / min | c(H <sub>2</sub> O <sub>2</sub> ) |                         |                         |                          |
|----------|-----------------------------------|-------------------------|-------------------------|--------------------------|
|          | 0 mmol dm <sup>-3</sup>           | 1 mmol dm <sup>-3</sup> | 5 mmol dm <sup>-3</sup> | 10 mmol dm <sup>-3</sup> |
| 0        | 0.00                              | 0.00                    | 0.00                    | 0.00                     |
| 10       | 11.16                             | 38.20                   | 40.10                   | 40.00                    |
| 20       | 21.31                             | 61.80                   | 63.90                   | 62.20                    |
| 30       | 29.47                             | 75.90                   | 77.70                   | 74.80                    |
| 40       | 37.15                             | 85.60                   | 88.40                   | 84.90                    |
| 50       | 43.82                             | 92.50                   | 94.10                   | 90.80                    |

TABLE S-II. RB52 degradation rate for 125-0 electrodes (125 µm granulation and 0 % of Fe) with different amounts H<sub>2</sub>O<sub>2</sub>

| τ, / min | c(H <sub>2</sub> O <sub>2</sub> ) |                         |                         |                          |
|----------|-----------------------------------|-------------------------|-------------------------|--------------------------|
|          | 0 mmol dm <sup>-3</sup>           | 1 mmol dm <sup>-3</sup> | 5 mmol dm <sup>-3</sup> | 10 mmol dm <sup>-3</sup> |
| 0        | 0.00                              | 0.00                    | 0.00                    | 0.00                     |
| 10       | 20.37                             | 31.62                   | 33.80                   | 32.40                    |
| 20       | 34.03                             | 54.41                   | 57.40                   | 56.20                    |
| 30       | 44.10                             | 69.95                   | 73.30                   | 71.21                    |
| 40       | 53.30                             | 79.94                   | 83.40                   | 81.70                    |
| 50       | 61.10                             | 86.62                   | 89.39                   | 89.20                    |

\* Corresponding author. E-mail: sladjana@chem.bg.ac.rs



TABLE S-III. RB52 degradation rate for 205-0 electrodes (205 µm granulation and 0 % of Fe) with different amounts H<sub>2</sub>O<sub>2</sub>

| $\tau$ , / min | c(H <sub>2</sub> O <sub>2</sub> ) |                         |                         |                          |
|----------------|-----------------------------------|-------------------------|-------------------------|--------------------------|
|                | 0 mmol dm <sup>-3</sup>           | 1 mmol dm <sup>-3</sup> | 5 mmol dm <sup>-3</sup> | 10 mmol dm <sup>-3</sup> |
| 0              | 0.00                              | 0.00                    | 0.00                    | 0.00                     |
| 10             | 17.26                             | 24.50                   | 31.50                   | 30.55                    |
| 20             | 31.35                             | 44.80                   | 54.50                   | 52.55                    |
| 30             | 41.64                             | 60.40                   | 71.82                   | 70.09                    |
| 40             | 51.37                             | 73.30                   | 83.84                   | 81.46                    |
| 50             | 59.79                             | 82.80                   | 92.00                   | 88.23                    |

TABLE S-IV. RB52 degradation rate for 70-2 electrodes (70 µm granulation and 2 % of Fe) with different amounts H<sub>2</sub>O<sub>2</sub>

| $\tau$ , / min | c(H <sub>2</sub> O <sub>2</sub> ) |                         |                         |                          |
|----------------|-----------------------------------|-------------------------|-------------------------|--------------------------|
|                | 0 mmol dm <sup>-3</sup>           | 1 mmol dm <sup>-3</sup> | 5 mmol dm <sup>-3</sup> | 10 mmol dm <sup>-3</sup> |
| 0              | 0.00                              | 0.00                    | 0.00                    | 0.00                     |
| 10             | 19.65                             | 61.71                   | 64.78                   | 55.38                    |
| 20             | 32.55                             | 85.72                   | 88.84                   | 78.89                    |
| 30             | 44.80                             | 92.52                   | 95.61                   | 89.18                    |
| 40             | 55.23                             | 95.46                   | 97.82                   | 92.76                    |
| 50             | 64.25                             | 96.89                   | 98.62                   | 94.59                    |

TABLE S-V. RB52 degradation rate for 125-2 electrodes (125 µm granulation and 2 % of Fe) with different amounts H<sub>2</sub>O<sub>2</sub>

| $\tau$ , / min | c(H <sub>2</sub> O <sub>2</sub> ) |                         |                         |                          |
|----------------|-----------------------------------|-------------------------|-------------------------|--------------------------|
|                | 0 mmol dm <sup>-3</sup>           | 1 mmol dm <sup>-3</sup> | 5 mmol dm <sup>-3</sup> | 10 mmol dm <sup>-3</sup> |
| 0              | 0.00                              | 0.00                    | 0.00                    | 0.00                     |
| 10             | 27.45                             | 57.40                   | 58.21                   | 54.40                    |
| 20             | 43.47                             | 81.86                   | 82.92                   | 77.90                    |
| 30             | 56.26                             | 90.40                   | 91.77                   | 88.20                    |
| 40             | 66.50                             | 93.30                   | 95.00                   | 91.40                    |
| 50             | 75.10                             | 94.50                   | 95.30                   | 92.60                    |

TABLE S-VI. RB52 degradation rate for 205-2 electrodes (205 µm granulation and 2 % of Fe) with different amounts H<sub>2</sub>O<sub>2</sub>

| $\tau$ , / min | c(H <sub>2</sub> O <sub>2</sub> ) |                         |                         |                          |
|----------------|-----------------------------------|-------------------------|-------------------------|--------------------------|
|                | 0 mmol dm <sup>-3</sup>           | 1 mmol dm <sup>-3</sup> | 5 mmol dm <sup>-3</sup> | 10 mmol dm <sup>-3</sup> |
| 0              | 0.00                              | 0.00                    | 0.00                    | 0.00                     |
| 10             | 11.58                             | 59.92                   | 63.78                   | 54.38                    |
| 20             | 23.02                             | 82.46                   | 85.80                   | 77.89                    |
| 30             | 33.31                             | 89.60                   | 91.61                   | 86.50                    |
| 40             | 42.20                             | 92.00                   | 94.20                   | 89.70                    |
| 50             | 50.10                             | 93.20                   | 95.62                   | 91.90                    |

TABLE S-VII. RB52 degradation rate for 70-7 electrodes (70 µm granulation and 7 % of Fe) with different amounts H<sub>2</sub>O<sub>2</sub>

| $\tau$ , / min | c(H <sub>2</sub> O <sub>2</sub> ) |                         |                         |                          |
|----------------|-----------------------------------|-------------------------|-------------------------|--------------------------|
|                | 0 mmol dm <sup>-3</sup>           | 1 mmol dm <sup>-3</sup> | 5 mmol dm <sup>-3</sup> | 10 mmol dm <sup>-3</sup> |
| 0              | 0.00                              | 0.00                    | 0.00                    | 0.00                     |
| 10             | 15.83                             | 26.09                   | 60.83                   | 76.00                    |
| 20             | 27.67                             | 46.83                   | 82.77                   | 93.88                    |
| 30             | 38.04                             | 61.20                   | 90.55                   | 97.93                    |
| 40             | 46.98                             | 72.39                   | 93.74                   | 99.16                    |
| 50             | 54.80                             | 79.30                   | 95.73                   | 99.31                    |

TABLE S-VIII. RB52 degradation rate for 125-7 electrodes (125 µm granulation and 7 % of Fe) with different amounts H<sub>2</sub>O<sub>2</sub>

| $\tau$ , / min | c(H <sub>2</sub> O <sub>2</sub> ) |                         |                         |                          |
|----------------|-----------------------------------|-------------------------|-------------------------|--------------------------|
|                | 0 mmol dm <sup>-3</sup>           | 1 mmol dm <sup>-3</sup> | 5 mmol dm <sup>-3</sup> | 10 mmol dm <sup>-3</sup> |
| 0              | 0.00                              | 0.00                    | 0.00                    | 0.00                     |
| 10             | 21.95                             | 50.96                   | 64.06                   | 76.36                    |
| 20             | 36.99                             | 75.38                   | 85.40                   | 90.13                    |
| 30             | 49.23                             | 87.93                   | 91.96                   | 94.92                    |
| 40             | 60.28                             | 92.68                   | 94.22                   | 97.02                    |
| 50             | 69.24                             | 93.75                   | 94.70                   | 98.10                    |

TABLE S-IX. RB52 degradation rate for 205-7 electrodes (205 µm granulation and 7 % of Fe) with different amounts H<sub>2</sub>O<sub>2</sub>

| $\tau$ , / min | c(H <sub>2</sub> O <sub>2</sub> ) |                         |                         |                          |
|----------------|-----------------------------------|-------------------------|-------------------------|--------------------------|
|                | 0 mmol dm <sup>-3</sup>           | 1 mmol dm <sup>-3</sup> | 5 mmol dm <sup>-3</sup> | 10 mmol dm <sup>-3</sup> |
| 0              | 0.00                              | 0.00                    | 0.00                    | 0.00                     |
| 10             | 12.59                             | 49.85                   | 60.98                   | 65.06                    |
| 20             | 25.00                             | 78.40                   | 83.30                   | 87.40                    |
| 30             | 35.30                             | 89.74                   | 91.88                   | 93.96                    |
| 40             | 44.20                             | 93.80                   | 95.45                   | 96.22                    |
| 50             | 51.70                             | 94.80                   | 96.70                   | 97.70                    |





*J. Serb. Chem. Soc.* 87 (1) 69–81 (2022)  
JSCS-5505

# Journal of the Serbian Chemical Society

JSCS@tmf.bg.ac.rs • www.schd.org.rs/JSCS

Original scientific paper  
Published 14 January 2022

## Comparison of non-destructive techniques and conventionally used spectrometric techniques for determination of elements in plant samples (coniferous leaves)

JOVANA ORLIĆ<sup>1\*</sup>, MIRA ANIČIĆ UROŠEVIĆ<sup>2</sup>, KONSTANTIN VERGEL<sup>3</sup>,  
INGA ZINICOVSCAIA<sup>3</sup>, SANJA STOJADINOVIC<sup>4</sup>, IVAN GRŽETIĆ<sup>1</sup>  
and KONSTANTIN ILIJEVIĆ<sup>1#</sup>

<sup>1</sup>*University of Belgrade – Faculty of Chemistry, Studentski trg 12–16, 11000 Belgrade, Serbia,*  
<sup>2</sup>*Institute of Physics Belgrade, University of Belgrade, Pregrevica 118, 11080 Belgrade, Serbia,*

<sup>3</sup>*Frank Laboratory of Neutron Physics, Joint Institute for Nuclear Research, Joliot-Curie 6, 141980 Dubna, Russian Federation and*<sup>4</sup>*University of Belgrade, Institute of Chemistry, Technology and Metallurgy (ICTM), Njegoševa 12, 11000 Belgrade, Serbia*

(Received 21 September, revised 17 November, accepted 24 November 2021)

**Abstract:** Conventionally used spectrometric techniques of inductively coupled plasma optical emission spectrometry (ICP-OES) and inductively coupled plasma optical emission spectrometry (ICP-MS) usually involve time-consuming sample preparation procedure of a sample dissolution which requires the usage of aggressive and toxic chemicals. The need for suitable and sustainable analytical methods for direct multi-elemental analysis of plant samples has been increased in recent years. Spectrometric techniques for direct sample analysis, instrumental neutron activation analysis (INAA) and X-ray fluorescence (XRF) have been applied in environmental studies and various fields of screening tests. Nevertheless, these techniques are not commonly used for plant sample analysis and their performances need to be evaluated. This research aimed to assess how reliable non-destructive techniques are in the determination of elements in plants compared to conventionally used spectrometric techniques. A total of 49 plant samples of four conifer species (*Pinus nigra*, *Abies alba*, *Taxus baccata* and *Larix decidua*) were measured using two conventionally applied (ICP-MS, ICP-OES) and two non-destructive techniques (wavelength dispersive XRF (WD-XRF), INAA). The comparison was performed by investigation of relative ratios of concentrations and by correlation analysis. Moreover, precision of the techniques was examined and compared. The quality control included analysis of NIST pine needles certified reference material (1575a) using all examined techniques. Our results suggest that addit-

\* Corresponding author. E-mail: jovanaorlic@chem.bg.ac.rs

# Serbian Chemical Society member.

<https://doi.org/10.2298/JSC210921101O>



ional analytical and quality control steps are necessary for reaching the highest accuracy of multi-elemental analysis.

**Keywords:** multi-element determination; WD-XRF; standardless analysis; INAA; ICP-OES; ICP-MS.

## INTRODUCTION

The chemical composition of plant matrices has been conventionally determined by spectrometric techniques such as atomic absorption spectrometry (AAS), inductively coupled plasma optical emission spectrometry (ICP-OES), and inductively coupled plasma mass spectrometry (ICP-MS).<sup>1–4</sup> The usage of these techniques usually involves demanding sample preparation procedures for sample dissolution. For total destruction of the sample matrix, wet mineralization (digestion) with strong acids has been commonly used.<sup>5,6</sup> Digestion of the sample can be performed in closed or open systems using a wide choice of reagents and their mixtures. The complete digestion in open systems (at atmospheric pressure) usually requires a long time for some plant materials (up to 10 h or even more), and also there is a problem of the loss of volatile compounds. Digestion in a closed system implies the usage of microwave ovens which shortens the time required for dissolution, reducing the volume of corrosive and environmentally non-friendly reagents, and avoiding analyte losses and contamination.<sup>7</sup> However, the required time, equipment, the use of aggressive and toxic chemicals during the sample preparation procedure are the main drawbacks of those conventionally used techniques.<sup>8–11</sup>

In recent years, the need for suitable, sustainable, or more diverse analytical methods for direct and multielemental analysis of plant samples has been increased. Such need arises from the necessity to comply with the principles of green chemistry, but also in order to overcome the shortcomings of multiple conventionally used techniques, related to the analysis of certain elements (*e.g.*, quantification of Na and K using ICP-OES, and Ni using ICP-MS).

The instrumental neutron activation analysis (INAA) is one of the techniques that do not require previous mineralization of samples.<sup>12</sup> This technique requires thermal neutrons produced within a nuclear reactor for the activation of sample elements to form radioactive isotopes. High costs of equipment and maintenance, the long time needed for analysis (several days), and the limited availability of a nuclear reactor are the greatest shortcomings of the INAA technique. INAA has been previously applied in environmental studies (soils, sediments, biological samples), nevertheless, it is not a commonly used technique especially for the vegetal samples, and therefore it is worth to further explore its potential and limitations for plant analysis.<sup>13–16</sup>

X-ray fluorescence (XRF) is another nondestructive technique that has also been used for plant material analysis.<sup>17–21</sup> XRF spectrometry provides the pos-

sibility of performing direct multielement analysis of solid samples with a wide dynamic range and low cost per measurement.<sup>22–29</sup> Using the XRF technique, it is possible to perform qualitative, semiquantitative, and quantitative determinations within a short time of analysis (high throughput). The limitations for more frequent usage of XRF spectrometry in environmental studies are higher detection limits for some environmentally important elements (*e.g.*, Pb and Cd).<sup>2,30</sup> The general characteristic of analytical techniques discussed in this study are described in research of Frontasyeva and Orlić *et al.*<sup>31,32</sup>

Conifers have been proven to be passive biomonitoring of atmospheric pollution because of their characteristics (thick epicuticular waxy layer) and their distribution all over the world, in urban and industrial environments, in natural forests, as well as in maintained habitats.<sup>33–36</sup>

Although several well-known analytical techniques which require wet digestion are successfully applied to multielemental analysis of plant samples, it is still necessary to explore the potential of the other analytical options for numerous reasons. Either because some elements cannot be accurately analyzed by one or more conventionally used analytical techniques or because total sample digestion can not be easily accomplished (*e.g.*, matrices with high Si content). Non-destructive techniques not only preserve samples for further analysis, but may also save a significant amount of resources and time. Investigated non-destructive techniques (WD-XRF and INAA) are still not routinely used for the analysis of plant samples, therefore it is important to compare their strengths and limitations to conventionally used analytical techniques (ICP-OES and ICP-MS), as well as the potential to replace or complement them. Another goal was to compare the standardless semiquantitative XRF method to other investigated techniques since it is expected that it has lower accuracy, but it also has the highest potential for fast screening studies, because it neither requires digestion of the sample nor any calibration standards.

## EXPERIMENTAL

A total of 49 plant samples of four conifer tree species, black pine (*Pinus nigra*), white fir (*Abies alba*), European yew (*Taxus baccata*), and larch (*Larix decidua*), were measured using four instrumental techniques (WD-XRF, ICP-MS, ICP-OES and INAA). Conifer needles were collected during spring (April and May) on four locations: Belgrade, Pančevo, Banatski Brestovac, and Šar Mountains. The studied locations represent urban and rural areas. The collected needles were up to one year old.

Needles samples were placed into plastic bags and delivered to the laboratory. In the laboratory, samples were air-dried for several days. Conifer needles were then grounded and drying was continued in the oven at 60 °C until a constant mass was reached.

Within WD-XRF analysis, the grounded and dried plant samples were pressed into 32 mm diameter pellets using Retsch PP25 hydraulic press with 15 tons pressure applied for 5 min. The prepared pellets contained around 4 g of plant samples and 20 wt. % of binder (Hoechst wax C micropowder, Merck, C.A.S. number: 110-30-5).

For INAA analysis, approximately 0.3 g of grounded conifer samples was pelletized in 10 mm diameter pellets. For short-term irradiation purposes, plant pellets were heat-sealed in polyethylene foil bags, whereas for long-term irradiation the samples were packed in aluminium cups. Further, polyethylene foils bags and aluminium cups were transferred by pneumo-transport system to the reactor for irradiation.

For ICP-OES and ICP-MS analysis, conifer powder samples (approximately 200 mg) were subjected to microwave digestion with 5 mL of 65 vol. % HNO<sub>3</sub> (Merck) and 2 mL of 30 vol. % H<sub>2</sub>O<sub>2</sub> (Merck).<sup>32</sup> A microwave oven Berghof (Speedwave, Berghof, Germany) was used for the sample digestion. After a cooling period, the samples were quantitatively transferred into a volumetric flask of 25 mL and diluted with ultra-pure water (Millipore Simplicity 185 system).

#### *Instrumental techniques*

*Wavelength dispersive X-ray fluorescence spectrometry (WD-XRF).* An ARL™ PERFORM'X sequential X-Ray fluorescence spectrometer (Thermo Fisher Scientific, Switzerland) equipped with a 4.2 kW Rh X-ray tube with a 50 µm Be window was applied. A primary beam spot size of 29 mm in diameter was used. The spectrometer was equipped with seven different crystals (AX16, AX03, AX09, Ge111, LiF200, LiF220 and PET), four collimators (0.15, 0.4, 1.0 and 2.6), and a tandem of detectors (flow proportional counter and scintillation counter). The analysis was performed in a high vacuum atmosphere (< 1 Pa). For qualitative analysis, spectral recording, and data processing, a software program Thermo Scientific™ OXSAS was used.<sup>37</sup> Two different types of quantitative analysis were used during the experimental work in this study, empirical calibration and standardless method. Empirical calibration was performed using artificial spiked cellulose standards (in further text WD-XRF). The procedure of cellulose standard preparation and calibration was described in the previous paper.<sup>32</sup> Table S-I (Supplementary material to this paper) shows the analytical lines and parameters for the analyzed elements. UniQuant (ThermoFisher Scientific, Integrated version), a standardless semi-quantitative to quantitative method for XRF analysis was used.<sup>38</sup>

*Instrumental neutron activation analysis (INAA).* INAA was performed using the pneumo-transport facility REGATA at the IBR-2 reactor (Frank Laboratory of Neutron Physics, Joint Institute for Nuclear Research FLNP, JINR, Dubna, Russia). The IBR-2 pulsed nuclear reactor has an average power of 2 MW and installed a pneumatic system.<sup>39</sup> Short-lived elements (Mg, Al, Cl, Ca, Ti, V, Mn and I) were irradiated for 3 min and measured for 15 min. Another aliquote of plant sample was irradiated for 3 days in the Cd-screened channel under the neutron flux of  $1.8 \times 10^{11} \text{ cm}^{-2} \text{ s}^{-1}$  to determine long-lived isotopes. The first group of long-lived isotopes (LLI 1; Na, K, As, Br, Mo, La, Sm, W, Au and U) were measured for 30 min after 4 days of decay, while the second group of long-lived isotopes (LLI 2; Sc, Cr, Fe, Co, Ni, Zn, Se, Rb, Sr, Zr, Sb, Cs, Ba, Ce, Nd, Eu, Tb, Yb, Hf, Ta and Th) were measured for 90 min after 20 days of decay. HPGe detector with a resolution of 2.5–3 keV for the 1332 keV line of the <sup>60</sup>Co was used for gamma spectra measurement. To display, analyze and store the gamma spectra Genie 2000 software was used.

*Inductively coupled plasma mass spectrometry (ICP-MS).* For plant samples analysis ICP-MS (iCAP Q, Thermo Scientific X series 2) was used. The entire system of ICP-MS is controlled with Qtegra Instrument Control Software. The analysis was carried out at the following operating parameters for the instrument: 1.548 kW radio frequency power, 13.9 L·min<sup>-1</sup> plasma gas flow, 1.09 L·min<sup>-1</sup> auxiliary gas flow, 0.80 L·min<sup>-1</sup> carrier gas flow, and 3.50 s acquisition time.

*Inductively coupled plasma optical emission spectrometry (ICP-OES).* Analysis of digested plant samples was carried out by an ICP-OES instrument (iCAP 6500 Duo; Thermo Scientific, Loughborough, UK). For data processing, the specialized iTEVA software was used. The quantification of 19 elements (Na, Mg, Al, K, Ca, Cr, Mn, Fe, Co, Ni, Cu, Zn, Sr, Ag, Cd, In, Tl, Bi and Pb) was carried out in axial mode and at the following operating parameters for the instrument: 1.150 kW radio frequency power, 12.0 L·min<sup>-1</sup> plasma gas flow, 0.50 L·min<sup>-1</sup> auxiliary gas flow, 0.50 L·min<sup>-1</sup> carrier gas flow.

#### *Quality control*

For the purpose of quality control, NIST pine needles certified reference material (1575a) was analyzed using all examined techniques. Table S-II of the Supplementary material shows the certified values and the measured ICP-MS, ICP-OES, INAA, UQ and WD-XRF concentrations in mg kg<sup>-1</sup> for investigated and detected elements. The measured concentrations were in good accordance with the certified for all investigated techniques.

## RESULTS AND DISCUSSION

Elements in the analyzed real sample set are present in a wide concentration range, as can be seen in Table S-III (Supplementary material), which sums up descriptive statistics of all investigated elements measured using different analytical techniques. Thereby, the results are shown as relative concentration ratios. The relative ratio values were calculated by dividing the element concentration measured, using the investigated analytical techniques with the concentration determined by ICP-MS and multiplied by 100. ICP-MS is the most commonly used technique within plant analysis, which possesses a very wide linear range, low detection limits, good accuracy, and precision. For that reason, the ICP-MS was used as the basis for comparisons of other investigated techniques in this research. Fig. 1 shows the median of the relative ratios of concentrations obtained using different analytical techniques compared with ICP-MS results for the same sample. Minimum, maximum, median, average, and standard deviations of relative ratios are presented in Table S-IV (Supplementary material).

The comparison of investigated techniques presented in Fig. 1 shows that concentrations of most of the analyzed elements are in good accordance, except for Na. UQ method is most often not in agreement with other techniques, which was expected, since this is a semi-quantitative method. Ratios of some elements were not presented for the WD-XRF technique because they were below the detection limit. The results also show that Na is a very difficult element for quantification, regardless of the type of the used technique.

The results obtained using ICP-OES were underestimated compared to ICP-MS for all analyzed samples, except for Na. On the contrary, the concentrations obtained using UQ method were overestimated compared to ICP-MS for all the analyzed elements, except for Mg. UQ as a standardless method for direct analysis shows a positive systematic error. Ratios of WD-XRF and ICP-MS did not show any trend of systematic errors (they are neither dominantly positive nor negative).

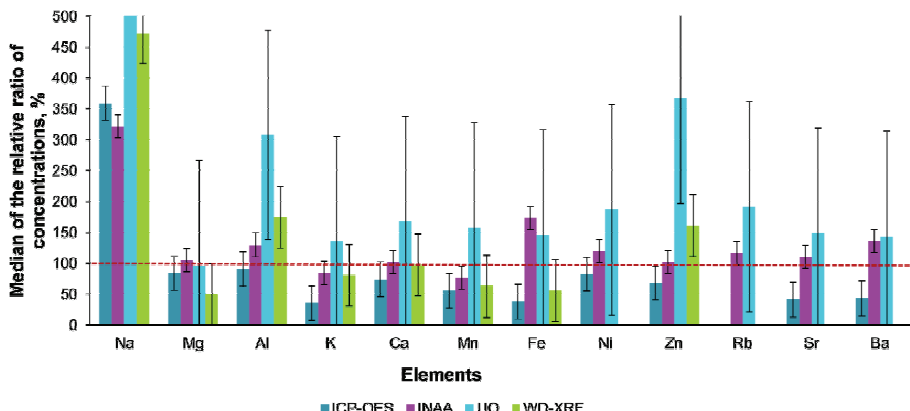


Fig. 1. Median values of the relative ratios of concentrations obtained using different techniques compared with ICP-MS concentration. The error bar represents  $\pm$  standard deviation the relative ratio values.

Relative ratios of INAA concentrations were always in the range of 70–130 % compared to ICP-MS concentrations, except for Na (332 %), Fe (173 %) and Ba (136 %), which indicated that this non-destructive technique produced results that were most similar to ICP-MS results.

The relative ratios of concentration of P and S, measured using only ICP-MS and UQ, are presented in Fig. 2. UQ method produces results that were in good accordance with ICP-MS for these two elements.

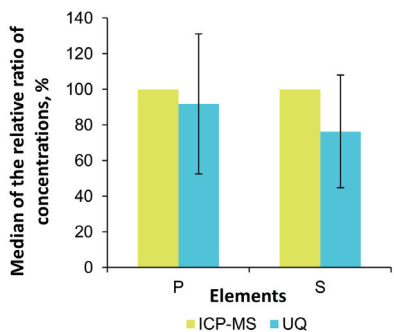


Fig. 2. Median of the relative ratio of concentrations of P and S obtained using ICP-MS and UQ.

#### Comparison of the techniques based on paired t-test

Paired *t*-test was applied in order to objectively estimate whether the difference among applied techniques is statistically significant. Table I shows the analyzed elements which were divided into three groups, according to the results of the paired *t*-test. The first group in the table gathered the elements whose concentrations did not show a statistical difference when investigated analytical techniques were compared, while in the other two groups (“Difference\*” and

“Difference\*\*”) difference was statistically significant at 0.05 and 0.01 levels, respectively.

TABLE I. Grouping of elements according to results of paired *t*-test applied to the compared analytical techniques. Boundaries between groups of elements are based on *P* values of the paired *t*-test (*P* = 0.05 and *P* = 0.01); \* – significant at the 0.05 level; \*\* – significant at the 0.01 level

| Compared techniques | Without difference | Difference* | Difference**                     |
|---------------------|--------------------|-------------|----------------------------------|
| ICP-MS and INAA     | Mg, Ca, Mn, Rb, Sr | Ba          | Na, Al, K, Fe, Ni                |
| ICP-MS and UQ       | Mg, P              | Mn          | Na, Al, K, Ca, S, Fe, Zn, Rb, Sr |
| ICP-MS and WD-XRF   | Na, Ca             | Mn          | Mg, Al, K, Fe, Zn                |
| ICP-OES and INAA    | Na, Mn, Ni, Zn     | Mg, Ba      | Al, K, Ca, Fe, Sr                |
| ICP-OES and UQ      |                    | –           | Na, Mg, Al, K, Ca, Mn, Fe, Zn    |
| ICP-OES and WD-XRF  | Na, Mn             | –           | Mg, Al, K, Ca, Fe, Zn            |
| INAA and UQ         | Mg                 | Mn, Fe      | Na, Al, K, Ca, Zn, Rb, Sr        |
| INAA and WD-XRF     | Na, Al, K, Ca, Mn  | Zn          | Mg, Fe                           |
| UQ and WD-XRF       | –                  | –           | Na, Mg, Al, K, Ca, Mn, Fe, Zn    |

From Table I it is possible to notice that ICP-MS did not show a statistically significant difference within the analysis of Mg, Ca, Mn, Rb and Sr compared with INAA; Mg and P compared with UQ; Na and Ca compared with WD-XRF. There was a statistically significant difference between ICP-MS and non-destructive techniques for all rest elements. ICP-OES did not show a statistically significant difference within the analysis of Na, Mn, Ni and Zn when compared with INAA; Na and Mn compared with WD-XRF. There is a statistically significant difference between ICP-OES and UQ for all analyzed elements. In comparison with XRF techniques, INAA did not show a significant difference within the analysis of Mg compared with UQ, and Na, Al, K, Ca and Mn compared with WD-XRF. There was a statistically significant difference between UQ and XRF methods for all analyzed elements.

According to the results of paired *t*-test, Fe showed a statistically significant difference within all compared techniques. UQ method differed from other techniques for the largest number of elements. Na, Mn, and Ca most frequently showed parity among compared techniques. Nevertheless, one must be careful during the interpretation of the *t*-test results, since some elements such as Na might show the absence of statistically significant differences not because the investigated techniques produce similar results, but because they all have low precision and large random error related to the analysis of this element.

#### *Comparison of the techniques based on correlation*

In the previous section, it was observed that investigated techniques may produce results with a statistically significant difference for a number of elements. The next logical question is to establish whether these measurements,

obtained from compared techniques, are correlated or not. Because if the results are well correlated then the difference between compared techniques is a consequence of systematic error related to one or both of compared techniques, which means that it can be more thoroughly described and corrected.

The correlations of concentrations of analyzed elements measured by investigated techniques were compared by nonparametric Spearman's correlation coefficients ( $\rho$ ) which are presented in Table II.

TABLE II. Spearman's correlation coefficient ( $\rho$ ) for elements of all compared techniques; \* – significant at the 0.05 level; \*\* – significant at the 0.01 level; \*\*\* – significant at the 0.001 level

| Element | ICP-MS<br>and<br>INAA | ICP-MS<br>and UQ | ICP-MS<br>and WD-<br>XRF | ICP-OES<br>and<br>INAA | ICP-OES<br>and<br>UQ | ICP-OES<br>and WD-<br>XRF | INAA<br>and UQ | INAA<br>and WD-<br>XRF | UQ and<br>WD-<br>XRF |
|---------|-----------------------|------------------|--------------------------|------------------------|----------------------|---------------------------|----------------|------------------------|----------------------|
| Na      | 0.836***              | 0.354*           | 0.182                    | 0.424*                 | 0.041                | 0.168                     | 0.455**        | 0.159                  | 0.081                |
| Mg      | 0.714***              | 0.334*           | 0.641***                 | 0.622***               | 0.437**              | 0.681***                  | 0.263          | 0.526***               | 0.194                |
| Al      | 0.884***              | 0.753***         | 0.823***                 | 0.818***               | 0.786***             | 0.833***                  | 0.720***       | 0.801***               | 0.932***             |
| K       | 0.938***              | 0.707***         | 0.813***                 | 0.681***               | 0.611***             | 0.774***                  | 0.729***       | 0.855***               | 0.837***             |
| Ca      | 0.873***              | 0.690***         | 0.845***                 | 0.880***               | 0.855***             | 0.970***                  | 0.764***       | 0.900***               | 0.877***             |
| P       | –                     | 0.723***         | –                        | –                      | –                    | –                         | –              | –                      | –                    |
| S       | –                     | 0.412**          | –                        | –                      | –                    | –                         | –              | –                      | –                    |
| Mn      | 0.766***              | 0.607***         | 0.711***                 | 0.734***               | 0.731***             | 0.835***                  | 0.669***       | 0.786***               | 0.822***             |
| Fe      | 0.417***              | 0.535***         | 0.770***                 | 0.472***               | 0.500***             | 0.586***                  | 0.269*         | 0.434***               | 0.646***             |
| Ni      | 0.779***              | –                | –                        | 0.470*                 | –                    | –                         | –              | –                      | –                    |
| Zn      | 0.647***              | 0.267            | 0.097                    | 0.621***               | 0.361*               | 0.164                     | 0.334*         | -0.017                 | 0.631***             |
| Rb      | 0.767***              | 0.814***         | –                        | –                      | –                    | –                         | 0.814***       | –                      | –                    |
| Sr      | 0.936***              | 0.753***         | –                        | 0.979***               | 0.688**              | –                         | 0.802***       | –                      | –                    |
| Ba      | 0.930***              | 0.5              | –                        | 0.864**                | –                    | –                         | –              | –                      | –                    |

The statistically significant correlation at the 0.001 level was found for all elements within ICP-MS and INAA comparison. The correlation between the ICP-MS and XRF techniques (UQ and WD-XRF) was statistically significant at the 0.001 level for the most of the investigated elements, except for Na and Mg ( $P < 0.05$ ) and S ( $P < 0.01$ ) with UQ method (Table II). There was no statistically significant correlation for Zn within ICP-MS and WD-XRF, and for Zn and Ba within ICP-MS and UQ comparisons.

The comparison of ICP-OES with non-destructive techniques showed similar results as when they were compared to ICP-MS. The statistically significant correlation at the 0.001 level was observed for most of the investigated elements. The correlation between ICP-OES and INAA was statistically significant at the 0.01 level for Ba, at the 0.05 level for Na and Ni. The correlation between ICP-OES and UQ was statistically significant only at the 0.01 level for Mg and Sr, only at the 0.05 level for Zn, and it was without statistical significance for Na.

The comparison with WD-XRF method did not show a statistically significant correlation for Na and Zn.

The statistically significant correlation between the INAA and UQ was found for Al, K, Ca, Mn, Rb and Sr ( $P < 0.001$ ); Na ( $P < 0.01$ ); Fe and Zn ( $P < 0.05$ ), while for Mg there was no statistically significant correlation. For INAA and WD-XRF comparison the statistically significant correlation at 0.001 level was found for all observed elements, except Na and Zn, for which there was no statistically significant correlation.

Comparison of the results of two XRF methods showed statistically significant correlation at the 0.001 level for all observed elements, with exception of Na and Mg (no statistically significant correlation).

Results in Table II demonstrated that measurements of the investigated techniques were well correlated, but not for all elements and all instrumental techniques. Sometimes instrumental techniques have difficulties producing accurate results due to technical reasons: *e.g.*, some ICP-MS instruments have sampler and skimmer cones created from Ni, which hinders quantification of this element by ICP-MS, while XRF instruments may have problems to accurately quantify Zn if the sample holder contains this element *etc.* On the other side were elements that are immanently difficult for quantification for one or even more techniques. The best example was Na which is inconvenient for ICP-OES because it had a small number of lines that were often burdened with spectral interferences, while XRF techniques suffer from very low sensitivity when they analyze spectral lines of Na. Fe was another element in our research without very good agreement among applied techniques results which could be attributed to lower concentrations compared to other macro elements (Al, Mg, Ca, K), but this cannot be the only reason for the discordance among applied techniques since other elements with low concentrations were very well correlated (*e.g.*, Sr, Br, Ni).

The fact that measurements from compared techniques were well correlated (Table II) and that some techniques had lower (ICP-OES vs. ICP-MS) or higher (UQ vs. ICP-MS) correlation coefficients for all investigated elements implied that the systematic error significantly affects observed discrepancies among investigated instrumental techniques. Nevertheless, a systematic error can be corrected if it is properly characterized.

#### *Comparison of techniques' precisions*

Every plant sample was analyzed multiple times with each of the investigated techniques, therefore it was possible to calculate the relative standard deviation ( $RSD$ ) for every measurement, which was used for comparisons of techniques' precisions. The Medians of relative standard deviations of repeated measurements of all investigated techniques are presented in Fig. 3. Minimum, maximum, average, and medians of  $RSD$  are presented in Table S-V (Supplementary material). Mea-

surements of all investigated analytical techniques were performed with low *RSD* values. Except for Ni, *RSD* of ICP-MS was lower than 5 % for all analyzed elements. *RSD* of non-destructive techniques (INAA, UQ and WD-XRF) was sometimes lower than *RSD* of ICP-MS and *RSD* medians are for the most elements lower than 10 %.

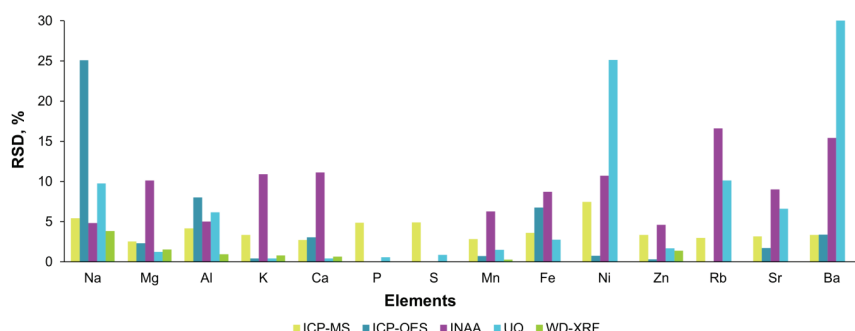


Fig. 3. Medians of relative standard deviations of repeated measurements of elements content, obtained using all investigated techniques.

## CONCLUSION

Comparisons in this study confirmed that the non-destructive spectroscopic techniques (INAA, WD-XRF, UQ) can be successfully applied to the analysis of plant samples which is valuable because sample preparation for these techniques can be fast and in good accordance with the principles of green chemistry. Even the semi-quantitative UQ method can produce either similar or at least well-correlated results, when it is compared to other techniques based on calibration standards. Although all investigated techniques have had comprehensive QC programs which included analysis of certified reference materials (CRM), their results have in some cases demonstrated discrepancies. Studies like ours, which analyze a large number of elements in samples from the environment (with potentially difficult matrices), rely on multi-element standards for calibration. The multi-element standards may have some interfering elements in much higher concentrations than in the analyzed samples and *vice versa*. On the other side, CRMs may not be enough similar to all analyzed samples within one research (either by the composition or by concentration) which limits their ability to control the accuracy of the technique. Our results suggest that if the highest possible accuracy is a priority for the analysis, the additional analytical and QC steps must be taken, such as the use of internal standards or standard addition.

## SUPPLEMENTARY MATERIAL

Additional data and information are available electronically at the pages of journal website: <https://www.shd-pub.org.rs/index.php/JSCS/article/view/11186>, or from the corresponding author on request.

*Acknowledgment.* This research was funded the Ministry of Education, Science and Technological Development of the Republic of Serbia (Grants No: 451-03-68/2020-14/200168 and 451-03-9/2021-14/200026). A part of research was supported by the project of bilateral cooperation between Institute of Physics Belgrade and Joint Institute for Nuclear Research, Dubna, Russia. There are no potential conflicts-of-interest to declare.

## ИЗВОД

ПОРЕЂЕЊЕ НЕДЕСТРУКТИВНИХ И КОНВЕНЦИОНАЛНО КОРИШЋЕНИХ  
СПЕКТОМЕТРИЈСКИХ ТЕХНИКА ЗА ОДРЕЂИВАЊЕ ЕЛЕМЕНТА У БИЉНОМ  
МАТЕРИЈАЛУ (ИГЛИЦЕ ЧЕТИНАРА)

ЈОВАНА ОРЛИЋ<sup>1</sup>, МИРА АНИЧИЋ УРОШЕВИЋ<sup>2</sup>, КОНСТАНТИН ВЕРГЕЛ<sup>3</sup>, ИНГА ЗИНИКОВСКАЈА<sup>3</sup>,  
САЊА СТОЈАДИНОВИЋ<sup>4</sup>, ИВАН ГРЖЕТИЋ<sup>1</sup> и КОНСТАНТИН ИЛИЈЕВИЋ<sup>1</sup>

<sup>1</sup>Универзитет у Београду – Хемијски факултет, Студентски тајм 12–16, 11000 Београд, <sup>2</sup>Институт за физику у Београду, Универзитет у Београду, Прећевица 118, 11080 Београд, <sup>3</sup>Frank Laboratory of Neutron Physics, Joint Institute for Nuclear Research, Joliot-Curie 6, 141980 Dubna, Russian Federation

<sup>4</sup>Универзитет у Београду, Институт за хемију, технологију и металургију (ИХТМ),  
Новоштадска 12, 11000 Београд

Конвенционално коришћене спектрометријске технике (ICP-OES, ICP-MS) обично подразумевају дуготрајну процедуру припреме узорка која захтева коришћење агресивних и токсичних хемикалија за минерализацију. У последњих неколико година расте потреба за погодним и одрживим аналитичким методама за директну мулти-елементарну анализу биљних узорака. Спектрометријске технике за директну анализу (INAA, XRF) се већ примењују у еколошким истраживањима и у различитим пољима скрининг испитивања. Ипак, ове технике нису уобичајено коришћене за анализу биљака и њихове перформансе морају бити процењене. Циљ овог истраживања је био да се процени колико су недеструктивне технике поуздане код одређивања елемената у биљном материјалу, у односу на рутински коришћене спектрометријске технике. Укупно 49 узорака четири врсте четинара (*Pinus nigra*, *Abies alba*, *Taxus baccata* и *Larix decidua*) су анализирани помоћу две рутински коришћене (ICP-MS и ICP-OES) и две недеструктивне технике (WD-XRF и INAA). Технике су упоређене испитивањем релативних односа концентрација и помоћу корелационе анализе. Поред тога, испитана је и упоређена прецизност техника. Програм контроле квалитета је обухватао анализу сертификованог референтног материјала, иглица бора (NIST 1575a) помоћу свих коришћених техника. Резултати нашег истраживања сугеришу да су неопходни додатни аналитички и кораци контроле квалитета како би се постигла максимална тачност мулти-елементарне анализе.

(Примљено 21. септембра, ревидирано 17. новембра, прихваћено 24. новембра 2021)

## REFERENCES

- W. E. Stephens, A. Calder, *Anal. Chim. Acta* **527** (2004) 89 (<https://doi.org/10.1016/j.aca.2004.08.015>)
- I. Queralt, M. Ovejero, M. L. Carvalho, A. F. Marques, J. M. Llabrés, *X-Ray Spectrom.* **34** (2005) 213 (<https://doi.org/10.1002/xrs.795>)
- C. Kilbride, J. Poole, T. R. Hutchings, *Environ. Pollut.* **143** (2006) 16 (<https://doi.org/10.1016/j.envpol.2005.11.013>)
- S. Reidinger, M. H. Ramsey, S. E. Hartley, *New Phytol.* (2015) 699 (<https://doi.org/10.1111/j.1469-8137.2012.04179.x>)

5. H. Polkowska-Motrenko, B. Danko, R. Dybczyński, A. Koster-Ammerlaan, P. Bode, *Anal. Chim. Acta* **408** (2000) 89 ([https://doi.org/10.1016/S0003-2670\(99\)00867-3](https://doi.org/10.1016/S0003-2670(99)00867-3))
6. S. C. C. Arruda, A. P. M. Rodriguez, M. A. Z. Arruda, *J. Braz. Chem. Soc.* **14** (2003) 470 (<https://doi.org/10.1590/S0103-50532003000300023>)
7. E. Marguí, I. Queralt, M. L. Carvalho, M. Hidalgo, *Anal. Chim. Acta* **549** (2005) 197 (<https://doi.org/10.1016/j.aca.2005.06.035>)
8. A. Gałuszka, Z. M. Migaszewski, P. Konieczka, J. Namieśnik, *Trends Anal. Chem.* **37** (2012) 61 (<https://doi.org/10.1016/j.trac.2012.03.013>)
9. S. Armenta, S. Garrigues, M. de la Guardia, *Trends Anal. Chem.* **71** (2015) 2 (<https://doi.org/10.1016/j.trac.2014.12.011>)
10. J. Płotka-Wasylka, *Talanta* **181** (2018) 204 (<https://doi.org/10.1016/j.talanta.2018.01.013>)
11. K. Chojnacka, M. Mikulewicz, *Trends Anal. Chem.* (2019) 254 (<https://doi.org/10.1016/j.trac.2019.02.013>)
12. M. V. Frontasyeva, *Phys. Part. Nucl.* **42** (2011) 332 (<https://doi.org/10.1134/S1063779611020043>)
13. A. Taftazani, R. Roto, N. R. Ananda, S. Murniasih, *Indones. J. Chem.* **17** (2017) 228 (<https://doi.org/10.22146/ijc.17686>)
14. E. T. Tousi, M. M. Firoozabadi, M. Shiva, E. Taghizadeh, M. Mehdi, M. Shiva, *Measurement* **90** (2016) 20 (<https://doi.org/10.1016/j.measurement.2016.04.020>)
15. R. Acharya, P. K. Pujari, *Forensic Chem.* **12** (2019) 107 (<https://doi.org/10.1016/j.forc.2018.01.002>)
16. K. Vergel, I. Zinicovscaia, N. Yushin, M. V. Frontasyeva, *Bull. Environ. Contam. Toxicol.* **103** (2019) 435 (<https://doi.org/10.1007/s00128-019-02672-4>)
17. C. Anderson, F. Moreno, F. Geurts, C. Wreesmann, M. Ghomshei, J. Meech, *Microchem. J.* **81** (2005) 81 (<https://doi.org/10.1016/j.microc.2005.01.004>)
18. G. Budak, I. Aslan, A. Karabulut, E. Tiraşoğlu, *J. Quant. Spectrosc. Radiat. Transf.* **101** (2006) 195 (<https://doi.org/10.1016/j.jqsrt.2005.11.013>)
19. N. Ekinci, R. Ekinci, R. Polat, G. Budak, *J. Radioanal. Nucl. Chem.* **260** (2004) 127 (<https://doi.org/10.1023/B:JRNC.0000027071.72742.ee>)
20. M. Z. Abdullah, A. Saat, Z. Hamzah, *Am. J. Eng. Appl. Sci.* **4** (2011) 355 (<https://doi.org/10.3844/ajeassp.2011.355.362>)
21. J. Orlić, I. Gržetić, K. Ilijević, *Spectrochim. Acta, B* **184** (2021). (<https://doi.org/10.1016/j.sab.2021.106258>) 106258
22. C. M. Wu, H. T. Tsai, K. H. Yang, J. C. Wen, *Environ. Forensics* **13** (2012) 110 (<https://doi.org/10.1080/15275922.2012.676603>)
23. D. Andrey, J. P. Dufrier, L. Perring, *Spectrochim. Acta, B* **148** (2018) 137 (<https://doi.org/10.1016/j.sab.2018.06.014>)
24. T. Radu, D. Diamond, *J. Hazard. Mater.* **171** (2009) 1168 (<https://doi.org/10.1016/j.jhazmat.2009.06.062>)
25. C. Vanhoof, V. Corthouts, K. Tirez, *J. Environ. Monit.* **6** (2004) 344 (<https://doi.org/10.1039/b312781h>)
26. A. S. G. Thaisa, P. D. G. Rennan, D. S. Severina, E. R. M. C. M. Mário, E. M. D. Maria, M. F. D. F. Rossana, T. M. Ricardo, *Afr. J. Biotechnol.* **14** (2015) 3333 (<https://doi.org/10.5897/ajb2015.14925>)
27. E. V. Chuparina, T. N. Gunicheva, *J. Anal. Chem.* **58** (2003) 856 (<https://doi.org/10.1023/A:1025689202055>)

28. T. J. Morgan, A. George, A. K. Boulamanti, P. Álvarez, I. Adanouj, C. Dean, S. V. Vassilev, D. Baxter, L. K. Andersen, *Energy Fuels* **29** (2015) 1669 (<https://doi.org/10.1021/ef502380x>)
29. L. Perring, D. Andrey, *X-Ray Spectrom.* **33** (2004) 128 (<https://doi.org/10.1002/xrs.725>)
30. R. M. Rousseau, *Rigaku J.* **18** (2001) 33 ([https://www.researchgate.net/publication/228687395\\_Detection\\_limit\\_and\\_estimate\\_of\\_uncertainty\\_of\\_analytical\\_XRF\\_results](https://www.researchgate.net/publication/228687395_Detection_limit_and_estimate_of_uncertainty_of_analytical_XRF_results))
31. M. V. Frontasyeva, *Phys. Part. Nucl.* **42** (2011) 332 (<https://doi.org/10.1134/S1063779611020043>)
32. J. Orlić, I. Gržetić, W. Goessler, S. Braeuer, J. Čáslavský, J. Pořízka, K. Ilijević, *Nucl. Ins. Methods Phys. Res., B* **502** (2021) 106 (<https://doi.org/10.1016/j.nimb.2021.06.012>)
33. D. Čeburnis, E. Steinnes, *Atmos. Environ.* **34** (2000) 4265 ([https://doi.org/10.1016/S1352-2310\(00\)00213-2](https://doi.org/10.1016/S1352-2310(00)00213-2))
34. M. Pietrzykowski, J. Socha, N. S. van Doorn, *Sci. Total Environ.* **470–471** (2014) 501 (<https://doi.org/10.1016/j.scitotenv.2013.10.008>)
35. M. M. Al-Alawi, K. L. Mandiwana, *J. Hazard. Mater.* **148** (2007) 43 (<https://doi.org/10.1016/j.jhazmat.2007.02.001>)
36. S. M. Serbula, T. S. Kalinovic, A. A. Ilic, J. V Kalinovic, M. M. Steharnik, *Aerosol Air Qual. Res.* **13** (2013) 563 (<https://doi.org/10.4209/aaqr.2012.06.0153>)
37. Oxsas, [https://www.thermofisher.com/content/dam/tfs/ATG/CAD/CAD/Documents/Product/Manuals&Specifications/Elemental/Analysis/XRF/X\\_R-PS41141-OXSAS-XRF-Hi-0713.pdf](https://www.thermofisher.com/content/dam/tfs/ATG/CAD/CAD/Documents/Product/Manuals&Specifications/Elemental/Analysis/XRF/X_R-PS41141-OXSAS-XRF-Hi-0713.pdf) (accessed September 13, 2021)
38. UniQuant®, <http://www.uniquant.com> (accessed September 13, 2021)
39. M. V. Frontasyeva, S. S. Pavlov, V. N. Shvetsov, *J. Radioanal. Nucl. Chem.* **286** (2010) 519 (<https://doi.org/10.1007/s10967-010-0814-z>).



SUPPLEMENTARY MATERIAL TO  
**Comparison of non-destructive techniques and conventionally  
used spectrometric techniques for determination of elements in  
plant samples (coniferous leaves)**

JOVANA ORLIĆ<sup>1\*</sup>, MIRA ANIČIĆ UROŠEVIĆ<sup>2</sup>, KONSTANTIN VERGEL<sup>3</sup>,  
INGA ZINICOVSCAIA<sup>3</sup>, SANJA STOJADINOVIC<sup>4</sup>, IVAN GRŽETIĆ<sup>1</sup>  
and KONSTANTIN ILIJEVIĆ<sup>1</sup>

<sup>1</sup>University of Belgrade – Faculty of Chemistry, Studentski trg 12–16, 11000 Belgrade,  
Serbia, <sup>2</sup>Institute of Physics Belgrade, University of Belgrade, Pregrevica 118, 11080  
Belgrade, Serbia, <sup>3</sup>Frank Laboratory of Neutron Physics, Joint Institute for Nuclear Research,  
Joliot-Curie 6, 141980 Dubna, Russian Federation and <sup>4</sup>University of Belgrade, Institute of  
Chemistry, Technology and Metallurgy (ICTM), Njegoševa 12, 11000 Belgrade, Serbia

J. Serb. Chem. Soc. 87 (1) (2022) 69–81

TABLE S-I. Analytical lines and parameters of analysed elements

| Element | Line   | Wavelength, Å | Crystal | Detector | Count time, s | Filter     |
|---------|--------|---------------|---------|----------|---------------|------------|
| Na      | Ka 1,2 | 11.9101       | AX03    | FPC      | 40            | None       |
| Mg      | Ka 1,2 | 9.89          | AX03    | FPC      | 40            | None       |
| Al      | Ka 1,2 | 8.3401        | PET     | FPC      | 24            | None       |
| K       | Ka 1,2 | 3.7424        | LiF200  | FPC      | 24            | None       |
| Ca      | Ka 1,2 | 3.3595        | LiF200  | FPC      | 24            | None       |
| Cr      | Ka 1,2 | 2.291         | LiF200  | FPC      | 24            | None       |
| Mn      | Ka 1,2 | 2.1031        | LiF200  | FPC      | 24            | None       |
| Fe      | Ka 1,2 | 1.9374        | LiF200  | FPC      | 24            | None       |
| Co      | Ka 1,2 | 1.7903        | LiF200  | FPC      | 24            | None       |
| Ni      | Ka 1,2 | 1.6592        | LiF200  | SC       | 24            | None       |
| Cu      | Ka 1,2 | 1.5418        | LiF200  | SC       | 24            | None       |
| Zn      | Ka 1,2 | 1.4364        | LiF200  | SC       | 24            | None       |
| Ga      | Ka 1,2 | 1.3414        | LiF200  | SC       | 24            | None       |
| Sr      | Ka 1,2 | 0.8766        | LiF200  | SC       | 16            | None       |
| Ag      | Ka 1,2 | 0.5609        | LiF200  | SC       | 40            | Cu 0.27 mm |
| Cd      | Ka 1,2 | 0.5365        | LiF200  | SC       | 40            | Cu 0.27 mm |
| In      | Ka 1,2 | 0.5136        | LiF200  | SC       | 24            | Cu 0.27 mm |
| Tl      | La 1   | 1.2074        | LiF200  | SC       | 24            | None       |
| Pb      | La 1   | 1.175         | LiF200  | SC       | 24            | None       |
| Bi      | La 1   | 1.1439        | LiF200  | SC       | 24            | None       |

\* Corresponding author. E-mail: jovanaorlic@chem.bg.ac.rs



TABLE S-II. Certified and measured (using ICP-MS, ICP-OES, INAA, UQ, and WD-XRF) values with the relative standard deviation (RSD) of the three repeated measurements and uncertainties values (SD) for the reference material

| Ele-<br>ment | Certified              |        | ICP-MS                 |        | ICP-OES                |        | INAA                   |        | UQ                     |        | WD-XRF                 |        |
|--------------|------------------------|--------|------------------------|--------|------------------------|--------|------------------------|--------|------------------------|--------|------------------------|--------|
|              | c / mg L <sup>-1</sup> | RSD, % | c / mg L <sup>-1</sup> | RSD, % | c / mg L <sup>-1</sup> | RSD, % | c / mg L <sup>-1</sup> | RSD, % | c / mg L <sup>-1</sup> | RSD, % | c / mg L <sup>-1</sup> | RSD, % |
| Na           | 63                     | 1      | 53                     | 3      | 112                    | 115    |                        |        | 343                    | 44     | 15                     | 7      |
| Mg           | 1060                   | 170    | 854                    | 33     | 945                    | 18     | 1067                   | 105    | 1267                   | 6      | 923                    | 52     |
| Al           | 580                    | 30     | 489                    | 28     | 539                    | 8      | 681                    | 155    | 710                    | 11     | 574                    | 34     |
| P            | 1070                   | 80     | 1054                   | 79     |                        |        |                        |        | 1367                   | 15     |                        |        |
| K            | 4170                   | 70     | 3733                   | 158    | 3120                   | 49     |                        |        | 4727                   | 124    | 3849                   | 128    |
| Ca           | 2500                   | 100    | 2269                   | 97     | 2421                   | 41     | 2667                   | 115    | 2707                   | 64     | 2542                   | 71     |
| Mn           | 488                    | 12     | 472                    | 30     | 462                    | 10     | 496                    | 48     | 595                    | 19     | 500                    | 10     |
| Fe           | 45                     | 2      | 45                     | 3      | 50                     | 13     |                        |        | 46                     | 4      | 47                     | 1      |
| Ni           | 1.47                   | 0.1    | 1.2                    | 0.1    | 1.5                    | 0.2    |                        |        |                        |        |                        |        |
| Zn           | 38                     | 2      | 41                     | 3      | 35                     | 2      |                        |        | 100                    | 4      | 20                     | 25     |
| Rb           | 16.5                   | 0.9    | 16                     | 1      |                        |        |                        |        | 5                      | 9      |                        |        |
| Ba           | 6                      | 0.2    | 5.4                    | 0.2    | 5.6                    | 0.1    |                        |        |                        | 2      | 1                      |        |

TABLE S-III. Descriptive statistics of all investigated elements measured using different analytical techniques: minimum, maximum, median, arithmetic mean (AR), and standard deviation (SD), median relative ratio (RR) of content and number of analysed samples (n)

| Content, mg kg <sup>-1</sup> | ICP-MS ICP-OES INAA UQ WD-XRF |        |        |        |       | ICP-MS ICP-OES INAA UQ WD-XRF |        |        |        |       |      |
|------------------------------|-------------------------------|--------|--------|--------|-------|-------------------------------|--------|--------|--------|-------|------|
|                              | Na                            |        |        |        |       | Mg                            |        |        |        |       |      |
| Minimum                      | 1.8                           | 2.4    | 18.3   | 229.5  | 0.5   | 527.7                         | 414.1  | 185.0  | 528.5  | 304.4 |      |
| Maximum                      | 1840.6                        | 1633.5 | 2160.0 | 1815.0 | 216.5 | 1812.4                        | 1494.5 | 1740.0 | 1770.0 | 914.9 |      |
| Median                       | 13.6                          | 83.8   | 39.3   | 384.3  | 91.3  | 1030.2                        | 854.2  | 1120.0 | 1055.0 | 509.4 |      |
| AR                           | 83.7                          | 144.5  | 135.9  | 434.8  | 87.3  | 1051.1                        | 872.1  | 1084.5 | 1022.7 | 524.9 |      |
| SD                           | 266.8                         | 252.3  | 359.6  | 245.9  | 45.8  | 256.7                         | 219.0  | 282.9  | 303.0  | 116.2 |      |
| RR <sup>a</sup> , %          | 100                           | 359    | 322    | 2210   | 473   | 100                           | 84     | 105    | 96     | 50    |      |
| n                            | 49                            | 41     | 36     | 46     | 46    | 49                            | 35     | 39     | 48     | 49    |      |
| Content, mg kg <sup>-1</sup> | Al                            |        |        |        |       | K                             |        |        |        |       |      |
|                              | Minimum                       | 3.9    | 2.4    | 12.2   | 16.5  | 6.6                           | 3334   | 1591   | 2700   | 3285  | 2475 |
| Maximum                      | 256.0                         | 324.7  | 297.0  | 545.5  | 416.1 | 20011                         | 5722   | 20800  | 29500  | 16901 |      |
| Median                       | 30.8                          | 30.5   | 38.9   | 77.3   | 47.1  | 9896                          | 3555   | 8300   | 13100  | 7488  |      |
| AR                           | 51.0                          | 46.9   | 62.6   | 129.3  | 90.1  | 10089                         | 3673   | 8549   | 13175  | 7809  |      |
| SD                           | 54.2                          | 54.7   | 63.7   | 121.2  | 91.7  | 4434                          | 1117   | 3970   | 6134   | 3790  |      |
| RR <sup>a</sup> , %          | 100                           | 90     | 130    | 308    | 174   | 100                           | 36     | 84     | 135    | 81    |      |
| n                            | 49                            | 47     | 39     | 46     | 49    | 49                            | 40     | 39     | 48     | 49    |      |
| Content, mg kg <sup>-1</sup> | Ca                            |        |        |        |       | P                             |        |        |        |       |      |
|                              | Minimum                       | 618    | 425    | 370    | 806   | 636                           | 876    | /      | /      | 681   | /    |
| Maximum                      | 17690                         | 13093  | 16200  | 22200  | 16348 | 5646                          | /      | /      | 5540   | /     |      |
| Median                       | 3620                          | 2513   | 3100   | 4548   | 3347  | 2977                          | /      | /      | 2418   | /     |      |
| AR                           | 4297                          | 3266   | 4231   | 6319   | 3894  | 2948                          | /      | /      | 2635   | /     |      |
| SD                           | 3448                          | 2904   | 3458   | 5196   | 3172  | 1405                          | /      | /      | 1321   | /     |      |
| RR <sup>a</sup> , %          | 100                           | 74     | 101    | 167    | 97    | 100                           | /      | /      | 92     | /     |      |
| n                            | 49                            | 49     | 39     | 48     | 49    | 49                            | /      | /      | 48     | /     |      |

|                              | ICP-MS              | ICP-OES | INAA | UQ   | WD-XRF | ICP-MS | ICP-OES | INAA | UQ   | WD-XRF |
|------------------------------|---------------------|---------|------|------|--------|--------|---------|------|------|--------|
|                              | S                   |         |      |      |        | Mn     |         |      |      |        |
| Content, mg kg <sup>-1</sup> | Minimum             | 667     | /    | /    | 446    | /      | 14      | 7    | 11   | 25     |
|                              | Maximum             | 2145    | /    | /    | 2100   | /      | 1300    | 533  | 600  | 1740   |
|                              | Median              | 1288    | /    | /    | 893    | /      | 85      | 36   | 56   | 123    |
|                              | AR                  | 1319    | /    | /    | 1007   | /      | 157     | 78   | 89   | 227    |
|                              | SD                  | 372     | /    | /    | 414    | /      | 230     | 105  | 116  | 308    |
|                              | RR <sup>a</sup> , % | 100     | /    | /    | 76     | /      | 100     | 56   | 77   | 158    |
| <i>n</i>                     |                     | 49      | /    | /    | 48     | /      | 49      | 48   | 38   | 48     |
|                              | Fe                  |         |      |      |        | Ni     |         |      |      |        |
| Content, mg kg <sup>-1</sup> | Minimum             | 21      | 4    | 38   | 24     | 10     | 0       | 0    | 1    | 9      |
|                              | Maximum             | 146     | 136  | 359  | 251    | 95     | 10      | 35   | 6    | 13     |
|                              | Median              | 55      | 20   | 98   | 81     | 27     | 2       | 2    | 2    | 11     |
|                              | AR                  | 62      | 26   | 111  | 83     | 34     | 2       | 3    | 3    | 11     |
|                              | SD                  | 35      | 23   | 67   | 49     | 21     | 2       | 6    | 1    | 2      |
|                              | RR <sup>a</sup> , % | 100     | 38   | 173  | 146    | 56     | 100     | 82   | 120  | 187    |
| <i>n</i>                     |                     | 49      | 46   | 35   | 48     | 49     | 49      | 36   | 30   | 2      |
|                              | Zn                  |         |      |      |        | Rb     |         |      |      |        |
| Content, mg kg <sup>-1</sup> | Minimum             | 10      | 7    | 9    | 35     | 1      | 0.4     | /    | 0.4  | 11.0   |
|                              | Maximum             | 84      | 271  | 81   | 337    | 215    | 36.2    | /    | 41.0 | 45.5   |
|                              | Median              | 36      | 24   | 44   | 127    | 55     | 4.3     | /    | 5.2  | 16.5   |
|                              | AR                  | 40      | 32   | 44   | 135    | 63     | 6.5     | /    | 7.7  | 20.8   |
|                              | SD                  | 17      | 37   | 17   | 62     | 36     | 6.6     | /    | 8.1  | 10.4   |
|                              | RR <sup>a</sup> , % | 100     | 68   | 102  | 367    | 161    | 100     | /    | 116  | 192    |
| <i>n</i>                     |                     | 49      | 49   | 39   | 44     | 44     | 49      | /    | 39   | 17     |
|                              | Sr                  |         |      |      |        | Ba     |         |      |      |        |
| Content, mg kg <sup>-1</sup> | Minimum             | 0.5     | 0.1  | 3.4  | 10.0   | /      | 0.1     | 0.02 | 3    | 104    |
|                              | Maximum             | 59.8    | 32.7 | 91.0 | 67.5   | /      | 100     | 18   | 103  | 139    |
|                              | Median              | 6.5     | 2.1  | 14.4 | 28.5   | /      | 4       | 3    | 10   | 131    |
|                              | AR                  | 11.9    | 3.9  | 19.6 | 30.5   | /      | 12      | 5    | 25   | 125    |
|                              | SD                  | 13.2    | 5.7  | 18.5 | 15.0   | /      | 22      | 6    | 30   | 18     |
|                              | RR <sup>a</sup> , % | 100     | 42   | 111  | 149    | /      | 100     | 44   | 136  | 143    |
| <i>n</i>                     |                     | 49.0    | 40.0 | 26.0 | 23.0   | /      | 49      | 18   | 23   | 3      |

<sup>a</sup>The median relative ratio (%) values calculated by dividing the element concentration measured using different techniques with ICP-MS concentration of the same plant sample

TABLE S-IV. Minimum, maximum, median, arithmetic mean (AR), and standard deviations (SD) of relative ratios of elements content

|         | ICP-OES    | INAA | UQ    | WD-XRF | ICP-OES | INAA | UQ  | WD-XRF |
|---------|------------|------|-------|--------|---------|------|-----|--------|
|         | Content, % |      |       |        |         |      |     |        |
|         | Na         |      |       |        |         |      |     |        |
| Minimum | 9          | 117  | 99    | 1      | 64      | 20   | 46  | 31     |
| Maximum | 5888       | 1826 | 15424 | 4367   | 116     | 214  | 196 | 74     |
| Median  | 359        | 322  | 2210  | 473    | 84      | 105  | 96  | 50     |
| AR      | 925        | 468  | 4169  | 869    | 86      | 107  | 100 | 51     |
| SD      | 1445       | 384  | 4503  | 1055   | 11      | 26   | 31  | 9      |
|         | Al         |      |       |        |         |      |     |        |
| Minimum | 23         | 0    | 26    | 12     | 18      | 0    | 57  | 24     |
| Maximum | 285        | 314  | 831   | 514    | 51      | 135  | 299 | 143    |
| Median  | 90         | 130  | 308   | 174    | 36      | 84   | 135 | 81     |
| AR      | 99         | 133  | 319   | 197    | 35      | 82   | 138 | 79     |
| SD      | 56         | 67   | 172   | 103    | 7       | 20   | 48  | 18     |
|         | Ca         |      |       |        |         |      |     |        |
| Minimum | 7          | 17   | 14    | 11     | /       | /    | 17  | /      |
| Maximum | 281        | 447  | 542   | 300    | /       | /    | 229 | /      |
| Median  | 74         | 101  | 167   | 97     | /       | /    | 92  | /      |
| AR      | 79         | 110  | 171   | 100    | /       | /    | 98  | /      |
| SD      | 39         | 61   | 98    | 47     | /       | /    | 39  | /      |
|         | S          |      |       |        |         |      |     |        |
| Minimum | /          | /    | 27    | /      | 3       | 0    | 5   | 2      |
| Maximum | /          | /    | 178   | /      | 418     | 111  | 964 | 524    |
| Median  | /          | /    | 76    | /      | 56      | 77   | 158 | 64     |
| AR      | /          | /    | 79    | /      | 66      | 71   | 183 | 76     |
| SD      | /          | /    | 32    | /      | 67      | 21   | 148 | 80     |
|         | Fe         |      |       |        |         |      |     |        |
| Minimum | 0          | 99   | 26    | 12     | 1       | 45   | 156 | /      |
| Maximum | 139        | 638  | 336   | 78     | 962     | 604  | 218 | /      |
| Median  | 38         | 173  | 146   | 56     | 82      | 120  | 187 | /      |
| AR      | 43         | 219  | 143   | 56     | 188     | 139  | 187 | /      |
| SD      | 25         | 126  | 59    | 12     | 226     | 95   | 43  | /      |
|         | Zn         |      |       |        |         |      |     |        |
| Minimum | 32         | 62   | 97    | 4      | /       | 16   | 82  | /      |
| Maximum | 455        | 236  | 838   | 529    | /       | 558  | 843 | /      |
| Median  | 68         | 102  | 367   | 161    | /       | 116  | 192 | /      |
| AR      | 78         | 119  | 363   | 177    | /       | 126  | 292 | /      |
| SD      | 58         | 44   | 175   | 111    | /       | 83   | 242 | /      |
|         | Sr         |      |       |        |         |      |     |        |
| Minimum | 7          | 66   | 84    | /      | 0,5     | 74   | 131 | /      |
| Maximum | 162        | 175  | 326   | /      | 380     | 305  | 251 | /      |
| Median  | 42         | 111  | 149   | /      | 44      | 136  | 143 | /      |
| AR      | 47         | 112  | 160   | /      | 62      | 142  | 175 | /      |
| SD      | 27         | 26   | 59    | /      | 83      | 52   | 66  | /      |
|         | Ba         |      |       |        |         |      |     |        |

TABLE S-V. Minimum, maximum, median, arithmetic mean (AR) of relative standard deviation (RSD) of repeated measurements of elements content

|         | ICP-MS | ICP-OES | INAA | UQ  | WD-XRF | ICP-MS | ICP-OES | INAA | UQ  | WD-XRF |
|---------|--------|---------|------|-----|--------|--------|---------|------|-----|--------|
|         | RSD, % |         |      |     |        |        |         |      |     |        |
|         | Na     |         |      |     |        |        |         |      |     |        |
| Minimum | 0.8    | 0.6     | 3    | 0.8 | 0      | 0.8    | 0.2     | 9.8  | 0   | 0      |
| Maximum | 23     | 95      | 7    | 38  | 18     | 12     | 9       | 41   | 11  | 3      |
| Median  | 5      | 25      | 5    | 10  | 4      | 3      | 2       | 10   | 1   | 2      |
| AR      | 7      | 34      | 5    | 10  | 4      | 3      | 2       | 11   | 2   | 2      |
|         | Al     |         |      |     |        |        |         |      |     |        |
| Minimum | 0.5    | 1.2     | 4    | 0   | 0      | 0.4    | 0.0     | 11   | 0   | 0.5    |
| Maximum | 19     | 94      | 23   | 65  | 7      | 15     | 1       | 12   | 69  | 1      |
| Median  | 4      | 8       | 5    | 6   | 1      | 3      | 0       | 11   | 0.4 | 0.8    |
| AR      | 5      | 12      | 6    | 11  | 1      | 4      | 0       | 11   | 2   | 0.8    |
|         | Ca     |         |      |     |        |        |         |      |     |        |
| Minimum | 0.3    | 0.3     | 11   | 0   | 0.4    | 0.9    | /       | /    | 0   | /      |
| Maximum | 9      | 23      | 15   | 118 | 1      | 16     | /       | /    | 101 | /      |
| Median  | 3      | 3       | 11   | 0.4 | 0.6    | 5      | /       | /    | 0.6 | /      |
| AR      | 3      | 5       | 11   | 3   | 0.7    | 5      | /       | /    | 3   | /      |
|         | S      |         |      |     |        |        |         |      |     |        |
| Minimum | 1      | /       | /    | 0   | /      | 0.5    | 0.1     | 6    | 0   | 0      |
| Maximum | 12     | /       | /    | 54  | /      | 12     | 3       | 8    | 109 | 7      |
| Median  | 5      | /       | /    | 0.8 | /      | 3      | 1       | 6    | 1   | 0.3    |
| AR      | 5      | /       | /    | 4   | /      | 4      | 1       | 6    | 5   | 1      |
|         | Fe     |         |      |     |        |        |         |      |     |        |
| Minimum | 0.5    | 1.1     | 6    | 0   | 0      | 1      | 0       | 8    | 17  | 0      |
| Maximum | 17     | 38      | 18   | 17  | 7      | 533    | 35      | 18   | 33  | 13     |
| Median  | 4      | 7       | 9    | 3   | 0      | 8      | 1       | 11   | 25  | 0      |
| AR      | 4      | 10      | 9    | 4   | 1      | 30     | 4       | 12   | 25  | 1      |
|         | Zn     |         |      |     |        |        |         |      |     |        |
| Minimum | 0.3    | 0.04    | 4    | 0   | 3      | 0.6    | /       | 17   | 0   | /      |
| Maximum | 15     | 1       | 11   | 14  | 47     | 19     | /       | 18   | 44  | /      |
| Median  | 3      | 0       | 5    | 2   | 1      | 3      | /       | 17   | 10  | /      |
| AR      | 4      | 0       | 7    | 3   | 0.4    | 4      | /       | 17   | 15  | /      |
|         | Sr     |         |      |     |        |        |         |      |     |        |
| Minimum | 0.3    | 0.4     | 8    | 1   | /      | 0.2    | 0.4     | 13   | 15  | /      |
| Maximum | 11     | 17      | 13   | 44  | /      | 14     | 32      | 17   | 47  | /      |
| Median  | 3      | 2       | 9    | 7   | /      | 3      | 3       | 15   | 38  | /      |
| AR      | 4      | 3       | 9    | 9   | /      | 4      | 7       | 15   | 35  | /      |
|         | Rb     |         |      |     |        |        |         |      |     |        |
| Minimum | 0.3    | 0.4     | 8    | 1   | /      | 0.2    | 0.4     | 13   | 15  | /      |
| Maximum | 11     | 17      | 13   | 44  | /      | 14     | 32      | 17   | 47  | /      |
| Median  | 3      | 2       | 9    | 7   | /      | 3      | 3       | 15   | 38  | /      |
| AR      | 4      | 3       | 9    | 9   | /      | 4      | 7       | 15   | 35  | /      |
|         | Ba     |         |      |     |        |        |         |      |     |        |
| Minimum | 0.3    | 0.4     | 8    | 1   | /      | 0.2    | 0.4     | 13   | 15  | /      |
| Maximum | 11     | 17      | 13   | 44  | /      | 14     | 32      | 17   | 47  | /      |
| Median  | 3      | 2       | 9    | 7   | /      | 3      | 3       | 15   | 38  | /      |
| AR      | 4      | 3       | 9    | 9   | /      | 4      | 7       | 15   | 35  | /      |





## Some examples of interactions between certain rare earth elements and soil

ZLATKO NIKOLOVSKI<sup>1</sup>, JELENA ISAILOVIĆ<sup>2\*</sup>, DEJAN JEREMIĆ<sup>3#</sup>,  
SABINA KOVAC<sup>4</sup> and ILIJA BRČESKI<sup>2#</sup>

<sup>1</sup>Institute MOL d.o.o., Nikole Tesle 15, 22300 Stara Pazova, Serbia, <sup>2</sup>Faculty of Chemistry, University of Belgrade, Studentski trg 12–16, 11000 Belgrade, Serbia, <sup>3</sup>Innovation Center of Faculty of Chemistry, University of Belgrade, Belgrade, Serbia and <sup>4</sup>Department of Mineralogy, Crystallography, Petrology and Geochemistry, Laboratory of Crystallography, Faculty of Mining and Geology, University of Belgrade, Đušina 7, 11000 Belgrade, Serbia

(Received 6 October, revised 9 November, accepted 11 November 2021)

**Abstract:** The rare earth elements represent an increasingly more and more important industrial resource. The increased use may result in waste generation, and their impact upon the environment quality has not been studied sufficiently. Their interaction with soil has been studied in this paper. The Freundlich adsorption isotherm has been determined for lanthanum, erbium and gadolinium at three different soil types (humus, clay and sand type), whereas the sequential extraction at these soil types has been applied for lanthanum and neodymium. The interaction of certain rare earth elements with soil components has been tested as well as the quantity in which these elements are bound to soil and later on extracted in solutions. The objective was to determine the soil capacity for disposal, first of all, of the electronic waste that contains these elements and to assume their fate in the environment.

**Keywords:** Freundlich adsorption isotherm; sequential extraction; metallic ions; ICP-OES.

### INTRODUCTION

The demand in rare earth elements (REE) has been increasingly greater year in the previous year, as their application in military, pharmaceutical and nuclear industry, metallurgy, electronics, medicine, chemical engineering,<sup>1</sup> agriculture<sup>2</sup> and others has been on the upscale. The reason of their widespread use in important fields are their different chemical, electrical, magnetic, metallurgical, optical and catalyst properties.<sup>1,3</sup> In nature they crop up in the lithophylle part of the earth's crust<sup>4,5</sup> and are widely prevalent in small quantities, with the average concen-

\* Corresponding author. E-mail: jelena.isailovic00@gmail.com

# Serbian Chemical Society member.

<https://doi.org/10.2298/JSC211006095N>

tration in the earth's crust between 130–240 µg g<sup>-1</sup>.<sup>6</sup> There are significant reserves also in the oceans for which it has been assumed to be in greater quantities than in the earth's crust and that are more cost effective than the earth's resource.<sup>7,8</sup> The ionic radiiuses of these elements are such that enable an easy replacement with alkaline and alkaline-earth metals, adsorbing at the surface<sup>9</sup> and at the interlayer places of clay mineral. In addition to adsorption being greater, there also comes to more rapid equilibrium establishment.<sup>10,11</sup> The result of their properties is their widespread use and as the consequence of the widespread use there is an increased quantity of waste that is disposed and often in the inappropriate manner and ends up in the nature, disrupting the resources such as water and soil. The contamination occurs due to insufficient legal regulations and controls both in mining and also in the processing fields.<sup>12</sup> The effect contamination, resulting as the consequence of the improper waste disposal, are seen very quickly.<sup>13</sup>

In this paper, the equilibrium between the liquid and solid phase has been studied which can contribute to the elimination of these elements from the contaminated soil. To describe the affinity of the rare earth elements to soil, the Freundlich adsorption isotherm has been used since it is suitable for working with heterogeneous surfaces, such as in soil, and for working with medium and high concentrations.<sup>14</sup> Sequential extraction (SE) was used for the desorption of these elements from the soil.

## EXPERIMENTAL

### *Materials and methods*

The soils used for the analysis are: humus, clay and sand type of soils. The soil fractions do not mutually differentiate as per the particles sizes but also as per mineralogical composition and therefore as per physical and chemical properties. The soil preparation comprised cleaning from foreign bodies (twigs, leaves and stones), air drying for 7 days and following the determination of the hygroscopic moisture content. The mineralogical soil sample composition was determined by X-ray diffraction method (Rigaku SmartLab, X-ray diffractometer) under the conditions provided in Table I. The humus content has been determined by volumetric method<sup>15</sup> and the clay content by hydrometric method.<sup>16</sup> The sorption capacity for all three soil types has been determined.

TABLE I. Test conditions for samples on the diffractometer

|  |         |
|--|---------|
| Operating voltage, kV  | 40      |
| Current, mA  | 30      |
| X-ray radiation from the copper (Cu) anticathode, wavelength, nm | 15.4178 |
| Scan range, 2θ/°   | 2–70    |
| Step size, 2θ/°  | 0.01    |
| Time constant, °/min   | 10      |
| Scan range (clay minerals), 2θ/°                                 | 2–30    |
| Step size (clay minerals), 2θ/°                                  | 0.01    |
| Time constant (clay minerals), °/min                             | 5       |

As the source of lanthanum, erbium and gadolinium (III) ions, their nitrate hexahydrate salts (Sigma–Aldrich, 99.9 % trace metals basis,  $\leq 1500.0$  ppm, trace rare earth analysis) were used for determining Freundlich adsorption isotherm, whereas as the source of neodymium and lanthanum (III) ions,  $\text{NdCl}_3 \cdot 6\text{H}_2\text{O}$  (Merck, 99.9 % trace metals basis) and  $\text{La}_2(\text{CO}_3)_2$  (Sigma–Aldrich, 99.9% trace metals basis,  $\leq 1500.0$  ppm, trace rare earth analysis) were used for sequential extraction. The concentration of stock solution amounted to  $2000 \text{ mg L}^{-1}$ , and working solutions used for determining sorption capacity and Freundlich adsorption isotherm were in the range of  $500\text{--}1500 \text{ mg L}^{-1}$ . All solutions were analyzed by ICP-OES technique (Spectroblue TI). The calibration solutions were prepared from the stock solution of all these elements (certified reference material, Sigma–Aldrich, periodic table mix 3 for ICP) and the calibration curves were constructed for the stated elements. The imaging of the calibration solutions, extraction solutions and results processing was done as by the created “Rare Earths” method. The limit of detection (*LOD*) for this method for La amounts to  $0.23 \mu\text{g g}^{-1}$ , and the limit of quantification (*LOQ*)  $0.77 \mu\text{g g}^{-1}$ , whereas *LOD* for Nd amounts to  $0.52 \mu\text{g g}^{-1}$ , and *LOQ*  $1.74 \mu\text{g g}^{-1}$ .<sup>17,18</sup>

#### *Procedure for determining Freundlich adsorption isotherm*

Approximately 5 g of soil was measured and 50 mL of metallic ion aper (pores size  $< 2 \mu\text{m}$ ) into the 100 mL volumetric flasks. The sediments were rinsed thsolution added. The pH of the solution wasn't adjusted. The solutions were mixed at the shaker at the speed of 80 rpm for two hours, and then they were filtered through “blue band” filter pree times with 10 mL distilled water each and filled up with distilled water up to the line. The solutions prior to mixing and the solutions after the mixing were analyzed by ICP-OES. The values have been presented in Table II.<sup>17</sup>

The values obtained were graph presented as the dependence of the metallic ion adsorbed mass per mass of adsorbent on the equilibrium concentration of that ion in the solution – Freundlich adsorption isotherm. The parameters for adsorption intensity (*n*) and Freundlich isotherm constant (*k<sub>f</sub>*) are determined in the equation of the line, according to the Eq. (3).

Also, the sorption capacity or elimination efficiency was determined as well and it represents the ability of soil to bind to itself a certain quantity of metallic ion, until there comes to its saturation. Sorption capacity is represented by:

$$q = V(c_0 - c_1)/m \quad (1)$$

where *q* is sorption capacity ( $\text{mg g}^{-1}$ ), *c<sub>0</sub>* initial metallic ions solution concentration ( $\text{mg L}^{-1}$ ), *c<sub>1</sub>* equilibrium concentration ( $\text{mg L}^{-1}$ ), *m* adsorbent mass (g) and *V* the solution volume (L).<sup>19</sup>

#### *Preparation of soil samples for sequential extraction*

Dry samples of soil (sand, humus and clay type of soil, about 10 g) had previously been saturated separately with 100 ml of lanthanum (III) ion solution concentration of  $50 \text{ mg L}^{-1}$  and neodymium (III) ion solution concentration of  $50 \text{ mg L}^{-1}$ , so that their concentration would amount to  $500 \mu\text{g}$  of element per gram of soil. The soil samples and solutions for the saturation were placed in glass bottles and were agitated for 12 h at a rotational shaker for the soils to be saturated with the ions from the solutions. After the saturation process, the suspensions were filtered and the soil samples were dried for the extraction. The same solutions used for soil saturation were analyzed by ICP-OES before and after the saturation for the determination of their real concentrations. The total quantities of lanthanum and neodymium ions in the soil were obtained from calculating the difference of what was introduced and what remained in the solutions. The soils had previously been treated by microwave digestion<sup>20</sup> and analyzed by ICP-OES for verification and confirmation that lanthanum and neodymium were not present in the soil. These elements were below the detection limits.<sup>16</sup>

The sequential extraction was performed in five phases.<sup>21</sup>

*Phase I.* Saturated soils were extracted in glass bottles at rotational shaker with 100 mL of 1.0 mol L<sup>-1</sup> ammonium acetate solution each. The pH value of the obtained suspensions amounted to about 7. The control test was formed of 100 mL extraction agent. The extraction at rotational shaker lasted for two hours. Upon extraction the samples were left to age for 12 h for as better separation of phases. The liquid phases were filtered into 250 mL volumetric flask and were filled up to the line. The sediment was rinsed with bidistilled water up to negative reaction to ammonia ion and returned to the initial bottles.

*Phase II.* In each bottle containing soils from Phase I was added 100 mL of 0.2 mol L<sup>-1</sup> hydroxylamine hydrochloride and 0.02 mol L<sup>-1</sup> hydrochloric acid solutions. The pH value was adjusted by adding 0.6 mol L<sup>-1</sup> hydrochloric acid up to the value of about 4. The extraction at rotational shaker lasted for 12 h. Upon the extraction, the suspensions were filtered immediately, and the sediment rinsing was performed by bidistilled water as far as the absence of reaction to chlorides. The filtrates obtained were transferred to the 250 mL volumetric flasks and were filled up to the line as well as blank test. The sediments were transferred to the initial bottles.

*Phase III.* To each soil from Phase II, 50 mL of 0.4 mol L<sup>-1</sup> oxalic acid and 0.4 mol L<sup>-1</sup> ammonium oxalate was added. The control test was made up of the extraction solutions. At the rotational shaker the extraction lasted for 9 h, following which the suspensions were left to age for minimum 12 h for better phases separation. The samples were filtered, and the sediments rinsing was performed with bidistilled water as far as the negative reaction to oxalates. The filtrates obtained were transferred each to 250 mL volumetric flasks and filled up to the line. The sediments from the funnels were quantitatively transferred to 250 mL glasses each, by rinsing with 40 mL of 0.02 mol L<sup>-1</sup> nitric acid and 60 mL bidistilled water.

*Phase IV.* In each glass with suspension from Phase III, 10 mL of 30 % hydrogen peroxide was added, which was acidified by concentrated nitric acid up to pH 2. The control test was represented only by the acid solution of hydrogen peroxide. The glasses were covered by watch glass and were heated for two hours at water bath at 85 °C. Thereafter another 6 mL of the acidified hydroxide peroxide solution was added to each glass, and heated for another three hours with occasional stirring. Suspensions were then left to cool. After being transferred to the initial bottles, to each suspension was added 100 mL of 3.2 mol L<sup>-1</sup> ammonium acetate and filled up with bidistilled water up to 500 mL. The suspensions were mixed at the rotational shaker for 30 min and then the bottles were left to age overnight. Decanting was done same as in all phases, and the sediment was rinsed up to the negative reaction to ammonium ion. The filtrates obtained were concentrated to about 200 mL and then cooled and diluted in 250 mL volumetric flasks.

*Phase V.* For Phase V, about 0.5 g of each dried up soil from the preceding phase was taken for microwave digestion. In each vessel containing soil 9 mL of concentrated nitric acid (Merck), 3 mL concentrated hydrochloric acid (Merck) and 2 mL of concentrated hydrofluoric acid (Merck) were added. The samples were digested by microwave digestion (CEM microwave digestion system) 2×15 min with cooling between two digestions for 15 min. The control blank was formed of the acids added. Upon digestion and cooling the solutions were filtered into 50 mL volumetric flasks and diluted up to the line.

## RESULTS AND DISCUSSION

### *Freundlich adsorption isotherms*

An adsorption isotherm is defined as the diagram of the relationship between the quantity of the adsorbate adsorbed per mass of adsorbent and the quantity of

adsorbate remaining in the equilibrium solution following adsorption, whereby the distribution between the liquid and solid phase of adsorption solution for different concentrations is presented. Most often the information on adsorption intensity, adsorbed quantity as well as on maximum adsorption capacity of the adsorbent is obtained by adsorption isotherms.<sup>22,23</sup>

One of the most frequently used adsorption isotherms is the Freundlich isotherm. Freundlich isotherm is used for describing the physical adsorption, being the consequence of the van der Waals forces impact, it is reversible and there may come to adsorption in a number of layers.<sup>14,24</sup> The equation of Freundlich adsorption isotherm is:

$$q = k_f c_1^{1/n} \quad (2)$$

where  $q$  represents the quantity of adsorbed metallic ion per unit of mass ( $\text{mg g}^{-1}$ ),  $k_f$  is the Freundlich isotherm constant,  $c_1$  represents the solution equilibrium concentration ( $\text{mg L}^{-1}$ ) and  $1/n$  Freundlich constant that describes the adsorption intensity.<sup>25</sup>

TABLE II. Calculated values for  $x_0$  – initial mass of metallic ion and  $x_1$  – adsorbed mass of metallic ion in the soil sample ( $\text{mg g}^{-1}$ )

| Sample | La    |       | Er    |       | Gd    |       |
|--------|-------|-------|-------|-------|-------|-------|
|        | $x_0$ | $x_1$ | $x_0$ | $x_1$ | $x_0$ | $x_1$ |
| Humus  | 8.64  | 8.64  | 10.89 | 10.89 | 9.51  | 9.51  |
|        | 14.27 | 14.27 | 17.23 | 17.23 | 14.65 | 14.66 |
|        | 17.83 | 17.77 | 21.76 | 21.76 | 17.69 | 17.69 |
|        | 21.26 | 21.03 | 25.51 | 25.51 | 20.67 | 20.54 |
|        | 27.07 | 25.81 | 31.21 | 31.21 | 23.44 | 22.56 |
| Clay   | 8.76  | 8.74  | 10.88 | 10.88 | 9.51  | 9.51  |
|        | 14.27 | 13.90 | 17.22 | 17.22 | 14.81 | 14.41 |
|        | 17.69 | 16.55 | 21.88 | 20.74 | 18.16 | 16.64 |
|        | 21.34 | 19.05 | 25.89 | 22.94 | 20.33 | 17.48 |
|        | 27.96 | 23.77 | 30.11 | 23.92 | 23.53 | 18.18 |
| Sand   | 8.74  | 6.50  | 10.78 | 7.52  | 9.49  | 6.35  |
|        | 14.15 | 9.93  | 17.27 | 10.49 | 14.85 | 8.96  |
|        | 17.65 | 11.68 | 21.48 | 12.36 | 17.73 | 10.24 |
|        | 21.28 | 13.30 | 25.16 | 13.90 | 20.89 | 11.73 |
|        | 26.42 | 15.55 | 31.12 | 15.70 | 23.58 | 11.62 |

Freundlich adsorption isotherm is linearized by logarithmic computation for easier determination of parameters  $n$  and  $k_f$ , and thus the Eq. (3) is obtained:

$$\log q = \log k_f + (1/n)\log c_1, \quad (3)$$

where  $\log k_f$  in the diagram represents the intercept at  $y$  axis, and  $1/n$  the line inclination.<sup>26</sup>

Table II presents the values of the initial mass of the metallic ion,  $x_0$  – the mass of ions in solutions divided by the mass of the sorbent, and adsorbed mass of the metallic ion in the soil sample following agitation ( $x_1$ ).

The values obtained for determining humus and clay content, hygroscopic moisture content, pH value and soil sorption capacity have been presented in Table III.

TABLE III. Display of hygroscopic moisture, humus, clay and sand content, soil sorption capacity and pH; n.a. – not achieved

| Soil type | Content, % |            |            |            | $q / \text{mg g}^{-1}$ |       |       | pH   |
|-----------|------------|------------|------------|------------|------------------------|-------|-------|------|
|           | Moisture   | Humus      | Clay       | Sand       | La                     | Er    | Gd    |      |
| Humus     | 2.97       | 4.43       | $\leq 0.5$ | $\leq 0.5$ | 17.77                  | n.a.  | 20.54 | 7.45 |
| Clay      | 2.66       | $\leq 0.5$ | 12.59      | $\leq 0.5$ | 8.74                   | 20.74 | 14.41 | 6.64 |
| Sand      | 1.02       | $\leq 0.5$ | $\leq 0.5$ | 91.02      | 6.5                    | 7.52  | 6.35  | 5.53 |

The diffractogram presentation on the determined mineralogical content of sand, clay and humus soil is shown in Fig. 1.

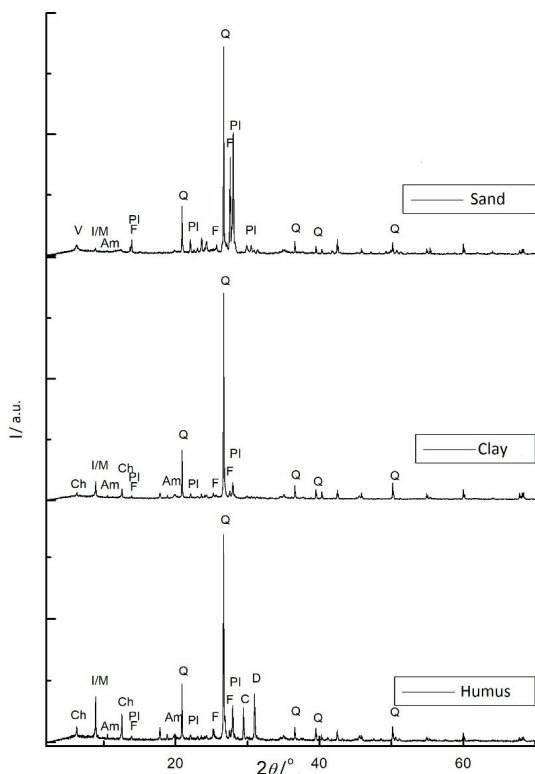


Fig. 1. X-ray diffractograms of powdered samples of sand, clay and humus type of soil.

Table IV shows the mineral phases of the samples and their presence in the tested samples as well as the phase designations used on the diffractograms.

Based on the values obtained from Table II, it was possible to determine Freundlich adsorption isotherms for lanthanum and gadolinium ions in the clay

and sand type of soil and erbium ions in the sand soil (Fig. 2). The values for Freundlich isotherm constant ( $k_f$ ) and the adsorption intensity ( $n$ ) have been provided in Table V.

TABLE IV. Mineral phases and their presence in tested samples

| Type of soil        | Humus | Clay | Sand |
|---------------------|-------|------|------|
| Quartz (Q)          | +     | +    | +    |
| Plagioclase (Pl)    | +     | +    | +    |
| Feldspar (F)        | +     | +    | +    |
| Amphibole (Am)      | +     | +    | +    |
| Calcite (C)         | +     |      |      |
| Dolomite (D)        | +     |      |      |
| Illite / Mica (I/M) | +     | +    | +    |
| Chlorite (Ch)       | +     | +    |      |
| Vermiculite (V)     |       |      | +    |

The sorption capacity of the clay soil for all three elements is approximately the same. The greatest sorption capacities are in the clay soil for erbium ions and humus soil for gadolinium ions (Table III). The sorption capacity of humus soil for erbium ions has not been achieved, meaning that it has much greater adsorption capacity than the applied concentration of erbium (III) ions. The Freundlich adsorption isotherms have been obtained in five cases (Fig. 2), whereas for all three ions in humus and erbium in clay soil they have not been achieved due to exceptional soil sorption capacity. The clay type of soil has been demonstrated as the best sorbent for lanthanum (III) ions. The parameters for other ions in clay and sand type of soils demonstrate that the adsorption rate is approximately the same, and as the adsorbents, these two soils are similar for the given ions. The exception being the sand type of soil for lanthanum (III) ions, where the adsorption rate is lower and where it has been demonstrated that sand type of soil is poorer adsorbent for this elements (Table V).

#### *The results of sequential extraction for lanthanum and neodymium*

Values of the initial concentration of lanthanum and neodymium ions in the soils result from the different phases of extraction and the extracted amount of metal ions from the different types of soil are presented in Table VI. The histogram presentation of the extracted lanthanum and neodymium ions through different phases of extraction has been shown in Figs. S-1 and S-2 of the Supplementary material to this paper, respectively.

Based on the results from Table VI it can be concluded that there is a difference between the results obtained for lanthanum and neodymium. The experimental results show that a significant metallic ions concentration have been extracted from sand soil 99.2 and 99.8 % from clay soil for lanthanum (Table VI). In humus soil about 56 % of lanthanum has been extracted. The lanthanum mobil-

ization happened in several different phases and the extraction in phases with milder agents had occurred.

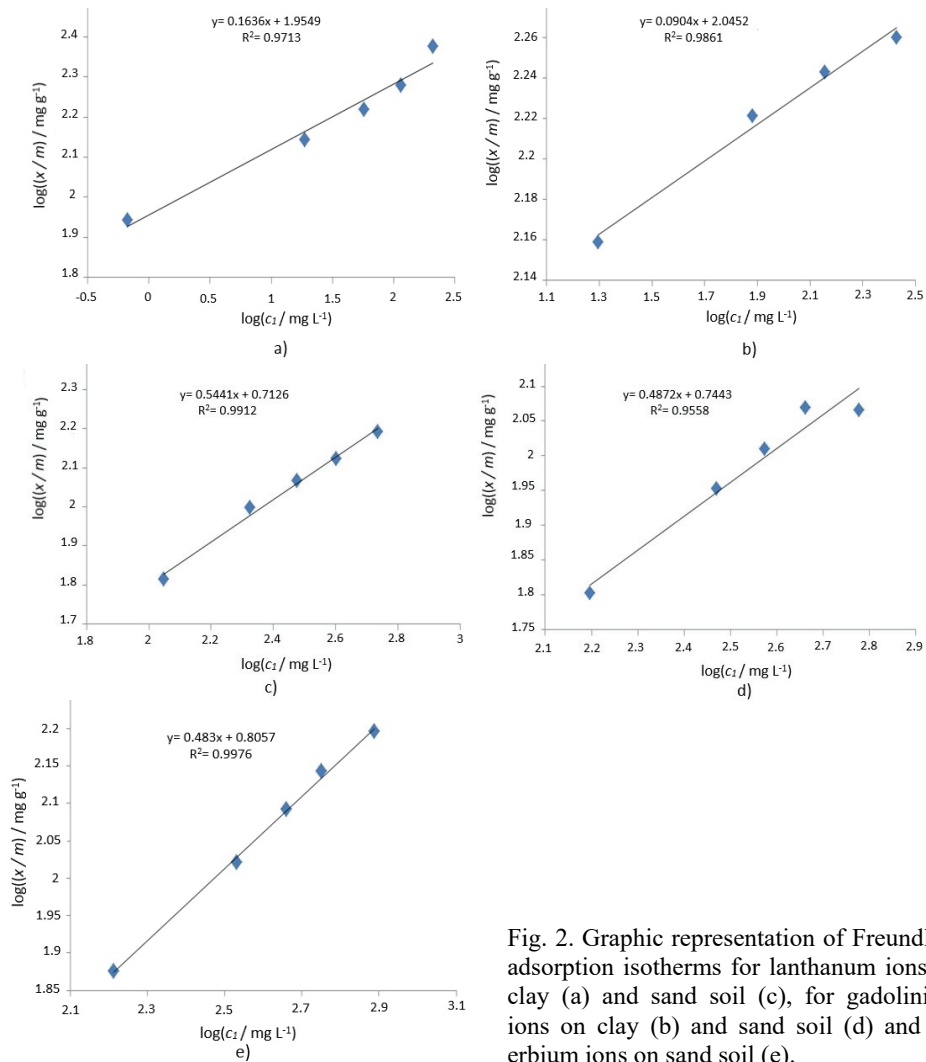


Fig. 2. Graphic representation of Freundlich adsorption isotherms for lanthanum ions on clay (a) and sand soil (c), for gadolinium ions on clay (b) and sand soil (d) and for erbium ions on sand soil (e).

TABLE V. Parameters for Freundlich adsorption isotherms

| Sample name  | $n$  | $k_f$ |
|--------------|------|-------|
| La-clay soil | 6.11 | 90.14 |
| Gd-clay soil | 2.07 | 6.39  |
| La-sand soil | 1.84 | 5.16  |
| Er-sand soil | 2.07 | 6.39  |
| Gd-sand soil | 2.05 | 5.55  |

TABLE VI. Concentration of rare earth elements (REE) in  $\mu\text{g g}^{-1}$  for three types of soil obtained by sequential extraction

| Element             | Type of soil |        |        | Element             | Type of soil |        |        |
|---------------------|--------------|--------|--------|---------------------|--------------|--------|--------|
| La                  | Sand         | Clay   | Humus  | Nd                  | Sand         | Clay   | Humus  |
| Initial conc.       | 448.08       | 447.95 | 447.97 | Initial conc.       | 527.64       | 527.44 | 527.64 |
| Phase I             | 229.34       | 3.42   | 47.52  | Phase I             | 305.21       | <1.74  | 2.32   |
| Phase II            | 10.69        | 1.14   | <0.77  | Phase II            | <1.74        | <1.74  | 2.56   |
| Phase III           | 7.14         | 12.73  | <0.77  | Phase III           | <1.74        | <1.74  | <1.74  |
| Phase IV            | 197.77       | 430.00 | <0.77  | Phase IV            | 118.42       | 506.09 | <1.74  |
| Phase V             | <0.77        | <0.77  | 203.69 | Phase V             | <1.74        | <1.74  | 107.61 |
| Extracted amount, % | 99.2         | 99.8   | 56     | Extracted amount, % | 80           | 96     | 20     |

In case of neodymium, the nature of soil is important in particular, since only in certain extraction phases there came to ion extraction, and also due to the slightly different neodymium properties because of the ionic diameter, where the ions were more tightly “bound” (complexed) to certain organic components characteristic for humus. The extraction was noticed in ion exchange phase (Phase I) and in extraction phases with acids (Phases IV and V).

The results show that in sand soil about 80 % of neodymium ions have been extracted and in the clay type of soil 96 % (Table VI). The extraction from humus soil was about 20 % (Table VI). This is a clear indicator that due to the complexity of interactions of lanthanum and neodymium ions with different soil components, it is not easy to effectively extract them using milder agents. It can be concluded that the extracted quantities depend on soil type, nature of extraction agent and metallic ion characteristics. Neodymium, first of all, reacts differently with soil, which is due to its ionic diameter. For that reason the extraction happened only with solutions of certain extraction agents depending on their nature and ionic forces.

#### CONCLUSION

The impact between the soil and rare earth elements and the soil capacity to adsorb these elements has been studied. Freundlich adsorption isotherms for the lanthanum, erbium and gadolinium have been presented in two soil types, the clay and sand soils. For humus soil the Freundlich adsorption isotherms have not been obtained for the used concentrations of these elements, and thus it has been assumed that humus soil possesses much greater adsorption capacity and that the equilibrium between the ions in the solution and at the soil surface is more rapidly established. It can be concluded that the examined soil possesses a certain capacity for binding the rare earth elements, so that physically unprotected soil does not present a suitable surface for the disposal of electronic waste. Should such waste be disposed on such soil types, it would be beneficial to protect the soil with polymer or similar non-permeable material.

The method of sequential extraction based on the results presented is suitable for the extraction of rare earth elements from sand and clay type of soils. Humus soil has demonstrated more intensive sorption properties, therefore these types of extractions are limited on it, namely this method is not so undemanding. The characteristics (composition) of soil, pH value and extraction solution composition are particularly important for the extraction effects. The suitability of the method presented is reflected in its simplicity, namely the rare earth elements ions can be extracted by this method from a complex matrix. The environment contamination on the occasion of these elements production is evident. With the exception of their natural occurrence, the anthropogenic factor is increasingly noticed, the waste caused by it is accumulating and the concentration of these elements increases rapidly. Developing the methodology of sequential extraction enables better predictions and further understanding of the elements fate as well as their potential hazard to the environment.

#### SUPPLEMENTARY MATERIAL

Additional data and information are available electronically at the pages of journal website: <https://www.shd-pub.org.rs/index.php/JSCS/article/view/11254>, or from the corresponding author on request.

#### ИЗВОД

#### НЕКИ ПРИМЕРИ ИНТЕРАКЦИЈА ПОЈЕДИНИХ ЕЛЕМЕНТА РЕТКИХ ЗЕМАЉА И ТЛА

ЗЛАТКО НИКОЛОВСКИ<sup>1</sup>, ЈЕЛЕНА ИСАИЛОВИЋ<sup>2</sup>, ДЕЈАН ЈЕРЕМИЋ<sup>3</sup>, САБИНА КОВАЧ<sup>4</sup> и ИЛИЈА БРЧЕСКИ<sup>2</sup>

<sup>1</sup>Институција МОЛ г.о.о., Николе Тесле 15, 22300 Стапара Пазова, <sup>2</sup>Хемијски факултет, Универзитет у Београду, Студенички трг 12–16, 11000 Београд, <sup>3</sup>Иновациони центар Хемијској факултети, Универзитет у Београду и <sup>4</sup>Департман за минералотехнолођију, кристалографију, петрологију и геохемију, Лабораторија за кристалографију, Рударско-геолошки факултет, Универзитет у Београду, Ђушина 7, 11000 Београд

Елементи ретких земаља представљају све важнији индустријски ресурс. Повећана употреба може довести до стварања отпада, а њихов утицај на квалитет животне средине није доволно проучен. У овом раду је испитивана њихова интеракција са земљиштем. Одређивана је Фројндлихова адсорпциона изотерма за елементе лантана, ербијума и гадолинијума на три различита типа земљишта (хумусном, глиновитом и песковитом), док је секвенцијална екстракција, на овим типовима земљишта, примењена за лантан и неодимијум. Испитивана је интеракција појединих елемената ретких земаља са компонентама земљишта, као и количина у којој се ови метали везују за тло, а касније и екстрагују у растворе. Циљ је био одредити капацитет земљишта за одлагање, превенствено, електронског отпада који садржи ове елементе и претпоставити њихову судбину у животној средини.

(Примљено 6. октобра, ревидирано 9. новембра, прихваћено 11. новембра 2021)

#### REFERENCES

- I. Anastopoulos, A. Bhatnagar, E. C. Lima, *J. Mol. Liq.* **221** (2016) 954  
(<https://doi.org/10.1016/j.molliq.2016.06.076>)

2. F. Tommasi, P. J. Thomas, G. Pagano, G. A. Perono, R. Oral, D. M. Lyons, M. Toscanesi, M. Trifuggi, *J. Arch. Environ. Contam. Toxicol.* **81** (2021) 531 (<https://doi.org/10.1007/s00244-020-00773-4>)
3. V. Balaram, *J. Geosci. Front.* **10** (2019) 1285
4. V. M. Goldschmidt, *J. Chem. Soc. (Resumed)* (1937) 655 (<https://doi.org/10.1039/JR9370000655>)
5. M. Bernat, *Cah. ORSTOM Ser. Geol* **7** (1975) 65 (<https://core.ac.uk/download/pdf/39881849.pdf>)
6. V. Zepf, in: *Rare Earth Elements*, Springer, Berlin, 2013, pp. 11–39 ([https://doi.org/10.1007/978-3-642-35458-8\\_2](https://doi.org/10.1007/978-3-642-35458-8_2))
7. Y. Takaya, K. Yasukawa, T. Kawasaki, K. Fujinaga, J. Ohta, Y. Usui, K. Nakamura, J. Kimura, Q. Chang, M. Hamada, G. Dodbiba, T. Nozaki, K. Iijima, T. Morisawa, T. Kuwahara, Y. Ishida, T. Ichimura, M. Kitazume, T. Fujita, Y. Kato, *Sci. Rep.* **8** (2018) (<https://doi.org/10.1038/s41598-018-23948-5>)
8. Y. Kato, K. Fujinaga, K. Nakamura, Y. Takaya, K. Kitamura, J. Ohta, R. Toda, T. Nakashima, H. Iwamori, *Nature Geosci.* **4** (2011) 535 (<https://doi.org/10.1038/ngeo1185>)
9. Y. Wan, C. Liu, *J. Rare Earths* **23** (2005) 377
10. G. W. Beall, B. H. Ketelle, R. G. Haire, G. D. O'Kelley, *ACS Symp. Ser.* **100** (1979) 201 (<http://dx.doi.org/10.1021/bk-1979-0100.ch012>)
11. F. Coppin, G. Berger, A. Bauer, S. Castet, M. Loubet, *Chem. Geology* **182** (2002) 57 ([https://doi.org/10.1016/S0009-2541\(01\)00283-2](https://doi.org/10.1016/S0009-2541(01)00283-2))
12. IAEA, Radiation protection and NORM residue management in the production of rare earths from thorium containing minerals, Safety Reports Series **68** (2011) 259
13. G. Haxel, *US Geological Survey* **87** (2002) (<https://pubs.usgs.gov/fs/2002/fs087-02>)
14. C. Ng, J. N. Losso, W. E. Marshall, R. M. Rao, *Biores. Technol.* **85** (2002) 131 ([https://doi.org/10.1016/S0960-8524\(02\)00093-7](https://doi.org/10.1016/S0960-8524(02)00093-7))
15. S. McLeod, *Notes Soil Tech.* (1973) 73
16. D. P. Gangwar, M. Baskar, *Texture determination of soil by hydrometer method for forensic purpose*, Central Forensic Science Laboratory, Chandigarh, 2019 (<http://dx.doi.org/10.13140/RG.2.2.16057.60001>)
17. J. Isailović, *Master Thesis*, Faculty of Chemistry, Belgrade, 202 (in Serbian)
18. Z. Nikolovski, *Master Thesis*, Faculty of Chemistry, Belgrade, 2021 (in Serbian)
19. A. Guša, M. Đolić, B. Lekić, V. Rajaković-Ognjanović, *Water Manage.* **47** (2015) 67 (<http://grafar.grf.bg.ac.rs/handle/123456789/656>) (in Serbian)
20. EPA M 3051A, Microwave assisted acid digestion of sediments, sludges, soils and oils, 2007
21. B. Stanimirović, J. Otašević, J. Petrović, D. Savić, D. Tonić, A. Šestak, Lj. Miličić, M. Savić, S. Jovanović, *Possibilities of extraction of high-value useful ions and ionic species from ash TPP JP EPS*, Institute MOL d.o.o. Stara Pazova, Institute IMS a.d., Belgrade, 2016, p. 33 (in Serbian)
22. D. L. Jensen, A. Ledin, T. H. Christensen, *Water Res.* **33** (1999) 2642 (<https://doi.org/10.1177%2F0734242X04042146>)
23. J. U. Keller, R. Staudt, *Gas adsorption equilibria: experimental methods and adsorptive isotherms*, Springer Science & Business Media, 2005, pp. 1–402 (ISBN 978-0-387-23598-1)
24. A. S. Erses, M. A. Fazal, T. T. Onay, W. H. Craig, *J. Hazard. Mater.* **121** (2005) 223 (<https://doi.org/10.1016/j.jhazmat.2005.02.011>)

25. S. Veli, B. Alyüz, *J. Hazard. Mater.* **149** (2007) 226  
(<https://doi.org/10.1016/j.hazmat.2007.04.109>)
26. A. Özer, H. B. Pirincci, *J. Hazard. Mater.* **137** (2006) 849  
(<https://doi.org/10.1016/j.hazmat.2006.03.009>).

SUPPLEMENTARY MATERIAL TO  
**Some examples of interactions between certain rare earth  
elements and soil**

ZLATKO NIKOLOVSKI<sup>1</sup>, JELENA ISAILOVIĆ<sup>2\*</sup>, DEJAN JEREMIĆ<sup>3</sup>,  
SABINA KOVAC<sup>4</sup> and ILIJA BRČESKI<sup>2</sup>

<sup>1</sup>Institute MOL d.o.o., Nikole Tesle 15, 22300 Stara Pazova, Serbia, <sup>2</sup>Faculty of Chemistry,  
University of Belgrade, Studentski trg 12–16, 11000 Belgrade, Serbia, <sup>3</sup>Innovation Center of  
Faculty of Chemistry, University of Belgrade, Belgrade, Serbia and <sup>4</sup>Department of  
Mineralogy, Crystallography, Petrology and Geochemistry, Laboratory of Crystallography,  
Faculty of Mining and Geology, University of Belgrade, Đušina 7, 11000 Belgrade, Serbia

J. Serb. Chem. Soc. 87 (1) (2022) 83–94

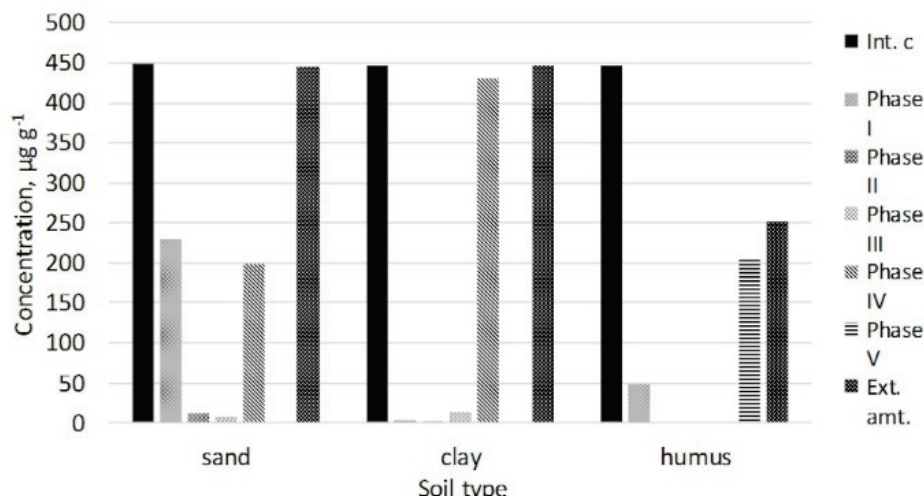


Fig. S-1. Histogram presentation of initial concentrations of lanthanum and extracted ions in different extraction agents.

\* Corresponding author. E-mail: jelena.isailovic00@gmail.com

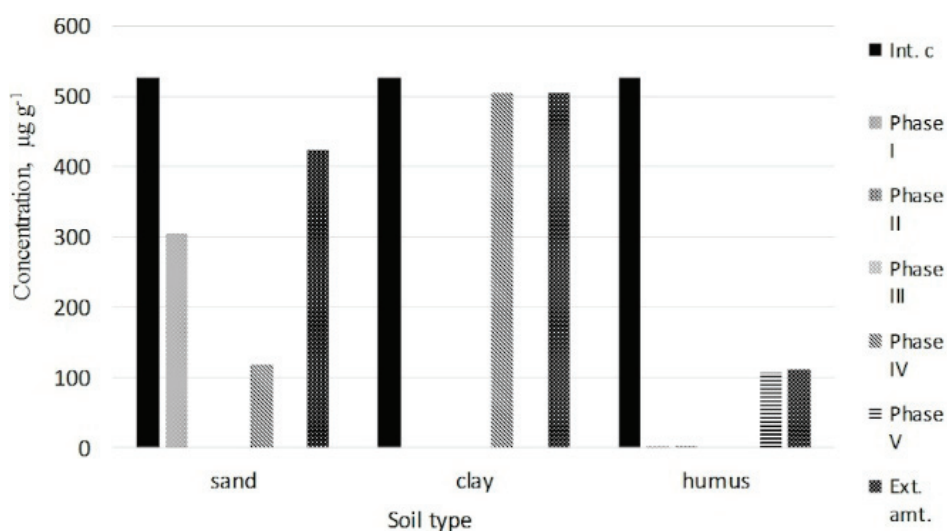


Fig. S-2. Histogram presentation of initial concentrations of neodymium and extracted ions in different extraction agents.



*J. Serb. Chem. Soc.* 87 (1) 95–107 (2022)  
JSCS-5507

# Journal of the Serbian Chemical Society

JSCS-info@shd.org.rs • www.shd.org.rs/JSCS

Original scientific paper

Published 14 January 2022

## Bioremediation of river sediment polluted with polychlorinated biphenyls: A laboratory study

ALEKSANDRA ŽERAĐANIN<sup>1\*</sup>, KRISTINA JOKSIMOVIĆ<sup>1#</sup>, JELENA AVDALOVIĆ<sup>1#</sup>,  
GORDANA GOJGIĆ-CVIJOVIĆ<sup>1#</sup>, TAKESHI NAKANO<sup>2</sup>, SRĐAN MILETIĆ<sup>1#</sup>,  
MILA ILIĆ<sup>1#</sup> and VLADIMIR P. BEŠKOSKI<sup>3#</sup>

<sup>1</sup>University of Belgrade – Institute of Chemistry, Technology and Metallurgy, Serbia, <sup>2</sup>Osaka University, Research Center for Environmental Preservation, Japan and <sup>3</sup>University of Belgrade – Faculty of Chemistry, Serbia

(Received 17 December, accepted 24 December 2021)

**Abstract:** Persistent organic pollutants (POPs) are lipophilic, constant and bio-accumulative toxic compounds. In general, they are considered resistant to biological, photolytic, and chemical degradation with polychlorinated biphenyls (PCBs) belonging to these chemicals. PCBs were never produced in Serbia, but they were imported and mainly used in electrical equipment, transformers, and capacitors. Our study aimed to analyse sequential multi-stage aerobic/anaerobic microbial biodegradation of PCBs present in the river sediment from the area known for long-term pollution with these chemicals. The study with an autochthonous natural microbial community (NMC model system) and NMC augmented with allochthonous hydrocarbon-degrading (AHD) microorganisms (isolated from location contaminated with petroleum products) (NMC-AHD model system) was performed in order to estimate the potential of these microorganisms for possible use in future bioremediation treatment of these sites. The laboratory biodegradation study lasted 70 days, after which an overall >33 % reduction in the concentration of total PCBs was observed. This study confirmed the strong potential of the NMC for the reduction of the level of PCBs in the river sediment under alternating multi-stage aerobic/anaerobic conditions.

**Keywords:** persistent organic pollutants (POPs); remediation; Topčider River; Čukarički Rukavac.

### INTRODUCTION

Persistent organic pollutants (POPs) are lipophilic toxic compounds that persist in the environment. They can bioaccumulate through the food chain and cause adverse effects on human health and the environment.<sup>1,2</sup> Production of

\* Corresponding author. E-mail: aleksandra.zeradjanin@ihtm.bg.ac.rs

# Serbian Chemical Society member.

<https://doi.org/10.2298/JSC211217113Z>

POPs in the last century was deliberate and focused on defence against pests and production of more robust industrial materials. It was not until several decades had passed that they were considered toxic, and now, in many countries, production and usage of these compounds is prohibited.<sup>3,4</sup> Their resistance to photolytic and chemical degradation is based on the exceptional strength of the carbon-chlorine bond, and with a higher degree of substitution of hydrogen with chlorine atoms, greater resistance of the chlorine to degradation occurs.<sup>5</sup> Resistance to degradation and the fact that POPs are generally aromatic structures with stronger connections than those in aliphatic compounds contribute to the low aqueous solubility.<sup>6</sup> However, in spite of their chemical stability, several micro-organisms are described in the literature with a potential to biotransform or mineralize the PCBs aerobically or anaerobically.<sup>7</sup> Aerobic oxidation and anaerobic dechlorination are the best known biodegradation pathways of PCBs.<sup>8,9</sup> Pollution with POPs can lead to disorder of the reproductive, immune, endocrine and the nervous system, as well as to carcinogenesis, mutagenesis and teratogenesis.<sup>10</sup> The problem of their high potential for bioaccumulation and toxicity to humans and the environment led to the 2004 adoption of the Stockholm Convention on POPs chemicals. Its primary objective is to protect human health and the environment from POPs. The countries that signed this Convention should determine, prohibit or restrict production, sale, and usage of POPs, and have additional obligation to reduce or eliminate emissions of POPs.<sup>11</sup>

Based on the Convention, POPs are classified into three categories: pesticides, such as aldrin, dieldrin, chlordane, toxaphene, mirex, endrin, heptachlor, hexachlorobenzene (HCB), dichloro-diphenyl-trichloroethane (DDT), *etc.*; industrial chemicals (PCBs); and by-products of industrial processes, and combustion processes as polychlorinated dibenzo-*p*-dioxins (PCDD), polychlorinated dibenzo-*p*-furans (PCDF) and polycyclic aromatic hydrocarbons (PAH). In addition, from 2017, the production and use of the perfluorooctane sulfonic acid (PFOS), its salts and perfluorooctane sulfonyl fluoride (PFOSF) was under restriction and based on the latest revised Convention from 2019, the production and use of perfluorooctanoic acid (PFOA), its salts and PFOA related compounds, together with PFOS, its salts and PFOSF should be eliminated, except for some cases as stated in the Convention.<sup>11–14</sup>

Among POPs, PCBs have a special place. There are ten groups of PCBs, from mono- to decachlorobiphenyl. With an increase in the percentage of substitution, solubility decreases,<sup>15</sup> and these compounds are extremely chemically inert, heat resistant, non-combustible with a high dielectric constant.<sup>16</sup> In Serbia, PCB-based fluids were never produced, but they were imported and used in transformers, capacitors, electric motors with liquid cooling, hydraulic systems, heat transfer systems, electromagnets, fluorescent light fittings, fluid-filled cables, and as additives to pesticides, inks, oils, lubricants, *etc.* A preliminary

inventory of PCBs was conducted in the framework of preparation of the first National Implementation Plan of the Stockholm Convention.<sup>17</sup> Besides PCB fluids in electrical equipment, waste consisting of, containing, or contaminated with, PCBs can be found in different physical forms, including: solvents, construction waste, contaminated oils, soil, sediments, sludge, rock and aggregates, tanks, barrels and containers.

For the treatment of this material, export from Serbia for incineration was the dominant method of choice. However, bioremediation can be of potential use for the treatment of soil and sediment polluted with low levels of PCBs, having in mind that industrial-scale bioremediation of soil contaminated with petroleum hydrocarbons was previously confirmed.<sup>18</sup> Based on the current knowledge, biodegradation of PCB can be conducted to some extent, using a variety of bacteria and/or fungi. The biodegradation of PCBs can include two main microbial metabolic steps: anaerobic reductive dehalogenation in which the PCB acts as an electron acceptor, and thus, hydrogen replaces chlorine, so the compound becomes less chlorinated,<sup>4,8,15,16</sup> and aerobic decomposition of the biphenyl structure, which is operative only on the PCBs that are less chlorinated (less than five atoms of chlorine).<sup>8,10,16</sup> Complete mineralization of biphenyl and some PCBs was confirmed using microorganisms from the following bacterial genus: *Pseudomonas*, *Alcaligenes*, *Burkholderia*, *Comamonas*, *Sphingomonas*, *Ralstonia*, *Cupriavidus*, *Achromobacter*, *Acidovorax*, *Nocardia* and *Acinetobacter* as Gram-negative strains, and *Rhodococcus*, *Corynebacterium* and *Bacillus* as Gram-positive strains.<sup>3,9</sup>

The aim of this study was to analyse the potential of the autochthonous natural microbial community (NMC model system), and NMC augmented with allochthonous hydrocarbon-degrading (AHD) microorganisms (isolated from location contaminated with petroleum products, NMC-AHD model system) for biodegradation of PCBs present in the river sediments to protect the environment and estimate future treatment of these sites. Sequential multi-stage aerobic/anaerobic microbial bioremediation of sediment polluted with PCBs was applied to stimulate both oxidative and reductive processes, respectively. The river sediments were collected in Belgrade, Serbia, from the confluence of Topčider River with Čukarički Rukavac (CR), which is known for long-term pollution with various organic and inorganic pollutants.<sup>19</sup> In the study, a combined multi-stage aerobic/anaerobic process was applied.

## EXPERIMENTAL

### *Sediment sampling*

River sediment samples were collected in Belgrade, Serbia, from the confluence of Topčider River with Čukarički Rukavac. Sediments were sampled from four depths in undisturbed conditions: 0–1, 1–3, 3–6 and 6–10 cm.

### *Basic physicochemical and chemical analysis of the sediment*

The content of total petroleum hydrocarbons (TPH) in the sediment was extracted as per method ISO 16703<sup>20</sup> and determined gravimetrically in accordance with DIN EN 14345<sup>21</sup> as previously described.<sup>18</sup> Sediments were analysed for: the content of sand, clay, and silt, moisture, pH, total, organic and inorganic carbon, sulphur and nitrogen using standard methods.<sup>22,23</sup> Sediments were dried and PCBs were extracted using a Soxhlet apparatus according to the modified method 3540C during 24 h with 5 cycles per hour.<sup>24</sup> Extraction was carried out using a 1:1 volumetric mixture of acetone:hexane, and the PCB content in the extracts (after clean-up) was analysed using GC–MS/MS (Bruker, 320MS). All solvents and reagents used were HPLC grade.

### *Microbiological analysis of the sediment*

The number of microorganisms in the river sediments was determined by plating appropriate serial dilutions on agar plates incubated at 28 °C. The media used were: nutrient agar for total chemoorganoheterotrophs (TC); nutrient agar with 0.5 % glucose for total anaerobic chemoorganoheterotrophs (TAC); malt agar for yeast and molds (YM), and; a mineral base medium containing 2 g of standard D2 diesel fuel in 1 L of medium<sup>25</sup> for hydrocarbon degraders (HD).

### *Bioremediation study*

After analysis of the sediments, a composite sample from all four sediments was produced for the bioremediation study, with the mass ratio of sediments from the different depths (0–1, 1–3, 3–6 and 6–10 cm) of 1:2:3:4. Composite sediment and sand were mixed in a 1:1 mass ratio and added to Bushnell–Haas modified medium (chloride-free): magnesium sulphate heptahydrate, 0.2 g L<sup>-1</sup>; calcium carbonate, 0.2–0.5 %; potassium dihydrogen phosphate, 1.0 g L<sup>-1</sup>; dipotassium hydrogen phosphate, 1.0 g L<sup>-1</sup>; ammonium nitrate, 1.0 g L<sup>-1</sup>; iron sulphate, trace; Tween 80, 0.1 g L<sup>-1</sup>; pH ~7. Bioremediation of polluted sediment lasted 70 days with alternating anaerobic and aerobic cycles: anaerobic (static, in a CO<sub>2</sub> atmosphere, 28 °C, three weeks (0–21 days)); aerobic (rotary shaker at 200 rpm, 28 °C, three weeks, (21–42 days)); anaerobic two weeks (42–56 days), aerobic two weeks (56–70 days). In parallel, the activity of microorganisms in NMC and NMC-AHD model systems was monitored. In the NMC-AHD model system, bioaugmentation using AHD was conducted at the beginning, 21<sup>st</sup> and 56<sup>th</sup> day under sterile conditions. The pH of suspensions in the model systems was measured on days 0, 42 and 70. Abiotic control was sterilized in an autoclave prior to incubation in order to monitor abiotic changes. All analyses were conducted in triplicate and results are given as mean values.

### *Allochthonous hydrocarbon-degrading microorganisms used for bioaugmentation*

Bioaugmentation was carried out by inoculation of AHD biomass (enriched in laboratory conditions) which were previously isolated from sites contaminated with petroleum products: *Pseudomonas* (*sp.* NS009 – GenBank: JF826528.1 and CHNSH-17 –GenBank: JQ292806.1), *Rhodococcus* (*sp.* RNP05 – GenBank: JQ065876.1 and CHP-NR31 – GenBank: JX965395.1) and *Achromobacter* (*sp.* NS014 – GenBank: JF826529.1).<sup>26,27</sup>

### *Instrumental analysis*

The content of PCBs was analysed using GC–MS/MS (Bruker, 320MS). For PCB congener-specific analysis, an HT8-PCB capillary column (60 m, 0.25 mm i.d., Kanto Kagaku, Japan) was used. As standard for PCB determination EC5433 (Cambridge Isotope Labor-

atories, USA) was used. As an internal standard, <sup>13</sup>C-labeled PCB congener mixture MBP-CG (Wellington Laboratories, Ontario, Canada) was used.

## RESULTS AND DISCUSSION

### *Chemical and microbiological properties of sediments*

The river sediments were characterized by neutral pH, relatively high content of organic carbon and high content of inorganic carbon (Table I). Silt, particularly fine silt, was the dominant granulometric fraction in all sediments. Among microorganisms determined, the dominant fraction comprised TC microorganisms. The number of TC increased with the depth of the sediment layers, together with HD (Table I). The high counts, determined for all microbial groups examined, suggested that intensive aerobic and anaerobic microbiological processes were occurring in the river sediments, and so these materials would form a suitable matrix for studying possible biotic transformations of organic contaminants, such as PCBs.

TABLE I. Basic chemical and microbiological properties of the river sediments studied; in all standard results:  $\pm$  deviation for three measurements

| Parameter                                    | Sediment layer depth, cm |                     |                     |                     |
|--|--------------------------|---------------------|---------------------|---------------------|
|  | 0–1                      | 1–3                 | 3–6                 | 6–10                |
| pH   | 7.30                     | 7.22                | 7.23                | 7.25                |
| Amount of total carbon, %                    | 3.2±0.1                  | 3.9±0.1             | 4.3±0.1             | 4.7±0.1             |
| Amount of organic carbon, %                  | 1.8±0.1                  | 2.1±0.1             | 2.3±0.1             | 2.6±0.1             |
| Amount of inorganic carbon, %                | 1.4±0.2                  | 1.8±0.1             | 2.0±0.1             | 2.1±0.1             |
| Amount of nitrogen, %                        | 0.32±0.04                | 0.24±0.04           | 0.28±0.04           | 0.22±0.04           |
| Amount of sulfur, %                          | 0.21±0.02                | 0.19±0.02           | 0.24±0.02           | 0.23±0.02           |
| Amount of sand, %                            | 9.7                      | 8.2                 | 8.1                 | 6.3                 |
| Amount of silt + clay, %                     | 90.3                     | 91.8                | 91.9                | 93.7                |
| Concentration of TPH, g kg <sup>-1</sup> dw  | 0.97±0.2                 | 1.12±0.2            | 0.88±0.2            | 1.54±0.2            |
| Concentration of PCBs, ng g <sup>-1</sup> dw | 305±10                   | 173±10              | 220±10              | 169±10              |
| Number of TC, CFU g <sup>-1</sup>            | 2.1×10 <sup>6</sup>      | 8.9×10 <sup>5</sup> | 5.1×10 <sup>5</sup> | 6.3×10 <sup>4</sup> |
| Number of TAC, CFU g <sup>-1</sup>           | 1.2×10 <sup>3</sup>      | 5.6×10 <sup>3</sup> | 9.8×10 <sup>3</sup> | 1.2×10 <sup>4</sup> |
| Number of YM, CFU g <sup>-1</sup>            | 5.4×10 <sup>3</sup>      | 5.1×10 <sup>3</sup> | 6.9×10 <sup>2</sup> | 8.4×10 <sup>2</sup> |
| Number of HD, CFU g <sup>-1</sup>            | 1.1×10 <sup>5</sup>      | 5.9×10 <sup>5</sup> | 1.8×10 <sup>5</sup> | 2.3×10 <sup>3</sup> |

### *PCBs in the sediments*

The distribution of PCBs in the sediments is given in Fig. 1. The PCBs are water-insoluble chemicals that accumulate in sediments depending on the partition coefficient.<sup>28</sup> The high level of PCBs in the sediment sample is probably due to historical reasons since industrial plant Minel located upstream of Topčider River, was known for the production of transformers and capacitors in the past. The Topčider River water body is small, thus leading to the accumulation of PCBs in sediment. The dominant PCBs in the sediments were pentachlorinated,

followed by tetra, tri and hexachlorinated compounds. The highest concentration was determined in the upper layer (0–1 cm), followed by 3 to 6 cm, 1 to 3 cm and 6 to 10 cm layer, respectively. This finding suggests that possible recent contamination also occurred.

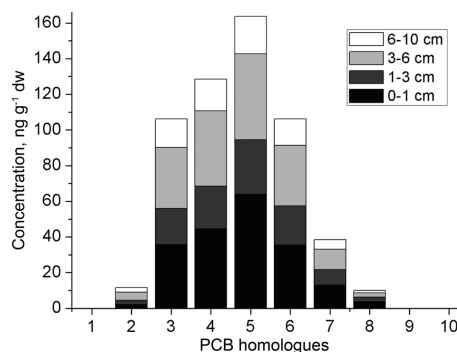


Fig. 1. Distribution of PCBs in the river sediments.

#### *Numbers of microorganisms during the biodegradation study*

The number of microorganisms during biodegradation is given in Table II. The number of microorganisms in the NMC model system was reasonably stable, with slight decreases. However, in the NMC-AHD model systems, numbers of TC and HD microorganisms increased by two orders of magnitude by day 42 and then reduced by one order of magnitude by day 70 (Table II).

TABLE II. Numbers of microorganisms (CFU g<sup>-1</sup>) in the NMC and NMC-AHD model systems on days 42 and 70, and in abiotic control after 70 days

| Microorganism | Model              |        |                   |                   |                   |                   |
|---------------|--------------------|--------|-------------------|-------------------|-------------------|-------------------|
|               | Abiotic control    |        | NMC               |                   | NMC-AHD           |                   |
|               | Day 0              | Day 70 | Day 42            | Day 70            | Day 42            | Day 70            |
| TC            | $7.0 \times 10^5$  | <1     | $5.0 \times 10^5$ | $2.5 \times 10^5$ | $4.9 \times 10^7$ | $10^7$            |
| TAC           | $2.1 \times 10^4$  | <1     | $1.3 \times 10^5$ | $6.2 \times 10^4$ | $3.9 \times 10^5$ | $2.0 \times 10^5$ |
| YM            | $1.15 \times 10^3$ | <1     | $2.5 \times 10^3$ | $4.5 \times 10^3$ | $2.9 \times 10^4$ | $4.0 \times 10^4$ |
| HD            | $1.7 \times 10^5$  | <1     | $2.0 \times 10^5$ | $2.3 \times 10^5$ | $2.6 \times 10^7$ | $4.7 \times 10^6$ |

#### *Change in suspension pH during the biodegradation study*

The pH values of suspensions in the biodegradation study, measured in the suspensions after stopping the bioremediation process by autoclaving, are shown in Fig. 2. In NMC model systems, the suspension pH decreased from initial pH 7.2 to 6.1 and 6.0 after 42 and 70 days, respectively. In NMC-AHD model systems, the pH decreased from initial 7.2 to 6.0 and 5.8 after 42 and 70 days, respectively. In the abiotic control, sterilized at the beginning of the process, the pH remained the same after 70 days. This change in pH indicated that the activity of microorganisms under aerobic/anaerobic conditions resulted in the decomposition of present hydrocarbons followed by the formation of organic acids as

one of the oxidation products during the aerobic step of the study. In addition, in the NMC-AHD model system, the pH decreases slightly more comparing to NMC, which is the result of the microbial activity of AHD used for bioaugmentation of the river sediment.

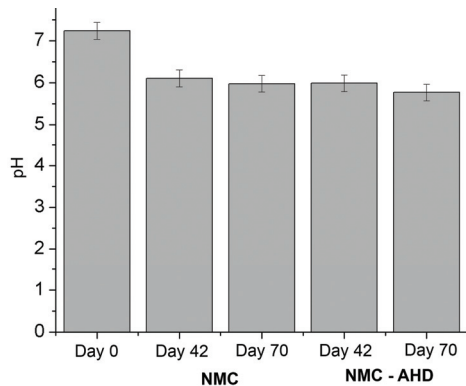


Fig. 2. Change in pH during the bioremediation study in different model systems.

#### *PCB concentrations during the biodegradation study*

The amount of PCBs and level of substitution through the bioremediation process was analysed using GC-MS/MS and the results are given in Fig. 3. At the beginning of the bioremediation, the total amount of PCBs was  $287.5 \text{ ng g}^{-1}$  (day 0). In the NMC model system, the concentration of PCBs was 276.8 and  $198.5 \text{ ng g}^{-1}$  after 42 days and 70 days, respectively. Therefore, significant ( $>30\%$ ) decrease in PCBs concentration occurred after 70 days.

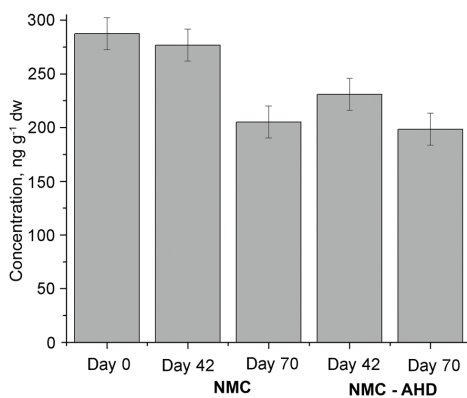


Fig. 3. Change in PCB concentration during the bioremediation study in different model systems.

In the NMC-AHD model systems, a faster decrease in the concentration of PCB in the first 42 days was determined ( $231.0 \text{ ng g}^{-1}$ ). After 70 days, the concentration was  $195.2 \text{ ng g}^{-1}$ . These reductions were 20 and 32 %, respectively, after 42 and 70 days. A slight decline in PCB levels in the abiotic control was

also observed, suggesting that sorption processes occurred. Surprisingly, the concentration of PCBs in the NMC and NMC-AHD model systems after 70 days was almost the same, suggesting that NMC, already present in the sediment, has important biodegradation potential for reducing PCBs and carry a major part of the bioremediation potential. Some previous studies also confirmed that PCBs contaminated soils can be the source of PCBs and biphenyl degrading microorganisms.<sup>29</sup> However, it should be emphasized that in our study, bioaugmentation (a process of adding allochthonous hydrocarbon-degrading microorganisms to supplement the autochthonous population) proved to be very useful because it leads to accelerated bioremediation.

#### *Changes in the PCB congener and PCB homologue patterns during the biodegradation study*

Changes in the PCB congener pattern during the biodegradation study are given in Fig. 4. The sediment sample contained from mono to octachlorinated biphenyls, wherein the dominant were pentachlorinated congeners (control suspension). A change in congener concentrations and profiles was observed during the bioremediation study. The level of higher substituted congeners was reduced and increases in the level of trichlorinated biphenyls were noticed.

These changes were noticed after the applied anaerobic/aerobic alteration cycles, suggesting that reductive dehalogenation occurred and that the increase in the concentration of trichlorinated biphenyls resulted from dehalogenation of higher congeners. This is supported by the previous studies in which tetra-, penta-, hexa- and hepta-chlorobiphenyls were produced during the dechlorinated process of deca- and hepta-chlorobiphenyls.<sup>30–32</sup> In the study of Song *et al.*<sup>33</sup> the rise of tetra-, penta-, hexa- and hepta-chlorobiphenyls was attributed to the loss of deca- and hepta-chlorobiphenyls. It should also be emphasized that the degree of chlorination and position of chlorine atoms on biphenyl rings may influence the biodegradability of different PCB congeners.

To follow the change in the homologue pattern of the PCBs during the bioremediation study, dihalogenated and trihalogenated homologues were given special attention. Table III lists the analysed homologues, while Figs. 5 and 6 depicts differences in the homologue patterns during bioremediation in NMC-AHD model systems.

The concentration of different PCB congener homologues was different in NMC-AHD model systems after 70 days compared to day 0. PCB12 was completely degraded while the concentrations of PCB-8, PCB-11 and PCB-15 were reduced by 60, 50 and 20 %, respectively. As for trihalogenated PCBs, PCB-18 and PCBs 19, 31 and 33 were the most susceptible to biodegradation, while PCB-28 and PCB-37 were reduced by less than 10 % by the biodegradation processes that occurred. In abiotic control after 70 days, significant changes were not noticed.

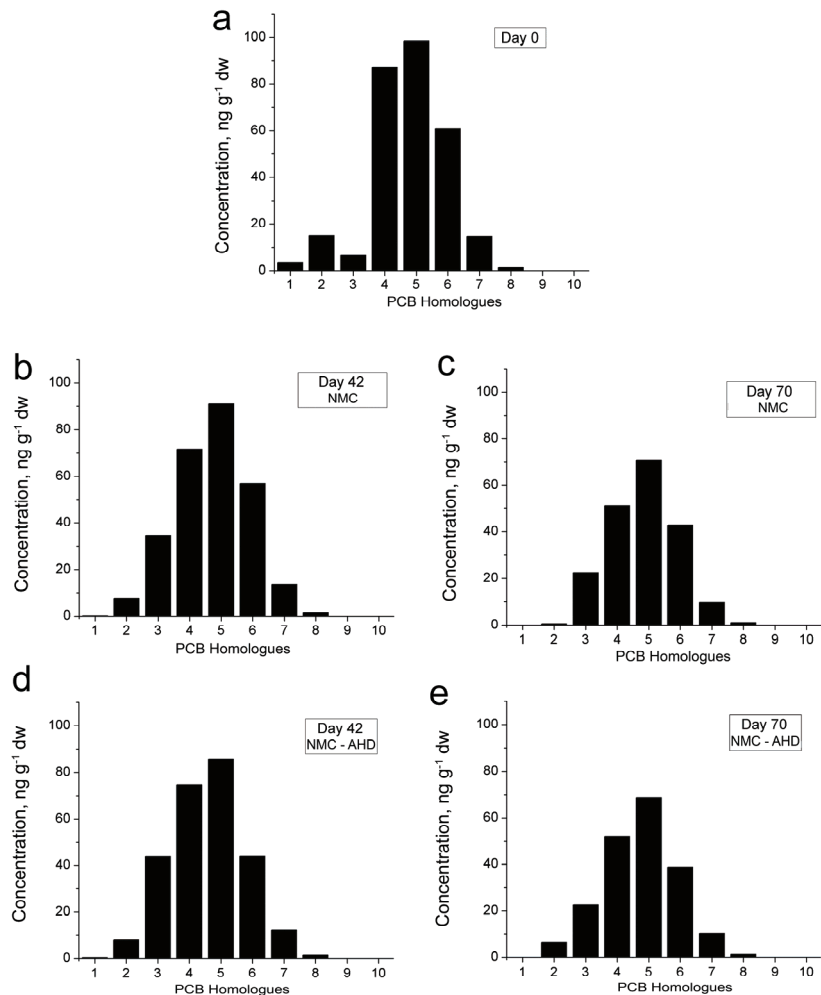


Fig. 4. Change in PCB congener patterns obtained during the bioremediation study in different model systems: day 0 (a), day 42 NMC (b), day 70 NMC (c), day 42 NMC-AHD (d) and day 70 NMC-AHD (e).

TABLE III. List of dihalogenated and trihalogenated PCB homologues analysed

| PCB 2 Cl | IUPAC | PCB 3 Cl | IUPAC |
|----------|-------|----------|-------|
| —        | —     | 2, 2', 6 | 19    |
| 2, 6     | 10    | 2, 2', 5 | 18    |
| 2, 2'    | 4     | 2, 4', 5 | 31    |
| 2, 5     | 9     | 2, 4, 4' | 28    |
| 2, 4'    | 8     | 2', 3, 4 | 33    |
| 3, 3'    | 11    | 3, 4, 5  | 38    |
| 3, 4     | 12    | 3, 3', 4 | 35    |
| 4, 4'    | 15    | 3, 4, 4' | 37    |

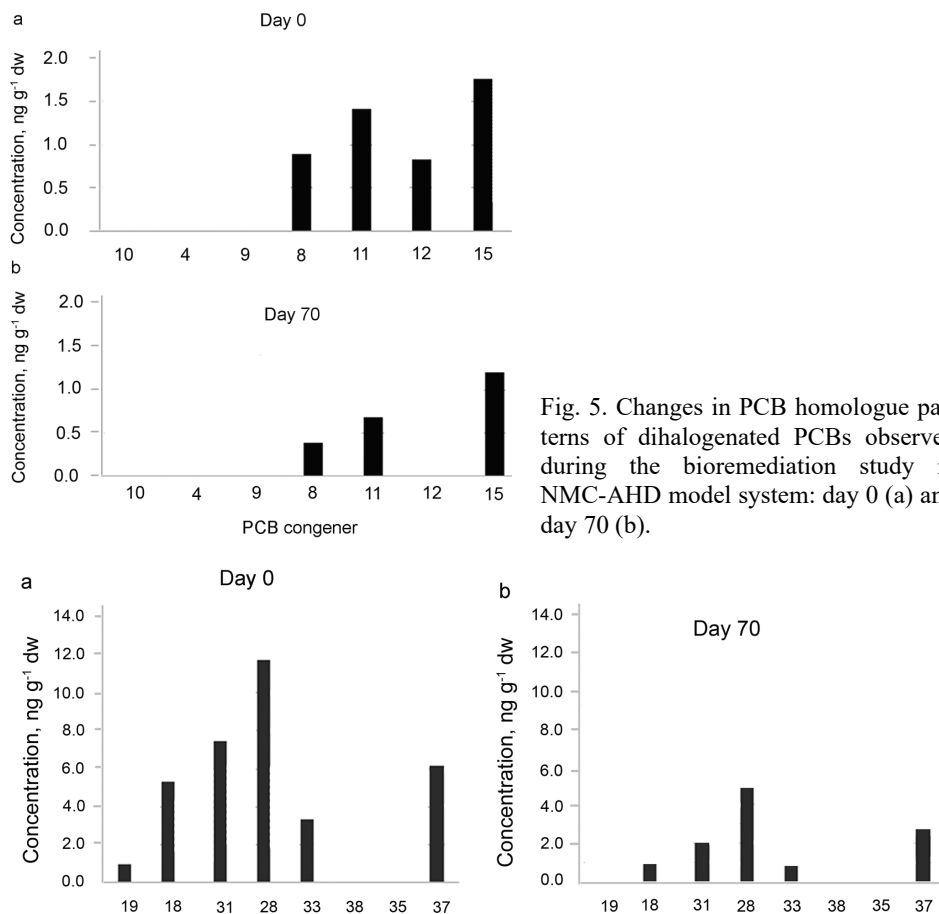


Fig. 5. Changes in PCB homologue patterns of dihalogenated PCBs observed during the bioremediation study in NMC-AHD model system: day 0 (a) and day 70 (b).

Fig. 6. Changes in PCB homologue patterns of trihalogenated PCBs observed during the bioremediation study in NMC-AHD model system: day 0 (a) and day 70 (b).

#### CONCLUSION

After 70 days in the both model systems, one with the autochthonous natural microbial community (NMC consortium) and the second with NMC augmented with AHD microorganisms (*Pseudomonas* (*sp.* NS009 – GenBank: JF826528.1 and CHNSH-17 –GenBank: JQ292806.1), *Rhodococcus* (*sp.* RNP05 – GenBank: JQ065876.1 and CHP-NR31 – GenBank: JX965395.1) and *Achromobacter* (*sp.* NS014 – GenBank: JF826529.1) about a 33 % reduction in the concentration of PCBs was observed. Tests have confirmed that NMC consortia can reduce the level of PCBs in the contaminated river sediment under laboratory conditions and that presence of AHD microorganisms facilitates this degradation. The results indicate the strong bioremediation potential of NMC present at the contaminated site if alternating anaerobic/aerobic cycles are used for the treatment of sediments

or soils contaminated with PCB compounds. Changes in the level of dominant congeners, *i.e.*, a reduction of the substituted higher fraction and an increase of the substituted lower fraction, during the course of the biodegradation corresponded to the occurrence of anaerobic reductive dehalogenation.

*Acknowledgements.* This study was supported by the Ministry of Education, Science and Technological Development of Republic of Serbia (Contract number: 451-03-9/2021-14/200168 and Contract number: 451-03-9/2021-14/200026) and Japan International Cooperation Agency (JICA) grassroot project “Environmental Improvement in Pančevo, Serbia, through the Collaborations Among Academia, Government, Industry and Citizens.

#### ИЗВОД

#### БИОДЕГРАДАЦИЈА ПОЛИХЛОРОВАНИХ БИФЕНИЛА У РЕЧНОМ СЕДИМЕНТУ: ЛАБОРАТОРИЈСКА СТУДИЈА

АЛЕКСАНДРА ЖЕРАЂАНИН<sup>1</sup>, КРИСТИНА ЈОКСИМОВИЋ<sup>1</sup>, ЈЕЛЕНА АВДАЛОВИЋ<sup>1</sup>, ГОРДАНА ГОГИЋ-ЦВИЈОВИЋ<sup>1</sup>, ТАКЕШИ НАКАНО<sup>2</sup>, СРЂАН МИЛЕТИЋ<sup>1</sup>, МИЛА ИЛИЋ<sup>1</sup> и ВЛАДИМИР П. БЕШКОСКИ<sup>3</sup>

<sup>1</sup>Универзитет у Београду - Институт за хемију, технолоџију и мешавине - Институт ог националној значају за Републику Србију, Београд, <sup>2</sup>Osaka University, Research Center for Environmental Preservation, Japan и <sup>3</sup>Универзитет у Београду - Хемијски факултет, Београд

Дуготрајне органске загађујуће супстанце (POPs) су липофилна, постојана и биоакумулативна токсична једињења. Уопште говорећи, сматрају се отпорним на биолошку, фотолитичку и хемијску деградацију, а полихлоровани бифенили (PCBs) спадају у групу ових хемикалија. У Србији се PCBs никада нису производили, али су се увозили и углавном користили у електроопреми, трансформаторима и кондензаторима. Циљ нашег истраживања био је да се анализира секвенцијална вишестепена аеробна/анаеробна микробиолошка разградња PCBs присутних у речном седименту са подручја познатог по дуготрајном загађењу овим једињењима. Проучавање активности конзорцијума аутохтоних природно присутних микроорганизама (NMC конзорцијум) и NMC суплементисаних конзорцијумом алохтоних угљоводоник деградирајућих (HD) микроорганизама (изолованих са локација контаминираних нафтним дериватима) (NMC-HD конзорцијум) је изведено како би се проценила способност ових микроорганизама за потренцијалну употребу у будућим биоремедијационим третманима оваквих локалитета. Лабораторијска студија биоразградње је трајала 70 дана, након чега је уочено смањење концентрације укупних PCBs за >33 %. Ово истраживање је потврдило снажан потенцијал аутохтоних микроорганизама за смањење нивоа PCBs у речном седименту у наизменичним вишестепеним аеробним/анаеробним условима.

(Примљено 17. децембра, прихваћено 24. децембра 2021)

#### REFERENCES

1. L. Xu, Y. Teng, Z. G. Li, J. M. Norton, Y. M. Luo, *Sci. Total Environ.* **408** (2010) 1007 (<https://doi.org/10.1016/j.scitotenv.2009.11.031>)
2. M. Matthies, K. Solomon, M. Vighi, A. Gilman, J. V. Tarazona, *Environ. Sci.- Proc. Imp.* **18** (2016) 1114 (<https://doi.org/10.1039/c6em00311g>)
3. A. V. B. Reddy, M. Moniruzzamana, T. M. Aminabhavi, *Chem. Eng. J.* **358** (2019) 1186 (<https://doi.org/10.1016/j.cej.2018.09.205>)

4. R. Villemur, *Philos. Trans. R. Soc. Lond. B Biol. Sci.* **368** (2013) 20120319 (<https://doi.org/10.1098/rstb.2012.0319>)
5. M. Diez, *J. Soil Sci. Plant Nut.* **10** (2010) 244 (<https://doi.org/10.4067/S0718-95162010000100004>)
6. P. I. Nikel, D. Pérez-Pantoya, V. de Lorenzo, *Philos. Trans. R. Soc. Lond. B Biol. Sci.* **368** (2013) 20120377 (<https://doi.org/10.1098/rstb.2012.0377>)
7. F. Khalid, M. Z. Hashmi, N. Jamil, A. Quadir, M. I. Ali, *Environ. Sci. Pollut. Res.* **28** (2021) 10474 <https://doi.org/10.1007/s11356-020-11996-2>.
8. L. Passatore, S. Rossetti, A. A. Juwarkar, A. Massacci, *J. Hazard. Mater.* **278** (2014) 189 (<https://doi.org/10.1016/j.jhazmat.2014.05.051>)
9. P. K. Arora, *Microbial Metabolism of Xenobiotic Compounds*, Springer, Singapore, 2019, pp. 165–188 (<https://doi.org/10.1007/978-981-13-7462-3>)
10. M. Seeger, M. Hernández, V. Méndez, B. Ponce, M. Córdova, M. González, *J. Soil Sci. Plant Nut.* **10** (2010) 320 (<https://doi.org/10.4067/S0718-95162010000100007>)
11. Stockholm Convention on POPs. Text of the Convention, <http://www.pops.int/TheConvention/Overview/TextoftheConvention/tabid/2232/Default.aspx> (accessed 17 December 2021)
12. M. A. Ashraf, *Environ. Sci. Pollut. R.* **5** (2015) 4223 (<https://doi.org/10.1007/s11356-015-5225-9>)
13. EPA Persistent Organic Pollutants: A Global Issue, A Global Response, <https://www.epa.gov/international-cooperation/persistent-organic-pollutants-global-issue-global-response> (accessed 17 December 2021)
14. Stockholm convention on POPs. The 12 initial POPs under Stockholm convention, <http://www.pops.int/TheConvention/ThePOPs/The12InitialPOPs/tabid/296/Default.aspx> (accessed 17 December 2021)
15. D. L. Bedard, K. M. Ritalahti, F. E. Löffler, *Appl. Environ. Microb.* **73** (2007) 2513 (<https://doi.org/10.1128/AEM.02909-06>)
16. J. Wiegel, Q. Wu, *FEMS Microbiol. Ecol.* **32** (2000) 1 (<https://doi.org/10.1111/j.1574-6941.2000.tb00693.x>)
17. NIP-National Implementation Plan for the implementation of the Stockholm Convention, the Ministry of Environment and Spatial Planning of the Republic of Serbia, 2010
18. V. P. Beškoski, G. Gojgić - Cvijović, J. Milić, M. Ilić, S. Miletić, T. Šolević, M.M. Vrvić, *Chemosphere* **83** (2011) 34 (<https://doi.org/10.1016/j.chemosphere.2011.01.020>)
19. G. Dević, S. Sakan, D. Đorđević, *Environ. Sci. Pollut. Res.* **23** (2016) 282 (<https://doi.org/10.1007/s11356-015-5808-5>)
20. ISO 16703: Soil Quality – Determination of Content of Hydrocarbon in the Range C10 to C40 by Gas Chromatography, 2004
21. DIN EN 14345: Characterization of Waste. Determination of Hydrocarbon Content by Gravimetry, 2004
22. R. Margesin, F. Schinner, *Manual for soil analysis-monitoring and assessing soil bioremediation*, Springer-Verlag, Berlin, 2005, pp. 47–95 (<https://doi.org/10.1007/3-540-28904-6>)
23. M. Pansu, J. Gautheyrou, *Handbook of soil analysis- mineralogical, organic and inorganic methods*, Springer-Verlag, Berlin, 2006 (<https://doi.org/10.1007/978-3-540-31211-6>)

24. D. Leys, L. Adrian, H. Smidt, *Philos. Trans. R. Soc., B* **368** (2013) 20120316 (<https://doi.org/10.1098/rstb.2012.0316>)
25. C. J. Hurst, R. L. Crawford, G. R. Knudsen, M. J. McInerney, L. D. Stetzenbach. *Manual of Environmental Microbiology*, 2<sup>nd</sup> ed., ASM Press, Washington DC, 2002, p. 934 (ISBN 978-1555811990)
26. G. D. Gojic-Cvijovic, J. S. Milic, T. M. Solevic, V. P. Beskoski, M. V. Ilic, L. S. Djokic, T. M. Narancic, M. M. Vrvic, *Biodegradation* **23** (2012) 1 (<https://doi.org/10.1007/s10532-011-9481-1>)
27. NCBI – The national center for biotechnology information, *Nucleotide database*, <https://www.ncbi.nlm.nih.gov> (accessed 17 December 2021)
28. I. Liska, F. Wagner, M. Sengl, K. Deutsch, J. Slobodnik, *Joint Danube Survey 3 — Final Scientific Report*, International Commission for the Protection of the Danube River, Vienna, 2015, pp. 249–259 ([http://www.danubesurvey.org/jds3/jds3-files/nodes/documents/jds3\\_final\\_scientific\\_report\\_1.pdf](http://www.danubesurvey.org/jds3/jds3-files/nodes/documents/jds3_final_scientific_report_1.pdf))
29. C. Tu, Y. Teng, Y. Luo, X. Li, X. Sun, Z. Li, W. Liu, P. Christie, *J. Hazard. Mater.* **186** (2011) 1438 (<https://doi.org/10.1016/j.jhazmat.2010.12.008>)
30. A. C. Alder, M. M. Haggblom, S. R. Oppenheimer, L.Y. Young, *Environ. Sci. Technol.* **27** (1993) 530 (<https://doi.org/10.1021/es00040a012>)
31. L. Dabrowska, A. Rosinska, *Chemosphere* **88** (2012) 168 (<https://doi.org/10.1016/j.chemosphere.2012.02.073>)
32. R.B. Payne, H.D. May, K.R. Sowers, *Environ. Sci. Technol.* **45** (2011) 8772 (<https://doi.org/10.1021/es201553c>)
33. M. Song, C. Luo, F. Li, L. Jiang, Y. Wang, D. Zhang, G. Zhang, *Sci. Total. Environ.* **502** (2015) 426 (<https://doi.org/10.1016/j.scitotenv.2014.09.045>).





J. Serb. Chem. Soc. 87 (1) 109–119 (2022)  
JSCS-5508

# Journal of the Serbian Chemical Society

JSCS@tmf.bg.ac.rs • www.schd.org.rs/JSCS

Original scientific paper  
Published 14 January 2022

## Determination of bisphenol A traces in water samples from the Vrbas River and its tributaries, Bosnia and Herzegovina

DAJANA SAVIĆ<sup>1\*</sup>, MILICA BALABAN<sup>2</sup>, NEBOJŠA PANTELIĆ<sup>1</sup>, DEJANA N. SAVIĆ<sup>2</sup>,  
MALIŠA ANTIĆ<sup>1</sup>, RADOSLAV DEKIĆ<sup>2</sup> and VESNA ANTIĆ<sup>1</sup>

<sup>1</sup>University of Belgrade – Faculty of Agriculture, Nemanjina 6, Belgrade-Zemun, Serbia and

<sup>2</sup>University of Banja Luka, Faculty of Natural Sciences and Mathematics, Mladena Stojanovića 2, Banja Luka, Bosnia and Herzegovina

(Received 1 October, accepted 15 November 2021)

**Abstract:** The bisphenol A (BPA) concentration was determined in 12 surface water samples of the Vrbas River and its five tributaries. The samples were taken in the area that belongs to the city of Banja Luka (Bosnia and Herzegovina). BPA was isolated using micro liquid–liquid extraction followed by derivatization and gas chromatography–mass spectrometry analysis (GC–MS). Silylation was used as a derivatization method to increase volatility and allow the GC–MS determination of BPA. The limits of detection (*LOD*) and quantification (*LOQ*), obtained by validating the procedure, were determined at 4 and 10 ng L<sup>-1</sup>, respectively. The concentrations of BPA were ranged between 33 and 354 ng L<sup>-1</sup>, and all were above the *LOQ* value. The lowest amount of BPA was found in the sample collected in the river Vrbas, near Švrakava estuary upstream from the city of Banja Luka. The highest concentration of BPA was recorded at the confluence of the Crkvena and Vrbas rivers, which is located in the city center. This study shows that population and human activity could affect the level of BPA in the environment.

**Keywords:** bisphenol A; GC–MS; microextraction; derivatization; river water.

### INTRODUCTION

It is well known that the presence of certain chemicals in the environment adversely affects human health by damaging the endocrine system.<sup>1</sup> These compounds can interact with specific receptors and therefore interfere with the hormonal action and function of human cells.<sup>2</sup>

Bisphenol A (BPA; 4,4'-dihydroxy-2,2-diphenyl propane) is a chemical synthesized worldwide with over 5.5 million tons per year and is defined as one of the endocrine-disrupting compounds (EDCs).<sup>3</sup> BPA is known as a monomer – for the synthesis of polycarbonate plastics, epoxy, and polyester resins, and it is

\* Corresponding author. E-mail: dajana.savic@agrif.bg.ac.rs  
<https://doi.org/10.2298/JSC211001098S>



also used in the production of thermal paper.<sup>4,5</sup> Consequently, it can be found in materials which are used to produce CDs and DVDs, baby bottles, containers for beverages and foods, toys, and medical devices.<sup>6,7</sup> Traces of BPA can leak from these materials leading to releases into the environment and causing pollution. Some studies have shown that the BPA is mainly found in water, soil, and sediments.<sup>8</sup> The primary sources of BPA in the aquatic environment are domestic and industrial wastewater and runoff from agriculture.<sup>9</sup> It has been found that the presence of BPA in the aquatic ecosystem may have a potentially harmful influence on the reproductive system and metabolic processes of organisms such as fish and mussels.<sup>10</sup> In addition, BPA has been detected in human serum, urine, saliva, and breast milk.<sup>11</sup> Some studies indicate that BPA could be effective as estradiol in activating specific receptor responses and may act as an androgen receptor antagonist.<sup>12,13</sup> Furthermore, it has been reported that human exposure to BPA could cause several health issues, including various types of cancers, obesity, cardiovascular and neurodegenerative disorders.<sup>14–17</sup>

Canada is the first country to consider BPA regulation more strictly and ban its presence in infant feeding bottles.<sup>18</sup> Moreover, BPA is listed among compounds considered hazardous to human health and the environment.<sup>19</sup> BPA-contained products are forbidden in some American states. At the same time, in the EU, France was the first state that banned the production, trade, and marketing of food cans coated with epoxy-resins containing BPA in January 2015.<sup>20</sup> Realizing the seriousness of the negative impact on human health, the European Food Safety Authority (EFSA) has recently set a new specific migration limit (*SML*) of BPA that can migrate from the plastic food contact material into the food at 50 µg kg<sup>-1</sup>.<sup>21</sup> The new *SML* is based on a temporary tolerable daily intake (*t-TDI*) of BPA, which from 2015 onwards amounts to 4 µg (kg BW)<sup>-1</sup> day<sup>-1</sup>.<sup>22</sup> Further, according to the European Water Framework Directive and the Environmental Quality Standards Directive, BPA has recently been listed as a priority hazardous pollutant.<sup>23,24</sup>

Due to the toxicity and widespread human exposure to BPA, it is necessary to monitor the presence of this compound in the environment. The examinations of wastewater, surface water, and drinking water samples collected in Germany showed that the BPA concentration in drinking water samples ranged from 0.5 to 2 ng L<sup>-1</sup>, while the mean BPA concentration in river water samples and the wastewater was 4.7 and 16 ng L<sup>-1</sup>, respectively.<sup>25</sup> A study conducted by measuring BPA in the Danube River, near Novi Sad in Serbia, showed that the concentration of BPA varies significantly depending on the seasons and is highest in summer, probably due to increased human activities and weather conditions.<sup>26</sup>

Accordingly, our study aimed to determine the amount of bisphenol A in real water samples collected in the Vrbas River and its tributaries using the GC–MS technique. The samples were collected in early July 2021, during the low water

levels. BPA was isolated from water samples by a very simple and accessible micro-liquid–liquid extraction technique, followed by a derivatization step by silylation with BSTFA reagent (*N,O*-bis(trimethylsilyl)-trifluoroacetamide). Silylated BPA was quantified by GC–MS due to increased volatility.

## EXPERIMENTAL

### Chemicals

BPA was purchased from Sigma–Aldrich with a minimum of 98% purity. Deuterated bisphenol A-*d*<sub>16</sub> (BPA-*d*<sub>16</sub>), purchased from Sigma–Aldrich, was used as an internal standard (IS). The stock solution was prepared by dissolving a certain amount of BPA in acetone (HPLC purity, Fisher Scientific, UK). Working solutions for recovery check and calibration were prepared by diluting the stock solution at the required concentrations in acetone. All solutions were stored in the refrigerator before analysis. During the experiment, only equipment made of glass was used. Sodium chloride and dichloromethane (both from Lach-Ner, Czech Republic) were used for the microextraction. The derivatization process was performed using the following derivatization reagent: BSTFA (*N,O*-bis(trimethylsilyl)trifluoroacetamide) + 1% TMCS (trimethylchlorosilane) reagent (Supelco, Sigma–Aldrich). The silylated derivative of BPA was dissolved in hexane (HPLC purity, Fisher Scientific, UK) before GC–MS analysis.

### Description of the sampling sites

Details related to the sampling sites are given in Supplementary material to this paper.

### Pretreatment and micro liquid-liquid extraction of the samples

150 g of NaCl was dissolved in a 500 mL water sample. Afterward, the pH value was adjusted between 3 and 5 by adding diluted HCl (1:1).<sup>27,28</sup> The sample was transferred to a separatory funnel connected to a mechanical stirrer. Then 3.5 mL of dichloromethane and 20 μL of BPA-*d*<sub>16</sub> (*c* = 0.5 mg mL<sup>-1</sup>) were added to the funnel. The content of the funnel was stirred for 1 min at 900 rpm.<sup>29</sup> After mixing, the organic phase (bottom layer) was discharged directly through a separatory funnel into a vial, via a layer of anhydrous Na<sub>2</sub>SO<sub>4</sub> and cotton wool, to remove residual water due to sensitivity of the derivatizing agent to moisture.

### Derivatization and GC–MS (SIM) analysis

The dichloromethane phase obtained after microextraction was exposed to a gentle stream of nitrogen to remove the solvent. Then derivatization of the residue (extracted BPA) was performed by adding 100 μL of derivatization reagent (BSTFA + 1 % TMCS). The content was stirred on vortex and heated to 80 °C for 30 min. After derivatization, the solution was evaporated to dryness under a stream of nitrogen. The residue was redissolved in 100 μL of hexane.<sup>30</sup>

The samples were analyzed using the GC–MS technique (Varian 450-GC gas chromatograph with 220-MS IT mass spectrometer, USA). The separation of compounds was performed on FactorFour capillary column VF-5ms 30 m × 0.25 mm with 0.25 μm film thickness (Varian). The injector temperature was 270 °C, and the injection volume was 1 μL in splitless mode. The carrier gas was helium at a constant flow rate of 1 mL min<sup>-1</sup>. The oven program started at 50 °C. Afterward, the temperature was incremented at 50 °C per min to reach 150 °C, and then immediately at 30 °C per minute until it reached 270 °C, where it was held for 5 min. The parameters for MS analysis were as follows: EI (70 eV) temperature 200 °C, solvent cut time 6 min, scan 45–650 *m/z*. The identification was based on comparing a particular compound's mass spectra and retention time with the reference materials using the “Wiley regis-

try™ of mass spectral data” library. The quantitative analysis was performed using the internal standard (BPA-*d*<sub>16</sub>, IS), which was added to each sample in the same amount and considered the relative response of the analyte to the IS. The calibration curve, which was used for quantification, is described in the “linearity” section.

#### The validation of the method

The validation was performed by determining several important parameters, such as linearity, precision and trueness, limit of detection (*LOD*), and quantification (*LOQ*). Deionised water without adding BPA was analyzed as a blank sample before each analysis in order to track the residual amounts of BPA in solvents and the used reagent.

**Linearity.** The linearity of the method was determined by calibration curve construction. A series of dilutions (50, 100, 200, 400, 600 and 800 ng mL<sup>-1</sup>) were made from the working solution (2000 ng mL<sup>-1</sup>) to obtain a calibration curve with six different concentration levels in hexane: 0.1, 0.2, 0.4, 0.8, 1.2 and 1.6 ng μL<sup>-1</sup>. Each concentration level was analyzed in duplicate. In addition, lower concentrations were also analyzed (0.02 and 0.05 ng μL<sup>-1</sup>), in order to determine the *LOD* and *LOQ*. The calibration curve was formed based on the peak area ratio of the BPA and the BPA-*d*<sub>16</sub>. The internal standard was always added at the same concentration of 0.2 ng μL<sup>-1</sup> hexane. The linearity of the calibration curve was determined by the coefficient of determination (Table I). The obtained calibration curve was used for the quantification of BPA in water samples.

***LOD* and *LOQ*.** The quantification limit is presented as the lowest concentration that can be quantified with a precision lower than 5 %. The sample with the minimum concentration of 0.02 ng in 1 μL hexane was analyzed in six replicates and the standard deviation (*SD*) was calculated.

The detection limit was calculated according to the following equation:

$$LOD = X + \frac{3SD}{m} \quad (1)$$

where *X* is the average value of concentrations found in analyzed samples and *m* is the slope of a calibration curve.

The detection limit was calculated according to the following equation:

$$LOQ = X + \frac{10SD}{m} \quad (2)$$

The *LOQ* and *LOD* values are shown in Table I.

**Precision and trueness.** Trueness was proved by the spiking/recovery method. Precision was calculated as the relative standard deviation (*RSD*, %) of concentrations found after the repetition of spiking six times per day. The validation was performed in duplicate by spiking the deionised water samples (test portion 500 mL) with the BPA to obtain the following concentrations: 80, 120 and 160 ng L<sup>-1</sup>. The IS was added to each sample in the same concentration of 40 ng L<sup>-1</sup>. The amount of recovered BPA ranged between 72.5 and 82.5 wt. %, with a mean value of 77.5 wt. %, calculated based on the initial weight of BPA. The obtained results are given in Table I.

TABLE I. The validation parameters of the microextraction – GC–MS method for the analysis of BPA in water samples

| <i>m/z</i> | <i>R</i> <sup>2</sup> | Method trueness – recovery ± <i>RSD</i> , wt. % | <i>LOQ</i> / ng L <sup>-1</sup> | <i>LOD</i> / ng L <sup>-1</sup> |
|------------|-----------------------|---|---------------------------------|---------------------------------|
| 357/372    | 0.9982                | 77.50±5.42                                      | 10                              | 4                               |

## RESULTS AND DISCUSSION

The real water samples collected at the locations, as shown in Fig. S-1 of the Supplementary material, were tested to determine the content of BPA. After microextraction and derivatization processes, the prepared samples were analyzed by GC-MS technique. The qualitative analysis was performed using a characteristic retention time and at least two  $m/z$  values. The first, always required, was the basic ion. The second was the molecular ion or characteristic/reference ion of a given compound. The characteristic total ion chromatogram and mass spectra of identified silylated BPA and silylated BPA- $d_{16}$  for the sample T4 are presented in Fig. 1.

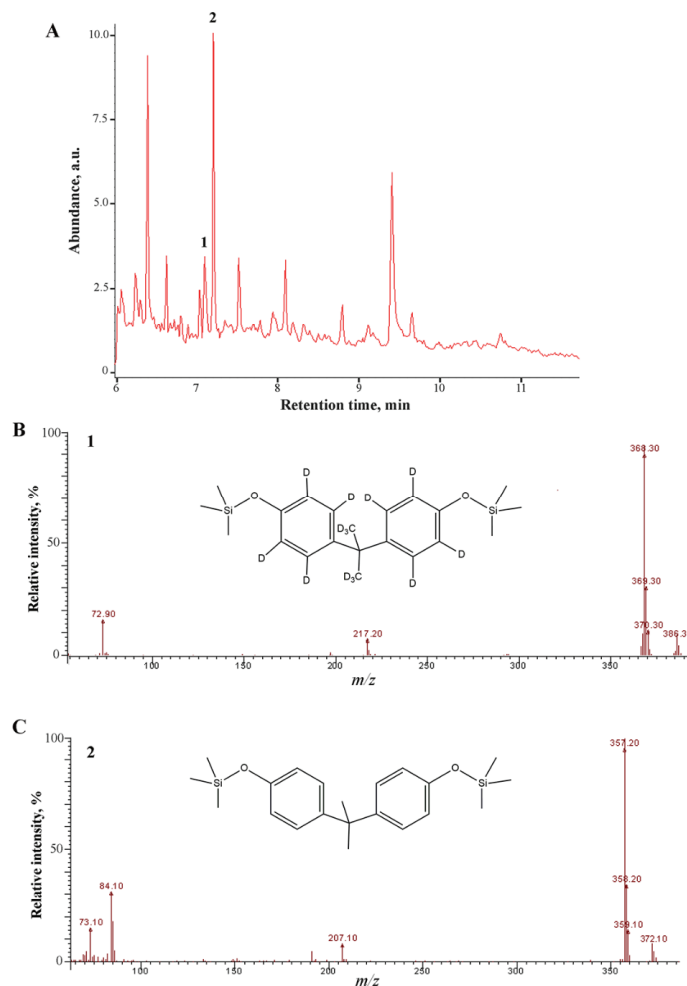


Fig. 1. The total ion chromatogram (A) and mass spectra of identified silylated BPA- $d_{16}$  (B) and silylated BPA (C) for the sample T4.

The main required ions used for the identification were 357 and 368 for silylated BPA and silylated BPA<sub>d</sub>, respectively. As a second characteristic ion, the molecular ion of a particular compound is generally sought, which was 372 (silylated BPA) and 386 (silylated BPA-*d*<sub>16</sub>).

The obtained results are shown in Table II. The mass of BPA (ng) in 1 µL hexane, which was injected in the GC column, was calculated using the calibration curve. The mass of BPA in 100 µL hexane was the same found in 500 mL of the initial sample before any treatment. It can be seen that the concentration of BPA in the investigated river samples ranged from 33 to 354 ng L<sup>-1</sup>. The highest concentration was measured in the samples collected at the mouth of the Crkvena into the Vrbas River (MT2). The lowest value of BPA was recorded in the sample taken at the location where the Švrakava River flows into the Vrbas upstream from the city (V1).

TABLE II. Results of GC-MS analysis of the water samples

| Sample | BPA concentration   |                    |
|--------|---------------------|--------------------|
|        | ng µL <sup>-1</sup> | ng L <sup>-1</sup> |
| T1     | 0.32                | 65                 |
| T2     | 0.34                | 69                 |
| T3     | 0.77                | 153                |
| T4     | 0.49                | 99                 |
| T5     | 0.96                | 193                |
| MT1    | 0.60                | 121                |
| MT2    | 1.77                | 354                |
| MT3    | 0.67                | 133                |
| V1     | 0.16                | 33                 |
| V2     | 0.42                | 84                 |
| V3     | 0.80                | 159                |
| V4     | 0.52                | 104                |

Additionally, it can be observed that in all analyzed samples, the BPA concentration was higher than the *LOQ* value, which was 0.06 ng µL<sup>-1</sup>. The obtained results indicated the contamination of the Vrbas River and its tributaries at all sampling sites.

The river Švrakava is a right tributary of the Vrbas, with the mouth around 15 km upstream from the city center, positioned in a relatively clean but populated area called Karanovac. It was not unexpected that the lowest BPA values were determined for the samples T1 and V1, although agricultural land and partly construction facilities are located immediately before the mouth along the riverbank. Both samples were clear, with no visible contaminants.

The course and the catchment area of the river Suturlja, which is about 17 km long, is located in the area southwest of Banja Luka. The river flows through a relatively uninhabited area, however, at the confluence into the Vrbas River in

Srpske Toplice, at the altitude of 159 m, it is under a certain anthropogenic factor. The mouth of the river Suturlija in the Vrbas is located just before the beginning of the inner city zone. The results show that the concentration of BPA in the sample taken at the mouth of the river Suturlija in the Vrbas (MT1) is two-fold higher than the concentration found in the sample taken in the river itself (T2). All samples taken in this area were clear, with no visible contaminants.

The Crkvena River, with its course of 11.5 km, flows through a very populated and active area. It finally flows into the Vrbas directly into the city centre and near the Kastel fortress. The last part of the stream, about 1.5 km long, is located in an underground tunnel under the road. This tunnel ends 100 m before the mouth of the Vrbas at the sewer in the central zone of Banja Luka. This could explain the high concentration of BPA recorded in the sample taken at the mouth of this river in the Vrbas (MT2), which is the highest value obtained in this study. The water samples taken from the Crkvena River were visibly polluted, turbid, and had an unpleasant odour.

The river Vrbanja is more than 90 km long and the largest tributary of the Vrbas. The river Vrbas upstream from the mouth of the Vrbanja is burdened with discharges. This could be why the higher measured concentration of BPA at the location V3, compared to the results obtained at locations T4 and MT3 (Table II). Furthermore, the Vrbanja samples were clear, with no visible contaminants. However, the sample of the Vrbas (V3) in this area was somewhat stained.

The source of the river Dragočajska is located on the hill Ruštevac. Its confluence into the Vrbas is near the settlement Zalužani. The length of the stream is about 21 km. In the middle and lower course, this river is of a flat character, with many tributaries. A significant part of the flow of this watercourse passes through a densely populated area and is under significant anthropogenic influence. The sample of the Dragočajska River was visibly polluted and turbid, while the sample of the Vrbas River (V4) was slightly stained. Moreover, at the time of sampling on the banks and in the river itself, the last few hundred meters before the mouth, plastic waste (bottles and bags) could be seen. The concentration of BPA in the Dragočajska sample was the highest (T5), which can be attributed to its position. In addition, it should be noted that one of the tributaries of the Dragočajska river (Ivaštanka) is located near the municipal landfill in Ramići, whose leachate could contribute to higher BPA value. It flows into the Vrbas about 9 km downstream from the central zone of the city of Banja Luka, which may explain the lower concentration of BPA in the sample of the Vrbas River in the zone downstream from the mouth (V4).

A study similar to ours, conducted in southern India, has shown that the BPA concentration ranged from 2.8 to 136 ng L<sup>-1</sup>, in the samples collected from three rivers (Kaveri, Vellar and Tamiraparani).<sup>31</sup> The values of BPA are comparable to those found in the Vrbas River area. In addition, in the study performed in the

Danube River (Serbia) and its tributaries the Tisa and the Sava, the BPA concentration varies from the area where the samples were taken.<sup>32</sup> Moreover, high amounts of BPA were detected near industrial zones (up to 338 ng L<sup>-1</sup>), which agrees with the result obtained in our study (sample MT2). On the other side, a much lower concentration was measured in the samples taken in the municipal areas ranging from 0.6 to 31.2 ng L<sup>-1</sup>. This finding confirms the observation obtained in our study that waste such as plastics and other contaminants could significantly impact the level of BPA in water resources. Furthermore, similar observation can be found in the study where sampling was performed from three wastewater treatment plants in Poland and municipal surface waters.<sup>33</sup> The obtained results have demonstrated extremely high concentration of BPA in wastewater (up to 1465 ng L<sup>-1</sup>), while this parameter was even higher in surface water (up to 3113 ng L<sup>-1</sup>), which is significantly higher than the concentrations found in surface water analyzed in this study.

#### CONCLUSION

The concentration of bisphenol A in the Vrbas River and its tributaries was examined by GC-MS technique. For that purpose, 15 samples were taken from three locations around 5 tributaries of the Vrbas River. The presence of BPA was detected in all analyzed samples, with the concentrations higher than the *LOQ* value. The highest BPA concentration was recorded at the mouth of the river Crkvena in the Vrbas River, where the Crkvena flows into the Vrbas direct to the city centre. On the other side, the lowest amount of BPA was found in the sample collected in the river Vrbas near Švrakava estuary upstream from the city of Banja Luka. This study indicates that population and human activity could influence the level of BPA in the environment and therefore the monitoring this compound is required. According to the legislation of the Western Balkan countries, the maximum permitted concentration of BPA is not defined. Thus, it is important to calculate the exposure rates of this pollutant as an endocrine-disrupting compound. Compared to the available literature data, the concentrations of BPA found in this study are not considered extremely hazardous to human health and the environment.

#### SUPPLEMENTARY MATERIAL

Additional data and information are available electronically at the pages of journal website: <https://www.shd-pub.org.rs/index.php/JSCS/article/view/11238>, or from the corresponding author on request.

*Acknowledgment.* This work was done within the agreement between the Faculty of Agriculture and the Ministry of Education, Science and Technological Development of the Republic of Serbia (Contract No: 451-03-9/2021-14/200116).

## ИЗВОД

## ОДРЕЂИВАЊЕ ТРАГОВА БИСФЕНОЛА А У УЗОРЦИМА ВОДЕ ИЗ РЕКЕ ВРБАС И ЊЕНИХ ПРИТОКА, БОСНА И ХЕРЦЕГОВИНА

ДАЈАНА САВИЋ<sup>1</sup>, МИЛИЦА БАЛАБАН<sup>2</sup>, НЕБОЈША ПАНТЕЛИЋ<sup>1</sup>, ДЕЈАНА Н. САВИЋ<sup>2</sup>, МАЛИША АНТИЋ<sup>1</sup>, РАДОСЛАВ ДЕКИЋ<sup>2</sup> и ВЕСНА АНТИЋ<sup>1</sup>

<sup>1</sup>Универзитет у Београду-Политехнички факултет, Немањина 6, Београд-Земун и <sup>2</sup>Универзитет у Бањој Луци, Природно-математички факултет, Младена Стојановића 2, Бања Лука, Босна и Херцеговина

Концентрација бисфенола А (BPA) одређена је у 12 узорака површинских вода реке Врбас и њених пет притока. Узорци су узети на подручју које припада граду Бања Лука (Босна и Херцеговина). BPA је изолован микро течно-течном екстракцијом, након чега је уследила дериватизација и гасно хроматографска-масено спектрометријска анализа (GC-MS). Силиловање је коришћено као метода дериватизације, како би се повећала испарљивост и омогућило GC-MS одређивање BPA. Границе детекције (*LOD*) и квантификације (*LOQ*), су утврђене валидацијом коришћене процедуре, и износиле су 4 и 10 ng L<sup>-1</sup>, редом. Концентрације BPA су се кретале између 33 и 354 ng L<sup>-1</sup>, и све су биле изнад вредности *LOQ*. Највиша количина BPA пронађена је у узорку узетом из реке Врбас код ушћа Шврнакаве, узводно од града Бања Лука. Највећа концентрација BPA забележена је на ушћу реке Црквене у Врбас, које се налази у центру града. Ова студија показује да би број становника и људска активност могли да утичу на ниво BPA у животној средини, па је стога потребно стално праћење концентрације овог једињења.

(Примљено 1. октобра, прихваћено 15. новембра 2021)

## REFERENCES

- P. Ascenzi, A. Bocedi, M. Marino, *Mol. Aspect. Med.* **27** (2006) 299 (<https://doi.org/10.1016/j.mam.2006.07.001>)
- M. M. Tabb, B. Blumberg, *Mol. Endocrinol.* **20** (2006) 475 (<https://doi.org/10.1210/me.2004-0513>)
- P. S. Bailin, M. Byrne, L. Sanford, R. Liroff, *Public Awareness Drives Market for Safer Alternatives: Bisphenol A Market Analysis Report*, New York, 2008
- C. Staples, P. Dome, G. Klecka, S. T. Oblock, *Chemosphere* **36** (1998) 2149 ([https://doi.org/10.1016/S0045-6535\(97\)10133-3](https://doi.org/10.1016/S0045-6535(97)10133-3))
- S. Biedermann, P. Tschudin, K. Grob, *Anal. Bioanal. Chem.* **398** (2010) 571 (<https://doi.org/10.1007/s00216-010-3936-9>)
- Y. Q. Huang, C. K. Wong, J. S. Zheng, H. Bouwman, R. Barra, B. Wahlström, L. Neretin, M. H. Wong, *Environ. Int.* **42** (2012) 91 (<http://dx.doi.org/10.1016/j.envint.2011.04.010>)
- L. N. Vandenberg, R. Hauser, M. Marcus, N. Olea, W. V. Welshons, *Reprod. Toxicol.* **24** (2007) 139 (<https://doi.org/10.1016/j.reprotox.2007.07.010>)
- I. Cousins, C. Staples, G. Klecka, D. Mackay, *Hum. Ecol. Risk Assess.* **8** (2002) 1107 (<https://doi.org/10.1080/1080-700291905846>)
- J. S. Ra, S. H. Lee, J. Lee, H. Y. Kim, B. J. Lim, S. H. Kim, S. D. Kim, *J. Environ. Monit.* **13** (2011) 101 (<https://doi.org/10.1039/C0EM00204F>)
- S. Mortazavi, A. R. Bakhtiari, A. E. Sari, N. Bahramifar, F. Rahbarizadeh, *Bull. Environ. Contam. Toxicol.* **90** (2013) 578 (<https://doi.org/10.1007/s00128-013-0964-0>)

11. L. N. Vandenberg, I. Chahoud, J. J. Heindel, V. Padmanabhan, F. J. R. Paumgartten, G. Schoenfelder, *Environ. Health Perspect.* **118** (2010) 1055 (<https://doi.org/10.1289/ehp.0901716>)
12. R. W. Stahlhut, W. V. Welshons, S. H. Swan, *Environ. Health Perspect.* **117** (2009) 784 (<https://doi.org/10.1289/ehp.0800376>)
13. R. Urbatzka, A. van Cauwenberge, S. Maggioni, L. Viganò, A. Mandich, E. Benfenati, I. Lutz, W. Kloas, *Chemosphere* **67** (2007) 1080 ([10.1016/j.chemosphere.2006.11.041](https://doi.org/10.1016/j.chemosphere.2006.11.041))
14. L. Pisapia, G. Del Pozzo, P. Barba, L. Caputo, L. Mita, E. Viggiano, G. L. Russo, C. Nicolucci, S. Rossi, U. Bencivenga, D. G. Mita, N. Diano, *Gen. Comp. Endocrinol.* **178** (2012) 54 (<https://doi.org/10.1016/j.ygcen.2012.04.005>)
15. R. Bhandari, J. Xiao, A. Shankar, *Am. J. Epidemiol.* **177** (2013) 1263 (<http://dx.doi.org/10.1093/aje/kws391>)
16. K. M. Donohue, R. L. Miller, M. S. Perzanowski, A. C. Just, L. A. Hoepner, S. Arunajadai, S. Arunajadai, S. Canfield, D. Resnick, A. M. Calafat, F. P. Perera, R. M. Whyatt, *J. Allergy Clin. Immunol.* **131** (2013) 736 (<http://dx.doi.org/10.1016/j.jaci.2012.12.1573>)
17. F. Perera, J. Vishnevetsky, J. B. Herbstman, A. M. Calafat, W. Xiong, V. Rauh, S. Wang, *Environ. Health Perspect.* **120** (2012) 1190 (<https://doi.org/10.1289/ehp.1104492>)
18. S. Flint, T. Markle, S. Thomson, E. Wallace, *J. Environ. Manage.* **104** (2012) 19 (<https://doi.org/10.1016/j.jenvman.2012.03.021>)
19. Government of Canada, *Chemical Substances: Bisphenol A*. Retrieved on October 15, 2011 (<http://www.chemicalsubstanceschimiques.gc.ca>)
20. French Republic, Law No. 2012-1442 for the Suspension of the Manufacture, Import, Export and Marketing of All-Purpose Food Packaging Containing Bisphenol A, *J. Off. Répub. Fran.*, JORF n° 0300:20395. ([https://www.legifrance.gouv.fr/eli/loi/2012/12/24/AFSX1240700L/jo/article\\_1](https://www.legifrance.gouv.fr/eli/loi/2012/12/24/AFSX1240700L/jo/article_1))
21. Commission Regulation (EU) 2018/213 of 12 February 2018 on the use of bisphenol A in varnishes and coatings intended to come into contact with food and amending Regulation (EU) No 10/2011 as regards the use of that substance in plastic food contact materials, *Off. J. Eur. Union*, L41/6-L41/12 (<https://eurlex.europa.eu/legalcontent/EN/TXT/PDF/?uri=CELEX:32018R0213&from=EN>)
22. EFSA CEF Panel on Food Contact Materials, Enzymes, Flavourings and Processing Aids, Scientific Opinion on the risks to public health related to the presence of bisphenol A (BPA) in foodstuffs: Executive summary, *EFSA J.* **13** (2015) 397 (<https://efsajournals.onlinelibrary.wiley.com/doi/pdf/10.2903/j.efsa.2015.3978>)
23. European Commission, European Commission Directive 2000/60/EC of the European Parliament and of the Council of 23 October 2000 establishing a framework for Community actions in the field of water policy, *Off. J. Eur. Union* **22** (2000) 1 (<http://data.europa.eu/eli/dir/2000/60/oj>)
24. European Commission, European Commission Directive 2008/105/EC of the European Parliament and of the Council of 16 December 2008 on environmental quality standards in the field of water policy, *Off. J. Eur. Union* **384** (2008) 84 (<http://data.europa.eu/eli/dir/2008/105/oj>)
25. H. M. Kuch, K. Ballschmiter, *Environ. Sci. Technol.* **35** (2001) 3201 (<http://dx.doi.org/10.1021/es010034m>)
26. M. Milanović, J. Sudji, N. Grujić Letić, J. Radonić, M. Turk Sekulić, M. Vojinović Miloradov, N. Milić, *J. Serb. Chem. Soc.* **80** (2016) 333 (<http://dx.doi.org/10.2298/JSC150721095M>)

27. O. Ballesteros , A. Zafra, A. Navalón , J. L. Vilchez, *J. Chromatogr., A* **1121** (2006) 154 (<https://doi.org/10.1016/j.chroma.2006.04.014>)
28. H. Fromme, T. Küchler, T. Otto, K. Pilz, J. Müller, A. Wenzel, *Water Res.* **36** (2002) 1429 ([https://doi.org/10.1016/S0043-1354\(01\)00367-0](https://doi.org/10.1016/S0043-1354(01)00367-0))
29. M. del Olmo, A. Zafra, A.B. Jurado, J.L. Vilchez, *Talanta* **50** (2000) 1141. ([https://doi.org/10.1016/S0039-9140\(99\)00176-9](https://doi.org/10.1016/S0039-9140(99)00176-9))
30. K. Szyrwińska, A. Kołodziejczak, I. Rykowska, W. Wasiak, J. Lulek, *Acta Chromatogr.* **18** (2007) 49. (<https://www.infona.pl/resource/bwmeta1.element.baztech-article-BAT8-0006-0019>)
31. K. K. Selvaraj, G. Shanmugam, S. Sampath, D. G. J. Larsson, B. R. Ramaswamy, *Ecotox. Environ. Safe.* **99** (2014) 13 (<http://dx.doi.org/10.1016/j.ecoenv.2013.09.006>)
32. M. Čelić, B. D. Škrbić, S. Insa, J. Živančev, M. Gros, M. Petrović, *Environ. Pollut.* **262** (2020) 114344 (<https://doi.org/10.1016/j.envpol.2020.114344>)
33. M. Caban, P. Stepnowski, *Environ. Sci. Pollut. R.* **27** (2020) 28829 (<https://doi.org/10.1007/s11356-020-09123-2>).



SUPPLEMENTARY MATERIAL TO  
**Determination of bisphenol A traces in water samples from the  
Vrbas River and its tributaries, Bosnia and Herzegovina**

DAJANA SAVIĆ<sup>1\*</sup>, MILICA BALABAN<sup>2</sup>, NEBOJŠA PANTELIĆ<sup>1</sup>, DEJANA N. SAVIĆ<sup>2</sup>,  
MALIŠA ANTIĆ<sup>1</sup>, RADOSLAV DEKIĆ<sup>2</sup> and VESNA ANTIĆ<sup>1</sup>

<sup>1</sup>University of Belgrade – Faculty of Agriculture, Nemanjina 6, Belgrade-Zemun, Serbia and

<sup>2</sup>University of Banja Luka, Faculty of Natural Sciences and Mathematics, Mladena  
Stojanovića 2, Banja Luka, Bosnia and Herzegovina

J. Serb. Chem. Soc. 87 (1) (2022) 109–119

DESCRIPTION OF THE SAMPLING SITES

The Vrbas is a river that springs below the mountain Zec, and after a 250 km long course, it flows into the river Sava near Srbac, at 96 m above elevation. The catchment area of this river is about 5,900 km<sup>2</sup>, and about 500 thousand inhabitants live on its banks.

In this paper, the water of five tributaries of the Vrbas, which flow into the Vrbas at different locations, was taken in the summer at low water levels in the area of the city of Banja Luka. Water samples were taken from the river Švrakava (it flows into the Vrbas upstream from the city), the rivers Suturlija, Crkvena and Vrbanja (they flow into the Vrbas in the city itself), and from the river Dragočajska, which flows into the Vrbas downstream from the city of Banja Luka. Water samples were also taken at the mouth of the tributaries to the Vrbas. In addition, river water samples taken from the Vrbas at locations which are 50–70 m downstream of the mouth of each of the Vrbas tributaries were analyzed. Fig. S-1 shows a map of Banja Luka's city and the Vrbas River's position and its tributaries with the sampling points. The tributaries are marked by a number denoting locations related to the Vrbas from south to north. The numbers from 1 to 5 denote Švrakava, Suturlija, Crkvena, Vrbanja, and Dragočajska River, respectively. Water samples taken from tributaries are designated as T1–T5, while water samples taken at the mouth of the tributary are designated as MT1–MT3. Water samples from the Vrbas River taken 50–70 m downstream from the mouth of the tributary are marked V1–V4.

\* Corresponding author. E-mail: dajana.savic@agrif.bg.ac.rs

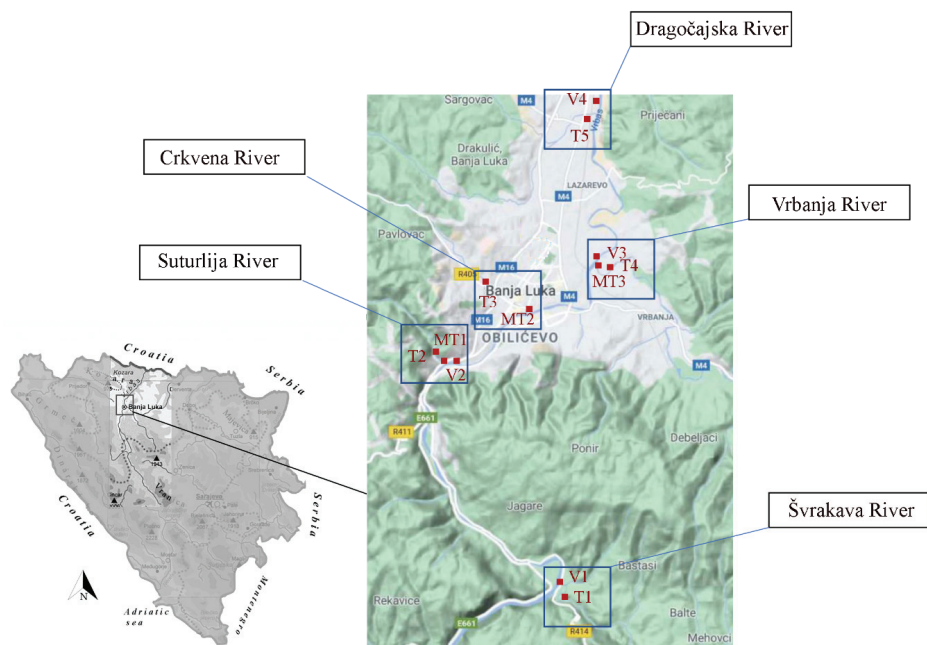


Fig. S-1. The river flow of Vrbas and five tributaries (Švrakava, Suturlja, Crkvena, Vrbanja, and Dragočajska) with indicated sampling locations of river water.





## Groundwater quality assessment of protected aquatic eco-systems in cross-border areas of Serbia and Croatia

BORIS B. OBROVSKI<sup>1</sup>, IVANA J. MIHAJLOVIĆ<sup>1\*</sup>, MIRJANA B. VOJNOVIĆ<sup>1</sup>, MILORADOVIĆ<sup>1#</sup>, MAJA M. SREMAČKI<sup>1</sup>, IVAN ŠPANIK<sup>2</sup> and MAJA Z. PETROVIĆ<sup>1</sup>

<sup>1</sup>University of Novi Sad, Faculty of Technical Sciences, Department of Environmental Engineering and Occupational Safety and Health, Trg Dositeja Obradovica 6, 21000 Novi Sad, Serbia and <sup>2</sup>Institute of Analytical Chemistry, Faculty of Chemical and Food Technology, STU, Radlinského 9, 81237 Bratislava, Slovakia

(Received 23 September, revised 6 December, accepted 7 December 2021)

**Abstract:** Research results define basis for specific monitoring programs of groundwater quality in wetland eco-systems in Serbia and Croatia. The main purpose of the research was to determine the impact of nonpoint diffuse source pollution on the groundwater quality, as well as seasonal variations on the concentration levels of selected physicochemical parameters. Statistical analyses, PCA, HCA, ANOVA and *t*-test, encompass 18 monitored parameters in groundwater. Statistical data indicated that protected area in Serbia has a significantly higher load of pollution from agricultural activities compared to Wetlands Tompojevci. The highest load in groundwater was detected from total nitrogen, ammonia and nitrogen anions, indicating contamination of groundwater by nitrogen-based fertilizers. The results obtained within the two-year seasonal monitoring program, from 2018 to 2020, are highly essential for achieving a comprehensive database that could be used as platform for high-quality groundwater management in selected protected areas with the aim of minimizing environmental pollution.

**Keywords:** sensitive water bodies; physicochemical parameters; monitoring; agricultural activities.

### INTRODUCTION

Environmental impact assessment (EIA) of protected areas is an imperative, particularly in the terms of groundwater quality, conservation of biodiversity, environmental sustainability and finally climate changes. Long-term anthropogenic pollution, as well as the changes within groundwater quality could be improved with data obtained by long-term monitoring programmes. The information

\* Corresponding author. E-mail: ivanamihajlovic@uns.ac.rs

# Serbian Chemical Society member.

<https://doi.org/10.2298/JSC210923107O>

on the groundwater quality in protected areas is sporadic and scarce. The lack of comprehensive and reliable data and databases on the current state of the groundwater quality in protected areas require development of specific monitoring programmes for minimization of groundwater and surrounding areas contamination.

Lakes and wetland areas are sensitive and vulnerable ecosystems where all human activities promptly affect groundwater contamination and quality.<sup>1,2</sup> Anthropogenic activities, such as agriculture, industry, urbanization and waste disposal, disturb and impair the natural aquatic ecosystems.<sup>3</sup> Groundwater contamination is attributed to nonpoint sources of contamination (excessive use of pesticides, mineral and natural fertilizers), adaptation of old wells into permeable septic tanks, unsanitary landfills, uncontrolled waste disposal and discharge of untreated wastewater.<sup>4–6</sup>

Temporal and spatial distribution of physicochemical pollutants, mainly nitrogen compounds is essential for evaluation of groundwater quality.<sup>7–9</sup> The uncontrolled urbanization in the vicinity of protected areas affect groundwater quality causing the contamination with nutrients from agriculture, waste disposal and discharge of untreated mixed urban wastewater.

Within the Interreg IPA CBC Croatia–Serbia Project Active sensor monitoring network and environmental evaluation for protection and wiSe use of wetlands and other surface waters – SeNs Wetlands, the groundwater quality in two cross-border protected areas, Lake Zobnatica, Serbia and Wetlands Tompojevci, Croatia, was investigated.<sup>10</sup> The two selected sites are within hydrological systems of watercourses recognised as ecological corridors. The Wetlands Tompojevci in Croatia has a direct influence on the quality of the Natura 2000 site. The Natura 2000 is the largest coordinated network of protected areas in the world that has the aim to ensure the long-term survival of Europe's most valuable and threatened species and habitats.<sup>11</sup> The protected area of the national Nature Park of Lake Zobnatica, Serbia, is environmentally interconnected with the Tompojevci Wetlands, indirectly linked to the Natura 2000 Network. Recognized protected ecosystems have similar and comparative characteristic – urban settlements around the water body, agricultural land in the close proximity of water bodies with the same types of crops (wheat, corn and sunflower), connection to the Danube River and Sava River Basin, and unevolved management and protection of sensitive aquatic systems.<sup>12</sup> Throughout the two years monitoring period (2018–2020), physicochemical parameters that affect the quality of the groundwater in protected areas were monitored – pH, electrical conductivity ( $\sigma$ ), dissolved oxygen (DO), chemical oxygen demand (COD), orthophosphate, nitrite, nitrate, ammonia, total nitrogen ( $N_{tot}$ ), sulfate, chloride, fluoride, total chlorine ( $Cl_{tot}$ ), chromium (VI), nickel, iron, zinc and copper ions.

The aim of this research paper is to identify the sources of groundwater contamination in cross-border protected areas.

To reduce the volume of collected data the multivariate statistical analysis was applied, extracting the data relevant for EIA. Seasonal variations of the parameter concentration levels in groundwater and long-term groundwater pollution were also assessed. The results of this study can provide successful design and application of protective measures on the specific environmental problems and weak points in protected areas and sensitive water bodies.

The operative groundwater protective measures considered in selected protected areas are development and maintenance of multifunctional vegetation belt (vegetation that have a potential of sorption of pollutants); optimization of chemicals used for fertilization and pest control (fertilizers, pesticides, herbicides, etc.); and recommendations for water control and management in the vicinity of the sensitive aquatic systems.

This type of research was initiated and conducted for the first time on sensitive cross-border protected areas in Western Balkan Region, as one of planned objectives within the Interreg IPA Project SeNs Wetlands.

#### EXPERIMENTAL

Details related to the sampling sites are given in the Supplementary material to this paper.

Samples were collected with mechanical bailer than transferred into 1 L bottles. After proper collection, the samples were stored in refrigerator at 4 °C, and transported to the laboratory for analyses. The sampling procedure was conducted according to the Standards SRPS EN ISO 5667-1:2008 (Guidelines for development of sampling programs), SRPS EN ISO 5667-3:2007 (Guidelines for protection and handling of the sample), SRPS EN ISO 5667-11:2005 (Guidance on sampling of groundwater).

Measurement of pH, dissolved oxygen and electrical conductivity was performed *in-situ* via a multiparameter device using standard EPA methods (EPA 150.1, EPA 360.1, EPA 120.1).

Orthophosphates were prepared and analysed by standard EPA method (EPA 365.3), while chemical oxygen demand, nitrite, nitrate, sulphate, chloride, fluoride, ammonium ions, total nitrogen and total chlorine were measured according HACH methods (LCI 500, HACH 8507, HACH 8192, HACH 8155, HACH 10208, HACH 8051, HACH 8113, HACH 8029 and HACH 8167, respectively). Metal ions chromium (VI), nickel, iron, zinc and copper were also analysed according to HACH methods (HACH 8023, Method 8150, Method 8146, Method 8009 and Method 8143, respectively). The concentrations of selected parameters were measured in the laboratory by UV–Vis spectrophotometer (DR 5000, HACH, Germany). The measurements were performed on maximum wavelengths suggested in EPA and HACH methods based on Standard Methods for the Examination of Water and Wastewater.<sup>13</sup> The recoveries were carried out by the addition of the standards of each element at different levels. Recoveries ranged from 89 to 97 %. Blanks were included in each batch of analysis. Calibration curves for the determination of selected parameters were processed with different dilutions of the standard stock solutions. The linear regression lines were acquired with correlation coefficient value of more than 0.9.

The IBM Statistical Package of Social Science (SPSS) software package version 25 was used for statistical data analyses. Descriptive statistic, principal component analyses (PCA), hierarchical cluster analyses (HCA), one-way ANOVA and independent sample *t*-test were performed for the purpose of data evaluation. A statistical analysis was applied for deter-

mining the basic aggregated functions (mean, minimum and maximum) of the observed physicochemical parameters. PCA was used to extract the relevant data and determine the most polluted locations of protected areas, Lake Zobnatica and Wetlands Tompojevci. One-way ANOVA was applied to detect the effect of seasonal variations on the concentration levels of physicochemical parameters in analysed samples of groundwater. Independent sample *t*-test was used to compare the cumulative groundwater pollution between the two observed cross-border protected areas.

#### RESULTS AND DISCUSSION

Within two-year monitoring programme (2018–2020), eighteen physicochemical parameters in the vicinity of Lake Zobnatica and Wetlands Tompojevci were investigated in groundwater. Statistical analysis was used to determine mean and the range for all physicochemical parameters (Table I).

TABLE I. Statistical results for analysed parameters in groundwater; COD: chemical oxygen demand; DO: dissolved oxygen; N<sub>tot</sub>: total nitrogen; Cl<sub>tot</sub>: total chloride; TV: threshold value from Croatian legislation; SD: standard deviation

| Parameter   | Zobnatica Lake      |       |       | Wetlands Tompojevci |       | TV    |
|---|---------------------|-------|-------|---------------------|-------|-------|
|   | Mean $\pm$ SD       | Min.  | Max.  | Mean $\pm$ SD       | Min.  |       |
| pH  | 7.77 $\pm$ 0.461    | 6.95  | 9.14  | 7.82 $\pm$ 0.95     | 6.961 | 12.8  |
| $\sigma$ / $\mu$ S cm <sup>-1</sup>                   | 1016 $\pm$ 319.45   | 477   | 1728  | 858.71 $\pm$ 253.3  | 248   | 1442  |
| c <sub>O<sub>2</sub></sub> / mg L <sup>-1</sup> (DO)  | 5.01 $\pm$ 1.287    | 0.8   | 7.53  | 4.48 $\pm$ 1.789    | 0.1   | 9     |
| c <sub>PO<sub>4</sub>3-</sub> / mg L <sup>-1</sup>    | 0.469 $\pm$ 0.788   | 0.005 | 4.075 | 0.942 $\pm$ 1.587   | 0.005 | 9.741 |
| c <sub>NO<sub>2</sub>-</sub> / mg L <sup>-1</sup>     | 0.076 $\pm$ 0.149   | 0.001 | 0.628 | 0.028 $\pm$ 0.052   | 0.001 | 0.291 |
| c <sub>NO<sub>3</sub>-</sub> / mg L <sup>-1</sup>     | 0.965 $\pm$ 0.971   | 0.01  | 4.52  | 0.34 $\pm$ 0.632    | 0.01  | 2.73  |
| c <sub>NH<sub>4</sub>+</sub> / mg L <sup>-1</sup>     | 0.119 $\pm$ 0.285   | 0.005 | 1.51  | 0.837 $\pm$ 1.152   | 0.005 | 3.88  |
| c <sub>SO<sub>4</sub>2-</sub> / mg L <sup>-1</sup>    | 46.17 $\pm$ 28.4    | 1     | 85    | 24.13 $\pm$ 27.57   | 1     | 98    |
| c <sub>Cl-</sub> / mg L <sup>-1</sup>                 | 43.22 $\pm$ 42.15   | 0.05  | 232.8 | 14.06 $\pm$ 10.93   | 0.6   | 45.4  |
| c <sub>F-</sub> / mg L <sup>-1</sup>                  | 0.25 $\pm$ 0.367    | 0.01  | 2.56  | 0.58 $\pm$ 0.872    | 0.01  | 4.32  |
| c <sub>Cl<sub>tot</sub></sub> / mg L <sup>-1</sup>    | 0.033 $\pm$ 0.039   | 0.01  | 0.16  | 0.116 $\pm$ 0.152   | 0.01  | 0.45  |
| c <sub>Cr<sup>6+</sup></sub> / mg L <sup>-1</sup>     | 0.0131 $\pm$ 0.2    | 0.005 | 0.11  | 0.066 $\pm$ 0.148   | 0.04  | 0.743 |
| c <sub>N<sub>tot</sub></sub> / mg L <sup>-1</sup>     | 12.06 $\pm$ 14.577  | 0.5   | 76.23 | 7.08 $\pm$ 10.3     | 0.5   | 46.99 |
| c <sub>Ni</sub> / mg L <sup>-1</sup>                  | 0.0054 $\pm$ 0.014  | 0.003 | 0.112 | 0.009 $\pm$ 0.013   | 0.003 | 0.062 |
| c <sub>Fe</sub> / mg L <sup>-1</sup>                  | 0.113 $\pm$ 0.14    | 0.01  | 0.88  | 0.486 $\pm$ 0.65    | 0.01  | 2.92  |
| c <sub>Zn</sub> / mg L <sup>-1</sup>                  | 0.455 $\pm$ 0.355   | 0.005 | 1.53  | 0.466 $\pm$ 0.31    | 0.01  | 1.31  |
| c <sub>Cu</sub> / mg L <sup>-1</sup>                  | 4.476 $\pm$ 7.16    | 0.5   | 35    | 8.15 $\pm$ 11.96    | 0.5   | 50    |
| c <sub>O<sub>2</sub></sub> / mg L <sup>-1</sup> (COD) | 17.843 $\pm$ 29.859 | 0     | 155   | 30.61 $\pm$ 35.15   | 0.137 | 170   |

According to the Groundwater Quality Standards (GWQS) of the respective national legislation (Official Gazette no. 50/2012 for Serbia and Official Gazette no. 96/19 for Croatia) and EU Groundwater Directive (GWD) 2006/118/EC, nitrates are set as definitive parameter for monitoring of groundwater pollution with threshold value of 50 mg L<sup>-1</sup>. In Serbian legislation, nitrates are also determined as key parameter; however, the threshold value of 50 mg L<sup>-1</sup> is determined as annual average concentration.

Furthermore, the other significant parameter is stated as active component of pesticides, their metabolites and products of degradation and chemical reaction, with threshold value of  $0.1 \mu\text{g L}^{-1}$ , with total concentration of all detected and quantified pesticides no higher than  $0.5 \mu\text{g L}^{-1}$ .

The EU GWD is stating that EU member states have to develop threshold values for arsenic, cadmium, lead, mercury, ammonia, chloride, sulphate, trichloroethylene, tetrachloroethylene and electrical conductivity, and if necessary to expand the list. The defined threshold values from Croatian By-Law are stated in the Table I. In Serbian By-Law, other pollutant are only listed (Lists I and II) without defined threshold values: organic compounds of halogens, phosphorus; oils and hydrocarbons; metals, metalloids and their compounds; cyanides; biocides and derivate; ammonia, fluorides, inorganic compounds of phosphorus and other.

Comparing the results in Table I and requirements of respective national legislation (Official Gazette of the RS 50/2012 for Serbia and Official Gazette no. 96/19 for Croatia), it was concluded that following parameters can be excluded from further analyses: pH, total chlorine and fluoride (as parameters that are not listed for assessment of groundwater quality status in legislation), cations of nickel, chromium and copper (the low concentrations were found to be insignificant for this research).

Correlation analysis was used to classify the strength of relationships between parameters (Table II).

TABLE II. Correlation coefficient values for the observed parameters;  $\text{N}_{\text{tot}}$  – total nitrogen; A – Serbia, Zobnatica lake; B – Croatia, Wetlands Tompojevci

| Parameter | B                           |                             |                        |                   |                   |                     |                        |                   |                             |                   |                   |                             |       |
|-----------|-----------------------------|-----------------------------|------------------------|-------------------|-------------------|---------------------|------------------------|-------------------|-----------------------------|-------------------|-------------------|-----------------------------|-------|
|           | $\sigma$                    | $c_{\text{O}_2}^{\text{a}}$ | $c_{\text{PO}_4^{3-}}$ | $c_{\text{NO}_2}$ | $c_{\text{NO}_3}$ | $c_{\text{NH}_4^+}$ | $c_{\text{SO}_4^{2-}}$ | $c_{\text{Cl}^-}$ | $c_{\text{N}_{\text{tot}}}$ | $c_{\text{Fe}}$   | $c_{\text{Zn}}$   | $c_{\text{O}_2}^{\text{b}}$ |       |
|           | $\mu\text{S cm}^{-1}$       | $\text{mg L}^{-1}$          |                        |                   |                   |                     |                        |                   |                             |                   |                   |                             |       |
| A         | $\sigma$                    | 1                           | -0.23                  | 0.26              | -0.47             | -0.58 <sup>a</sup>  | 0.11                   | -0.24             | 0.21                        | -0.13             | 0.39              | 0.18                        | -0.07 |
|           | $c_{\text{O}_2}^{\text{a}}$ | -0.24                       | 1                      | -0.16             | 0.24              | 0.07                | -0.16                  | 0.16              | -0.14                       | -0.06             | -0.28             | -0.28                       | -0.33 |
|           | $c_{\text{PO}_4^{3-}}$      | -0.09                       | -0.16                  | 1                 | -0.31             | -0.09               | 0.13                   | -0.1              | 0.02                        | 0.11              | 0.07              | 0.24                        | 0.14  |
|           | $c_{\text{NO}_2}$           | 0.39                        | -0.25                  | 0.01              | 1                 | 0.79 <sup>a</sup>   | -0.09                  | 0.48              | -0.08                       | 0.11              | -0.17             | -0.22                       | -0.14 |
|           | $c_{\text{NO}_3}$           | 0.08                        | 0.29                   | -0.23             | -0.01             | 1                   | -0.17                  | 0.41              | -0.24                       | 0.11              | -0.19             | -0.13                       | -0.13 |
|           | $c_{\text{NH}_4^+}$         | -0.1                        | -0.35                  | 0.20              | 0.03              | -0.15               | 1                      | -0.24             | 0.17                        | 0.77 <sup>a</sup> | 0.54 <sup>a</sup> | 0.34                        | 0.42  |
|           | $c_{\text{SO}_4^{2-}}$      | -0.01                       | 0.34                   | -0.27             | -0.14             | 0.59 <sup>a</sup>   | -0.26                  | 1                 | -0.19                       | -0.22             | -0.34             | -0.17                       | -0.13 |
|           | $c_{\text{Cl}^-}$           | 0.10                        | -0.01                  | -0.20             | -0.16             | 0.30                | 0.10                   | 0.27              | 1                           | -0.03             | 0.63 <sup>a</sup> | 0.13                        | 0.37  |
|           | $c_{\text{N}_{\text{tot}}}$ | -0.01                       | 0.31                   | -0.20             | -0.16             | 0.47                | -0.16                  | 0.35              | 0.20                        | 1                 | 0.27              | 0.19                        | 0.32  |
|           | $c_{\text{Fe}}$             | 0.11                        | -0.42                  | 0.37              | 0.13              | -0.27               | 0.51 <sup>a</sup>      | -0.37             | -0.13                       | -0.18             | 1                 | 0.27                        | 0.26  |
|           | $c_{\text{Zn}}$             | -0.01                       | -0.06                  | 0.08              | -0.11             | 0.23                | 0.12                   | 0.29              | 0.13                        | 0.15              | 0.21              | 1                           | 0.2   |
|           | $c_{\text{O}_2}^{\text{b}}$ | 0.22                        | -0.18                  | 0.05              | 0.64 <sup>a</sup> | -0.28               | -0.09                  | -0.15             | -0.26                       | -0.15             | 0.17              | -0.33                       | 1     |

<sup>a</sup>DO – dissolved oxygen; <sup>b</sup>COD – chemical oxygen demand

Based on the correlation coefficient, it was concluded that there is a high positive correlation between nitrate and sulphate ions ( $r = 0.59$ ), nitrite and chemical

oxygen demand ( $r = 0.64$ ), as well as ammonia and iron ions ( $r = 0.51$ ) in groundwater in Zobnatica, Serbia. Samples from Croatia revealed a significant positive correlation between nitrite and nitrate ( $r = 0.79$ ), total nitrogen and ammonia ion ( $r = 0.77$ ), ammonia and iron ions ( $r = 0.54$ ), iron and chloride ions ( $r = 0.63$ ); and negative correlation between electrical conductivity and nitrate ( $r = -0.58$ ).

Elevated concentration levels of nitrates in groundwater can be explained by the widespread use of nitrogen-based fertilizers in agriculture and atmospheric deposition, whereas sulphate groundwater pollution can be explained by atmospheric deposition, geothermal processes, and mineral dissolution and precipitation processes.<sup>14</sup> The product of nitrogen-based fertilizers decomposition is ammonia, enabling infiltration and migration of ammonia into the groundwater through the permeable soil. Iron naturally occurs in groundwater as a result of mineral dissolution processes in the soil.<sup>15</sup>

Principal component analyses (PCA) was applied to minimize the volume and abundance of data by extracting the key physicochemical parameters for monitoring and evaluation of groundwater quality. Kaiser's coefficient for overall measure of sample adequacy is 0.61 (Zobnatica Lake) and 0.60 (Wetlands Tompojevci) and Bartlett's test of sphericity ( $p < 0.05$ ) indicate that the data are appropriate for the PCA. The scree diagram, as graphical tool, was used to determine the number of significant factors in PCA. To interpret the scree plot it is necessary to identify the scree point, the point at which the curve sharply changes shape and direction (Fig. S-2 of the Supplementary material). The number of significant factors contributing the most to total variance is the number of points which are equal to or above the scree point. The scree plots (Fig. S-2) derived from PCA indicate that two factor score (Zobnatica Lake) and three factor score (Wetlands Tompojevci) are suitable for examined data. Significant factors were adopted to clarify groundwater quality status. Following the selection of significant factors, varimax rotation was used to redistributing the influence of factors from the main factor (Table III).

Measure of sampling adequacy (MSA) of 0.5 and greater was used to quantify the correlation of physicochemical parameters and for factor analysis confirmation (Table IV).

Two significant factors for Zobnatica Lake explained 42.786 % of total variance, while three significant factors for Wetlands Tompojevci explained 57.731 % of the total variance pointing groundwater pollution.

In Factor 1, nitrate, sulphate, iron and zinc ions were isolated as significant parameters for Zobnatica Lake, while electrical conductivity, nitrite, nitrate and sulphate were isolated for Wetlands Tompojevci. Nitrate and sulphate as the key parameters for assessment of groundwater pollution, overlap in cross-border areas for Factor 1. The main source of nitrate in groundwater is treatment of wheat, corn, and sunflower with fertilizer such as potassium nitrate ( $\text{KNO}_3$  – 13 % nitrogen),

urea-carbamide, uric acid ( $\text{CO}(\text{NH}_2)_2$  – 46 % nitrogen) and ammonium nitrate ( $\text{NH}_4\text{NO}_3$  – 33–34 % nitrogen), while main source of groundwater contamination with sulphate are natural phenomena such as atmospheric deposition, geothermal processes and mineral dissolution and precipitation processes. Based on the obtained results Factor 1 is interpreted as “contamination of groundwater by nitrate-based fertilizers”.

TABLE III. Factor loading of variables obtained by principal component analysis (PCA); DO: dissolved oxygen;  $N_{\text{tot}}$ : total nitrogen; COD: chemical oxygen demand;  $\lambda$ : eigenvalue;  $Var(X)$ : variance;  $Var(X)_c$ : cumulative variance; PC – principal component

| Parameter                               | Component          |                     |                     |                    |                    |
|---|--------------------|---------------------|---------------------|--------------------|--------------------|
|   | Zobnatica Lake     |                     | Wetlands Tompojevci |                    |                    |
|   | PC1                | PC2                 | PC1                 | PC2                | PC3                |
| $\sigma/\mu\text{S cm}^{-1}$            | 0.095              | 0.121               | -0.653 <sup>a</sup> | -0.197             | 0.204              |
| $c_{\text{O}_2}/\text{mg L}^{-1}$ (DO)  | 0.355              | -0.613 <sup>a</sup> | 0.079               | -0.005             | -0.294             |
| $c_{\text{PO}_4^{3-}}/\text{mg L}^{-1}$ | -0.087             | 0.444               | -0.043              | 0.045              | -0.107             |
| $c_{\text{NO}_2^-}/\text{mg L}^{-1}$    | -0.051             | 0.053               | 0.890 <sup>a</sup>  | 0.017              | 0.001              |
| $c_{\text{NO}_3^-}/\text{mg L}^{-1}$    | 0.791 <sup>a</sup> | -0.141              | 0.901 <sup>a</sup>  | 0.026              | -0.106             |
| $c_{\text{NH}_4^+}/\text{mg L}^{-1}$    | -0.194             | 0.733 <sup>a</sup>  | -0.129              | 0.864 <sup>a</sup> | 0.250              |
| $c_{\text{SO}_4^{2-}}/\text{mg L}^{-1}$ | 0.745 <sup>a</sup> | -0.271              | 0.630 <sup>a</sup>  | -0.338             | -0.121             |
| $c_{\text{Cl}^-}/\text{mg L}^{-1}$      | 0.233              | 0.137               | -0.110              | -0.046             | 0.916 <sup>a</sup> |
| $c_{\text{Ntot}}/\text{mg L}^{-1}$      | -0.131             | 0.784 <sup>a</sup>  | 0.097               | 0.934 <sup>a</sup> | -0.008             |
| $c_{\text{Fe}}/\text{mg L}^{-1}$        | 0.610 <sup>a</sup> | 0.509 <sup>a</sup>  | -0.229              | 0.308              | 0.769 <sup>a</sup> |
| $c_{\text{Zn}}/\text{mg L}^{-1}$        | 0.648 <sup>a</sup> | -0.186              | -0.155              | 0.261              | 0.084              |
| $c_{\text{O}_2}/\text{mg L}^{-1}$ (COD) | -0.254             | -0.128              | 0.024               | 0.398              | 0.457              |
| $\lambda$                               | 2.950              | 2.184               | 2.676               | 2.271              | 1.980              |
| $Var(X)/\%$                             | 24.586             | 18.200              | 22.299              | 18.929             | 16.503             |
| $Var(X)_c/\%$                           | 24.586             | 42.786              | 22.299              | 41.228             | 57.731             |

<sup>a</sup>MSA at the level  $\geq 0.5$

TABLE IV. Comparison of seasonal variations for Zobnatica Lake; DO: dissolved oxygen;  $N_{\text{tot}}$ : total nitrogen; SD: standard deviation

| Parameter                               | Spring            | Summer            | Autumn            | Winter            | <i>p</i> -value      |
|---|-------------------|-------------------|-------------------|-------------------|----------------------|
|   | Mean $\pm$ SD     |                   |                   |                   |                      |
| $c_{\text{O}_2}/\text{mg L}^{-1}$ (DO)  | 5.84 $\pm$ 0.58   | 4.65 $\pm$ 1.53   | 4.17 $\pm$ 1.03   | 5.28 $\pm$ 1.12   | <0.0005 <sup>a</sup> |
| $c_{\text{NO}_3^-}/\text{mg L}^{-1}$    | 0.92 $\pm$ 1.05   | 0.704 $\pm$ 0.62  | 1.18 $\pm$ 0.89   | 1.4 $\pm$ 1.49    | 0.25                 |
| $c_{\text{NH}_4^+}/\text{mg L}^{-1}$    | 0.09 $\pm$ 0.135  | 0.068 $\pm$ 0.091 | 0.264 $\pm$ 0.52  | 0.033 $\pm$ 0.026 | 0.124                |
| $c_{\text{Ntot}}/\text{mg L}^{-1}$      | 34.17 $\pm$ 24.32 | 6.21 $\pm$ 7.94   | 7.73 $\pm$ 4.98   | 13.09 $\pm$ 9.46  | 0.178                |
| $c_{\text{SO}_4^{2-}}/\text{mg L}^{-1}$ | 52.62 $\pm$ 22.47 | 36.65 $\pm$ 31.41 | 47.31 $\pm$ 28.81 | 58.37 $\pm$ 24.79 | <0.0005 <sup>a</sup> |
| $c_{\text{Fe}}/\text{mg L}^{-1}$        | 0.065 $\pm$ 0.052 | 0.14 $\pm$ 0.085  | 0.132 $\pm$ 0.225 | 0.111 $\pm$ 0.16  | 0.391                |
| $c_{\text{Zn}}/\text{mg L}^{-1}$        | 0.603 $\pm$ 0.288 | 0.296 $\pm$ 0.376 | 0.544 $\pm$ 0.387 | 0.435 $\pm$ 0.147 | 0.035 <sup>a</sup>   |

<sup>a</sup>Statistical significance at the level of 0.05

In Factor 2, dissolved oxygen, ammonium ion, total nitrogen and iron ion were isolated as significant parameters for Zobnatica Lake, while ammonium ion and total nitrogen were isolated for Wetlands Tompojevci. Ammonium ion and

total nitrogen overlap in Factor 2 which could lead to the conclusion that the main potential source is treatment of surrounding agricultural soil with ammonium phosphate ( $(\text{NH}_4)_3\text{PO}_4$  – 11 % nitrogen and 52 % phosphorus), ammonium nitrate and nitrogen–phosphorus–potassium (NPP, 15 % N, 15 % P and 15 % Na). Based on the obtained results Factor 2 could be interpreted as “contamination of groundwater by ammonia-based fertilizers”.

Factor 3 for Wetlands Tompojevci isolated iron and chloride ions as significant parameters and could be interpreted as “infiltration processes and dissolution of minerals and rocks” since iron and chloride ions reach groundwater naturally by infiltration from soil.<sup>15,16</sup>

Based on the conducted PCA, it can be concluded that the main sources of groundwater pollution are agricultural activities (use of nitrogen-based fertilizers as the most dominant factor, F1), which corresponds to the fact that wheat, corn, and sunflower are grown on the studied area.

The most polluted locations were investigated using hierarchical cluster analysis (HCA) in respect to observed selected parameters in groundwater. From Fig. S-3 of the Supplementary material it can be concluded that the piezometers B3, B7, B1, B4 and B8 were in the separate cluster due to the lowest concentration level of physicochemical parameters (Table S-II of the Supplementary material). Locations B2 and B5 were isolated in the second cluster, as the most polluted sites and differ from other piezometers in groundwater quality, as a consequence of the high concentrations of nitrates, sulphates, chloride ions and total nitrogen for the Lake Zobnatica (Table S-II). Locations P2 and P8 in Wetlands Tompojevci (Fig. S-3) were grouped in a specific cluster and correspond to the most polluted sampling areas. Concentrations of nitrite, nitrate and total nitrogen are highly elevated on these locations compared to other locations (Table S-III of the Supplementary material). Locations P4, P5, P3, P7, P1, P6 and P8 are in second cluster which correspond to low groundwater pollution.

Seasonal variations on concentration levels for selected parameters extracted by PCA were assessed within research activities. One-way ANOVA test was used to examine differences in concentration levels of physicochemical parameters in relation to seasonal variations. Four groups of parameters were compared, arranged by seasons. Statistically significant differences in seasonal concentration levels were determined for dissolved oxygen, sulfate and zinc ions (Zobnatica Lake) and chloride ion (Wetlands Tompojevci), Tables IV and V.

Dissolved oxygen is an important parameter to consider when assessing quality of every water type and it is a highly sensitive factor in terms of seasonal variations and other prevailing conditions. The predominant part of groundwater recharge process is in the winter-spring period and higher concentrations of dissolved oxygen in groundwater are observed in winter, as the solubility of oxygen is lower in water with higher temperature. The lower concentration of dis-

solved oxygen in groundwater can also be the consequence of the intensified oxidation and reduction processes of organic and inorganic pollutants.<sup>17,18</sup>

TABLE V. Comparison of seasonal variations for Wetlands Tompojevci; N<sub>tot</sub>: total nitrogen; SD: standard deviation

| Parameter                                 | Spring        | Summer       | Autumn        | Winter        | <i>p</i> -value      |
|---|---------------|--------------|---------------|---------------|----------------------|
|   | Mean ± SD     |              |               |               |                      |
| $\sigma / \mu\text{S cm}^{-1}$            | 900.56±260.18 | 912.42±226.6 | 798.14±306.18 | 820.46±220.42 | 0.541                |
| $c_{\text{NO}_2^-} / \text{mg L}^{-1}$    | 0.032±0.027   | 0.02±0.035   | 0.033±0.075   | 0.03±0.053    | 0.923                |
| $c_{\text{NO}_3^-} / \text{mg L}^{-1}$    | 0.432±0.812   | 0.425±0.628  | 0.208±0.49    | 0.242±0.49    | 0.72                 |
| $c_{\text{NH}_4^+} / \text{mg L}^{-1}$    | 0.571±1.01    | 0.991±1.24   | 0.8±1.16      | 0.9±1.26      | 0.878                |
| $c_{\text{Ntot}} / \text{mg L}^{-1}$      | 6.31±16.43    | 6.55±5.69    | 7.24±7.07     | 7.96±11.96    | 0.403                |
| $c_{\text{SO}_4^{2-}} / \text{mg L}^{-1}$ | 30.12±26.78   | 30.07±33.65  | 13.85±19.74   | 25.75±28.25   | 0.99                 |
| $c_{\text{Fe}} / \text{mg L}^{-1}$        | 0.121±0.067   | 0.464±0.73   | 0.72±0.81     | 0.483±0.34    | 0.229                |
| $c_{\text{Cl}^-} / \text{mg L}^{-1}$      | 10.15±4.28    | 5.4±4.38     | 21.62±12.73   | 19.9±7.71     | <0.0005 <sup>a</sup> |

<sup>a</sup>Statistical significance at the level of 0.05

The concentration of sulphate anion is the highest in spring and late autumn, when agricultural land is treated with fertilizers and fungicides. In autumn, the concentration of sulphate anion increases in comparison to the summer due to higher precipitation, which increases soil erosion. Chloride anions occur naturally in groundwater by dissolution of minerals and their concentration depends on atmospheric deposition.<sup>16</sup> Chloride anions concentration is directly correlated to the atmospheric precipitation, when the precipitation is lowest, in summer months, the concentration levels of chlorides is lower and inversely.

Independent sample *t*-test was used to examine difference in concentration of parameters between two compared groups, Zobnatica Lake and Wetlands Tompojevci. There is a statistically significant difference between the groundwater quality of two observed protected areas for the concentration levels of nitrite, nitrate, ammonia, sulphate and iron ions (Table VI).

TABLE VI. Comparison of physicochemical parameters in groundwater by locations; N<sub>tot</sub>: total nitrogen; SD: standard deviation

| Parameter                                 | Zobnatica Lake | Wetlands Tompojevci | <i>p</i> -value      |
|---|----------------|---------------------|----------------------|
|   | Mean ± SD      |                     |                      |
| $c_{\text{NO}_2^-} / \text{mg L}^{-1}$    | 0.076±0.149    | 0.028±0.052         | 0.021 <sup>a</sup>   |
| $c_{\text{NO}_3^-} / \text{mg L}^{-1}$    | 0.965±0.971    | 0.34±0.632          | <0.0005 <sup>a</sup> |
| $c_{\text{NH}_4^+} / \text{mg L}^{-1}$    | 0.119±0.28     | 0.837±1.152         | <0.0005 <sup>a</sup> |
| $c_{\text{Ntot}} / \text{mg L}^{-1}$      | 12.06±14.57    | 7.08±10.3           | 0.085                |
| $c_{\text{SO}_4^{2-}} / \text{mg L}^{-1}$ | 46.17±28.4     | 24.13±27.57         | <0.0005 <sup>a</sup> |
| $c_{\text{Fe}} / \text{mg L}^{-1}$        | 0.115±0.139    | 0.486±0.65          | 0.001 <sup>a</sup>   |

<sup>a</sup>Statistical significance at the level of 0.05

Based on the statistical comparison, it can be concluded that Zobnatica Lake has a higher groundwater contamination load (Table VI). The concentrations of nitrite and nitrate in groundwater are higher in Zobnatica Lake, which confirm the oxic conditions compared to the anoxic environment in Wetlands Tompojevci (higher concentration of ammonia).

Agricultural activities as the main source of contamination indicate that nitrate-based fertilizers are predominantly used in Zobnatica Lake, while ammonia-based fertilizers are predominantly used in Wetlands Tompojevci. Mineral dissolution as the main source of groundwater pollution with sulphate confirms that Zobnatica Lake is more exposed to sulphate contamination due to mineral composition compared to Wetlands Tompojevci. Iron cation concentrations were evaluated in anoxic environment which corresponds to higher concentrations of iron in Wetlands Tompojevci compared to Zobnatica Lake.

Data obtained within the scope of the IPA Project SeNs Wetlands enabled the proposition of the coastal multifunctional vegetation belt which contributes to a greater reduction of pollutants that enter the water from the surrounding areas.

The multifunctional vegetation belt is buffer system and physical barrier for the sensitive water bodies.<sup>19</sup> In order to ensure that the amount of pollution that reaches the water is halved, a green buffer strip 16 m wide is needed, made of grass and shrubs, but species-rich plant communities. Multi-layered green buffer system 20 m wide retains up to 75 % of pollutants, also in experiments with phosphorus.<sup>20</sup> Woody vegetation has the best results in restricting the pollutants wind transmission and is considerably more effective than medium and low height vegetation.

#### CONCLUSION

The conducted study research indicates the agricultural activities as the main source of the groundwater pollution in the cross border protected areas in Serbia and Croatia. The groundwater quality status assessment of selected protected areas, 18 physicochemical parameters were examined from 2018 to 2020. Six parameters (pH, total chlorine, fluoride, nickel, chromium and copper ions) have been excluded from discussion due to the results of statistical evaluation. The most significant correlations have been observed between chemical oxygen demand, electrical conductivity, nitrite, nitrate, sulfate, ammonia, iron and chlorine ions on both sites, Lake Zobnatica, Serbia and Wetlands Tompojevci, Croatia. The PCA analyses indicate that a two-factor score is appropriate for Zobnatica Lake data and three factor score for data from Wetlands Tompojevci. Based on the statistical assessment, it could be concluded that protected area in Serbia is more affected by agricultural activities compared to Wetlands Tompojevci due to the higher groundwater contamination load. Locations with the observed highest level of pollution were B2 and B5 in Zobnatica, Serbia and P2 and P6 in Tompojevci, Croatia. The nitrogen compounds have been identified as the most dom-

inant pollutants, since the nitrite, nitrate and total nitrogen were isolated in statistical evaluation. The results of this research have shown that the most significant pathways of pollution are agricultural activities and use of nitrogen and phosphorus-based fertilizers. The findings of this study have been used for development and maintenance of vegetation belt in protected areas. The results obtained within the two-year monitoring programme are highly essential on achieving a comprehensive database that could be used as platform for high-quality groundwater management in selected protected areas with the aim of minimizing environmental pollution.

#### SUPPLEMENTARY MATERIAL

Additional data and information are available electronically at the pages of journal website: <https://www.shd-pub.org.rs/index.php/JSCS/article/view/11194>, or from the corresponding author on request.

*Acknowledgments.* The authors acknowledge for the funding provided by the Ministry of Education, Science and Technological Development, Republic of Serbia, through the project no. 451-03-68/2020-14/200156: “Innovative scientific and artistic research from the FTS domain”, Interreg IPA CBC Croatia–Serbia Project „Active sensor monitoring Network and environmental evaluation for protection and wiSe use of wetlands and other surface waters“ AF\_HR-RS135\_SeNs\_Wetlands, the Bilateral project funded by the Ministry of Education, Science and Technological Development of the Republic of Serbia (contract no. 337-00-107/2019-09/16), Slovak Research and Development Agency under contract SK-SRB-18-0020 and the Slovak Research and Development Agency under Contract No. APVV-19-0149.

#### ИЗВОД

ПРОЦЕНА КВАЛИТЕТА ПОДЗЕМНИХ ВОДА ЗАШТИЋЕНИХ АКВАТИЧНИХ МОЧВАРНИХ ЕКОСИСТЕМА У ПРЕКОГРАНИЧНИМ ПОДРУЧЈИМА СРБИЈЕ И ХРВАТСКЕ

БОРИС Б. ОБРОВСКИ<sup>1</sup>, ИВАНА Ј. МИХАЛОВИЋ<sup>1</sup>, МИРЈАНА Б. ВОЈНОВИЋ МИЛОРАДОВ<sup>1</sup>,  
МАЈА СРЕМАЧКИ<sup>1</sup>, ИВАН ШПАНИК<sup>2</sup> и МАЈА З. ПЕТРОВИЋ<sup>1</sup>

<sup>1</sup>Универзитет у Новом Саду, Факултет техничких наука, Департман за инжењерство заштите животне средине и заштите на раду, Три Доситеја Обрадовића 6, 21000 Нови Сад и <sup>2</sup>Institute of Analytical Chemistry, Faculty of Chemical and Food Technology, STU, Radlinského 9, 81237 Bratislava, Slovakia

Резултати истраживања дефинишу основу за специфичне програме праћења квалитета подземних вода у мочварним екосистемима у Србији и Хрватској. Основни циљ истраживања био је утврђивање утицаја загађења из дифузних извора на квалитет подземних вода, као и сезонских варијација концентрационих нивоа селектованих физичко-хемијских параметара. Статистичке анализе, РСА, НСА, ANOVA и *t*-тест, обухватају 18 параметара анализираних у подземним водама. Статистички подаци су показали да заштићено подручје у Србији има значајно веће оптерећење загађивањима из пољопривредних активности у поређењу са мочварним подручјем Томпојевци. Највеће оптерећење подземних вода забележано је од укупног азота, амонијака и азотних анјона, што указује на загађење подземних вода ђубривима на бази азота. Резултати добијени у оквиру двогодишњег мониторинг програма, од 2018. до 2020. године, од изузетног су значаја за формирање свеобухватне базе података која би се могла користити као

платформа за добро управљање подземним водама у изабраним заштићеним подручјима са циљем смањења загађења животне средине.

(Примљено 23. септембра, ревидирано 6. децембра, прихваћено 7. децембра 2021)

#### REFERENCES

1. D. McLaughlin, M. Cohen, *Ecol. Appl.* **23** (2013) 1619 (<https://doi.org/10.1890/12-1489.1>)
2. W. Chen, C. Cao, D. Liu, R. Tian, C. Wu, Y. Wang, Y. Qian, G. Ma, D. Bao, *China Sci. Total. Environ.* **666** (2019) 1080 (<https://doi.org/10.1016/j.scitotenv.2019.02.325>)
3. S. van Asselen, P. Verburg, J. Vermaat, J. Janse, *PLOS One* **8** (2013) e81292 (<https://doi.org/10.1371/journal.pone.0081292>)
4. D. Tilman, K. G. Cassman, P. A. Matson, R. Naylor, S. Polasky, *Nature* **418** (2002) 671 (<https://doi.org/10.1038/nature01014>)
5. R. Balestrini, E. Sacchi, D. Tidili, C. A. Delconte, A. Buffagni, *Agric. Ecosyst. Environ.* **221** (2016) 132 (<https://doi.org/10.1016/j.agee.2016.01.034>)
6. D. Merchan, L. Sanz, A. Alfaro, I. Perez, M. Goñi, F. Solsona, I. Hernandez-García, C. Perez, J. Casalí, *Sci. Total Environ.* **706** (2020) 135701 (<https://doi.org/10.1016/j.scitotenv.2019.135701>)
7. J. Heil, H. Vereecken, N. Brüggemann, *Eur. J. Soil Sci.* **67** (2016) 23 (<https://doi.org/10.1111/ejss.12306>)
8. N. Wells, V. Hakoun, S. Brouyere, K. Knoller, *Water Res.* **98** (2016) 363 (<https://doi.org/10.1016/j.watres.2016.04.025>)
9. M. Gutierrez, R. N. Biagiomi, M. T. Alarcon-Herrera, B. A. Rivas-Lucero, *Sci. Total Environ.* **624** (2018) 1513 (<https://doi.org/10.1016/j.scitotenv.2017.12.252>)
10. Active Sensor monitoring Network and environmental evaluation for protection and wiSe use of WETLANDS and other surface waters – SeNs Wetlands, Interreg IPA CBC Croatia–Serbia, <https://www.interreg-croatia-serbia2014-2020.eu/project/sens-wetlands/> (accessed 17.09.2021)
11. European Commission, *Natura 2000, Environment*, [https://ec.europa.eu/environment/natura2000/index\\_en.htm](https://ec.europa.eu/environment/natura2000/index_en.htm) (accessed 17.09.2021)
12. M. Sremački, B. Obrovski, M. Petrović, I. Mihajlović, P. Dragićević, J. Radić, M. Vojinović Miloradov, *Environ. Monit. Assess.* **187** (2020) 192 (<https://doi.org/10.1007/s10661-020-8141-5>)
13. R.B. Baird, A.D. Eaton, E.W. Rice, *Standard methods for the examination of water and wastewater*, American Public Health Association, Washington, D.C., 2017, p. 1546 (<https://doi.org/10.2105/SMWW.2882.216>)
14. D. Ityel, *Filtr. Sep.* **48** (2011) 26 ([https://doi.org/10.1016/S0015-1882\(11\)70043-X](https://doi.org/10.1016/S0015-1882(11)70043-X))
15. J.A. Torres-Martínez, A. Mora, P.S.K. Knappett, N. Ornelas-Soto, J. Mahlknecht, *Water Res.* **182** (2020) 115962 (<https://doi.org/10.1016/j.watres.2020.115962>)
16. E. Custodio, J. Jódar, C. Herrera, J. Custodio-Ayala, A. Medina, *J. Hydrol.* **556** (2018) 427 (<https://doi.org/10.1016/j.jhydrol.2017.11.035>)
17. T. Scheytt, *Hydrogeol. J.* **5** (1997) 86 (<https://doi.org/10.1007/s100400050123>)
18. I. Sharma, S. Sood, G. Duggirala, *Indian J. Sci. Technol.* **10** (2017) 1 (<https://doi.org/10.17485/ijst/2017/v10i30/115534>)
19. T. Schmitt, M. Dosskey, K. Hoagland, *J. Environ. Qual.* **28** (1999) 1479 (<https://doi.org/10.2134/jeq1999.00472425002800050013x>)
20. J. Dorioz, D. Wang, J. Poulenard, D. Trevisan, *Agric. Ecosys. Environ.* **117** (2006) 4 (<https://doi.org/10.1016/j.agee.2006.03.029>)



SUPPLEMENTARY MATERIAL TO  
**Groundwater quality assessment of protected aquatic  
eco-systems in cross-border areas of Serbia and Croatia**

BORIS B. O BROVSKI<sup>1</sup>, IVANA J. MIHAJLOVIĆ<sup>1\*</sup>, MIRJANA B. VOJNOVIĆ  
MILORADOV<sup>1</sup>, MAJA M. SREMAČKI<sup>1</sup>, IVAN ŠPANIK<sup>2</sup> and MAJA Z. PETROVIĆ<sup>1</sup>

<sup>1</sup>*University of Novi Sad, Faculty of Technical Sciences, Department of Environmental  
Engineering and Occupational Safety and Health, Trg Dositeja Obradovica 6, 21000 Novi  
Sad, Serbia and <sup>2</sup>Institute of Analytical Chemistry, Faculty of Chemical and Food  
Technology, STU, Radlinského 9, 81237 Bratislava, Slovakia*

J. Serb. Chem. Soc. 87 (1) (2022) 121–132

SAMPLING SITES

Lake Zobnatica with an area of 250 ha is in the North Bačka District near the town of Bačka Topola. Zobnatica was declared as the national Nature Park in 1976. Water from the Lake is applied for irrigation of agricultural land as main human activity in this region. Industrial facilities, predominantly meat industry, are located 7 km from the Lake. The urbanization of the surrounding area resulted in the development of tourist attractions (sport facilities, beaches, catering, and hospitality industry facilities, etc.). Wetlands Tompojevci are wetlands of 5700 ha located in the eastern part of Vukovar-Srijem District, Tompojevci municipality. Agriculture is one of the main activities in the Tompojevci region. The total length of Tompojevci Wetland is 48 km, with a natural depression depth of up to 15 m where run-off water from agricultural land is naturally aggregated.

Within the IPA Project 8 piezometers surrounding the Lake Zobnatica (B1–B8) and Wetlands Tompojevci (P1–P8) were constructed (Fig. S-1 and GPRS coordinates in Table S-I) and used for collection of groundwater sample. The sampling campaigns were conducted for period of two years, from May of 2018 until February of 2020. Analyses were carried out in accredited laboratory for environmental and occupational monitoring, Department of Environmental Engineering and Occupational Safety, Faculty of Technical sciences, University of Novi Sad.

\* Corresponding author. E-mail: ivanamihajlovic@uns.ac.rs

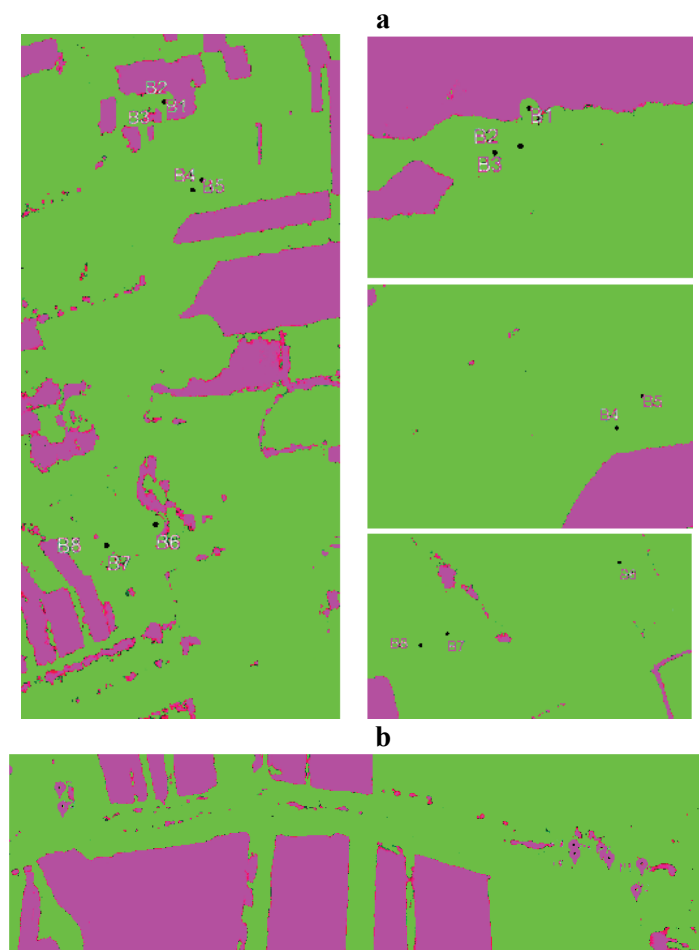


Fig. S-1. Sampling site for a) Zobnatica Lake and b) Wetlands Tompojevci.

TABLE S-I. GPRS coordinates of water sampling sites from Serbia and Croatia

| Location | Zobnatica lake, Serbia               | Location | Wetlands Tompojevci, Croatia         |
|----------|--------------------------------------|----------|--------------------------------------|
| B1       | (45° 53' 9.11" N, 19° 36' 55.25" E)  | P1       | (45° 14' 35.78" N, 19° 6' 39.72" E)  |
| B2       | (45° 53' 8.58" N, 19° 36' 54.78" E)  | P2       | (45° 14' 34.05" N, 19° 6' 38.89" E)  |
| B3       | (45° 53' 8.68" N, 19° 36' 55.16" E)  | P3       | (45° 14' 35.99" N, 19° 6' 37.13" E)  |
| B4       | (45° 52' 45.94" N, 19° 37' 5.01" E)  | P4       | (45° 14' 36.54" N, 19° 6' 36.60" E)  |
| B5       | (45° 52' 48.69" N, 19° 37' 7.82" E)  | P5       | (45° 14' 36.65" N, 19° 6' 34.37" E)  |
| B6       | (45° 51' 26.94" N, 19° 36' 57.38" E) | P6       | (45° 14' 36.07" N, 19° 6' 34.36" E)  |
| B7       | (45° 51' 21.73" N, 19° 36' 43.64" E) | P7       | (45° 14' 38.05" N, 19° 05' 51.56" E) |
| B8       | (45° 51' 20.88" N, 19° 36' 41.56" E) | P8       | (45° 14' 36.80" N, 19° 05' 52.11" E) |

TABLE S-II. Mean value for piezometer B1 to B8 in Zobnatica Lake

| Parameter                                      | Location |        |       |       |        |       |       |       |
|--|----------|--------|-------|-------|--------|-------|-------|-------|
|  | B1       | B2     | B3    | B4    | B5     | B6    | B7    | B8    |
| $\sigma / \mu\text{S cm}^{-1}$                 | 853.1    | 1147.1 | 918.9 | 931.5 | 1506.4 | 998.1 | 1021  | 839.5 |
| $c_{\text{O}_2} / \text{mg L}^{-1}$ (DO)       | 5.04     | 4.64   | 5.69  | 5.14  | 5.15   | 4.53  | 5.17  | 4.77  |
| $c_{\text{PO}_4^{3-}} / \text{mg L}^{-1}$      | 0.46     | 0.26   | 0.48  | 0.61  | 0.25   | 0.32  | 0.43  | 1.04  |
| $c_{\text{NO}_2^-} / \text{mg L}^{-1}$         | 0.09     | 0.22   | 0.04  | 0.1   | 0.08   | 0     | 0.04  | 0.04  |
| $c_{\text{NO}_3^-} / \text{mg L}^{-1}$         | 1.12     | 1.82   | 1.18  | 0.6   | 1.45   | 0.06  | 1.04  | 0.39  |
| $c_{\text{NH}_4^+} / \text{mg L}^{-1}$         | 0.07     | 0.06   | 0.21  | 0.02  | 0.04   | 0.07  | 0.07  | 0.47  |
| $c_{\text{SO}_4^{2-}} / \text{mg L}^{-1}$      | 36.38    | 55.13  | 42.5  | 35.75 | 74.38  | 15.38 | 78    | 29.86 |
| $c_{\text{Cl}^-} / \text{mg L}^{-1}$           | 28.93    | 43.58  | 32.92 | 41.89 | 104.86 | 38.77 | 16.34 | 37.84 |
| $c_{\text{N}_{\text{tot}}} / \text{mg L}^{-1}$ | 19.11    | 17.95  | 7.28  | 7.93  | 22.76  | 1.02  | 10.38 | 9.71  |
| $c_{\text{Fe}} / \text{mg L}^{-1}$             | 0.06     | 0.11   | 0.08  | 0.08  | 0.1    | 0.09  | 0.13  | 0.31  |
| $c_{\text{Zn}} / \text{mg L}^{-1}$             | 0.33     | 0.44   | 0.39  | 0.31  | 0.9    | 0.32  | 0.4   | 0.58  |
| $c_{\text{O}_2} / \text{mg L}^{-1}$ (COD)      | 20.15    | 35.45  | 6.7   | 13.49 | 11.89  | 14.13 | 18.51 | 23.07 |

DO: dissolved oxygen; N<sub>tot</sub>: total nitrogen COD: chemical oxygen demand

TABLE S-III. Mean value for piezometer P1 to P8 in Wetlands Tompojevci

| Parameters                                     | P1    | P2    | P3     | P4     | P5     | P6    | P7     | P8      |
|--|-------|-------|--------|--------|--------|-------|--------|---------|
| $\sigma / \mu\text{S cm}^{-1}$                 | 855.5 | 558   | 934.33 | 903.37 | 911.11 | 772   | 856.33 | 1051.33 |
| $c_{\text{O}_2} / \text{mg L}^{-1}$ (DO)       | 4.93  | 4.57  | 3.69   | 4.55   | 4.91   | 4.81  | 5.03   | 3.36    |
| $c_{\text{PO}_4^{3-}} / \text{mg L}^{-1}$      | 0.541 | 0.523 | 0.604  | 0.556  | 0.876  | 1.09  | 0.444  | 3.15    |
| $c_{\text{NO}_2^-} / \text{mg L}^{-1}$         | 0.007 | 0.135 | 0.009  | 0.019  | 0.008  | 0.033 | 0.017  | 0.018   |
| $c_{\text{NO}_3^-} / \text{mg L}^{-1}$         | 0.07  | 1.496 | 0.086  | 0.15   | 0.086  | 0.954 | 0.155  | 0.046   |
| $c_{\text{NH}_4^+} / \text{mg L}^{-1}$         | 0.216 | 0.328 | 0.213  | 0.44   | 1.335  | 2.715 | 0.43   | 1.572   |
| $c_{\text{SO}_4^{2-}} / \text{mg L}^{-1}$      | 57    | 62.8  | 7.71   | 11.5   | 15.14  | 6.75  | 28.25  | 7.4     |
| $c_{\text{Cl}^-} / \text{mg L}^{-1}$           | 13.36 | 8.98  | 10.7   | 12.61  | 12.45  | 6.65  | 22.27  | 28.04   |
| $c_{\text{N}_{\text{tot}}} / \text{mg L}^{-1}$ | 1.358 | 6.57  | 4.58   | 2.81   | 7.22   | 33.43 | 2.47   | 7.34    |
| $c_{\text{Fe}} / \text{mg L}^{-1}$             | 0.128 | 0.194 | 0.301  | 0.35   | 0.614  | 0.355 | 0.287  | 1.72    |
| $c_{\text{Zn}} / \text{mg L}^{-1}$             | 0.373 | 0.414 | 0.467  | 0.508  | 0.517  | 0.382 | 0.495  | 0.55    |
| $c_{\text{O}_2} / \text{mg L}^{-1}$ (COD)      | 18.9  | 10.76 | 19.07  | 23.26  | 27.08  | 55.58 | 67.05  | 45.32   |

DO: dissolved oxygen; N<sub>tot</sub> – total nitrogen; COD – chemical oxygen demand

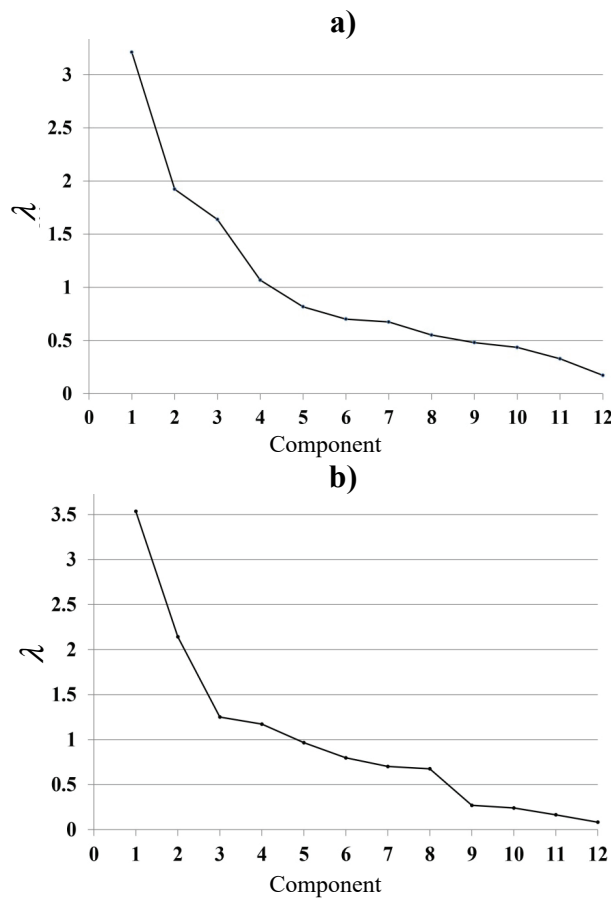


Fig. S-2. Scree plot of eigenvalues ( $\lambda$ ) for generated Components for  
a) Zobnatica Lake and b) Wetlands Tompojevci.

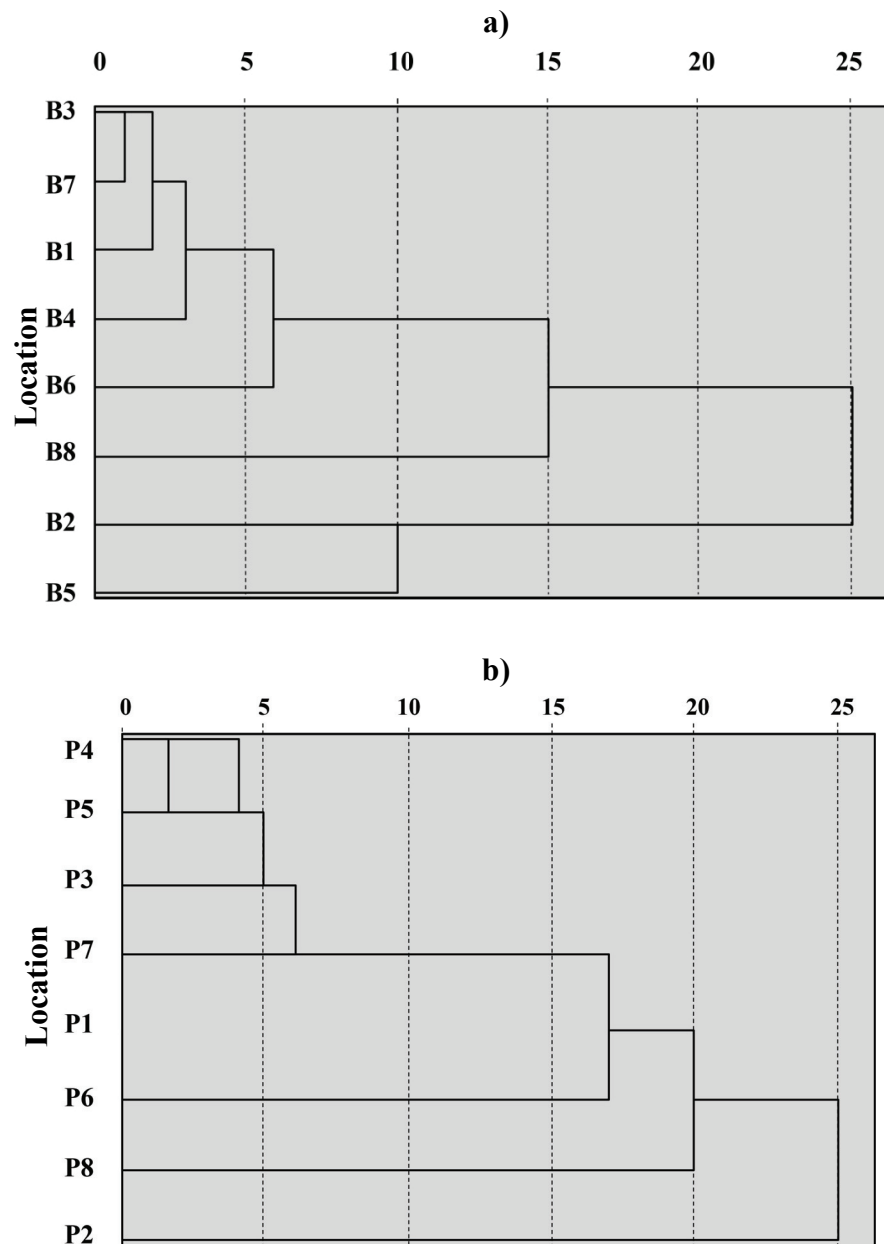


Fig S-3. Dendograms of Rescaled Distance Cluster Combined for sampling locations of  
a) Zobnatica Lake and b) Wetlands Tompojevci.



## Characterization of landfill deposited sediment from dredging process during different maturation stages

MILOŠ DUBOVINA, NENAD GRBA\*, DEJAN KRČMAR, JASMINA AGBABA#, SRDAN RONČEVIĆ#, ĐURĐA KERKEZ# and BOŽO DALMACIJA#

University of Novi Sad, Faculty of Sciences, Department of Chemistry, Biochemistry and Environmental Protection, Trg Dositeja Obradovica 3, 21000 Novi Sad, Serbia

(Received 30 August, revised and accepted 29 November 2021)

**Abstract:** A long-term monitoring of deposited sediment in the environment is considered in order to examine the mechanism of incorporation of Cu and Cd into mineral fractions and to investigate their bioavailability during landfill maturation. Using the sequential extraction technique (Community Bureau of Reference, BCR), the dominant presence of Cu and Cd in the oxidation and residual fraction was determined, which suggests a low risk of bioavailability of these metals in the environment. The maturation of the deposited sediment indicates that the Cu and Cd content decreases over time in the exchangeable fraction and increases in the oxidation fraction. X-ray techniques XRF and EDS indicated a prevalence of silicates in the tested samples, which suggests the possibility of presence of silicate compounds that can bind metals and thus convert them into less mobile forms in the sediment. By imaging the samples with a scanning electron microscope SEM, the formation of heterogeneous structures over time was determined, which confirms the formation of new minerals and the potential possibility of incorporating copper and cadmium in them. In order to determine the mineral forms and dominant compounds in the examined sediment samples, X-ray diffraction analysis was applied, and the transformation pathways were explained.

**Keywords:** bioavailability of Cu and Cd in sediment fractions; metals adsorption, sequential extraction; sediment maturation mechanism.

### INTRODUCTION

In this research a structural characterization, heavy metals binding pathways with risk assessment of dredged riverbed sediment and determination of different maturation stages are presented. The deposited sediment samples from three vertically hotspots landfill sites were subjected to long-term monitoring, over a period

\* Corresponding author. E-mail: nenad.grba@dh.uns.ac.rs

# Serbian Chemical Society member.

<https://doi.org/10.2298/JSC210830102D>

of 3 years (2017–2019) and become characterized as samples with variable values of heavy metals with the average composition (*e.g.*, Cu 245.15 mg/kg, Cd 9.16 mg/kg) mostly higher than of the upper continental crust (UCC).<sup>1,2</sup> In order to examine the bioavailability of high concentrations of Cu and Cd in the deposited sediment samples after dredging, an operational specification performed by the four-step BCR (Community Bureau of Reference) sequential extraction procedure was applied.<sup>3,4</sup> The structural characterization of the examined matrices using the scanning electron microscopy/energy dispersive X-Ray spectroscopy (SEM/EDS) and X-ray fluorescence analysis (XRF) characterized the qualitative and semi-quantitative distribution of elements that can represent an important instrumental analysis in order to determine the dominant binding mechanisms and mobility pathways of monitored metals in sediment system to stable forms.<sup>5,6</sup> X-ray diffraction (XRD) analysis determined the mineral forms of Cu and Cd, and in line with the analysis of other mineral forms present in the sediment, the mechanisms of potential metal adsorption were investigated.<sup>5</sup>

The general characterization of sediment using the mentioned techniques will contribute to the assessment of the risk of mobility of metal forms due to the influence of atmospheric precipitation, weathering reactions and leaching of sediment deposited on the landfill over long period of time.<sup>7</sup>

## EXPERIMENTAL

The research area is positioned in the coastal area of the Bega Canal near the border with Romania. After the sludge was deposited in the environment, an exploratory landfill was formed, where long-term monitoring was performed for a period of 3 years (2017–2019). Risk assessment of metal mobility or distribution of heavy metals by fractions in sediment deposits after dredging was determined using the conventional technique of sequential sediment extraction (BCR).<sup>8–10</sup> The procedure for determining the distribution of heavy metals in sediments by fractions consists of four steps. In the first step, 1 g of a dry sediment sample is weighed and mixed with 40 mL of acetic acid (0.11 mol/L) in a 100 mL vessel and extracted for 16 h at 22±5 °C. The samples are then centrifuged; the supernatant is decanted and used for analysis. In the second step, the sediment from phase 1 is used in the second phase by adding 40 mL of hydroxylamine hydrochloride (0.5 mol/L) to the sample and extracting for 16 h at 22±5 °C. Centrifugation is then performed, the supernatant is decanted and the metal content is analysed. Samples from this phase are used in phase 3. In the third step, 10 mL of hydrogen peroxide (8.8 mol/L) is added; digestion is performed at room temperature for 1 h with occasional shaking. Evaporation for 1 h in a water bath at 85±2 °C to 3 mL. 10 mL of hydrogen peroxide (8.8 mol/L) is added, followed by digestion for 1 hour in a water bath at 85±2 °C, and then evaporated to a volume of 1 mL. 50 mL of 1 mol/L ammonium acetate is added and extraction continued for 16 h at 22±5 °C. The sample is centrifuged, the supernatant is decanted and used for analysis. Finally, in the fourth step, the samples from the third phase are subjected to digestion with imperial water (9 mL of HCl and 3 mL of HNO<sub>3</sub>), after which the samples are filtered and analyzed for metal content.

Qualitative and quantitative distribution of elements in sediment samples was analyzed using two different X-ray techniques by energy dispersive X-ray spectrometry (EDS) in combin-

ation with scanning electron microscopy (SEM) and X-ray fluorescence analysis (XRF). For SEM/EDS analysis, the samples were dried, and the entire volumes were ground into a fine powder. The powder sample was applied to the carbon strip and recorded. SEM analysis of samples was performed on Quantax 70 EDS System – Hitachi Tabletop Microscope TM3000 – Brucker, Germany. The X-ray fluorescence XRF process begins by homogenizing the sediment sample and recording it by measuring the wavelength or energy of the photon and the intensity of the characteristic radiation emitted from the sample. A Delta Premium Handheld XRF Analyzer Specifications analyzer was used to record sediment samples.

X-ray diffraction (XRD) is a widespread analytical technique that has been applied to determine different forms of crystal structures in sediment.<sup>11</sup> For X-ray diffraction analysis, the entire volume of sediment was crushed, and a certain amount of sample was applied to a glass plate, measuring 20 mmx20 mm and with a recess of 0.5 mm. Analyses were performed on an automatic powder diffractometer Rigaku MiniFlex 600, Brag–Brentano geometry with a secondary graphite monochromator. Recording was done in step mode, with a stop time of 2 s. Radiation was performed via copper anodes, with a voltage of 40 kV and a current of 15 mA.

#### RESULTS AND DISCUSSION

By using conventional sequential extraction (BCR), an assessment of the potential risk of deposited sediment into the environment after dredging activity was determined.<sup>12</sup> Long-term monitoring, over a period of 3 years (2017–2019), of sediment quality was determined analysing the binding of elevated metals, dominantly of copper and cadmium, to certain fractions of sediment in order to establish their bioavailability.

##### *Sediment related results from conventional sequential extraction (BCR) procedure*

The distribution of Cu and Cd (Figs. 1 and 2) show a dominant presence in the oxidable and residual phases, which suggests that these metals are mainly bound to organic matter, sulphides and minerals and therefore less available in the environment.<sup>13,14</sup> Individually inspection at each of the metal binding phases in the sediment, showed that copper is the most abundant in the residual fraction ranging from 44.42 to 50.95 %, while the binding to organic matter and sulphides

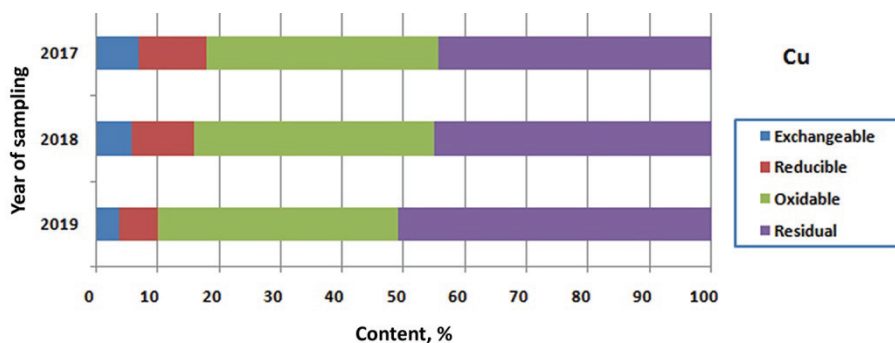


Fig. 1. Binding of Cu to different fractions during sediment maturation (2017–2019).

are also characterized by a high share of 37.51 to 38.92 % (Fig. 1). A similar trend of sediment binding is shown by Cd with a somewhat more dominant presence in the mineral fraction from 48.52 to 54.16 %, which indicates a low risk of bioavailability to biota (Fig. 2).<sup>15</sup>

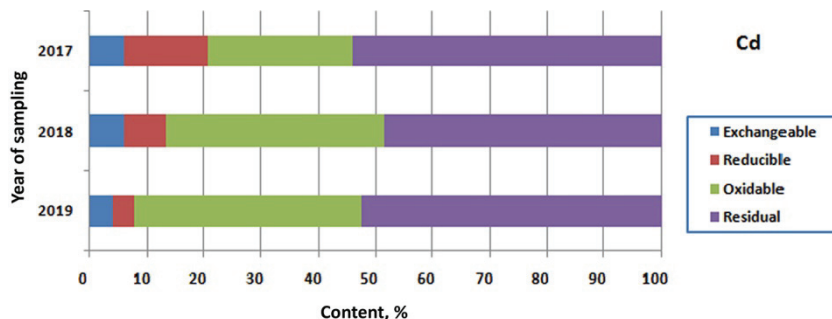


Fig. 2. Binding of Cd to different fractions during sediment maturation (2017–2019).

During long-term monitoring of sludge sediments, the percentage of Cu and Cd decreased in the dissolved phase (2018 (Cu 5.82 %; Cd 5.75 %), 2019 (Cu 3.90 %; Cd 3.70 %)), while the oxidative phase was characterized by a higher presence of these two metals. The change in the distribution of Cu and Cd in the sediment fractions indicates the formation of organic complexes and sulphides during the aging of the sediment at the landfill.<sup>16</sup>

#### *Semi quantitative to quality comparisons of different heavy metals indicators*

Comparison of XRF and EDS techniques and related results from XRF analysis of the hot spots of the investigated sediments (chronologically: S1 sample (2017), S2 sample (2018) and S3 sample (2019)), were scale up based on the increasing content of Si in the landfill sediment over time (Table I). The predominantly low Ca/Si ratio during all monitoring periods indicates sediment

TABLE I. Comparative quantitative spot analysis in selected areas of exploratory deposited samples using Energy dispersive X-ray spectrometry (EDS) and X-ray fluorescence analysis (XRF) techniques

| Parameter    | Year of characterization of deposited sediment |       |       |       |       |       |
|--------------|--|-------|-------|-------|-------|-------|
|              | EDS  |       |       | XRF   |       |       |
|              | 2017   | 2018  | 2019  | 2017  | 2018  | 2019  |
| Content, %   |  |       |       |       |       |       |
| Ca           | 1.89   | 1.21  | 0.89  | 1.72  | 0.93  | 1.89  |
| Al           | 8.25   | 10.51 | 13.53 | 9.41  | 9.71  | 13.11 |
| Si           | 18.59  | 22.72 | 24.35 | 20.92 | 23.64 | 25.21 |
| Atomic ratio |  |       |       |       |       |       |
| Ca/Si        | 0.10   | 0.05  | 0.04  | 0.08  | 0.04  | 0.07  |
| Si/Al        | 2.25   | 2.16  | 1.80  | 2.22  | 2.43  | 1.92  |

characterized by a high Si presence. Accordingly, the presence of Si suggests that silicate compounds predominate in the sediment, which is very important from the aspect of binding metals by silicate substances in the process of landfill maturation and thus reduces their mobility.<sup>5</sup>

The scanning electron microscopy shows a different microstructural nature or variations in the semi-homogeneous structure as well as visible macro/meso porosity. The formation of new minerals due to mineralogical changes is visible in Figs. 3–5 due to the formation of larger aggregates.

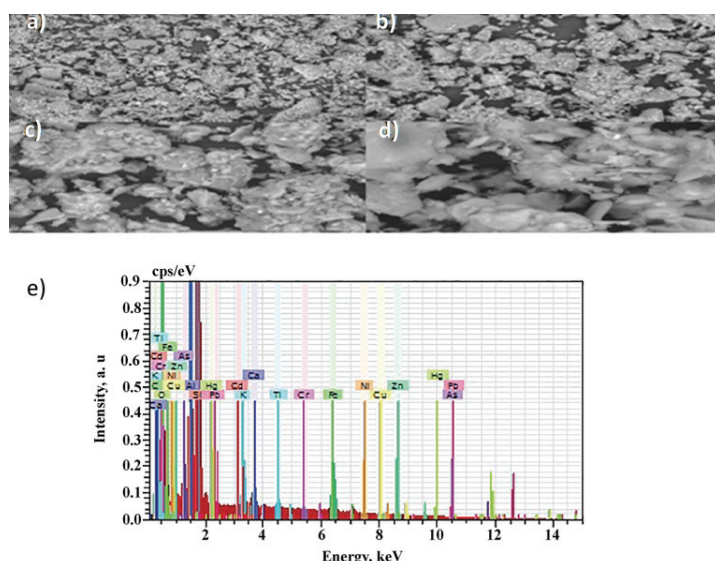


Fig. 3. Analysis of deposited sediment sample from 2017 using a scanning electron microscope (SEM) with magnification: a) 500×, b) 1000×, c) 2000×, d) 4000×; e) analysis of energy dispersive X-ray spectrometry (EDS).

The application of EDS and XRF analysis indicates that the sediment from 2019 has a slightly more heterogeneous structure, with a lower Si/Al ratio of about 1.80 (EDS) and 1.92 (XRF), respectively, compared to other periods of sediment characterization (Table I), which may also indicate a higher binding capacity of heavy metals during sediment landfill maturation.<sup>17</sup> This can also be explained by the presence of aluminosilicates with increased aluminium content.<sup>18,19</sup>

#### *Maturation and characterisation of sediments and heavy metals binding pathways*

As it was investigated in the geological classification of northern part of Serbia (Vojvodina) including cross-border geological units to Romania, the loess–paleosol section (LPS) of this region is dominantly represented and characterized by irregularities in sedimentological properties, magnetic susceptibility

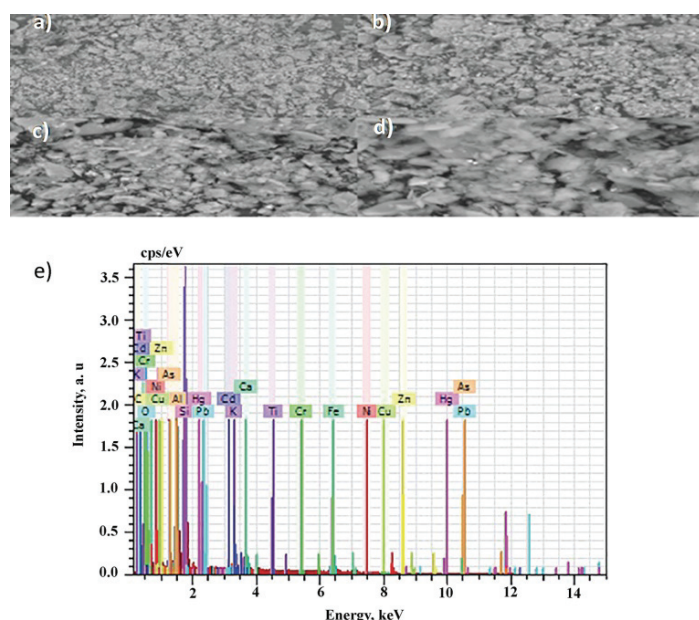


Fig. 4. Analysis of deposited sediment sample from 2018 using a scanning electron microscope (SEM) with magnification: a) 500 $\times$ , b) 1000 $\times$ , c) 2000  $\times$ , d) 4000 $\times$ ; e) analysis of energy dispersive X-ray spectrometry (EDS).

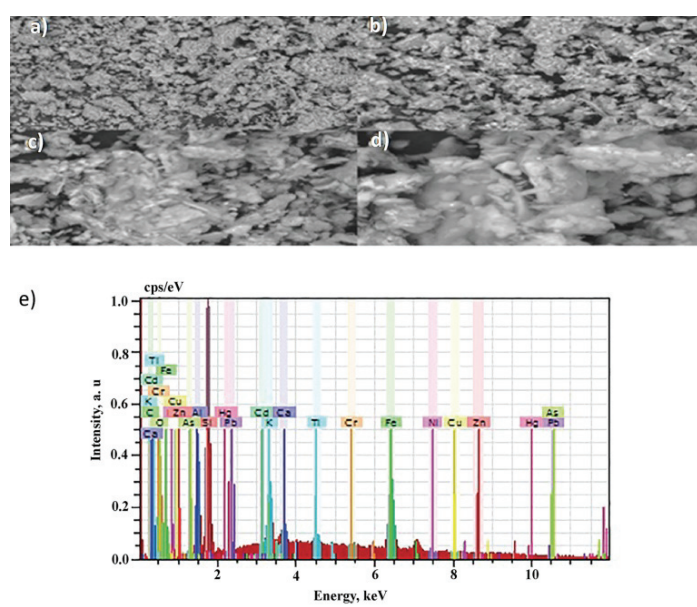


Fig 5. Analysis of deposited sediment sample from 2019 using a scanning electron microscope (SEM) with magnification: a) 500 $\times$ , b) 1000 $\times$ , c) 2000 $\times$ . d) 4000 $\times$ ; e) analysis of energy dispersive X-ray spectrometry (EDS).

and color of the sediment with a unique sedimentology differing from all other investigated sections in Serbia.<sup>20</sup> Characterization of three different time periods (2017–2019) by target samples using XRD analysis show elevated picks of minerals, shifting of high intensity of, *e.g.*, quarz to lower and alternating muscovite and albite (Fig. 6).

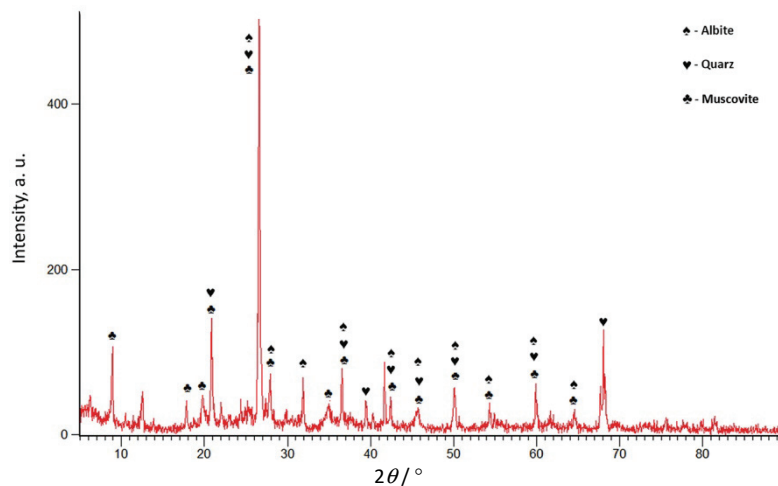


Fig. 6. The dominant selected minerals from sample 1 (2017).

Quartz ( $\text{SiO}_2$ ) and albite a sodium aluminosilicate ( $\text{NaAlSi}_3\text{O}_8$ ), Table II, are non-clay minerals and the albite as a feldspathic mineral can act as a sintering aid and sinter raw material at dominantly higher temperatures (rock forming mineral is possible also at 20 °C), 50 and 80 °C,<sup>21</sup> or pressure which can render the reactivity of it when exposed to an alkaline environment during the synthesis of the zeolite.<sup>22</sup>

TABLE II. Identified minerals in sample 1 (2017)

| Compound name                         | Chemical formula  |
|---------------------------------------|---|
| <b>Silicon oxide</b>                  | $\text{SiO}_2$  |
| Copper indium sulfide                 | $\text{CuInS}_2$  |
| Copper rhodium oxide                  | $\text{CuRh}_2\text{O}_4$   |
| Copper oxide                          | $\text{Cu}_2\text{O}$   |
| Copper telluride                      | $\text{Cu}_{2.8}\text{Te}_2$  |
| Aluminum silicate                     | $\text{Al}_2\text{SiO}_5$   |
| Potassium aluminum silicate hydroxide | $\text{KAl}_3\text{Si}_3\text{O}_{10}(\text{OH})_2$                   |
| <b>Sodium aluminum silicate</b>       | <b>Na (<math>\text{AlSi}_3\text{O}_8</math>)</b>                      |
| Copper hydroxide sulfate hydrate      | $\text{Cu}_{15}(\text{OH})_{22}(\text{SO}_4)_4(\text{H}_2\text{O})_6$ |

Albite may be most widely found in pegmatites and felsic igneous rocks such as granites. It was also found in low-grade metamorphic rocks and as authi-

genic albite in certain sedimentary varieties.<sup>23</sup> In our samples the authigenic form is likely to occur in muscovite–albite granite form. Muscovite can be usually found in sedimentary rocks rather than in igneous rocks of intermediate, mafic, and ultramafic composition,<sup>24</sup> but this kind of rocks with higher metals content could be also found in near region as Posavina.<sup>25</sup>

Decreasing of quartz mechanisms binding of heavy metals (dominantly Cu and Cd) is replaced by phryopilite, ilite and albite (Fig. 7), which during the hydrothermal alteration in combination with oxidation, pH values and different precipitations and weathering conditions could act like zeolites based minerals with high capacity of long term capturing of pilar heavy metals clasters. Not dominant, but present, CHS polzonc reactions occur in heterogenic sediment structure in investigated Begej Cannal locations, with cross border pollution.<sup>26</sup> The CaCO<sub>3</sub> content in this region is high and varies from 9.2 to 31.8 % (average 19.3 %)<sup>16</sup> and consequently it can be assumed, that the genesis of CSH and related polzonc reactions could be time related including dependence from higher temperature, pressure, pH and other geochemical parameters. This could be the reason for encapsulating of heavy metals, including Cu and Cd in the river bed and later in landfill sediment site.

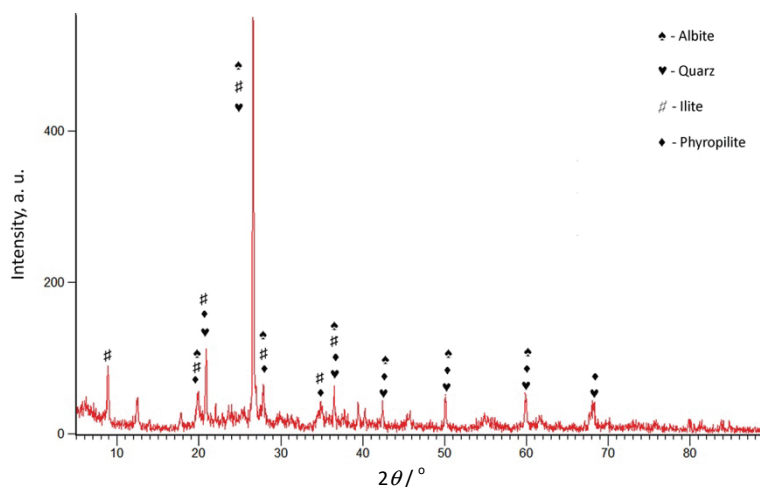


Fig. 7. The dominant selected minerals from sample 2 (2018).

These mineral complexations will lead to higher maturation as demonstrated in Table III and Fig. 8 in 2019 with potential encapsulation of Cu and Cd in mineral phases. Fig. 8 shows quartz and ilite as dominant peaks and from Table III silicon oxide, carbonates and aluminosilicates. The Cd and Cu captured in minerals are not available in free forms in sediment or water.

Literature data show that muscovite and illite have high heavy metals adsorption capacity.<sup>27</sup> The results show that for, e.g., Cu<sup>2+</sup> and Zn<sup>2+</sup> are adsorbed as

monovalent ions, probably as  $(\text{CuOH})^{+1}$  and  $(\text{ZnOH})^{+1}$  hydroxy surface complexes, due to their high ionic potential. SEM/EDS pushes a higher content of Al, Si, which confirms aluminosilicate sheets, as well as Ca and heavy metals, *e.g.*, Cu and Cd higher content in Figs. 3–5.

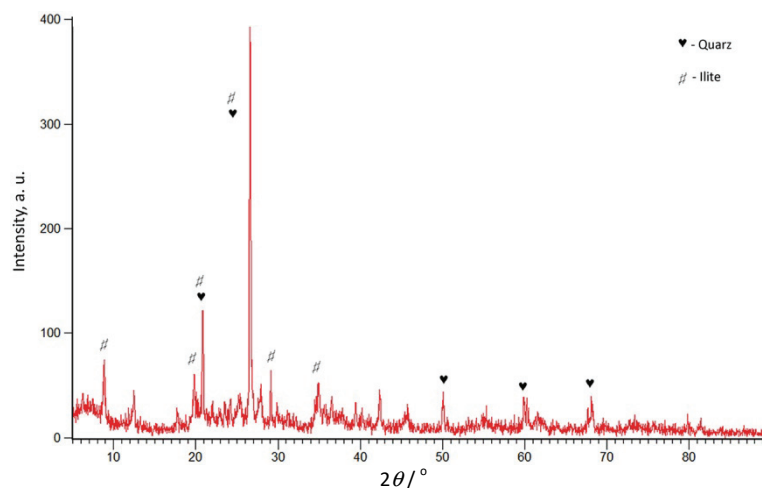


Fig. 8. The dominant selected minerals from sample 3 (2019).

TABLE III. Dominant related and other compounds in sample 3 (2019)

| Compound name                             | Chemical formula  |
|---|---|
| <b>Silicon oxide</b>                      | $\text{SiO}_2$  |
| <b>Calcium carbonate</b>                  | $\text{Ca}(\text{CO}_3)$  |
| Copper sulfate hydroxide hydrate          | $\text{Cu}_4(\text{SO}_4(\text{OH})_6\text{H}_2\text{O})\text{H}_2\text{O}$   |
| <b>Sodium aluminum silicate</b>           | $\text{NaAlSiO}_4$  |
| Aluminum tetrahydroxodisilicate formamide | $\text{Al}_2\text{Si}_2\text{O}_5(\text{OH})_4(\text{HCONH}_2)$               |
| Gallium cadmium copper oxide              | $\text{Ga}_2\text{Cd}_{.75}\text{Cu}_{.25}\text{O}_4$                         |
| Copper hydroxide sulfate hydrate          | $\text{Cu}_{15}(\text{OH})_{22}(\text{SO}_4)_4(\text{H}_2\text{O})_6$         |
| Copper zinc sulfate hydroxide hydrate     | $(\text{Cu}_6\text{Zn})(\text{SO}_4)_2(\text{OH})_{10}(\text{H}_2\text{O})_3$ |
| Copper silicate hydroxide                 | $\text{Cu}_5\text{Si}_4\text{O}_{12}(\text{OH})_2$                            |
| Potassium aluminum silicate hydroxide     | $\text{KA}_{12}(\text{Si}_3\text{Al})\text{O}_{10}(\text{OH})_2$              |

#### CONCLUSION

The long-term characterization of sediment from the landfill after dredging activity is presented, in order to determine the potential bioavailability of Cu and Cd metals characterized as a potential risk in the examined matrix. Using sequential BCR extraction, it was observed that the maturation of the deposited sludge leads to a decrease in the metal content in the available sediment fraction. This distribution of metals indicates that during the maturation of the landfill, metals are incorporated into stable mineral forms and thus become less available in other environmental media due to potential atmospheric influences. The application of

SEM/EDS and XRF analysis has contributed to the quantification of elements of interest such as Al and Si. Increase in the percentage of Si, suggests that the maturation of the landfill in the sediment is dominated by silicate compounds, and consequently the metals changed into more stable forms what was confirmed by sequential analysis. Mineral changes were characterized by the formation of new minerals, detected by the formation of larger aggregates and recorded by a scanning electron microscope. Previous studies showed that non-clay minerals (quartz and albite) can act as a sinter raw material at low to higher range of temperature and pressure, and that clay minerals (muscovite and illite) are also good adsorbent of dominantly monovalent ions. Temperature, pH or pressure are the well-known parameters in the mechanism for the encapsulation of heavy metals, confirmed in this research. Also the most important process is mixing of sediment after dredging that showed the high level results only few months after applying the best available technique (BAT). This could be taken into account for further analysis on implementing plan for longtime waste disposal process.

#### ИЗВОД

#### КАРАКТЕРИЗАЦИЈА ИЗМУЉЕНОГ СЕДИМЕНТА ТОКОМ РАЗЛИЧИТИХ ФАЗА САЗРЕВАЊА ДЕПОНИЈЕ

МИЛОШ ДУБОВИНА, НЕНАД ГРБА, ДЕЈАН КРЧМАР, ЈАСМИНА АГБАБА, СРЂАН РОНЧЕВИЋ, ЂУРЂА КЕРКЕЗ  
и БОЖО ДАЛМАЦИЈА

*Универзитет у Новом Саду, Природно-математички факултет, Департиман за хемију, биохемију и  
заштиту животне средине, Три Доситеја Обрадовића 3, 21000 Нови Сад*

У овом раду размотрен је дугорочни мониторинг депонованог седимента у животну средину како би се испитао механизам инкорпорирања Cu и Cd у минералним фракцијама и размотрила њихова биодоступност током сазревања депоније. Применом технике секвенцијалне екстракције, утврђена је доминантна заступљеност Cu и Cd у оксидованој и резидуалној фракцији што указује на низак ризик биодоступности поменутих метала у животној средини. Сазревање депонованог седимента указује да се садржај Cu и Cd смањује током времена у изменљивој фракцији, а повећава у оксидованој. Рендгенске технике XRF и EDS су показале доминантну заступљеност силикатног узорцима, као и на могућност формирања силикатних једињења која имају способност да везују метале и тиме их преводе у мање мобилне форме у седименту. Снимајући узорке скенирајућим електронским микроскопом утврђено је формирање хетерогених структура током времена, што потврђује формирање нових минерала и потенцијалну могућност инкорпорирања бакра и кадмијума у њима. Како би се утврдиле минералне форме и доминантна једињења у испитиваним узорцима седимента, примењена је рендгенска дифракциони анализа и појашњени су путеви трансформације датих једињења током времена.

(Примљено 30. августа, ревидирано и прихваћено 29. новембра 2021)

#### REFERENCES

1. R. L. Rudnick, S. Gao, in *Treatise on Geochemistry, Vol. 3: The Crust*, R. L. Rudnick, Ed., Elsevier Science, 2004, pp. 1–64 (<https://doi.org/10.1016/B0-08-043751-6/03016-4>)

2. S. R. Taylor, S. M. McLennan, *Rev. Geophys.* **33** (1995) 241 (<https://doi.org/10.1029/95RG00262>)
3. I. Ahumada, A. Maricán, M. Retamal, C. Pedraza, L. Ascar, A. Carrasco, P. Richter, *J. Braz. Chem. Soc.* **21** (2010) 721 (<https://doi.org/10.1590/S0103-50532010000400020>)
4. G. Rauret, J.F. Lopez-Sánchez, A. Sahuquillo, R. Rubio, C. Davidson, A. Ure, P. Quevauviller, *J. Environ. Monit.* **1** (1999) 57 (<https://doi.org/10.1039/A807854H>)
5. D. Rađenović, *PhD Thesis*, University of Novi Sad, Novi Sad, 2020 (<https://www.cris.uns.ac.rs/record.jsf?recordId=114883&source=NaRDuS&language=sr>) (in Serbian)
6. N. Varga, *PhD Thesis*, University of Novi Sad, Novi Sad, 2017 ([https://nardus.mpn.gov.rs/bitstream/handle/123456789/8627/Disertacija\\_11467.pdf?sequence=6&isAllowed=y](https://nardus.mpn.gov.rs/bitstream/handle/123456789/8627/Disertacija_11467.pdf?sequence=6&isAllowed=y)) (in Serbian)
7. R. Zhang, F. Zeng, W. Liu, R.J. Zeng, H. Jiang, *J. Environ. Manage.* **53** (2014) 1119 (<https://doi.org/10.1007/s00267-014-0268-0>)
8. A. Sahuquillo, J. F. López-Sánchez, R. Rubio, G. Rauret, R. P. Thomas, C. M. Davidson, A. M. Ure, *Anal. Chim. Acta* **382** (1999) 317 ([https://doi.org/10.1016/S0003-2670\(98\)00754-5](https://doi.org/10.1016/S0003-2670(98)00754-5))
9. K. Nemati, N. K. A. Bakar, M. R. Abas, E. Sobhanezadeh, *J. Hazard. Mater.* **192** (2011) 402 (<https://doi.org/10.1016/j.jhazmat.2011.05.039>)
10. D. Rađenović, Đ. Kerkez, D. Tomašević-Pilipović, M. Dubovina, N. Grba, D. Krčmar, B. Dalmacija, *Sci. Total Environ.* **684** (2019) 186 (<https://doi.org/10.1016/j.scitotenv.2019.05.351>)
11. A. Q. R. Baron, in *Synchrotron Light Sources and Free-Electron Lasers*, E. Jaeschke, S. Khan, J. Schneider, J. Hastings, Eds., Springer, Cham, 2016, pp. 1643–1713 ([http://dx.doi.org/10.1007/978-3-319-14394-1\\_41](http://dx.doi.org/10.1007/978-3-319-14394-1_41))
12. Y. Juhua, C. Qiuwen, Z. Jianyun, Z. Jicheng, F. Chengxin, H. Liuming, S. Wenqing, Y. Wenyong, Z. Yinlong, *Sci. Total Environ.* **658** (2019) 501 (<https://doi.org/10.1016/j.scitotenv.2018.12.226>)
13. S. Pradhanang, *JIST* **19** (2014) 123 (<https://doi.org/10.3126/jist.v19i2.13865>)
14. B. A. Al-Mur, *Oceanologia* **62** (2020) 31 (<https://doi.org/10.1016/j.oceano.2019.07.001>)
15. A. V. Filqueiras, I. Lavilla, C. Bendicho, *J. Environ. Monit.* **4** (2002) 823 (<https://doi.org/10.1039/B207574C>)
16. D. Rađenović, Đ. Kerkez, D. Tomašević-Pilipović, M. Dubovina, N. Grba, D. Krčmar, B. Dalmacija, *Sci. Total Environ.* **684** (2019) 186 (<https://doi.org/10.1016/j.scitotenv.2019.05.351>)
17. A. M. Ziyath, P. Mahbub, A. Goonetilleke, M. O. Adebajo, S. Kokot, A. Oloyede, *J. Water Resour. Prot.* **3** (2011) 758 (<https://doi.org/10.4236/jwarp.2011.310086>)
18. Z. D. Mojović, *PhD Thesis*, University of Belgrade, Belgrade, 2009 ([fedorabg.bg.ac.rs/fedora/get/o:7915/bdef:Content/get](http://fedorabg.bg.ac.rs/fedora/get/o:7915/bdef:Content/get)) (in Serbian)
19. R. Sánchez-Hernández, I. Padilla, S. López-Andrés, A. LópezDelgado, *Desalination Water Treat.* **126** (2018) 181 (<https://doi.org/10.5004/dwt.2018.22816>)
20. I. Obreht, C. Zeeden, P. Schulte, U. Hambach, E. Eckmeier, A. Timar-Gabor, F. Lehmkuhl, *Aeolian Res.* **18** (2015) 69 (<https://doi.org/10.1016/j.aeolia.2015.06.004>)
21. B. Lothenbach, E. Bernard, U. Mäder, *Phys. Chem. Earth* **99** (2017) 77 (<https://doi.org/10.1016/j.pce.2017.02.006>)

22. S. Salimkhani, K. Siahcheshm, A. Kadkhodaie, H. Salimkhani, *Mater. Chem. Phys.* **271** (2021) 124 (<https://doi.org/10.1016/j.matchemphys.2021.124957>)
23. *Albite*, <https://www.britannica.com/science/albite> (accessed August 10, 2021)
24. *Muscovite*, <https://geology.com/minerals/muscovite.shtml> (accessed August 10, 2021)
25. N. Grba, F. Neubauer, A. Šajnović, K. Stojanović, B. Jovančićević, *J. Serb. Chem. Soc.* **80** (2015) 827 (<https://doi.org/10.2298/JSC140317047G>)
26. M. Dubovina, D. Krčmar, N. Grba, M. A. Watson, D. Rađenović, D. Tomašević-Pilipović, B. Dalmacija, *Environ. Pollut.* **236** (2018) 773 (<https://doi.org/10.1016/j.envpol.2018.02.014>)
27. S. Gier, W. D. Johns, *Appl. Clay Sci.* **16** (2000) 289 ([https://doi.org/10.1016/S0169-1317\(00\)0004-1](https://doi.org/10.1016/S0169-1317(00)0004-1)).



## UV light impact on phthalates migration from children's toys into artificial saliva

TATJANA D. ANĐELOKOVIĆ<sup>1\*</sup>, DANICA S. BOGDANOVIĆ<sup>1</sup>, IVANA S. KOSTIĆ KOKIĆ<sup>1</sup>, GORDANA M. KOĆIĆ<sup>2</sup> and RADMILA M. PAVLOVIĆ<sup>3</sup>

<sup>1</sup>University of Niš, Faculty of Science and Mathematics, Department of Chemistry, Višegradska 33, 18000 Niš, Serbia, <sup>2</sup>University of Niš, Faculty of Medicine, Department of Biochemistry, Bulevar dr Zorana Đindića 81, 18000 Niš, Serbia and <sup>3</sup>University of Milan, Department of Veterinary Science and Public Health, Via Celoria 10, 20133 Milan, Italy

(Received 28 September, revised and accepted 15 November 2021)

**Abstract:** Phthalates have been widely used in children's toys as plasticizers and softeners. Therefore, attention should be paid to plastic toys, especially those that children can put in their mouths. In this paper quantification of five phthalates: DMP, DnBP, BBP, DEHP and DnOP in plastic toys, as well as irradiation of toys with UV light was performed. After sample preparation and development of the liquid–liquid phthalate extraction method from artificial saliva phthalate quantitative determination using the GC–MS technique was performed. The mean recovery value for DEHP is  $77.03 \pm 2.76\%$ . The determination of phthalate in the recipient models (artificial saliva and *n*-hexane) was performed after 6, 15 and 30 days of the migration test using the GC–MS technique. Based on the known mass % DEHP in the analyzed toys, the percentage of phthalate migration from each analyzed toy to the recipient model after 6, 15 and 30 days of the migration test was calculated. The results show that there is no significant migration of DEHP into artificial saliva, due to high polarity of the recipient (artificial saliva is polar), unlike *n*-hexane where the migration of DEHP is significant because it is a non-polar solvent.

**Keywords:** plasticizers; PVC; leaching; GC–MS.

### INTRODUCTION

Phthalates represent a group of synthetic chemical compounds, formed in the reaction of phthalic anhydride and alcohol with an aliphatic or aromatic chain. These are the substances most used as a plasticizer, and as such can be found in many consumer products: medical devices, food packaging products, children's toys, cosmetics and pharmaceuticals and other polyvinyl chloride (PVC) materials. The annual production of phthalates is significant and amounted 8 million tons in

\* Corresponding author. E-mail: tatjana.andjelkovic@outlook.com  
<https://doi.org/10.2298/JSC210928097A>

2011 of which diethyl hexyl phthalate (DEHP) production was 4 million tons, corresponding to the fact that DEHP is the most used phthalate.<sup>1,2</sup> Under appropriate conditions such as high temperature, exposure to UV light, long storage time, the phthalates easily migrate from the polymer and are released in the environment, because phthalates are only mixed with the polymer, not chemically bonded.<sup>3–5</sup> Phthalates are classified as endocrine disruptors, because phthalates negatively affect the work of glands that secrete hormones and exposure to phthalates can cause various endocrinological and metabolic disorders.<sup>6–8</sup>

Phthalates has been widely used in children's toys as plastic plasticizers and softeners. Therefore, special attention should be paid to plastic toys, especially those that children can put in their mouths, because children are exposed to phthalates from plastic toys from the earliest stage of their development due to their small body weight and fast metabolism. Due to children's sensitivity to the effects of phthalates from plastic toys the European Commission has restricted the use of DEHP, di-*n*-butyl phthalate (DnBP) and butyl benzyl phthalate (BBP) as plasticizers in children's toys and childcare products, while the restriction on the use of diisononyl phthalate (DINP), diisodecyl phthalate (DIDP) and di-*n*-octyl phthalate (DnOP) only applies to toys that children can put in their mouths. According to Directive 2005/84/EC, products containing 0.1 % DEHP, DnBP and BBP (individually or together) by weight of a plastic product may not be placed on the market. Also, this directive prohibits the placing on the market plastic products that children can put in their mouths, which contain DINP, DIDP and DnOP in a concentration above 0.1 % by weight.<sup>9</sup>

Considering the fact the enormous amount of phthalates production, easy migration of phthalates from plastic materials and the negative impact on human health, various methods have been developed for the determination of phthalates in appropriate matrices. There is a special interest in determination of phthalates in plastic toys so the following instrumental techniques in defining determination methods have been developed till now: gas chromatography coupled with mass spectrometer as detector (GC–MS), high-performance liquid chromatography coupled with photodiode array detection (HPLC-PDA) or UV detection (HPLC-UV).<sup>10–13</sup>

The aim of this work is the detection and quantification of five phthalates – DMP, DnBP, BBP, DEHP and DnOP in plastic toys placed on the market without declaration, as well as irradiation of toys with UV light, in order to determine the influence of UV light on the migration of phthalates from plastic toys. Since these are toys that children can put in their mouths, the analysis of phthalate migration from plastic toys to artificial saliva was also performed and compared with the migration of phthalate to *n*-hexane as a model recipient.

## EXPERIMENTAL

### *Reagents*

The tetrahydrofuran (THF, HPLC grade) was purchased from Fischer scientific (USA). The *n*-hexane (HPLC grade) was purchased from Carlo Erba (France). DMP, DnBP, BBP, DEHP and DnOP were purchased (99.7 % purity) from Sigma–Aldrich. Dibutyl adipate (DBA) was purchased from Fluka (Switzerland) and used as an internal standard.

### *Apparatus and equipment*

Gas chromatographic analysis was performed by gas chromatograph 6890 (Hewlett-Packard, USA) equipped with a mass selective detector (MSD) 5973 (Hewlett-Packard), auto sampler 7683 (Agilent, USA) and SGE 25QC2/BPX5 0.25 capillary column (25 m×0.22 mm×0.25 µm, non-polar). The centrifuge Jouan C4I Benchtop (Termo Fisher) was used to separate the precipitate from the solution. The analytical balance (Kern, CA) with accuracy of ±0.00001 g for gravimetric measurements was used. The Vortex Genie (Scientific industries, USA) was used for vigorous shaking solution of artificial saliva with part of PVC plastic toys. A UV cylinder was used to irradiate UV-A with a wavelength of 365 nm. As a source of UV-C radiation, a UV photo reactor with low pressure mercury lamps, 28 W, with a maximum radiation at 254 nm, manufactured by Philips (Netherlands) was used.

### *Calibration standards*

In order to obtain calibration curves for investigated five phthalates and calibrate GC–MS instrument, five standard solutions with concentration ranged from 80 to 120 % of the expected phthalate concentration in the samples were prepared. Stock, intermediate and standard solutions of the tested phthalates (DMP, DnBP, BBP, DEHP, DnOP) were prepared in *n*-hexane according to the following procedure:

- first, individual stock solutions of each phthalate of concentration 1000 µg mL<sup>-1</sup> were made, which were diluted to obtain an intermediate solution in which the concentration of each phthalate separately was 100 µg mL<sup>-1</sup>;
- standard solutions of concentrations of 0.25, 0.50, 1.00, 1.50 and 2.50 µg mL<sup>-1</sup> were obtained by appropriate dilution of the intermediate solution and addition of DBA as an internal standard at a concentration of 1 µg mL<sup>-1</sup>.

The solutions were stored at 4 °C. The stock solutions are stable for one month, the working solutions are stable for 10 days. Each standard solution was recorded three times using the GC–MS technique, to ensure accuracy of the method.

### *Plastic materials*

In order to determine phthalates in plastic children's toys using the GC–MS technique, 19 plastic children's toys purchased from a market in Niš (Serbia) without a clearly stated declaration of composition were analysed. These are the toys intended for the youngest population – babies, who can put those toys in their mouths. These toys were numbered from 1–19, where the given numbering will be used in further work.

### *Artificial saliva*

For monitoring the migration of phthalates from plastic children's toys to the artificial saliva, artificial saliva was prepared according to the standard procedure of the European Commission.<sup>14</sup> The amounts of chemicals given in Table I were dissolved in 1 L of distilled water, the pH was adjusted to 6.8 with hydrochloric acid and the artificial saliva prepared in this way was stored in the dark.

### *GC–MS technique*

The gas chromatograph was operated in the split less injection mode. The oven temperature was programmed from initial temperature 90 °C (hold time 0 min) to 280 °C at a rate of 20 °C per min with hold time of 4 min, and post run 300 °C (2 min.). Helium was the carrier gas (flow rate of 1.0 mL min<sup>-1</sup>). The operating temperature of the MSD was 280 °C with the electron impact ionization (EI) voltage of 70 eV. The dwell time was 100 ms. The MSD was used in the single ion-monitoring mode (SIM), the quantification ion is *m/z* 149 for DnBP, BBP, DEHP and DnOP, *m/z* 163 for DMP and ion *m/z* 185 was chosen as representative ion of DBA. Analyte response was normalized to DBA as internal standard. The identification and quantification of target compound was based on the relative retention time, the presence of target ions and its relative abundance. Both data acquisition and processing were accomplished by Agilent MSD ChemStation® D.02.00.275 software.

Table I Salts used in the preparation of artificial saliva

| Chemical compound              | Molecular formula               | <i>c</i> / mmol L <sup>-1</sup> |
|--------------------------------|---------------------------------|---------------------------------|
| Magnesium chloride             | MgCl <sub>2</sub>               | 0.82                            |
| Calcium chloride               | CaCl <sub>2</sub>               | 1.00                            |
| Dipotassium hydrogen phosphate | K <sub>2</sub> HPO <sub>4</sub> | 3.30                            |
| Potassium carbonate            | K <sub>2</sub> CO <sub>3</sub>  | 3.80                            |
| Sodium chloride                | NaCl                            | 5.60                            |
| Potassium chloride             | KCl                             | 10.00                           |

### *Determination of phthalates in PVC children's toys*

To confirm that analysed plastic children's toys are made from polyvinyl chloride (PVC), 19 noted plastic toys were dissolved in THF. Dissolution of plastic toys is accelerated by using an ultrasonic bath with gentle heating. Among those 19 toys, even 18 toys were dissolved in THF, while only one toy remained undissolved, from which it follows that the undissolved toy was not made of PVC. The remaining 18 PVC toys, dissolved in THF, were analysed for phthalate content by GC–MS technique.

PVC children's toys were measured (0.01 g) and dissolved in 4 mL of THF. To precipitate the polymer, 10 mL of *n*-hexane was added in THF solutions of each plastic article. After centrifugation of the resulting blur solutions at 3500 rpm and filtration of the supernatant through a 0.45 µm PTFE micro filter, the exact volume of *n*-hexane-THF solution of each article (10 µL) was pipetted and diluted with *n*-hexane to 1 mL with the addition of DBA as an internal standard, after which the analysis of these items were performed by GC–MS technique.

### *Determination of phthalates in artificial saliva*

For monitoring the migration of phthalates from PVC children's toys into artificial saliva, first the optimization of the method for determining the concentration of phthalates in artificial saliva was performed. Artificial saliva (5 mL) was spiked with five analysed phthalates, so that the concentration of phthalates in artificial saliva is 1, 2, 3, 4 and 6 µg mL<sup>-1</sup>. The set conditions and parameters of liquid–liquid extraction (LLE) are as follows: extraction agent is *n*-hexane, extraction time is 10 min and type of agitation is manual shaking, following with 10 min agitation in an ultrasonic bath with ultrasonic waves. After the applied type of agitation and after clarification of the layers, the *n*-hexane layer was pipetted, and the phthalate concentration was determined using the GC–MS technique.

*Monitoring the migration of phthalates from plastic toys into the recipient model and artificial saliva*

Monitoring the migration of phthalates from two toys (Toy 8 and Toy 12) with a known content of DEHP was performed by setting migration tests. *n*-Hexane and artificial saliva were selected as phthalate recipients in order to compare the maximum degree of phthalate migration from plastic toys to *n*-hexane and the realistic scenario of phthalate migration into artificial saliva, because toys that children can put in their mouths were tested.

*Migration of phthalates from PVC toys to the recipient model*

Two noted PVC toys were cut into pieces with an area of about 0.5 cm<sup>2</sup>, where the weight of each item for analysis was about 0.02 g, whereby the measurement was performed with an accuracy of  $\pm 0.00001$  g. *n*-Hexane (5 mL) was added to each cut and measured plastic toys, after which the procedure of monitoring the migration of phthalate from PVC toys into the *n*-hexane recipient model was performed for 6, 15 and 30 days, so that after 6 days the recipient volume was pipetted (250  $\mu$ L) and diluted 4 times with *n*-hexane, then pipetted 10  $\mu$ L of this solution, added 100  $\mu$ L of DBA (10  $\mu$ g mL<sup>-1</sup>) and 890 mL of *n*-hexane. The prepared solution was analyzed by GC-MS technique. The analysis was repeated after the migration tests were performed for 15 and 30 days. To obtain reliable results with a certain standard deviation, the analysis of each item was performed three times.

*Migration of phthalates from PVC toys to artificial saliva*

Selected PVC toys were subjected to the following migration tests:

- PVC toy, with an area of about 1 cm<sup>2</sup>, was covered with artificial saliva (5 mL). Vigorous shaking was performed using a Vortex Genie for 10 min. Then the same piece of PVC toy was poured with a new volume of artificial saliva (5 mL), after which the vigorous shaking was repeated using a Vortex Genie for 10 min. Collect 10 mL of artificial saliva, which was further subjected to optimized LLE extraction with *n*-hexane according to the described procedure. This test approximately simulates real conditions in which a child chews a PVC toy vigorously for 20 min, whereby there is a potential migration of phthalates from the PVC toy into the child's saliva, which may expose the child to the effects of phthalates;
- PVC toy, surface area 0.5 cm<sup>2</sup>, was filled with 5 mL of artificial saliva. The migration test took place within 5, 15 and 30 days. After 5, 10, and 30 days, the artificial saliva potentially contaminated with phthalates was further subjected to optimized LLE extraction with *n*-hexane. This test is experimental, since it does not simulate the real conditions under which phthalates migrate from PVC toys to saliva and was set up to compare the results obtained after phthalate migration.

*Monitoring the influence of UV light on the migration of phthalates from PVC toys into the recipient model and artificial saliva*

The two toys (Toy 8 and Toy 12), in which the DEHP content was determined in this study, were irradiated with UV-A light and UV-C light for a certain time interval, in order to analyze the effects of UV -A and UV-C light on the change in the polymer structure of PVC articles, and thus on the migration of phthalates from these PVC articles. A UV cylinder was used as a source of UV-A irradiation wavelength of 365 nm. As a source of UV-C radiation, a UV photo reactor with low pressure mercury lamps, with a maximum radiation at 254 nm, was used. The toys were placed at 5 cm from these lamps. The UV-A radiation test somewhat imitates sunlight, while the UV-C radiation test sets up an experiment to compare the effects of these two radiations on the migration of phthalates from PVC toys. The PVC toys were

irradiated with UV-A light for 1, 2, 4, 6, 12, 24 h, while PVC toys were irradiated with UV-C light for 1 and 2 h.

To determine the percentage of phthalate migration from irradiated toys, before the migration tests, DEHP quantification was performed in irradiated PVC toys in the described manner.

After appropriate irradiation with UV-A and UV-C light, migration tests were performed:

- Conditions for migration of phthalates from irradiated PVC toys to the recipient model (*n*-hexane) are the same as for the migration of phthalates from non-irradiated toys;

The migration of phthalates from irradiated PVC toys into artificial saliva was also performed in the same way as the migration of phthalates from non-irradiated toys into artificial saliva.

## RESULTS AND DISCUSSION

The obtained calibration curves are linear in this concentration range with calibration coefficients higher than 0.995 for each phthalate and are given in Fig. 1.

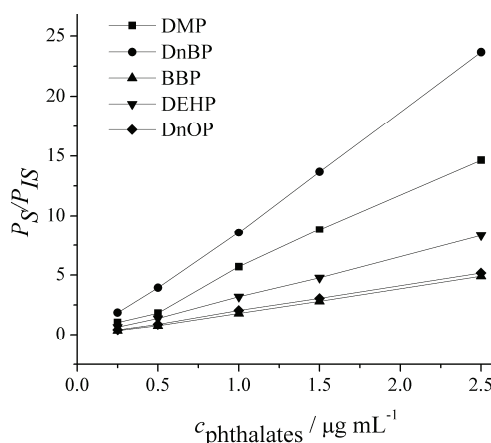


Fig. 1. GC-MS calibration curves in the concentration range  $0.25\text{--}2.5 \mu\text{g mL}^{-1}$  for: DMP, DnBP, BBP, DEHP and DnOP.

### Determination of phthalates in plastic materials by GC-MS technique

The phthalate concentrations in the appropriate prepared samples of 18 PVC toys were determined using the GC-MS technique. Of the five analyzed phthalates, only DEHP was detected. Based on the performed calibration, quantification of DEHP was performed and the results of DEHP quantification in 18 analyzed PVC toys are presented in Table II.

After appropriate sample preparation and development of the liquid-liquid phthalate extraction method from artificial saliva, DEHP quantitative determination was performed using the GC-MS technique and the results of this analysis are shown in Table III.

The mean recovery value for DEHP with standard deviation ( $77.03\pm2.76\%$ ) will be used to calculate the degree of DEHP migration from PVC toys to artificial saliva, given that only DEHP is detected and quantified in PVC toys.

TABLE II. Results of DEHP quantification in PVC children's toys by GC-MS technique

| Toy | $c_{DEHP}$ / mg g <sup>-1</sup> | $c_{DEHP}$ / mass % |
|-----|---------------------------------|---------------------|
| 1   | 532.42±27.2                     | 53.2±2.7            |
| 2   | 430.01±9.40                     | 43.0±0.9            |
| 3   | 406.89±9.19                     | 40.7±0.9            |
| 4   | 402.38±11.2                     | 40.2±1.1            |
| 5   | 400.05±19.5                     | 40.0±1.9            |
| 6   | 373.55±18.5                     | 36.9±1.6            |
| 7   | 368.72±16.1                     | 36.9±1.6            |
| 8   | 368.21±11.7                     | 36.8±1.2            |
| 9   | 364.38±6.43                     | 36.4±0.6            |
| 10  | 313.42±11.1                     | 31.3±1.1            |
| 11  | 295.02±6.31                     | 29.5±0.6            |
| 12  | 270.35±19.2                     | 27.0±1.9            |
| 13  | 102.68±3.06                     | 10.3±0.3            |
| 14  | 1.34±0.09                       | 0.13±0.01           |
| 15  | 1.20±0.20                       | 0.12±0.02           |
| 16  | 0.83±0.09                       | 0.08±0.01           |
| 17  | 0.47±0.02                       | 0.05±0.00           |
| 18  | 0.45±0.08                       | 0.05±0.01           |

TABLE III. Recovery of phthalate extraction from artificial saliva by optimized LLE (%)

| Spike concentration, µg L <sup>-1</sup> | Compound |       |       |       |       |
|---|----------|-------|-------|-------|-------|
|   | DMP      | DnBP  | BBP   | DEHP  | DnOP  |
| 1                                       | 79.44    | 63.16 | 91.11 | 77.15 | 82.23 |
| 2                                       | 76.30    | 66.27 | 95.64 | 73.12 | 79.21 |
| 3                                       | 64.20    | 60.18 | 86.31 | 76.89 | 80.36 |
| 4                                       | 71.11    | 64.98 | 90.60 | 77.10 | 79.32 |
| 6                                       | 66.57    | 65.41 | 90.52 | 80.91 | 82.10 |

#### *Phthalate migration into the recipient model and artificial saliva*

Based on the known mass % of DEHP in the analyzed toys, the degree of DEHP migration from each analyzed toy into the recipient model after 6, 15 and 30 days of the migration test was calculated using the GC-MS technique and the data are shown in Table IV. It was concluded that the degree of DEHP migration is higher for Toy 8 after each migration test, in different time periods. The reason for that is most likely that the PVC toys were cut into pieces with an area of 0.5 cm<sup>2</sup>, and since the piece of Toy 12 is thicker, the area of 0.5 cm<sup>2</sup> is therefore of greater mass. The contact model of the recipient and DEHP in the plastic material is more probable and it takes less time for DEHP to migrate from plastic layer to the recipient model when it comes to the Toy 8.

The obtained results of the migration test for 6, 15 and 30 days in which DEHP was migrated to artificial saliva and of the migration test which simulates

the real situation of chewing a toy in the mouth by a child for 1 day for 20 min, were shown in Table V.

TABLE IV. Degree of DEHP migration into *n*-hexane relative to the mass of DEHP in PVC toy (%)

| PVC toy | Mass of PVC toy<br>g | Mass of DEHP in PVC toy<br>μg | <i>t</i> / days |       |       |
|---------|----------------------|-------------------------------|-----------------|-------|-------|
|         |                      |                               | 6               | 15    | 30    |
| 8       | 0.0246               | 9057                          | 64.70           | 77.29 | 85.92 |
| 12      | 0.0426               | 11519                         | 60.97           | 73.26 | 80.63 |

TABLE V. Degree of DEHP migration into artificial saliva relative to the mass of DEHP in PVC toys

| Time of migration, day | Mass of PVC toy, g | Mass of DEHP in PVC toy, μg | Maximum amount of migrated DEHP, μg | Degree of DEHP migration, % |
|------------------------|--------------------|-----------------------------|-------------------------------------|-----------------------------|
| Toy 8                  |                    |                             |                                     |                             |
| 1                      | 0.1661             | 61158                       | 3.25                                | 0.005                       |
| 6                      | 0.0389             | 14324                       | 1.62                                | 0.011                       |
| 15                     | 0.0388             | 14286                       | 2.14                                | 0.015                       |
| 30                     | 0.0183             | 6738                        | 1.86                                | 0.028                       |
| Toy 12                 |                    |                             |                                     |                             |
| 1                      | 0.1632             | 44129                       | 6.21                                | 0.014                       |
| 6                      | 0.0491             | 13276                       | 2.10                                | 0.016                       |
| 15                     | 0.0441             | 11924                       | 2.14                                | 0.018                       |
| 30                     | 0.0415             | 11221                       | 3.36                                | 0.030                       |

*Results of determining the influence of factors on the migration of phthalates from PVC toys into the recipient model and artificial saliva*

The results show that migration was almost non-existent. The migration rate for DEHP ranges from 0.005 to 0.028 % for Toy 8, while for Toy 12 this rate ranges from 0.014 to 0.030 %. The mass of the migrated DEHP during migration that simulates real conditions was 3.25 μg for Toy 8 and 6.21 μg for Toy 12. The weight of migrated DEHP in relation to the body weight of a child at that age (10 kg) was 0.325 or 0.621 μg kg<sup>-1</sup>, which is far below the TDI value for DEHP which is 0.05 mg kg<sup>-1</sup>.

After UV-A and UV-C light irradiation of PVC Toy 8 and Toy 12, with an area of 1 cm<sup>2</sup>, a time period as a factor that influence the change in the structure of the polymer and thus the DEHP migration from these articles was determined. The migration degree was calculated after performing the following migration tests: DEHP migration into the recipient model (after 6, 15 and 30 days) and DEHP migration into artificial saliva (after 6, 15 and 30 days and within one day) and by performing liquid-liquid extractions of DEHP from artificial saliva by the optimized method.

In order to calculate the degree of DEHP migration based on the mass of DEHP in irradiated toys, DEHP in irradiated toys was quantified by the GC-MS technique after dissolving these toys in THF according to an optimized method. The quantification results were given in Table VII. The presented results showed the influence of UV-A and UV-C light on the properties of PVC toys in terms of DEHP content. By irradiating the toys, there is a weakening of the interaction strength between DEHP and the polymer and there is a migration of DEHP into the atmosphere, which affects the decreasing mass % DEHP in the toys with radiation time. The weight percentages of DEHP in Toy 12 decrease from 27.04 to 19.58 mass %, while this range for Toy 8 ranges from 36.82 to 30.81 mass %. UV-A radiation for 2 h leads to the most significant change in the percentage composition of PVC toys, while further radiation reduces the percentage composition of DEHP gradually.

TABLE VI. The degree of DEHP migration from irradiated PVC toy 12 to model recipient; a and b values with the same letter within a row are not statistically significant different at the  $p < 0.05$  level (Tukey's HSD test)

| PVC Toy | Type of radiation | Time of radiation, h | Content of DEHP in PVC toy, mass % | Degree of DEHP migration, % |                      |                    |
|---------|-------------------|----------------------|------------------------------------|-----------------------------|----------------------|--------------------|
|         |                   |                      |                                    | 6 days                      | 15 days              | 30 days            |
| 12      | UV-A              | 0                    | 27.04±1.92                         | 60.97 <sup>a</sup>          | 73.26 <sup>a,b</sup> | 80.63 <sup>b</sup> |
|         |                   | 2                    | 21.87±2.25                         | 65.60 <sup>a</sup>          | 80.46 <sup>a,b</sup> | 87.14 <sup>b</sup> |
|         |                   | 4                    | 21.45±1.08                         | 66.19 <sup>a</sup>          | 81.37 <sup>a,b</sup> | 88.01 <sup>b</sup> |
|         |                   | 6                    | 20.75±2.46                         | 67.76 <sup>a</sup>          | 81.66 <sup>a,b</sup> | 89.49 <sup>b</sup> |
|         |                   | 12                   | 21.67±1.12                         | 70.87 <sup>a</sup>          | 83.30 <sup>a,b</sup> | 90.44 <sup>b</sup> |
|         |                   | 24                   | 21.13±1.13                         | 71.52 <sup>a</sup>          | 84.45 <sup>a,b</sup> | 91.59 <sup>b</sup> |
|         |                   | 1                    | 20.03±0.11                         | 75.68 <sup>a</sup>          | 88.86 <sup>a,b</sup> | 96.47 <sup>b</sup> |
|         | UV-C              | 2                    | 19.58±0.17                         | 76.25 <sup>a</sup>          | 90.49 <sup>a,b</sup> | 97.25 <sup>b</sup> |

Also, Tables VI and VII show the results of DEHP migration tests to the recipient model after 6, 15 and 30 days of DEHP migration.

TABLE VII. The degree of DEHP migration from irradiated PVC toy 8 to model recipient; a and b values with the same letter within a row are not statistically significant different at the  $p < 0.05$  level (Tukey's HSD test)

| PVC Toy | Type of radiation | Time of radiation, h | Content of DEHP in PVC toy, mass % | Degree of DEHP migration, % |                      |                    |
|---------|-------------------|----------------------|------------------------------------|-----------------------------|----------------------|--------------------|
|         |                   |                      |                                    | 6 days                      | 15 days              | 30 days            |
| 8       | UV-A              | 0                    | 36.82±1.17                         | 64.70 <sup>a</sup>          | 77.29 <sup>a,b</sup> | 85.92 <sup>b</sup> |
|         |                   | 1                    | 33.75±0.21                         | 67.73 <sup>a</sup>          | 84.98 <sup>a,b</sup> | 90.69 <sup>b</sup> |
|         |                   | 2                    | 33.32±0.75                         | 71.39 <sup>a</sup>          | 83.84 <sup>a,b</sup> | 86.92 <sup>b</sup> |
|         |                   | 4                    | 33.59±1.02                         | 68.48 <sup>a</sup>          | 84.84 <sup>a,b</sup> | 91.72 <sup>b</sup> |
|         |                   | 6                    | 33.50±1.98                         | 72.02 <sup>a</sup>          | 83.23 <sup>a,b</sup> | 87.14 <sup>b</sup> |
|         |                   | 12                   | 33.04±1.41                         | 73.75 <sup>a</sup>          | 84.75 <sup>a,b</sup> | 91.61 <sup>b</sup> |
|         |                   | 24                   | 33.39±1.12                         | 75.08 <sup>a</sup>          | 86.30 <sup>a,b</sup> | 90.27 <sup>b</sup> |
|         | UV-C              | 1                    | 31.22±0.17                         | 79.56 <sup>a</sup>          | 90.44 <sup>a,b</sup> | 99.16 <sup>b</sup> |
|         |                   | 2                    | 30.81±0.19                         | 79.67 <sup>a</sup>          | 91.81 <sup>a,b</sup> | 99.41 <sup>b</sup> |

Unlike DEHP migration from non-irradiated toys where the percentage was 80.63 % for Toy 12 and 85.92 % for Toy 8 after 30 days, the percentage of migration after radiation of toys increases to 97.25 % for Toy 12 and 99.41 % for Toy 8 in relation to the mass of the toy. The same trend applies to migration tests lasting 6 and 15 days, which confirms that radiation disrupts the bonds that exist between DEHP and polymers in PVC toys, thus enabling easier migration.

In order to determine a significant difference between the results obtained after different migration periods (6, 15 and 30 days), the obtained mass concentrations of DEHP listed in Tables VI and VII were compared using Tukey's HSD test. Significant difference (*HSD*) values for each pair of results were calculated using the Origin<sup>©</sup> program, for  $p < 0.05$ , and compared with a tabular value of 3.70.<sup>15</sup> The obtained results show that there is a significant difference in DEHP migration after 6 and 30 days for all analyzed toys. There is no significant difference in DEHP migration after 6 and 15 days of migration, as well as after 15 and 30 days.

Tables VIII and IX show the results of performed migration tests during 6, 15 and 30 days, as well as for one day, in which DEHP was migrated from irradiated toys to artificial saliva.

TABLE VIII. The degree of DEHP migration from irradiated PVC toy 12 to artificial saliva

| PVC toy | Type of radiation | Time of radiation, h | Degree of DEHP migration, % |        |         |         |
|---------|-------------------|----------------------|-----------------------------|--------|---------|---------|
|         |                   |                      | During one day              | 6 days | 15 days | 30 days |
| 12      | UV-A              | —                    | 0.01                        | 0.02   | 0.02    | 0.03    |
|         |                   | 2                    | 0.02                        | 0.02   | 0.03    | 0.02    |
|         |                   | 4                    | 0.02                        | 0.03   | 0.05    | 0.02    |
|         |                   | 6                    | 0.02                        | 0.03   | 0.03    | 0.02    |
|         |                   | 12                   | 0.01                        | 0.02   | 0.02    | 0.02    |
|         |                   | 24                   | 0.01                        | 0.01   | 0.02    | 0.02    |
|         | UV-C              | 1                    | 0.01                        | 0.03   | 0.08    | 0.02    |
|         |                   | 2                    | 0.01                        | 0.02   | 0.02    | 0.02    |

TABLE IX. The degree of DEHP migration from irradiated PVC toy 8 to artificial saliva

| PVC toy | Type of radiation | Time of radiation, h | Degree of DEHP migration, % |        |         |         |
|---------|-------------------|----------------------|-----------------------------|--------|---------|---------|
|         |                   |                      | During one day              | 6 days | 15 days | 30 days |
| 8       | UV-A              | —                    | 0.01                        | 0.01   | 0.02    | 0.03    |
|         |                   | 1                    | 0.02                        | 0.04   | 0.02    | 0.02    |
|         |                   | 2                    | 0.01                        | 0.02   | 0.04    | 0.02    |
|         |                   | 4                    | 0.01                        | 0.02   | 0.03    | 0.02    |
|         |                   | 6                    | 0.01                        | 0.03   | 0.03    | 0.02    |
|         |                   | 12                   | 0.01                        | 0.02   | 0.03    | 0.02    |
|         |                   | 24                   | 0.02                        | 0.01   | 0.03    | 0.02    |
|         | UV-C              | 1                    | 0.01                        | 0.02   | 0.02    | 0.02    |
|         |                   | 2                    | 0.01                        | 0.01   | 0.01    | 0.02    |

The results show that there is no significant migration of DEHP into artificial saliva, which is the case with non-irradiated toys. The reason for this is the polarity of the recipient (artificial saliva is polar), unlike *n*-hexane where the migration of DEHP is significant because it is a non-polar solvent.

#### CONCLUSION

The results of determining the degree of migration of phthalates from PVC toys to artificial saliva show that the migration of phthalates is at very low level. However, there must be a concern present since the tested PVC toys contain up to 50 % phthalate. By changing certain conditions, like UV light irradiation, phthalates can migrate, due to mechanical pressure by the teeth. Due to the high exposure of children to phthalates from these toys and rapid metabolism and insufficient physiological maturity of children restriction on the use of phthalates should be followed. DEHP is the predominant plasticizer for PVC toys. It is commonly used at concentrations varying between 30 and 45 % by weight. Based on the known mass % DEHP in the analyzed toys, the percentage of phthalate migration from each analyzed toy to the recipient model after 6, 15 and 30 days of the migration test was calculated. The results show that there is no significant migration of DEHP into artificial saliva, due to high polarity of the recipient (artificial saliva is polar), unlike *n*-hexane where the migration of DEHP is significant because it is a non-polar solvent. By irradiation of toys, a weakening of the interaction strength between DEHP and the polymer occurs leading to migration of DEHP into the atmosphere, which affects the decreasing of mass % DEHP in the toys with radiation time. UV-A radiation for 2 h leads to the most significant change in the percentage composition of PVC toys, while further radiation reduces the percentage composition of DEHP gradually.

*Acknowledgment.* This study was performed within the research program – Contract No. 451-03-9/2021-14/200124.

#### ИЗВОД

#### УТИЦАЈ UV ЗРАЧЕЊА НА МИГРАЦИЈУ ФТАЛАТА ИЗ ДЕЧЈИХ ИГРАЧАКА У ВЕШТАЧКУ ПЉУВАЧКУ

ТАТЈАНА Д. АНЂЕЛКОВИЋ<sup>1</sup>, ДАНИЦА С. БОГДАНОВИЋ<sup>1</sup>, ИВАНА С. КОСТИЋ КОКИЋ<sup>1</sup>, ГОРДАНА М. КОЦИЋ<sup>2</sup>  
и РАДМИЛА М. ПАВЛОВИЋ<sup>3</sup>

<sup>1</sup>Универзитет у Нишу, Природно-математички факултет, Департањман за хемију, Вишеградска 33,  
18000 Ниш, <sup>2</sup>Универзитет у Нишу, Медицински факултет, Департањман за биохемију, Булевар  
гр Зорана Ђинђића, 18000 Ниш и <sup>3</sup>University of Milan, Department of Veterinary Science and Public  
Health, Via Celoria 10, 20133 Milan, Italy

Фталати се широко користе у дечјим играчкама као пластификатори и омекшивачи. Због тога треба обратити пажњу на пластичне играчке, посебно оне које деца могу ставити у уста. У овом раду извршена је квантификација пет фталата: DMP, DnBP, BBP, DEHP и DnOP у пластичним играчкама, као и зрачење играчака UV светлом. Након припреме узорака и развоја методе течно-течне екстракције фталата из вештачке пљувачке

извршено је квантитативно одређивање помоћу GC–MS технике. Средња *Recovery* вредност за DEHP је  $77,03 \pm 2,76\%$ . Одређивање фталата у модел реципијентима (вештачка пљувачка и *n*-хексан) изведено је након 6, 15 и 30 дана теста миграције применом GC–MS технике. На основу познатог масеног процента DEHP у анализираним играчкама, израчунат је проценат миграције фталата из сваке анализиране играчке у модел реципијент након 6, 15 и 30 дана миграционог тестира. Резултати показују да нема значајне миграције DEHP у вештачку пљувачку, због високе поларности реципијента (вештачка пљувачка је поларна), за разлику од *n*-хексана где је миграција DEHP значајна јер је растварач неполаран. Зрачењем играчака долази до слабљења снаге интеракције између DEHP и полимера што доводи до миграције DEHP у атмосферу, што утиче на смањење мас. % DEHP у играчкама с временом зрачења. UV-A зрачење током 2 сата доводи до најзначајније промене процентног састава DEHP у PVC играчкама, док даље зрачење поступно смањује процентни састав DEHP.

(Примљено 29. септембра, ревидирано и прихваћено 15. новембра 2021)

#### REFERENCES

1. S. Net, R. Sempere, A. Delmont, A. Paluselli, B. Ouddane, *Environ. Sci. Technol.* **49** (2015) 4019 (<https://doi.org/10.1021/es505233b>)
2. K. Stamatelatou, C. Pakou, G. Lyberatos, *Comprehen. Biotechnol.* **6** (2011) 473 (<https://doi.org/10.1016/B978-0-08-088504-9.00496-7>)
3. R. Rudel, L. Perovich, *Atmos. Environ.* **43** (2008) 170 (<https://doi.org/10.1016/j.atmosenv.2008.09.025>)
4. M. Criado, V. Fernandez Pinto, A. Badessari, D. Cabral, *Int. J. Food Microbiol.* **99** (2005) 343 (<https://doi.org/10.1016/j.ijfoodmicro.2004.10.036>)
5. I. Kostić, T. Andjelković, D. Andjelković, T. Cvetkovic, D. Pavlović, *J. Serb. Chem. Soc.* **83(10)** (2018) 1157 (<https://doi.org/10.2298/JSC180423058K>)
6. E. Gray, J. Ostby, J. Furr, M. Price, R. Veeramachaneni, L. Parks, *Toxicol. Sci.* **58** (2000) 350 (<https://doi.org/10.1093/toxsci/58.2.350>)
7. R. H. Waring, R. M. Harris, *Maturitas* **68** (2011) 111 (<https://doi.org/10.1016/j.maturitas.2010.10.008>)
8. S. S. S. Rowdhwal, J. Chen, *BioMed Res. Int.* (2018) 1 (<https://doi.org/10.1155/2018/1750368>)
9. Directive 2005/84/EC of the European Parliament and of the Council, *Off. J. Eur. Union*, 2005
10. M. Al-Natsheh, M. Alawi, M. Fayyada, I. Tarawneh, *J. Chrom., B* **985** (2015) 103 (<https://doi.org/10.1016/j.jchromb.2015.01.010>)
11. T. Yuzawa, C. Watanabe, R. Freeman, S. Tsuge, *Anal. Sci.* **25** (2009) 1057 (<https://doi.org/10.2116/analsci.25.1057>)
12. M. Akkbik, V. Ali Turksoy, S. Koçoğlu, *Toxicol. Mech. Methods* **30** (2020) 33 (<https://doi.org/10.1080/15376516.2019.1650145>)
13. U. Hauri, U. Schlegel, M. Wagmann, C. Hohl, *Mitt. Gebiete Lebensm. Hyg.* **93** (2002) 179
14. *Standard operation procedure for Determination of release of phthalate plasticizers in saliva simulant, Appendix I of report V3932*, Ref. Ares 4242543, 2015
15. R. Hampton, J. Havel, *Introductory biological statistics*, Waveland Press, Long Grove, IL, 2006, pp. 99–120.



## Modelling of gas–particle partitioning of PAHs according to ab/adsorption approach

MIRJANA VOJINOVIĆ MILORADOV<sup>1#</sup>, MAJA TURK SEKULIĆ<sup>1</sup>,  
LAZAR IGNJATOVIĆ<sup>2</sup>, SMILJA KRAJNOVIĆ<sup>1</sup>, DRAGAN ADAMOVIĆ<sup>1\*</sup>  
and JELENA RADONIĆ<sup>1</sup>

<sup>1</sup>University of Novi Sad, Faculty of Technical Sciences, Novi Sad, Serbia and <sup>2</sup>Jaroslav Černi Water Institute, Belgrade, Serbia

(Received 29 November, accepted 17 December 2021)

**Abstract:** The new approach of the study was to assess the consistency between the gas–particle partition coefficients of 16 EPA (Environmental Protection Agency) polycyclic aromatic hydrocarbons (PAHs) predicted by the Dachs–Eisenreich ab/adsorption model and the experimental results obtained within the field measurements. A total number of 29 air samples was obtained at 9 locations in Serbia. High volume air sampler was applied, with quartz filters for collecting the atmospheric particles and polyurethane foam filters (PUF) for retaining the free gas molecules of PAHs. The results predicted by the model and the experimental data were compared. The deviations between the measured and predicted *f* (fraction) values were less than one order of magnitude for Flo, Phe, Ant, Flu, Pyr, B(a)A and Chr. For the PAHs with high molecular mass, B(b)F, B(k)F, B(a)P, I(1,2,3-cd)P, D(ah)A and B(ghi)P, very good agreement was confirmed, except for the data measured at the Oil refinery in Pančevo. The applied model underestimated the concentrations of PAHs in gas-phase for the low-molecular mass PAHs.

**Keywords:** Dachs–Eisenreich model; high volume sampling; air pollution.

### INTRODUCTION

Gas/particle partitioning is a complex and sophisticated mechanism affecting the fate, transmission and transport of semivolatile organic compounds (SOCs), such as PAHs.<sup>1</sup> It gets the modelling of atmospheric distribution into the focus of recent investigations. During the previous decades, numerous methods have been suggested for modelling the sorption processes, ad/absorption and gas–particle

\* Corresponding author. E-mail: draganadamovic@uns.ac.rs

# Serbian Chemical Society member.

<https://doi.org/10.2298/JSC211129109V>

partitioning of SOC.<sup>1–5</sup> The atmosphere is the dominant medium for the transport and transformation processes of generated PAHs. In the atmosphere, PAHs can be present as free gas molecules (lower molecular mass PAHs) or can be ad/absorbed onto/into aerosol particles (higher molecular mass PAHs) and transmitted over the long distances.<sup>6</sup>

US EPA classified 16 PAHs (naphthalene, Nap; acenaphthylene, Acy; ace-naphthene, Ace; fluorene, Flo; phenanthrene, Phe; pyrene, Pyr; fluoranthene, Flu; anthracene, Ant; chrysene, Chr; benz[a]anthracene, B(a)A; benzo[b]fluoranthene, B(b)F; benzo[k]fluoranthene, B(k)F; benzo[a]pyrene, B(a)P; dibenz[a,h]anthracene, D(ah)A; benzo[ghi]perylene, B(ghi)P; indeno[1,2,3-c,d]pyrene, I(123cd)P) as priority pollutants, due to their high frequency of detection in soil, air and water samples.<sup>5</sup> The selected 16 PAHs can be classified according to the value of vapour pressure and molar mass in three groups: PAHs as free gas molecules (Nap, Acy, Ace, Flo, Phe, Ant), PAHs distributed between gas and particle phase (Chr, B(a)A, Pyr, Flu) and PAHs associated with particle phase (B(b)F, B(k)F, B(a)P, D(ah)A, B(ghi)P, I(123cd)P).<sup>5</sup>

The mostly investigated pathological effect of PAHs is their high toxicity and the most hazardous compound of the group is cancerogenic, teratogenic and genotoxic B(a)P. The main source of atmospheric PAHs is the incomplete combustion of organic matter. Soot particles are byproducts of the liquid and gaseous fuels combustion and PAHs perform an important role in soot formation and particle growth.<sup>7</sup> PAHs have a significant affinity for carbonaceous materials, so the adsorption of PAHs onto the soot fraction of atmospheric aerosols, or primary aerosol carbon with which it is highly correlated, may be a dominant mechanism affecting the gas-particle partitioning of PAHs.<sup>1</sup>

The main purpose of our study was to assess the consistency between the gas-particle partition coefficients of 16 EPA priority PAHs predicted by the Dachs-Eisenreich ab/adsorption model and the experimental results gained within the field measurements.

## EXPERIMENTAL

Air samples (gas and particulate) were taken in the urban and industrial area of the three cities in Serbia (Novi Sad, Pančevo, Kragujevac).

The three sampling sites in the city of Novi Sad were: N1, Oil Refinery Novi Sad (N 45° 16' 23,3"; E 19° 52' 12,1"), N2, Šangaj settlement, near the oil refinery (N 45° 16' 22,7"; E 19° 52' 24,1") and N3, city centre (N 45° 14' 54,3"; E 19° 50' 42,9"). The three sampling sites in the city of Pančevo were: P1, Oil refinery Pančevo (N 44° 49' 56,3"; E 20° 41' 25,4"), P2, Chemical Industry Pančevo (N 44° 49' 57,0"; E 20° 40' 17,0") and P3, city centre (N 44° 52' 12,8"; E 20° 38' 24,1"). In the city of Kragujevac, two samples were collected in the "Zastava" car factory: K1 (N 44° 0' 10,5"; E 20° 54' 46,6") and K2 (N 44° 0' 13,7"; E 20° 54' 45,9"). The third sample, K3 was collected in the city centre (N 44° 1' 4,2" E 20° 54' 45,9").<sup>5</sup>

Three air samples (gaseous and particle phase) were collected at sampling sites N1, N2, N3, P2, K1, K2 and K3 and four samples at the sites P1 and P3, therefore the total number of 29 air samples was obtained from 9 representative monitoring stations.

High volume air sampler, HVAS, was used, with quartz filters for collecting the atmospheric particles (GF) and polyurethane foam filters (PUF) for collecting the free gas molecules. The samples were analyzed using GC-MS instrument (HP 6890 – HP 5972) supplied with a J&W Scientific fused silica column DB-5MS. All analytical procedures were done in the laboratories of the Research Centre for Environmental Chemistry and Ecotoxicology (RECETOX), Masaryk University, Brno, Czech Republic.

#### *The gas-particle partition coefficient $K_p$ and particle bound fraction $\phi$*

The gas-particle partitioning could be quantified using partitioning coefficient,  $K_p$ , or particle-bound fraction,  $\phi$ . Fraction is defined as a ratio of compound concentration associated with the particle phase ( $F / \text{ng m}^{-3}$ ) over the sum of compound gaseous phase concentrations ( $A / \text{ng m}^{-3}$ ) and particle phase concentrations:<sup>8</sup>

$$\phi = \frac{F}{A + F} = \frac{K_p c_{\text{TSP}}}{1 + K_p c_{\text{TSP}}} \quad (1)$$

Coefficient  $K_p$  is a ratio of  $F/c_{\text{TSP}}$  over  $A$ , where  $c_{\text{TSP}}$  is the concentration of total suspended particles (TSP) in the air ( $\mu\text{g m}^{-3}$ ).<sup>8</sup>

$$K_p = \frac{F / c_{\text{TSP}}}{A} \quad (2)$$

#### *Dachs–Eisenreich sorption model*

The Dachs–Eisenreich sorption model, unlike other previously widely discussed adsorption and absorption models,<sup>1</sup> considers the partitioning of pollutants into two aerosol components: absorption into organic matter (OM) and adsorption to aerosol elemental carbon (EC).<sup>1</sup>

$$K_p = 10^{-12} [f_{\text{OM}} M_{\text{oct}} \gamma_{\text{oct}} / \rho_{\text{oct}} M_{\text{OM}} \gamma_{\text{OM}}] K_{\text{OA}} + f_{\text{EC}} (a_{\text{EC}} / a_{\text{SC}}) K_{\text{SA}} \quad (3)$$

where:  $f_{\text{OM}}$  and  $f_{\text{EC}}$  are fractions of organic matter and elemental carbon on the TSP, respectively,  $K_{\text{OA}}$  is octanol/air partition coefficient,  $K_{\text{SA}}$  is soot/air partition coefficient,  $\text{L kg}^{-1}$ ,  $M_{\text{oct}}$  is molecular weight of the octanol,  $130.23 \text{ g mol}^{-1}$ ,  $M_{\text{OM}}$  is molecular weight of the organic matter phase,  $\text{g mol}^{-1}$ ,  $\rho_{\text{oct}}$  is density of octanol,  $0.82 \text{ kg L}^{-1}$ ,  $10^{-12}$  comes from:  $10^{-9} \text{ kg } \mu\text{g}^{-1} \times 10^{-3} \text{ m}^3 \text{ L}^{-1}$ , units conversion factor,  $a_{\text{EC}}$  and  $a_{\text{SC}}$  are specific surface areas ( $\text{m}^2 \text{ g}^{-1}$ ) of the aerosol elemental carbon and the soot carbon, respectively, used to measure  $K_{\text{SA}}$  (the D-E model<sup>1</sup> assumes this ratio is equal to 1).

The model further presumes that  $M_{\text{oct}}/M_{\text{OM}}$  and  $\gamma_{\text{oct}}/\gamma_{\text{OM}}$  are equal to 1. The model assumes that well-known octanol and elemental carbon are good surrogates of organic matter and soot, respectively.

If the partition is calculated only with the first part of the equation,  $K_p$  values would be underpredicted by 10 to 50 times. It is in accordance with the known fact that the majority of PAHs family members express a greater tendency to sorb onto the soot phase than into the organic matter per mass of sorption phase.<sup>1</sup>

## RESULTS AND DISCUSSION

#### *TSP, EC and atmospheric PAHs concentrations*

The concentrations of TSP and EC applied in the modelling process are given in Table I.

TABLE I. TSP and EC concentrations

| Parameter                             | P1-P3                        | N1                            | N2                            | N3                            | K1-K3 <sup>a</sup> | S1-S4 <sup>a</sup> | T1-T5 <sup>a</sup> |
|---------------------------------------|------------------------------|-------------------------------|-------------------------------|-------------------------------|--------------------|--------------------|--------------------|
| $c_{\text{TSP}} / \mu\text{g m}^{-3}$ | 114<br>(47–173) <sup>b</sup> | 187<br>(116–267) <sup>b</sup> | 187<br>(116–267) <sup>b</sup> | 205<br>(124–256) <sup>b</sup> | 100                | 100                | 100                |
| $c_{\text{EC}} / \mu\text{g m}^{-3}$  | 3.4<br>(8–13) <sup>b</sup>   | 5<br>(1–13) <sup>b</sup>      | 5<br>(1–13) <sup>b</sup>      | 4<br>(1–12) <sup>b</sup>      | —                  | —                  | —                  |
| $f_{\text{EC}}$                       | 0.0298                       | 0.0267                        | 0.0267                        | 0.0195                        | 0.05               | 0.05               | 0.05               |

<sup>a</sup>Literature data; <sup>b</sup>range of concentrations

In the vicinity of the Pančevo centre, TSP concentrations ranged from 47 to 173  $\mu\text{g m}^{-3}$ , with the average value of 114  $\mu\text{g m}^{-3}$ . In Šangaj settlement, Novi Sad, TSP concentrations ranged from 116 to 267  $\mu\text{g m}^{-3}$  (average 187  $\mu\text{g m}^{-3}$ ) and in the Novi Sad centre, from 124 to 256  $\mu\text{g m}^{-3}$  (average 205  $\mu\text{g m}^{-3}$ ). The TSP concentration values measured at P3 were also applied for the modelling at the P1 and P2 locations. In the city of Pančevo, the EC concentrations ranged from 8 to 13  $\mu\text{g m}^{-3}$  (average 3.4  $\mu\text{g m}^{-3}$ ;  $f_{\text{EC}} = 0.0298$ ). In Šangaj settlement, the EC levels ranged from 1 to 13  $\mu\text{g m}^{-3}$  (average 5  $\mu\text{g m}^{-3}$ ;  $f_{\text{EC}} = 0.0267$ ) and, in the Novi Sad centre, from 1 to 12  $\mu\text{g m}^{-3}$  (average 4  $\mu\text{g m}^{-3}$ ;  $f_{\text{EC}} = 0.0195$ ). At the location P3 the TSP levels were lower than in Novi Sad, but the fraction of elemental carbon (soot phase),  $f_{\text{EC}}$ , was higher. There were no measured data for TSP, EC and  $f_{\text{EC}}$  for the cities of Kragujevac, Sarajevo and Tuzla, therefore the literature values were used. The TSP concentrations for different spatial conditions (suburban: 60  $\mu\text{g m}^{-3}$ , urban: 100  $\mu\text{g m}^{-3}$ ) are given by Whitby.<sup>9</sup> The mass fraction of elemental carbon  $f_{\text{EC}}$  in aerosol particles for urban conditions ( $f_{\text{EC}} = m_{\text{EC}}/m_{\text{TSP}} = 0.05$ ) is published by Jonkers and Koelmans,<sup>1</sup> Seinfeld and Pandis,<sup>7</sup> Vardar *et al.*<sup>10</sup> and Dachs and Eisenreich.<sup>11</sup>

The measured atmospheric concentrations of gas and particle phase of PAHs ( $\text{ng m}^{-3}$ ) at locations in Serbia are shown on Fig. 1.

Fig. 1 displays that gas molecule concentrations of lower molecular mass PAHs (Phe, Flu and Pyr) were about two to four times higher at Oil Refinery Pančevo and Chemical Industry Pančevo comparing to urban locations in Novi Sad. Gas concentrations at Oil Refinery Novi Sad are higher than in the city, but still lower than at Oil Refinery Pančevo and Chemical Industry Pančevo. The variability in the aerosol and gas molecule concentrations of PAHs is related to wind direction and EC concentrations in the aerosols.<sup>1</sup>

The most notably variations of measured  $\phi$  fractions are recorded for the group of PAHs presented in both, gas and particle phase (B(a)A, Chr), Fig. 2.

The particle bound fractions of 16 EPA PAHs (in percentage) were calculated for all nine locations in Serbia using the Eq. (1) and it is shown later in Figs. 3–7 as the “measured value”, when measured and predicted values are compared.

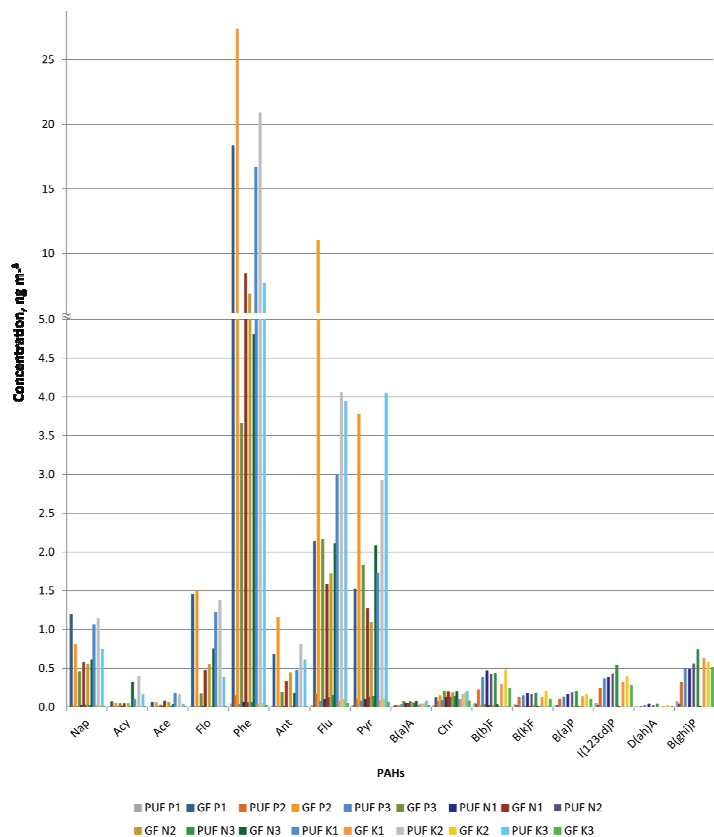


Fig. 1. Median values of measured atmospheric concentrations of PAHs gas (PUF) and particle phase (GF) at locations in Serbia.

#### *Dachs–Eisenreich model*

In order to perform the modelling process, values for the vapour pressure  $p_L^0$  and  $\log K_{OA}$  were obtained from Mackay *et al.*,<sup>12</sup> and the values for  $\log K_{SA}$  were calculated using the Eq. (4) except for the values for Flo, Phe, Ant, Flu, Pyr, Chr and B(a)P, which were taken from the Lohmann and Lammel:<sup>4</sup>

$$K_{SA} = -0.85 \log p_L^0 + 8.94 - \log \left( \frac{998}{a_{EC}} \right) \quad (4)$$

The data were not available for the organic matter fraction  $f_{OM}$ , the  $K_p$  and  $\phi$  values, so they were calculated using  $f_{OM} = 0.40$  for urban conditions and  $f_{OM} = 0.25$  for suburban conditions, recommended by Seinfeld and Pandis,<sup>7</sup> and also using  $f_{OM} = 0.20$ , proposed by Jonkers and Koelmans.<sup>11</sup> Values from Table I for TSP and  $f_{EC}$  were used to calculate the partition coefficient  $K_p$  by the Dachs–Eisenreich Equation:<sup>1</sup>

$$K_p = \frac{f_{OM}}{10^{12} \rho_{oct}} K_{OA} + \frac{f_{EC}}{10^{12}} K_{SA} \quad (5)$$

and the particle bound fraction  $\phi$  was calculated using Eq. (1).

The values for vapour pressure,  $\log K_{OA}$  and  $\log K_{SA}$  of 16 EPA priority PAHs are presented in Table II.

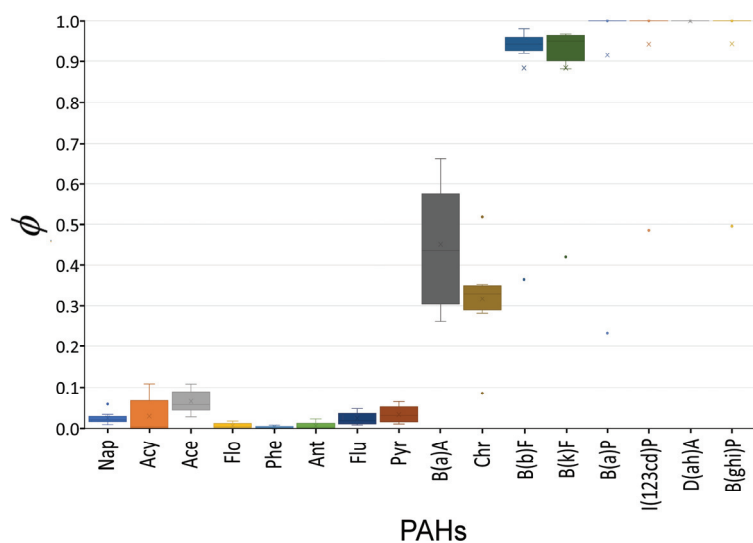


Fig. 2. Variations of  $\phi$  values at the locations in Serbia.

TABLE II. Vapour pressure,  $\log K_{OA}$  and  $\log K_{SA}$  for 16 EPA priority PAHs used in Dachs–Eisenreich model

| PAH       | $p_L^0 / \text{Pa}$  | $\log K_{OA}$ | $\log (K_{SA} / \text{L kg}^{-1})$ |
|-----------|----------------------|---------------|------------------------------------|
| Nap       | 1.00                 | 5.13          | 6.89                               |
| Acy       | 0.90                 | 6.23          | 7.78                               |
| Ace       | 0.30                 | 6.22          | 8.18                               |
| Flo       | 0.50                 | 6.68          | 8.60                               |
| Phe       | 0.08                 | 7.45          | 9.40                               |
| Ant       | 0.07                 | 7.34          | 9.50                               |
| Flu       | $6 \times 10^{-3}$   | 8.60          | 10.50                              |
| Pyr       | $5 \times 10^{-4}$   | 8.61          | 10.60                              |
| B(a)A     | $5 \times 10^{-4}$   | 9.54          | 10.54                              |
| Chr       | $1.7 \times 10^{-4}$ | 10.44         | 12.10                              |
| B(b)F     | $10^{-6}$            | 10.98         | 12.84                              |
| B(k)F     | $10^{-6}$            | 11.19         | 12.84                              |
| B(a)P     | $3 \times 10^{-6}$   | 10.77         | 13.00                              |
| I(123cd)P | $10^{-9}$            | 11.56         | 15.39                              |
| D(ah)A    | $10^{-8}$            | 13.90         | 14.54                              |
| B(ghi)P   | $10^{-8}$            | 11.01         | 14.54                              |

### Modelling gas-particle partition of PAHs

The discrepancy between the measured and the predicted values for higher molecular mass PAHs ( $B(b)F$ ,  $B(k)F$ ,  $B(a)P$ ,  $I(1,2,3\text{ cd})P$ ,  $D(ah)A$ ,  $B(ghi)P$ ) is negligible for all sampling locations in Serbia, except for Oil Refinery Pančevo (P1), where the measured values for  $\phi$  were 30–50 % lower than predicted (Fig. 3). The reason is higher rate of PAHs emission in the atmosphere at the location Oil Refinery Pančevo than the rate of sorption onto the soot in the air, causing the specific gas-particle partition comparing to urban conditions.

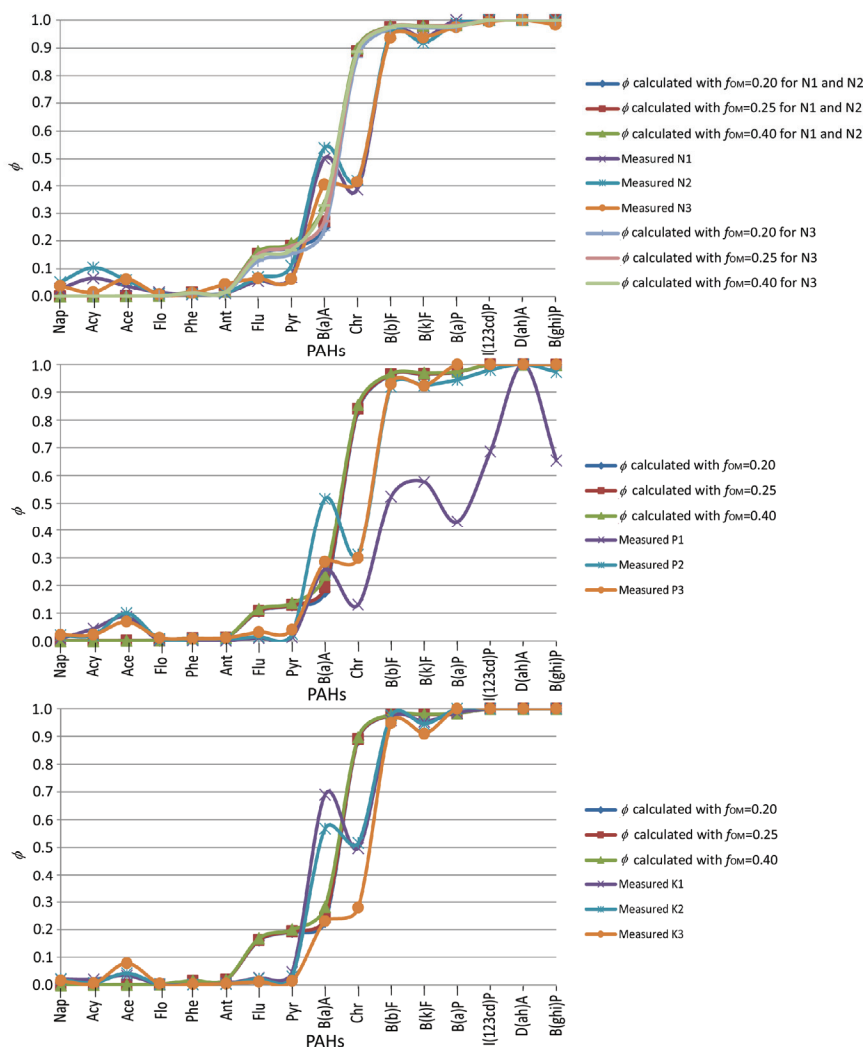


Fig. 3. Comparison of measured and predicted  $\phi$  values at all locations using Dachs-Eisenreich model.

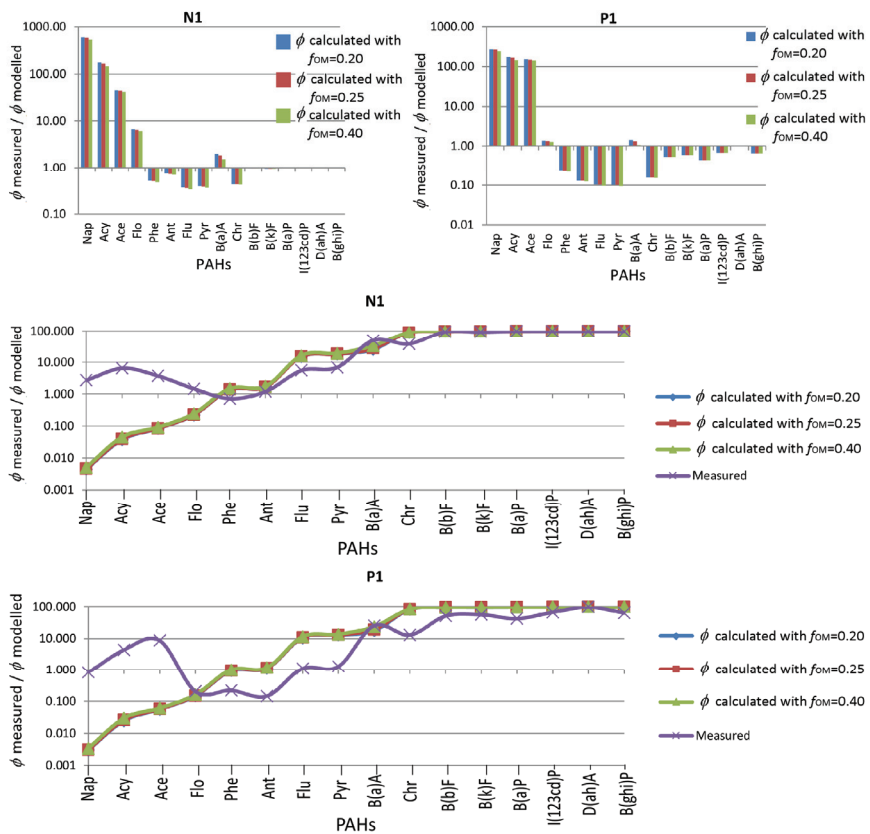
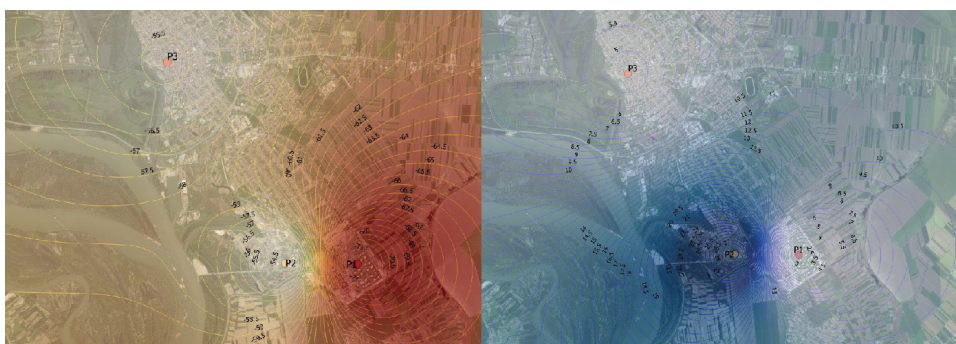
Other reasons for the presented discrepancy could be:

- the variations in the chemical contents of the atmospheric particles which were not adequately presented by the uniform values for  $f_{OM}$  and  $f_{EC}$ ;
- as indicated by Dachs and Eisenreich,<sup>1</sup> the temperature exerts a strong influence on the values of  $K_{OA}$  and  $K_{SA}$ ; the coefficient  $K_{SA}$  depends on the dimensionless Henry's law constant  $H$  and its value variates at different temperatures; the temperature influence on  $K_{OA}$  is defined by  $\log K_{OA} = A + B/T$ , whereas A and B are coefficients estimated by Harner and Bidleman by measurements of  $K_{OA}$  at different temperatures –  $T / K$ ,<sup>3</sup> but in our prediction, it was assumed that the temperature was 25 °C; the prediction should be more precise if the temperature influence was taken into account;
- since the liquid film of organic matter covers the elemental carbon, the reversible processes of SOCs ad/desorption onto and from the atmospheric aerosols are very slow and the reaching of equilibrium between gas and particle phase is delayed, the gaps between measured and real concentrations can be potentially caused;<sup>1</sup>
- according to the specific source of PAHs emissions at the Oil Refinery Pančevo (P1), the modelled values could be improved using the measured values for TSP and  $f_{EC}$  on the site;
- breakthrough of volatile PAHs from the PUF can lead to underestimation of the concentrations of gas-phase PAHs.

Three different scenarios for the  $f_{OM}$  value gave approximately identical levels of PAHs particle fraction  $\phi$ , which means that the process of absorption doesn't affect so much the overall partition of PAHs in the atmosphere. The research has shown that the Dachs and Eisenreich model provided the good prediction for urban locations, but underestimated the values in rural areas for one order of magnitude.<sup>10,13</sup>

To compare the results, the ratio of measured and modelled values is shown on logarithmic scale (for selected locations N1 and P1, Fig. 4). It is obvious that the Dachs and Eisenreich model points out the good predictions of gas-particle partition for higher molecular mass PAHs considering all three scenarios. As well, the predicted values obtained by Dachs and Eisenreich model for lower molecular mass PAHs are slightly closer to the measured ones, comparing to the other previously wide used mathematical models.<sup>14–16</sup> Nevertheless, the model needs the correction, at least for the Nap, Acy, Ace and Flo.

The differences between measured and modelled values for three cities are presented using QGIS software and shown on Figs. 5–7. The difference is positive if the measured value is higher than the modelled one, and *vice versa*. Only the  $\phi$  for Chr and B(a)A are pictured on the maps because these compounds showed the highest gaps between the measured and the modelled values.

Fig. 4. Measured and modelled  $\phi$  values at locations N1 and P1.Fig. 5. The differences between measured and modelled  $\phi$  values of Chr (a) and B(a)A (b) for the city of Pančevo, Serbia.

The  $\phi$  for Chr in Pančevo is significantly overestimated using the Dachs and Eisenreich model at the locality P1 and it is obvious that the model needs to be corrected. Particle bound fraction for Chr was also overestimated at the P2 and P3

locations, but not in such high extent. While the partition of B[a]A was acceptable, as predicted by the model at P1 and P3, it was underestimated at the locality Petrochemical Industry Pančevo.



Fig. 6. The differences between measured and modelled fractions  $\phi$  of Chr and B(a)A for the city of Novi Sad, Serbia.

The results were similar at the Oil Refinery Novi Sad. The model, once again, overestimated the particle fraction of Chr and underestimated the particle fraction of B(a)A, although the differences between the Oil Refinery and the city centre were minor.

For the city of Kragujevac (Fig. 7), the model overestimated Chr particle fraction for the city centre (60 %) and for the car factory (40 %). B(a)A particle fraction was modelled accurately for the city centre (K3), but again underestimated in the industrial area.



Fig. 7. The differences between measured and modelled fractions  $\phi$  of Chr and B(a)A for the city of Kragujevac, Serbia.

#### CONCLUSION

The results on modelling of the PAHs atmospheric distribution using the Dachs–Eisenreich ab/adsorption model displays gaps between the measured and predicted  $\phi$  values less than one order of magnitude for Flo, Phe, Ant, Flu, Pyr,

B(a)A and Chr. For the high molecular mass PAHs, namely B(b)F, B(k)F, B(a)P, I(1,2,3-cd)P, D(ah)A and B(ghi)P, very good corelation was confirmed.

Similar variability of the measured/modelled  $\phi$  values was obtained using the previously discussed theoretical and empirical, absorption and adsorption models, indicating the presence of non-exchangeable, inert fraction of PAHs in the suspended particles, which cannot be exchanged by the air. One of the possible reasons for the discrepancy between the measured and modelled  $\phi$  values could be the assumed constant values of  $f_{OM}$  and  $f_{EC}$ . For each specific locality, the influence of the local ambient conditions on both physical and chemical structure, concentration and dynamic of suspended particles formation should be considered.

For the PAHs with lower molecular mass, all models have significantly underestimated the concentrations of PAHs as the free gas molecules, but applying the Dachs and Eisenreich approach, the modelled values are slightly closer to the measured ones. For the second group of PAHs, in both the gas and particle phase, the variations between the measured and the predicted values are recorded using all models. For the third group of PAHs, the Dachs and Eisenreich model has predicted the partition processes precisely.

The application of the Dachs–Eisenreich sorption approach was examined and demonstrated and resulted in the modified regional-scale gas/particle atmospheric modelling. Our results can provide ground for the new research area development including the gas/particle spatial-temporal variations of  $\phi$  values for the variety of atmospheric pollutants distribution balance models, without the need for extensive additional field data collection.

#### ИЗВОД

#### МОДЕЛОВАЊЕ ГАС–ЧЕСТИЧНЕ РАСПОДЕЛЕ ПОЛИАРОМАТИЧНИХ УГЉОВОДОНИКА ПРИМЕНОМ АПСОРПЦИОНО/АДСОРПЦИОНОГ МОДЕЛА

МИРЈАНА ВОЈИНОВИЋ МИЛОРАДОВ<sup>1</sup>, МАЈА ТУРК СЕКУЛИЋ<sup>1</sup>, ЛАЗАР ИГЊАТОВИЋ<sup>2</sup>, СМИЉА КРАЈИНОВИЋ<sup>1</sup>, ДРАГАН АДАМОВИЋ<sup>1</sup> и ЈЕЛЕНА РАДОНИЋ<sup>1</sup>

<sup>1</sup>Универзитет у Новом Саду, Факултет техничких наука, Нови Сад и <sup>2</sup>Институт за водопривреду „Јарослав Черни“, Београд

Мотив истраживања био је да се процени конзистентност између гас–честичне расподеле 16 EPA полиароматичних угљоводоника предиктоване апсорпционо/адсорпционим Dachs–Eisenreich моделом и резултата добијених експерименталним теренским мерењима. На 9 препрезентативних локација у Србији прикупљено је укупно 29 узорака ваздуха. Примењена је експериментална метода прикупљања узорака ваздуха узорковањем велике запремине (high volume air sampler, HVAS), са квачним филтерима за атмосферске суспендоване честице и филтерима од полиуретанске пене (PUF) за слободне гасне молекуле полиароматичних угљоводоника. Упоређени су резултати добијени Dachs–Eisenreich моделом и подаци добијени теренским мерењима. Одступања између измерених и вредности модела била су мања од једног реда величине за Flo, Phe, Ant, Flu, Pir, B (a) A и Chr. За полиароматичне угљоводонике велике молекулске масе, B (b) F, B (k) F, B (a) P, I (1,2,3-cd) P, D (ah) A и B (ghi) P, потврђена је веома добра

корелација, осим код података са територије Рафинерије нафте у Панчеву. Примењени модел је показао знатно ниже вредности концентрација за слободне гасне молекуле полиароматичних угљоводоника мале молекулске масе.

(Примљено 29. новембра, прихваћено 17. децембра 2021)

#### REFERENCES

1. J. Dachs, S. J. Eisenreich, *Environ. Sci. Technol.* **34** (2000) 3690 ([https://doi.org/10.1021/es991201+\)](https://doi.org/10.1021/es991201+)
2. J. F. Pankow, *Atmos. Environ.* **28** (1994) 185 ([https://doi.org/10.1016/1352-2310\(94\)90093-0](https://doi.org/10.1016/1352-2310(94)90093-0))
3. T. Harner, T. F. Bidleman, *J. Chem. Eng. Data* **32** (1998) 1494 (<https://doi.org/10.1021/es970890r>)
4. R. Lohmann, G. Lammel, *Environ. Sci. Technol.* **38** (2004) 3793 (<https://doi.org/10.1021/es035337q>)
5. J. Radonić, *PhD Thesis*, Faculty of Technical Sciences, Novi Sad, 2009, <https://nardus.mpn.gov.rs/handle/123456789/1873> (in Serbian)
6. W. Wang, S. L. M. Simonich, W. Wang, B. Giri, J. Zhao, M. Xue, J. Cao, X. Lu, S. Tao, *Atmos. Res.* **99** (2011) 197 (<https://doi.org/10.1016/j.atmosres.2010.10.002>)
7. J. H. Seinfeld, S. N. Pandis, K. Noone, *Phys. Today* **51** (1998) 88 (<https://doi.org/10.1063/1.882420>)
8. J. Radonic, M. T. Sekulic, M. V. Miloradov, P. Čupr, J. Klánová, *Environ. Sci. Pollut. Res.* **16** (2009) 65 (<https://doi.org/10.1007/s11356-008-0067-3>)
9. K. T. Whitby, B. K. Cantrell, D. B. Kittelson, *Atmos. Environ.* **12** (1978) 313 ([https://doi.org/10.1016/0004-6981\(78\)90213-5](https://doi.org/10.1016/0004-6981(78)90213-5))
10. N. Vardar, Y. Tasdemir, M. Odabasi, K. E. Noll, *Sci. Total Environ.* **327** (2004) 163 (<https://doi.org/10.1016/j.scitotenv.2003.05.002>)
11. M. T. O. Jonker, A. A. Koelmans, *Environ. Sci. Technol.* **36** (2002) 3725 (<https://doi.org/10.1021/es020019x>)
12. D. Mackay, W.-Y. Shiu, W.-Y. Shiu, S. C. Lee, *Handbook of Physical-Chemical Properties and Environmental Fate for Organic Chemicals*, CRC Press, Boca Raton, FL, 2006, p. 4216 (<https://doi.org/10.1201/9781420044393>)
13. E. Galarneau, T. F. Bidleman, P. Blanchard, *Atmos. Environ.* **40** (2006) 182 (<https://doi.org/10.1016/j.atmosenv.2005.09.034>)
14. M. Turk Sekulic, J. Radonic, M. Vojinovic-Miloradov, N. Senk, M. Okuka, *Hem. Ind.* **65** (2011) 371 (<https://doi.org/10.2298/hemind101013046t>)
15. J. Radonić, D. Ćulibrk, M. V. Miloradov, B. Kukić, M. T. Sekulić, *Therm. Sci.* **15** (2011) 105 (<https://doi.org/10.2298/TSCI100809005R>)
16. M. Turk Sekulić, M. Okuka, N. Šenk, J. Radonić, M. Vojinović Miloradov, B. Vidicki, *Atmos. Res.* **128** (2013) 111 (<https://doi.org/10.1016/j.atmosres.2013.03.013>).